

(NASA-CR-175656) SHUTTLE PAYLOAD BAY
DYNAMIC ENVIRONMENTS: SUMMARY AND
CONCLUSION REPORT FOR STS FLIGHTS 1-5 AND 9
(Jet Propulsion Lab.) 166 p HC A08/HF A07

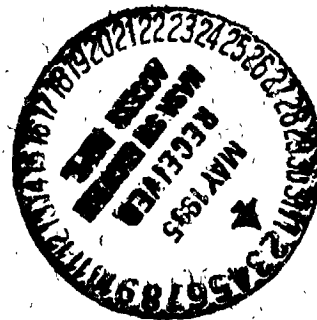
N85-23896

Unclas
CSCL 22B G3/16 14791

Shuttle Payload Bay Dynamic Environments

Summary and Conclusion Report for STS Flights 1-5 and 9

Michael O'Connell
John Garba
Dennis Kern



December 1, 1984

NASA

National Aeronautics and
Space Administration

Jet Propulsion Laboratory
California Institute of Technology
Pasadena, California

JPL PUBLICATION 84-88

Shuttle Payload Bay Dynamic Environments

Summary and Conclusion Report for STS Flights 1-5 and 9

Michael O'Connell
John Garba
Dennis Kern

December 1, 1984

NASA

National Aeronautics and
Space Administration

Jet Propulsion Laboratory
California Institute of Technology
Pasadena, California

The research described in this publication was carried out by the Jet Propulsion Laboratory, California Institute of Technology, under a contract with the National Aeronautics and Space Administration.

Reference herein to any specific commercial product, process, or service by trade name, trademark, manufacturer, or otherwise, does not constitute or imply its endorsement by the United States Government or the Jet Propulsion Laboratory, California Institute of Technology

ABSTRACT

This report summarizes the vibration, acoustic and low frequency loads data from the first 5 shuttle flights and presents the engineering analysis of that data. Vibroacoustic data from STS-9 are also presented because they represent the only data taken on a large payload. Payload dynamic environment predictions developed by the participation of various NASA and industrial centers are presented along with a comparison of analytical loads methodology predictions with flight data, including a brief description of the methodologies employed in developing those predictions for payloads. The review of prediction methodologies illustrates how different centers have approached the problems of developing shuttle dynamic environmental predictions and criteria. Ongoing research activities related to the shuttle dynamic environments are also described. This should increase the awareness of the user community as to what is being planned in an effort to resolve the areas of concern pertaining to the Space Transportation System (STS) dynamic environments. Analytical software recently developed for the prediction of payload acoustic and vibration environments are also described.

ACKNOWLEDGEMENTS

This task report was sponsored by the NASA Office of Aeronautics and Space Technology (OAST). The Jet Propulsion Laboratory (JPL) was the lead center for the task for OAST. This report represents the combined efforts of the NASA DATE Working Group members from various NASA and industrial centers, and the Air Force Space Division. The group was chaired by the Goddard Space Flight Center (GSFC). The DATE Working Group is charged with planning shuttle dynamic and thermal data acquisition, data reduction, dissemination of the data and its analysis. Other participating organizations include Rockwell International, the Aerospace Corporation, Johnson Space Center, Lockheed Missiles and Space Company, Marshall Space Flight Center and the Lewis Research Center. Contributions from these organizations are gratefully acknowledged.

It is anticipated that this report will prove to be useful to the STS user community in developing realistic dynamic environment design and test requirements for shuttle payloads.

Table of Contents

| Section | Page Number |
|----------------------------------|-------------|
| 1.0 INTRODUCTION | 1 |
| 2.0 OVERVIEW OF RESULTS | 2 |
| 2.1 Vibration and Acoustics | 2 |
| 2.2 Low Frequency Vibration | 3 |
| 3.0 FLIGHT DATA SYSTEMS | 5 |
| 3.1 Launch Vehicle Configuration | 5 |
| 3.2 Flight Data System | 5 |
| 3.3 Data System Errors | 9 |
| 4.0 DATA REDUCTION | 11 |
| 4.1 Acoustic Data Reduction | 11 |
| 4.2 Vibration Data Reduction | 11 |
| 5.0 FLIGHT DATA EVALUATION | 15 |
| 5.1 Acoustic Data Summary | 15 |
| 5.1.1 Perimeter Acoustic Data | 17 |
| 5.1.2 Payload Acoustic Data | 18 |
| 5.1.3 Aft Flight Deck Acoustics | 18 |
| 5.2 Vibration Data Summary | 45 |
| 5.2.1 Payload Bay Vibration | 45 |
| 5.2.2 Aft Flight Deck Vibration | 47 |

Table of Contents
(continued)

| Section | Page Number |
|---|--------------------|
| 5.3 Low Frequency Vibration | 76 |
| 5.3.1 Low Frequency Response During Ascent | 76 |
| 5.3.1.1 Low Frequency Response During Main Engine Ignition | 76 |
| 5.3.1.2 Low Frequency Response During Solid Rocket Booster Ignition | 77 |
| 5.3.2 Low Frequency Response During Landing | 77 |
| 5.3.2.1 Low Frequency Response During Main Landing Gear Touchdown | 77 |
| 5.3.2.2 Low Frequency Response During Nose Gear Touchdown | 77 |
| 6.0 ENVIRONMENTAL UNCERTAINTIES | 89 |
| 6.1 Spatial Bias Errors | 89 |
| 6.2 Payload Effects | 89 |
| 6.3 Spatial Variation | 90 |
| 6.4 Flight-to-Flight Variation | 90 |
| 6.4.1 Acoustic Environment | 90 |
| 6.4.2 Low Frequency Vibration | 91 |
| 7.0 DYNAMIC ENVIRONMENT AND LOADS PREDICTIONS | 92 |
| 7.1 Acoustic Predictions | 92 |
| 7.1.1 Jet Propulsion Laboratory Acoustic Predictions | 92 |
| 7.1.2 Lockheed Missiles and Space Company Acoustic Predictions | 93 |
| 7.1.3 Aerospace Corporation Acoustic Predictions | 95 |

Table of Contents
(continued)

| Section | | Page Number |
|----------------|--|--------------------|
| 7.1.4 | Rockwell International/Johnson Space Center Acoustic Predictions | 95 |
| 7.1.5 | Goddard Space Flight Center Acoustic Predictions | 95 |
| 7.2 | Computerized Acoustic and Vibration Predictions | 95 |
| 7.2.1 | PACES | 95 |
| 7.2.2 | VAPEPS | 96 |
| 7.3 | Vibration Predictions | 96 |
| 7.3.1 | Rockwell Vibration Prediction | 96 |
| 7.3.2 | Aerospace Corporation Vibration Prediction | 96 |
| 7.3.3 | GSFC Vibration Prediction | 96 |
| 7.4 | Flight Data and Analytical Loads Predictions | 98 |
| 7.4.1 | Comparison of Flight Data With Design Conditions | 98 |
| 7.4.2 | Comparison of Flight Data with Post-Flight Correlation Analyses | 100 |
| 8.0 | RELATED ACTIVITIES | 117 |
| 9.0 | CONCLUSIONS | 118 |
| 9.1 | Acoustic Data | 118 |
| 9.2 | High Frequency Vibration Data | 119 |
| 9.3 | Low Frequency Vibration Data | 120 |
| 9.4 | Data Deficiencies | 124 |

Table of Contents
(continued)

| Section | Page Number |
|---|--------------------|
| 9.4.1 Acoustics and High Frequency Vibration | 124 |
| 9.4.2 Low Frequency Vibration | 125 |
| 10.0 RECOMMENDATIONS | 126 |
| 10.1 STS Dynamic Data Base | 126 |
| 10.1.1 Vibration and Acoustic Data Base | 126 |
| 10.1.2 Low Frequency Data Base | 127 |
| 10.2 Large Payload Methodology | 128 |
| 10.3 Vent Tone Definition | 128 |
| 10.4 Vibroacoustic Transfer Functions | 128 |
| 10.5 Loads Combination Methodology | 128 |
| 10.6 VAPEPS Improvement | 129 |
| 10.7 Western Test Range Environment and Forcing Functions for Loads Analysis | 129 |
| 11.0 REFERENCES AND BIBLIOGRAPHY | 130 |
| 11.1 References | 130 |
| 11.2 Bibliography | 132 |
| APPENDIX | 134 |
| FIGURES | |
| 4-1 Typical Time History for Microphone 9219, Overall Flight, STS 1 | 13 |
| 4-2 Summary of Payload Mean Acoustic Levels for Significant Flight Conditions | 14 |

Table of Contents
(continued)

| | Page Number |
|---|--------------------|
| 5-1 Payload Bay Acoustic Level Statistics for All Bay Microphones, STS-1 Through STS-5 | 20 |
| 5-2 Perimeter and Payload Region Average Level Comparison With Average of Maximum Time Envelope Levels for Each Microphone | 21 |
| 5-3 Perimeter and Payload Region Maximum Acoustic Levels | 22 |
| 5-4 Perimeter and Payload Acoustic Level Standard Deviation | 23 |
| 5-5 Shuttle Payload Bay Acoustic Contours for Small Payloads/Empty Bay | 24 |
| 5-6 Mean of Acoustic Time Envelopes for Each Flight's Perimeter Microphones | 25 |
| 5-7 Maximum of Acoustic Time Envelopes for Each Flight's Perimeter Microphones | 26 |
| 5-8 Acoustic Envelope Statistics for Perimeter Microphones | 27 |
| 5-9 Flight-to-Flight Variation and Scatter of Each Flight's Perimeter Acoustic Mean Levels From Overall Perimeter Mean, STS-1 Through STS-5 | 28 |
| 5-10 Maximum Time Envelope for Acoustic Level 6 Feet From Payload Bay Centerline Near Payload Doors, Microphone 9231, STS-3 | 29 |
| 5-11 Maximum Time Envelope for Acoustic Level Between Pallet and Sidewall, Microphone 9256, STS-2 | 30 |
| 5-12 Spacelab Module External Acoustics vs. STS-2 Through STS-5 Pallet Envelope and STS-2 Pallet Side Levels | 31 |
| 5-13 Spacelab Tunnel Acoustics vs. STS-2 Through STS-5 Envelope | 32 |
| 5-14 Spacelab STS-9 Pallet Acoustics | 33 |
| 5-15 Discrete Tone, 315 Hz, During Transonic Flight, Microphone 9256, STS-2 | 34 |

Table of Contents
(continued)

| | Page |
|--|-------------|
| 5-16 Power Spectral Density of Transonic Flight Acoustic Measurements, STS-1, AM Cargo Bay Internal (250 - 350 Hz from T+20 to T-85 seconds) | 35 |
| 5-17 Power Spectral Density of Transonic Flight Acoustic Measurements, STS-2, AM LF OSTA-1 Pallet (250 - 350 Hz from T+20 to T-85 seconds) | 36 |
| 5-18 Mean of Acoustic Time Envelopes for Each Flight's Payload Microphones | 37 |
| 5-19 Maximum Envelope of Acoustic Time Envelopes for Payload Microphones | 38 |
| 5-20 Acoustic Data Time Envelope Statistics for Payload Microphones, All Flights | 39 |
| 5-21 Acoustic Data Time Envelope Statistics for Payload Microphones, STS-2 | 40 |
| 5-22 Acoustic Data Time Envelope Statistics for Payload Microphones, STS-3 | 41 |
| 5-23 Acoustic Data Time Envelope Statistics for Payload Microphones, STS-4 | 42 |
| 5-24 Acoustic Data Time Envelope Statistics for Payload Microphones, STS-5 | 43 |
| 5-25 Expanded Acoustic Data Time Envelope Statistics for Payload Microphones, All Flights | 44 |
| 5-26 Vibration Data for Longeron Bridge Fitting Mounted Payload | 48 |
| 5-27 Orbiter Longeron Vibration Criteria Derived From Flight Data | 49 |
| 5-28 DFI Payload Trunnion Vibration | 50 |
| 5-29 DFI Payload Longeron and Trunnion Vibration Comparison in X-Axis, STS-1 Through STS-3 | 51 |
| 5-30 DFI Payload Longeron and Trunnion Vibration Comparison in Y-Axis, STS-1 Through STS-3 | 52 |

Table of Contents
(continued)

| | Page Number |
|---|--------------------|
| 5-31 DFI Payload Longeron and Trunnion Vibration Comparison in Z-Axis, STS-1 Through STS-3 | 53 |
| 5-32 DFI Payload Pallet Center Vibration | 54 |
| 5-33 Orbiter Keel Fitting Flight Vibration Data | 55 |
| 5-34 Pallet Hardpoint/Experiment Interface Vibration | 56 |
| 5-35 OSTA-1 Payload Shelf Vibration | 57 |
| 5-36 OSS-1 Cold Plate Edge Vibration | 58 |
| 5-37 OSS-1 Experiment Support Bracket Vibration (Mounted on Small Shelf) | 59 |
| 5-38 Measured STS and Extrapolated Test Acceleration Spectral Density for OSS-1 Shelf, Experiment Support Bracket, Accelerometer 9295 | 60 |
| 5-39 Measured and Extrapolated Test Acceleration Spectral Density Level for OSS-1, Cold Plate Edge, Accelerometer 9301, Normal to Plate | 61 |
| 5-40 STS-3/OSS-1 vs. Acoustic Ground Test Payload Acoustic Environment | 62 |
| 5-41 Comparison of STS-4 Flight and Ground Test Vibration Data, DOD Pallet, Normalized to Extrapolated Ground Vibration Data | 63 |
| 5-42 Ground Test and STS Liftoff Acoustic Comparisons | 64 |
| 5-43 Comparison of STS-3 Flight and Ground Test Vibration Data, OSS-1 Pallet, Normalized to Extrapolated Ground Vibration Data | 65 |
| 5-44 STS-9 Pallet CPSS/Component Interface Vibration, Ground Acoustic Test vs. Flight Vibration | 66 |
| 5-45 STS-9 Vibration Input to SWAA at 1.3-m Ring, Ground Acoustic Test vs. Flight Vibration | 67 |
| 5-46 STS-9 Spacelab STT Fan Housing Interface Vibration, Ground Acoustic Test vs. Flight Vibration | 68 |

Table of Contents
(continued)

| | | Page Number |
|------|---|--------------------|
| 5-47 | OCE Shelf Shock Response Spectrum Time Envelope, Accelerometer 9247, STS-2 | 69 |
| 5-48 | OCE Shelf Shock Response Spectrum Time Envelope, Accelerometer 9248, STS-2 | 70 |
| 5-49 | DFI Pallet Beam Shock Response Spectrum Time Envelope, Accelerometer 9273, STS-3 | 71 |
| 5-50 | DFI Pallet Beam Shock Response Spectrum Time Envelope, Accelerometer 9274, STS-3 | 72 |
| 5-51 | Cold Plate Side Shock Response Spectrum Time Envelope, Accelerometer 9300, STS-3 | 73 |
| 5-52 | Cold Plate Side Shock Response Spectrum Time Envelope, Accelerometer 9301, STS-3 | 74 |
| 5-53 | Thermal Can Base Shock Response Spectrum Time Envelope, Accelerometer 9292, STS-3 | 75 |
| 5-54 | Response Spectra, Main Engine Ignition, Crew Cabin, Y Direction, Accelerometer V33A9215A | 78 |
| 5-55 | Response Spectra, Main Engine Ignition, Crew Cabin, Z Direction, Accelerometer V33A9216A | 78 |
| 5-56 | Response Spectra, Main Engine Ignition, Aft Bulkhead, X Direction, Accelerometer V34A9434A | 79 |
| 5-57 | Response Spectra, Main Engine Ignition, Aft Bulkhead, Y Direction, Accelerometer V34A9435A | 79 |
| 5-58 | Response Spectra, Main Engine Ignition, Aft Bulkhead, Z Direction, Accelerometer V34A9436A | 80 |
| 5-59 | Response Spectra, Solid Rocket Booster Ignition, Crew Cabin, Z Direction, Accelerometer V33A9215A | 81 |
| 5-60 | Response Spectra, Solid Rocket Booster Ignition, Crew Cabin, Z Direction, Accelerometer V33A9216A | 81 |
| 5-61 | Response Spectra, Solid Rocket Booster Ignition, Aft Bulkhead, X Direction, Accelerometer V34A9434A | 82 |
| 5-62 | Response Spectra, Solid Rocket Booster Ignition, Aft Bulkhead, Y Direction, Accelerometer V34A9435A | 82 |

Table of Contents
(continued)

| | Page Number | |
|------|---|-----|
| 5-63 | Response Spectra, Solid Rocket Booster Ignition, Aft Bulkhead, Z Direction, Accelerometer V34A9436A | 83 |
| 5-64 | Response Spectra, Solid Rocket Booster Ignition, Input to DFI Pallet, Y Direction, Right-Hand Bridge Fitting, Accelerometer V08D9261A | 84 |
| 5-65 | Response Spectra, Solid Rocket Booster Ignition, Input to DFI Pallet, Z Direction, Right-Hand Bridge Fitting, Accelerometer V08D9262A | 84 |
| 5-66 | Response Spectra, Solid Rocket Booster Ignition, Input to DFI Pallet, Z Direction, Left-Hand Bridge Fitting, Accelerometer V08D9264A | 85 |
| 5-67 | Response Spectra, Solid Rocket Booster Ignition, Input to DFI Pallet, Z Direction, Keel Bridge Fitting, Accelerometer V08D9265A | 85 |
| 5-68 | Response Spectra, Solid Rocket Booster Ignition, DFI Pallet Beam, X Axis, Accelerometer V08D9267A | 86 |
| 5-69 | Response Spectra, Solid Rocket Booster Ignition, DFI Pallet Beam, Y Axis, Accelerometer V08D9268A | 86 |
| 5-70 | Response Spectra, Solid Rocket Booster Ignition, DFI Pallet Beam, Z Axis, Accelerometer V08D9269A | 87 |
| 5-71 | Response Spectra, Landing, Main Landing Gear Contact, Aft Bulkhead, Z Direction, Accelerometer V34A9436A | 88 |
| 5-72 | Response Spectra, Landing, Nose Landing Gear Contact, Crew Cabin, Z Direction, Accelerometer V33A9216A | 88 |
| 7-1 | Small Payload/Empty Bay Acoustic Prediction Comparison | 101 |
| 7-2 | JPL STS Large Payload Acoustic Prediction | 102 |
| 7-3 | JPL 2-Sigma of Payload Acoustic Data, All Payload Microphones, STS-1 Through STS-5 | 103 |
| 7-4 | Large Payload Acoustic Prediction Comparison | 104 |
| 7-5 | Aerospace Corporation Adjustment for Large Payloads | 105 |

Table of Contents
(continued)

| | Page Number |
|--|-------------|
| 7-6 Rockwell International Comparison of Transonic Flight and Lift-Off Payload Bay Noise | 106 |
| 7-7 Aerospace Corporation Longeron/Bridge Fitting Payload Vibration for STS-1 Through STS-3 Liftoff | 107 |
| 7-8 Response Spectra, Comparison of Design Conditions With Flight Data, Liftoff, SSME Ignition +10 Seconds, Aft Bulkhead, X Direction | 108 |
| 7-9 Response Spectra, Comparison of Design Conditions With Flight Data, Liftoff, SSME Ignition +10 Seconds, Keel, Y Direction | 108 |
| 7-10 Response Spectra, Comparison of Design Conditions With Flight Data, Liftoff, SSME Ignition +10 Seconds, Left Longeron, Z Direction | 109 |
| 7-11 GSFC-Installed Measurement Locations on OSS-1 | 110 |
| 7-12 Response Spectra, Post Liftoff, SRB Ignition +4 Seconds, OSS-1 Experiment, X Direction, Accelerometer V08D9285A | 111 |
| 7-13 Response Spectra, Post Liftoff, SRB Ignition +4 Seconds, OSS-1 Experiment, Y Direction, Accelerometer V08D9286A | 111 |
| 7-14 Response Spectra, Post Liftoff, SRB Ignition +4 Seconds, OSS-1 Experiment, Z Direction, Accelerometer V08D9287A | 112 |
| 7-15 Response Spectra, Landing, Main Gear Contact +2 Seconds, OSS-1 Experiment, Z Direction, Accelerometer V08D9284A | 112 |
| 7-16 Response Spectra, Landing, Nose Gear Contact +2 Seconds, OSS-1 Experiment, Z Direction, Accelerometer V08D9284A | 113 |
| 7-17 Location of SBS/PAM-D Accelerometers, STS-5 | 114 |
| 7-18 Response Spectra, Comparison of Reconstructed Liftoff Analysis to STS-5 Flight Data, SRB Ignition +3 Seconds, PAM-D/SBS Interface, X Direction, Accelerometer P01A0002A | 115 |

Table of Contents
(continued)

| | | Page Number |
|-------------------|---|--------------------|
| 7-19 | Response Spectra, Comparison of Reconstructed Liftoff Analysis to STS-5 Flight Data, SRB Ignition +3 Seconds, PAM-D/SBS Interface, Y Direction, Accelerometer P01A0003A | 115 |
| 7-20 | Response Spectra, Comparison of Reconstructed Liftoff Analysis to STS-5 Flight Data, SRB Ignition +3 Seconds, FAM-D/SBS Interface, Z Direction, Accelerometer P01A0001A | 116 |
| 9-1 | Shock Spectra of Left Longeron Z ₀ Load Factor at X ₀ 823 for Flight Data and Analytical Design Cases, SRB Ignition to +3 Seconds | 123 |
| A-1 | STS-2 Microphone Locations | A-2 |
| A-2 | STS-3 Microphone Locations | A-2 |
| A-3 | STS-4 Microphone Locations | A-3 |
| A-4 | STS-5 Microphone Locations | A-3 |
| A-5 | STS-9 Microphone Locations | A-4 |
| A-6 | DFI Acceleration Measurement Locations | A-5 |
| A-7 | DATE Low Frequency Accelerometers at DFI Pallet in Identical Locations for Multiple Flights | A-6 |
| TABLES | | |
| 3-1 | Launch Vehicle Configuration | 5 |
| 3-2 | STS Instrumentation Summary | 6 |
| 3-3 | Summary of Low Frequency Acceleration Measurements for Orbiter Vehicle No. 102, STS-1 Through STS-5 | 7 |
| 3-4 | STS Dynamic Data System Errors | 10 |
| 5-1 | Microphone Region Category | 16 |
| 5-2 | Aft Flight Deck Acoustic Environment | 19 |
| 5-3 | Aft Flight Deck Vibration | 47 |

Table of Contents
(continued)

| | | Page Number |
|-----|--|--------------------|
| 7-1 | LMSC Acoustic Prediction Factors for Large DOD Payload | 94 |
| 7-2 | Baseline Random Vibration Environment Criteria for Shuttle Pallet Payload Subsystems Flight Levels | 97 |
| 9-1 | Maximum Load Factors for STS Lift-Off From the Orbiter Low-Frequency Accelerometers | 121 |
| 9-2 | Shuttle Quasi-Static Load Factors on STS-1 Through STS-5 | 121 |
| 9-3 | Landing Touchdown Conditions in Shuttle Test Flights | 122 |
| 9-4 | Maximum Load Factors for STS Landing From the Orbiter Low-Frequency Accelerometers | 122 |
| A-1 | DATE Accelerometers at DFI Pallet in Identical Locations for Multiple Flights | A-7 |
| A-2 | DFI Acceleration Measurement Information | A-8 |
| A-3 | DFI Acoustic Measurement Information | A-9 |
| A-4 | STS-2 DATE Measurement Information on DFI Pallet | A-10 |
| A-5 | STS-2 DATE Measurement Information on OSTA Pallet | A-11 |
| A-6 | STS-3 DATE Measurement Information on DFI Pallet | A-12 |
| A-7 | STS-3 DATE Measurement Information on OSS-1 | A-13 |
| A-8 | STS-4 DATE Measurement Information | A-14 |
| A-9 | STS-5 DATE Measurement Information | A-16 |

1.0 INTRODUCTION

This report summarizes the results of the dynamic environmental data taken during the first 5 space shuttle flights and STS-9. An evaluation of the data and its application to payloads are primary objectives of this report. Methods of payload dynamic environmental prediction developed by industry and several government centers, including prediction programs and loads methodologies, will also be discussed. The primary objectives of the low frequency flight data evaluation are the verification of analytical prediction methods and the compilation of a highly reliable data base. Finally, conclusions from the data are presented and recommendations on future activities are made.

The data in this report were acquired and reduced as part of the NASA DATE (Dynamic, Acoustic and Thermal Environments) activity, managed by Goddard Space Flight Center (GSFC). The data base consists of the flight measurements recorded on the DATE instrumentation and the Development Flight Instrumentation (DFI) system installed by Johnson Space Center (JSC). Marshall Space Flight Center (MSFC) installed transducers in Spacelab. DATE has disseminated its environmental data to the payload community through the DATE reports (References 1 through 5). However, to be of benefit to shuttle users for the development of payload loads and dynamic environment design and test criteria, engineering interpretation must be applied to the data. This report is intended to provide guidance to the payload community in developing vibration, acoustic and loads criteria for payloads.

DATE microphones, low frequency accelerometers, and high frequency accelerometers were present on flights 2 through 5. DFI microphones and low frequency accelerometers were present for all 5 flights. All DATE dynamic flight data were obtained on small pallet payloads. Microphones and high frequency accelerometers on STS-9 were provided by MSFC and were on a large payload.

2.0 OVERVIEW OF RESULTS

2.1 Vibration and Acoustics

The shuttle payload bay acoustic and vibration environments are summarized herein for pallet and small payloads based on the first 5 shuttle flights and for a large payload (Spacelab) on STS-9. Acoustic data are treated in a statistical manner, where appropriate, while vibration data has been enveloped. Vibroacoustic environments are generally below those predicted prior to the first STS flight. There are, however, exceptions to this, namely the longeron vibration, localized acoustic discrete tones near the pressure equalization vents (Reference 6), and localized acoustic levels around a large payload (Reference 12). Vibration requirements for the orbiter longeron have been increased. Uncertainties in the acoustic and vibration environments have also been quantified for the first five flights. These uncertainties include data acquisition and reduction errors, spatial bias errors, flight to flight variation and spatial deviation from the mean.

There is good agreement among NASA centers and industry in defining small payload acoustic environments. However, it is generally agreed by the DATE Working Group members that there are still significant deficiencies in the STS payload data base. In particular, the influence of large payloads, the acoustic environment near the payload bay doors, the acoustic discrete tones and the effects of the mechanically transmitted random vibration have not been well defined. A better statistical base for defining uncertainties in the environment is desired. The effect of future changes such as uprated engines, launches from the Western Test Range and shuttle configuration changes are unknown without more data. Additional flight dynamic data will allow a reduction of the uncertainty factors used in defining the vibroacoustic environments. This will eliminate overly conservative test levels, and reduce test failures, schedule slips and cost impacts.

The most severe vibroacoustic environments occurred during liftoff but some frequencies were dominated by acoustic discrete tones during transonic flight. The acoustic environment in the bay was uniform except for the areas near the bay perimeter. Higher levels were also measured near the payload bay doors and on the large Spacelab module.

The average payload bay acoustic level at liftoff of the first 5 flights was 132.9 dB overall (OA). When the microphones mounted on payloads are considered by themselves, the level is 131.8 dB and there is less scatter in the data. Acoustic levels were highest and had greater scatter at the bay perimeter. Average perimeter levels for the 5 flights was 135.3 dB. Discrete acoustic tones from the pressure equalization vents were significant in localized areas of the payload bay. Multiple discrete tones from the pressure equalization vents were present at frequencies from 280 Hz to 340 Hz. The one-third octave band level of the discrete tones was as high as 134 dB at the bay sidewall on STS-2. More generally, the level was 128-130 dB at the bay perimeter and was much less intense at the pallet payloads.

Some flight data indicates there are higher localized acoustic levels around large payloads. The only pallet data on the first five flights which demonstrated a definite payload effect was measured between the payload bay wall and the orbiter bridge fitting. This was further substantiated on STS-9.

Acoustic data on Space Lab shows a definite increase in acoustic levels for a large diameter payload.

Vibration environments on the pallet at its attach points were well below those at the orbiter payload support structure. Vibration on the pallet sill trunnions was as high as $0.02 \text{ G}^2/\text{Hz}$ for the first 5 flights, while levels on the orbiter sill longeron were $0.1 \text{ G}^2/\text{Hz}$. Measured keel orbiter fitting vibration was as high as $0.02 \text{ G}^2/\text{Hz}$. The highest levels were seen on pallet experiment shelves. Levels there were as high as $0.2 \text{ G}^2/\text{Hz}$ at 320 Hz.

Small payload acoustic predictions agree well (within ± 2 dB) among the contributing organizations. Various payload acoustic environment prediction methods used by each contributing NASA and industrial facility and opinions on how to predict large payload environments differ widely. Some centers do not account for large payload influences. However, among centers that do account for large payload effects in the local acoustic environment, predictions generally agree well. Most methods for predicting acoustic environments involve averaging of all or a specific portion of the microphone data. Probability levels and flight to flight variability are typically added to the mean levels. Another method is to envelope all the data in the payload bay. PACES (Payload Acoustic Environment for Shuttle), a computer code, is also available for predicting large payload effects.

2.2 Low Frequency Vibration

The loads or low frequency vibration environment is, in general, dependent on the dynamic characteristics of the coupled payload/launch vehicle system and the frequency content of the external forcing functions. The objectives of flight response measurements in the low frequency or loads regime differ from the objectives of the vibroacoustic regime. The former aims to define instrumentation for the verification of methodology, while the latter aims to define the flight environment statistically.

In light of these objectives, the low frequency (0-50 Hz) response data is examined in two areas. First, the degree of repeatability or flight-to-flight variation of the responses are studied. For nearly identical systems, such as STS-2 through STS-5, repeatability is an indication of the variations in the forcing functions. Such data are valuable in establishing realistic forcing functions for future missions. Next, the flight responses are compared to analytical predictions, specifically upper bound and nominal design cases from preflight analyses as well as analytical predictions from post-flight reconstruction analyses. The accuracy and adequacy of the existing flight data are discussed and recommendations for future acquisitions are made.

Low frequency response measurements made on STS-1 through STS-5 varied in number from 9 on STS-1 to a total of 33 on STS-3. These data were mainly utilized to assess the adequacy of the load prediction process in only the overall sense. Few, if any, detailed analyses were performed for such an evaluation. In making such assessments it is important to examine the accuracy and adequacy of the flight data. For the purpose of evaluating the loads methodology, the existing data had limitation in frequency response.

Furthermore, some of the payload mathematical models did not have the fidelity desired for such an evaluation. It should also be noted that flights STS-2 through STS-5 carried relatively light payloads; thus the data obtained from these flights are not necessarily representative of future payloads which will be heavier.

Given the above limitation, the loads data can be summarized as follows. The overall responses measured were generally within predicted levels for liftoff, landing, and the various quasi-static events. For liftoff, the Solid Rocket Booster (SRB) ignition rather than the Space Shuttle Main Engine (SSME) ignition produced the peak accelerations. Most landings were relatively benign due to low sink rates. STS-3 was an exception and resulted in some predictions being exceeded. Significant repeatability was observed in the low frequency responses at liftoff up to about 10 Hz. An apparent lack of correlation between flight and analysis was observed at frequencies between 10-50 Hz. Responses at 3 Hz were apparently underpredicted.

The above observations are deliberately stated as apparent since there are limitations in the frequency response of the flight data.

In general, improved correlations between analytical predictions and flight data are needed to achieve the desired confidence in the ability to predict the flight loads. It should also be noted that this problem has been recognized by the launch vehicle community and that efforts to correct this are under way.

3.0 FLIGHT DATA SYSTEMS

The STS vehicle and dynamic instrumentation configuration, instrumentation locations and dynamic data system errors for the data in this report are discussed in the following subsections.

3.1 Launch Vehicle Configuration

The STS configuration for the data taken during the first 5 flights and flight 9 is summarized in the Table 3-1 below (Reference 7). All payload pallets on these flights were of the type developed by the European Space Agency (ESA), except for the Development Flight Instrumentation (DFI) pallet.

Table 3-1. Launch Vehicle Configuration

| | STS 1 | STS 2-4 | STS 5 | STS 9 |
|--|----------|------------|----------|----------|
| a. OV-102 vehicle | X | X | X | X |
| b. Launch from Kennedy Space Center (KSC) | X | X | X | X |
| c. No thrust augmentation | X | X | X | X |
| d. Full thermal radiator panels | X | X | X | X |
| e. Payload bay vents open at all times | X | X | X | X |
| f. Payload bay with ESA pallet payloads | | X | X | X |
| g. Payload bay with DFI pallet payload | X | X | X | |
| h. Payload bay with DFI pallet and TELESAT payloads | | | X | |
| i. Large diameter payload | | | | X |

3.2 Flight Data System

Shuttle dynamic instrumentation for STS-1 through 5 and 9 consisted of microphones, low frequency accelerometers and high frequency accelerometers. The number and location of STS microphones and accelerometers were unique for each shuttle flight. These transducers were part of three separate data recording systems: the Development Flight Instrumentation (DFI), the Dynamic, Acoustic and Thermal Environment (DATE) instrumentation and instrumentation installed by MSFC. The DFI system was used on each of the first five flights of the shuttle. DATE measurements were taken on flights 1 through 5 and MSFC measurements were taken on STS-9.

Payload bay microphone locations for the first 5 flights are illustrated in Figures A-1 through A-4 in the appendix. Appendix Figure A-5 shows the STS-9 microphone locations. High frequency accelerometer locations on payloads and

in the payload bay are shown in the appropriate vibration data plots. DFI low frequency accelerometers are shown in Figure A-6. The numbers of DATE, DFI and MSFC accelerometers and microphones on each flight are summarized in Table 3-2 below. A further breakdown of the low frequency accelerometers is given by flight in Table 3-3. A listing of the transducers on each flight may be found in Tables A-1 through A-8, in the Appendix (References 1 through 5). No acoustic data has been taken in the forward one-third of the payload bay except for the forward bulkhead microphone.

Table 3-2. STS Instrumentation Summary

| Flight | DFI Low Frequency Accelerometers | DATE Low Frequency Accelerometers | DATE Mid Frequency Accelerometers | DFI Microphones | DATE Microphones |
|--------|----------------------------------|-----------------------------------|-----------------------------------|-----------------|------------------|
| 1 | 9 | 0 | 0 | 4 | 0 |
| 2 | 9 | 10 | 8 | 4 | 14 |
| 3 | 9 | 16 | 14 | 4 | 8 |
| 4 | 9 | 16 | 14 | 4 | 8 |
| 5 | 9 | 16 | 0 | 4 | 7 |

| Spacelab | Low Frequency Accelerometers | Mid Frequency Accelerometers | Microphones |
|----------|------------------------------|------------------------------|-------------|
| 9 | 29 | 31 | 3 |

DFI Instrumentation

Installation and calibration of the DFI transducers was the responsibility of JSC. DFI channels were recorded on the Ascent Recorder and the Mission Recorder. Most of the DFI data channels were allocated to monitoring the orbiter structure and subsystems. There were only 4 microphones internal to the bay and 9 low frequency accelerometers at the aft bulkhead, sill and keel longerons. The DFI accelerometers and microphones for all five flights were mounted at identical locations within the payload bay. The DFI microphones were of the piezoelectric vibration compensated type and were installed at the orbiter bay fore and aft bulkheads, the bay side wall and on the DFI pallet itself. Internal DFI microphones were manufactured by Gulton Industries, model number MC449-091-003. External microphones were model number MC449-0191-002. DFI microphone locations are given in Table A-3.

DFI low frequency accelerometer transducers were manufactured by Sunstrand, Q-Flex Model No. ME-449-0208. The sampling rate for these accelerometers was

100 samples/second. The response was flat to within $\pm 2\%$ from 0 to 14 Hz, down 29% (3dB) at 20 Hz, and rolled off at 18 dB/octave above that. Two of these transducers were located in the crew cabin approximately on the vehicle centerline measuring Y and Z accelerations. Three transducers were mounted on the sill longeron, two on the port or left-hand side and one on the starboard or right-hand side, all measuring Z direction acceleration. One accelerometer was mounted to measure keel longeron Y direction response. The remaining three measurements were made on the aft fuselage bulkhead recording the X, Y, and Z acceleration responses. A detailed definition of the locations of these transducers is contained in Table A-2 and Figure A-6, and also in References 1 through 5.

Table 3-3. Summary of Low Frequency Acceleration Measurements for Orbiter Vehicle No. 102, STS-1 Through STS-5

| STS NO. | PAYLOAD (P/L) | DFI INSTRUMENTATION 0-15 Hz | DATE EXPERIMENT INSTRUMENTATION | | | | | | OTHER |
|---------|---------------|-----------------------------|---------------------------------|-----|----------------------------|-----|-------------|-----|-------|
| | | | 0-50 Hz ORBITER INPUT TO | | 1.5-50 Hz ORBITER INPUT TO | | RESPONSE OF | | |
| | | | DFI | P/L | DFI | P/L | DFI | P/L | |
| 1 | - | 9 | - | - | - | - | - | - | - |
| 2 | OSTA | 9 | 5 | - | 1 | 3 | 3 | 3 | - |
| 3 | OSS-1 | 9 | 6 | - | - | - | - | 10 | 8 |
| 4 | DOD | 9 | - | 6 | 6 | - | 3 | 1 | - |
| 5 | TELESAT | 9 | - | 6 | 6 | - | 3 | 1 | 3 |

DATE Instrumentation

DATE instrumentation installation and calibration was the responsibility of Goddard Space Flight Center (GSFC). Both low and high frequency accelerometers were used in the DATE instrumentation package. DATE microphones were Endevco model number 2510 and were vibration isolated. High frequency accelerometers were also manufactured by Endevco, model numbers 2271A and 2271AM. The low frequency instrumentation flown as part of the DATE experiment on STS-2 through STS-5 consisted of six (6) zero frequency (0-50 Hz) servo-accelerometers, modified Sunstrand Model 303B, and ten (10) crystal vibration accelerometers (1.5-50 Hz) Endevco Models 2271A and 2271AM. DATE Instrumentation locations are given in Tables A-4 through A-8.

Signals from the DATE transducers were recorded on the Orbiter Experiments (OEX) wide band FM recorder. The frequency response curve of the zero frequency transducers was flat to within $\pm 2\%$ to 18 Hz, down 21% (2 dB) at 50 Hz, and 29% (3 dB) at 60 Hz. The characteristics of the crystal vibration accelerometers were down 21% (2 dB) at 1 Hz, flat from 1.5 to 40 Hz, and down 29% at 50 Hz. Post-flight data processing consisted of low pass filtering, either digital or analogue, and digitizing at 512 samples/second. The filter had a cutoff frequency, the 29% (3 dB) down point, of 63 Hz. Table A-1 and Figure A-7 show the DATE accelerometers at the DFI pallet that were in identical locations for multiple flights.

Two of the flights, STS-3 and STS-5, carried payload-peculiar accelerometers, (Table 3-3). The data obtained from this instrumentation has been included in the DATE reports for the respective flight (References 3 and 5). GSFC had responsibility for eight DC accelerometers mounted on the OSS-1 pallet on STS-3. These accelerometers were Sunstrand Data Control Model No. 979-0138-001 rated at 0-50 Hz. The data was sampled at 200 samples/second and recorded onboard in Pulse Code Modulation (PCM) format using a low pass filter, down 29% (3 dB) at 50 Hz. Prior to on-the-ground data reduction, the data was again filtered using a low pass filter, down 3 dB at 100 Hz. A detailed description of these data is contained in Reference 8. On STS-5, three DC accelerometers were mounted on the Satellite Business Systems Corporation (SBS) payload near the base at the PAM-D interface. These accelerometers were Systron Donner, Model 4311A with a flat frequency response from 0 to 50 Hz. A more detailed description of these data is contained in Reference 5.

Spacelab Instrumentation

Spacelab instrumentation and calibration was the responsibility of Marshall Space Flight Center. Both low and high frequency accelerometers were used on Spacelab but only the high frequency data will be discussed in this report. High frequency accelerometers and microphones were sensitive from 20 to 2,000 Hz. A more detailed discussion of the MSFC-installed instrumentation is beyond the scope of this report.

3.3 Data System Errors

Errors generally associated with dynamic transducers include errors in frequency response, sensitivity, distortion and calibration. The overall data system and reduction error is estimated to be ± 1 dB for both accelerometers and microphones. There are other sources of error that are peculiar to the shuttle instrumentation. Some error in the DATE microphone data may result from the interaction of the microphones and their isolation system. DFI microphones at the fore and aft bay bulkheads are housed in partial enclosures. These may interfere with the pressure field near the microphone. In addition, several of the microphones are in close proximity to orbiter surfaces and may give rise to pressure doubling type effects at the microphone. If only payload microphones are considered, these surface effects are minimized. These errors, detailed in Table 3-4, are more fully explained in Reference 9. These errors do not necessarily apply to Spacelab data systems but probably represent a close estimate of the errors for that data as well. Low frequency accelerometers which do not measure the DC component indicate an erroneous response at the initiation of a transient event such as liftoff and landing.

In addition, none of the acoustic data above 1000 Hz is considered valid. Some time histories in the DATE reports show the level above 800 Hz increases with increasing frequency. In fact, the data in most all cases are within 3 dB or less of the data acquisition noise floor. The rise in the noise floor with frequency exactly matches that seen in the data.

Table 3-4. STS Dynamic Data System Errors

Transducer, Signal Conditioner and Filter Clipper Bias Box

| Error Sources | Piezo-Electric Accelerometers | Piezo-Electric Microphones | Servo Accelerometers |
|--|----------------------------------|-------------------------------|-------------------------|
| Frequency Response* | ±5% | ±5% | ±5% |
| Sensitivity | ±2% | ±2% | ±1.3% |
| Distortion and Non-Linearity | ±2.25% | ±2.25% | ±0.05% |
| Gain Instability | ±3% | ±3% | ±0.75% |
| Calibration | ±6% | ±6% | -- |
| FM Multiplexer and Tape Recorder System | ±1.9% | ±1.9% | ±1.9% |
| Subtotal Estimated Root Sum Square Errors | ±9.1% | ±9.1% | ±5.6% |
| Estimated Data Reduction Errors not included in sub total | ±12% | ±12% | ±12% |
| Total Estimated Root Sum Square Errors | ±15.1% = 1 dB | ±15.1% = 1 dB | ±13.2% = 1 dB |

*Maximum frequency response error is observed at the high frequency end of the spectrum for all systems and at the low frequency end of the spectrum for piezo-electric transducers. Frequency response errors can increase if the data is used to the -3 dB frequencies on the response curve. The response error at the flat portion of the frequency response curve is probably on the order of ±1%. The transducer, a signal conditioner, and filter clipper bias box errors were measured as a system.

4.0 DATA REDUCTION

Data from STS-1 through STS-5 used in this study are taken from GSFC DATE reports 002 through 006 (References 1 through 5), and STS-9 data was taken from Reference 17. The DATE data reduction task was performed at two NASA Centers. The low frequency vibration DATE data was reduced at the Jet Propulsion Laboratory (JPL) while the high frequency vibration and acoustic DATE data were reduced at GSFC. Spacelab (STS-9) data was reduced by MSFC, but it was not DATE data. Acoustic data was reduced in the form of 1/3 octave band time histories. Both low and high frequency random vibration DATE data was reduced in the form of acceleration spectral density (ASD) plots, shock response spectrums and ASD time variant plots. These "water fall plots present the general character of the data in an intuitively meaningful visual image" (Reference 6). Averaging times (1 second) are probably too long to obtain useful spectral density values. Low frequency Spacelab vibration data is not included in this report.

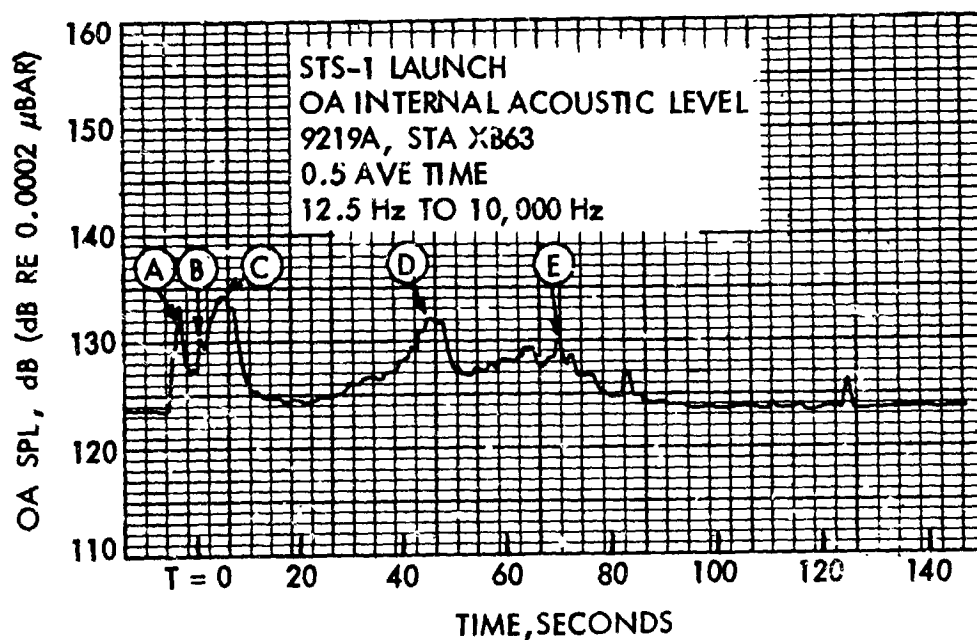
4.1 Acoustic Data Reduction

Acoustic data from the DATE reports were reduced in the form of 1/3 octave band time histories by using an analog RMS meter with band pass filters. A sample acoustic time history is seen in Figure 4-1. This time history presentation was chosen over typical spectral analysis because of the transient nature of the data. An averaging time of 0.5 seconds was used for most of the time history data. Transient acoustic time history data has its limitations and requires a systematic approach to develop acoustic environments. A conservative but widely accepted approach is to envelope the levels at each data channel with respect to time. All microphone acoustic data was tabulated for each of four significant flight events: Main Engines (at 20% thrust), liftoff, Transonic, and Supersonic. As an illustration, Figure 4-2 compares the levels on STS-2 for each of these flight events. The data for these events was enveloped to obtain a "time envelope" for each data channel. Therefore, maximum acoustic levels in each one-third octave band do not necessarily occur at the same time. DATE acoustic data above 800 Hz is considered "suspect" because of the high noise floor in the data acquisition system. STS-9 Spacelab data was also reduced by MSFC in the form of 1/3 octave band spectral plots by Fourier analysis of the time increment of the maximum overall level of the liftoff event.

4.2 Vibration Data Reduction

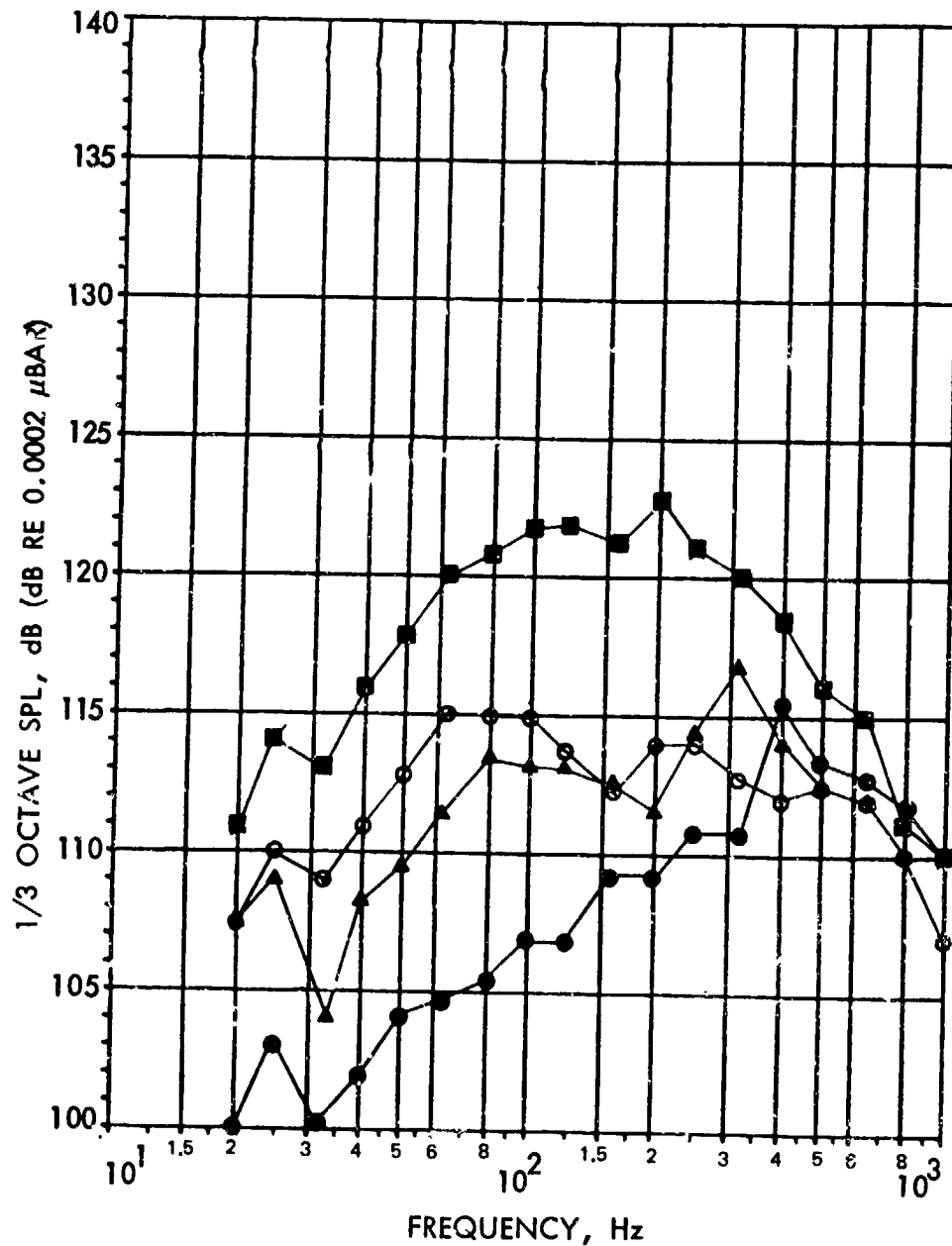
Both low and high frequency random vibration data were reduced in the form of acceleration spectral density (ASD) plots, shock response spectrums and ASD time variant plots. Averaging time of the "water fall" plots is probably too long to obtain useful spectral density values. Typical acceleration spectral density data were analyzed over short time slices for times throughout the shuttle launch event. These ASD plots were enveloped with respect to time with the same technique as was used on the acoustic data to obtain maximum vibration environments. Shock response plots were analyzed for the major transient events with dynamic amplifications of 10, 20 and 50. The low frequency vibration plots range from 0 Hz to 100 Hz but the value of the data is limited. DATE data frequency response was flat only to 50 Hz. Above this it rolled off at 18 dB per octave. The DFI low frequency accelerometer

at 18 dB/octave above that. All low frequency FM data was put through a low-pass Butterworth filter. The cutoff frequency of the filter was 63 Hz (see References 1 through 5). No Spacelab low frequency data is included in this report. High frequency Spacelab vibration was reduced in the form of ASD plots by MSFC similar to the method used in their acoustic data reduction.



- A SHUTTLE MAIN ENGINE
- B SRB IGNITION
- C MAXIMUM LIFT-OFF REFLECTION
- D TRANSONIC
- E SUPERSONIC, MAXIMUM Q

Figure 4-1. Typical Time History for Microphone 9219, Overall Flight STS-1



- = MAIN ENGINE START 125.5 dB OA
- = LIFTOFF 132.1 dB OA
- ▲ = TRANSONIC 124.6 dB OA
- = SUPERSONIC 123.3 dB OA

Figure 4-2. Summary of Payload Mean Acoustic Levels for Significant Flight Conditions

5.0 FLIGHT DATA EVALUATION

In general, the vibration and acoustic environments at liftoff (T = +3 seconds) were the most severe launch environments. Other launch events with significant higher frequency dynamic environments were "main engines at 20% rough burn", "transonic" and "supersonic". During transonic and supersonic flight, localized discrete tones from the bay pressure equalization vents appeared in the acoustic environment in the 315 Hz 1/3 octave band. Higher acoustic noise was measured around the perimeter of the Spacelab module indicating that large payloads do cause localized acoustic noise increases.

Flight data evaluation in the loads or low frequency regime (0-50 Hz) is aimed at the verification of loads prediction methods. By necessity, these load prediction methods must account for flight-to-flight variations in level and frequency content. In practice, these variations are accounted for by a series of forcing functions. A measure of flight-to-flight variations of the dynamic response data enables the analyst to assess how representative and ultimately how conservative these forcing functions are.

Of the Orbiter events analyzed, only those which produce substantial dynamic loading on the primary structure, namely ascent and landing, are assessed in the loads evaluation. Data for the other events, such as transonic, maximum dynamic pressure, SRB burnout, SRB separation, main engine cut-off, External Tank (ET) separation, main gear roll transient, and rollout were generally found to be more benign and are not included in this assessment. A complete set of these data is contained in References 1 through 5. These references contain time histories, response shock spectra, and power spectral densities. For purposes of establishing flight-to-flight variations, only the response shock spectra, using a gain of $Q = 20$, will be examined. Data from STS-1 is not included since it is deemed not representative of future flights. These data are contained in Reference 27.

5.1 Acoustic Data Summary

The mean, maximum and 97% probability levels of all the acoustic data taken in the payload bay for STS-1 through STS-5 are given in Figure 5-1. The bay mean level for the first five flights was 132.9 dB overall. DATE acoustic data above 1000 Hz is not considered good data because of the high noise floor in the data acquisition system above 800 Hz. Any acoustic data plotted above 1000 Hz was extrapolated linearly from the rest of the spectrum.

Probability levels for the data were obtained by adding the mean level to the standard deviation times an appropriate factor. For example, 2 sigma added to the mean represents the .97 probability level for a data set with Gaussian distribution. For small data sets or ones which may not be exactly Gaussian in nature, it is appropriate to say the probability level was approximately .97 for the mean plus 2 sigma value. A confidence interval describes the probability that the .97 probability level actually lies within a prescribed "tolerance band" about the .97 probability. However, estimation of confidence intervals requires large amounts of data and could not be estimated from the STS data set.

Figures 5-2 and 5-3 compare the means and the maximum levels for the perimeter microphones and those on pallet payloads for STS-1 through STS-5. The perimeter microphones are those mounted on or adjacent to the orbiter payload

bay sidewalls or bulkheads. The perimeter mean level, 135.3 dB overall (OA), was 6-8 dB higher than the payload mean levels, 131.8 dB OA, throughout much of the frequency range. The perimeter maximum levels were 10 dB or more higher than payload maximum levels throughout the frequency spectrum, except between 100 and 200 Hz (Figure 5-3). Over this narrow frequency range the spectral level difference was only 4 dB. Figure 5-4 indicates that the standard deviation () at the bay perimeter was also greater in general than for pallet payloads, particularly at lower frequencies. The small variance of the payload acoustic data indicates the acoustic environment in the bay was diffuse except for the perimeter of the bay. The standard deviation at the perimeter is biased, by an unknown amount, to the 4 locations that were on all 5 flights. The scatter on a given flight was also much greater in the perimeter than at the payloads and it closely followed the standard deviation curves of Figure 5-4.

On this basis the payload bay may be divided into distinct pallet or small payload and perimeter regions. The payload bay microphones for STS-1 through STS-5 are categorized in Table 5-1 below by region and flight. The contour plots of Figure 5-5 illustrate the size and shape of the acoustic zones with small payloads or an empty bay. The contour delineates the region of the diffuse acoustic field and the bay perimeter for small payloads only. The contours on the right were typical for all flight conditions and frequencies except during lift off between 50 to 400 Hz. In this frequency range there was also a higher intensity noise field below the payload bay doors as seen in the left contour plot (Figure 5-5)

Table 5-1 Microphone Region Category

| Perimeter Microphones | | Pallet Payload Microphones | | | | |
|-----------------------|-------|----------------------------|---------|---------|---------|---------|
| STS 1,3-5 | STS-2 | STS-1 | STS-2 | STS-3 | STS-4 | STS-5 |
| 9219 | 9256 | 9220 | 9220 | 9220 | 9220 | 9220 |
| 9403 | 9255 | | 9252-54 | 9231-34 | | 9275-81 |
| 9405 | 9219 | | 9257,58 | 9275 | 9275-79 | |
| | 9403 | | 9275-81 | 9281 | 9281 | |
| | 9405 | | | | | |

5.1.1 Perimeter Acoustic Data

The mean and maximum perimeter levels for Flights 1 through 5 are shown in Figures 5-6 and 5-7, respectively. The mean, 97% probability and maximum levels for all perimeter flight data for all 5 flights combined are shown in Figure 5-8.

Flight to flight variation is best indicated by the scatter in the perimeter mean levels (Figure 5-7), because these microphones were present on all the first 5 flights. The ensemble of the perimeter flight mean levels in Figure 5-9 had a general scatter of ± 1.5 dB throughout the spectrum. The scatter of maximum levels is ± 2 dB below 150 Hz (Figure 5-7). Above 150 Hz the scatter of the maximum was ± 2.5 dB. This is because flight 2 had unusually high levels above 150 Hz at the bay perimeter (Figure 5-7). The standard deviation, however, was smaller above 150 Hz as seen by comparing the maximum and the 97% curves of Figure 5-8.

Higher acoustic levels near the bay doors were measured at liftoff on STS-3 (Figure 5-10). These door levels were 2.4σ (99% probability level) above the small payload mean. Although the data is from one microphone on the OSS-1 pallet, it appears that the environment near the doors is characteristically higher than the general payload level. Higher levels near the payload bay doors were predicted prior to the first STS flight (References 10, 11 and 12).

The noise level between the OAST-1 (STS-2) pallet outer surface and the STS bay bridge fitting plate was much higher than the payload mean level (Figure 5-11). There is approximately 38.1 centimeters (15 inches) of space between the pallet outer surface and the bay side wall. A payload of a 4.27 meter (14 foot) diameter would have the same amount of space between itself and the bay side wall. The data between the pallet and sidewall may give an indication of what localized acoustic levels can be expected for large diameter payloads.

Spacelab module acoustic data (STS-9, Reference 17) also shows levels well above those measured on pallet payloads (Figure 5-12). In fact, Spacelab module levels exceed pallet sidewall levels between 60-300 Hz even though the Spacelab module diameter is only 4.05 meters (13.3 feet). The acoustic levels at the Spacelab tunnel (Figure 5-13) and pallet (Figure 5-14) were comparable to pallet levels measured on Flights 1 through 5. Therefore, Spacelab data also indicates higher local acoustic levels for a payload in close proximity to an orbiter surface. The high acoustic environment at the Spacelab module is probably a combination of a payload effect and of higher levels near the bay doors. This payload effect was predicted prior to the first STS flight (Reference 10). It should be noted that the Spacelab ASD data was reduced by MSFC in a different way from the way the DATE acoustic data was reduced and plotted (maximum 1/3 octave band levels) in this report. The Spacelab data was reduced by Fourier analysis with 1-second time slices. This difference may result in some minor discrepancy when comparing the DATE data with the Spacelab acoustic data.

During transonic flight, a discrete tone of up to 134 dB at 315 Hz appeared in the shuttle bay acoustic environment, at microphone 9256 near a pressure equalization vent (Figure 5-15). This level was measured on STS-2 between the pallet outer wall and the orbiter sidewall near the bay perimeter, but this microphone location was not repeated on subsequent flights. For the other 4

flights the discrete tone ranged from 128 dB to 130 dB at different microphone locations. This tone is the result of cavity resonances at the bay pressure equalization vents during transonic and supersonic flight. The mean level of this discrete tone was 12 dB lower at the pallet payloads than for the perimeter (Figure 5-8). Thus the discrete tone can be treated principally as a localized effect for payloads near the pressure equalization vents.

High resolution analysis of this discrete tone revealed that there were actually multiple discrete tones in two groups in the 315 Hz 1/3 octave band. One group of discrete tones was centered at 295 Hz while a second group was at 320 Hz. Different spikes that existed at the same moment may have been produced by different pressure equalization vents. As Figures 5-16 and 5-17 show, the frequencies of the discrete tones shifted upward with time (i.e., with mach number). This behavior is characteristic of fluctuating pressure discrete tones produced by aerodynamic resonances within a cavity in an air flow. The noise intensity at each vent is, presently, unknown and will depend on the direction of air flow through it during transonic flight. Some vents ingest air, while others expel it from the bay.

A second low level discrete tone at 120 dB overall was seen in the aft bulkhead acoustic data. The discrete frequency, 630 Hz, matches the Auxiliary Power Unit (APU) pump frequency which is mounted to the aft bulkhead. No high frequency vibration data was taken at the aft bulkhead so the intensity of the vibration at 630 Hz is unknown.

5.1.2 Payload Acoustic Data

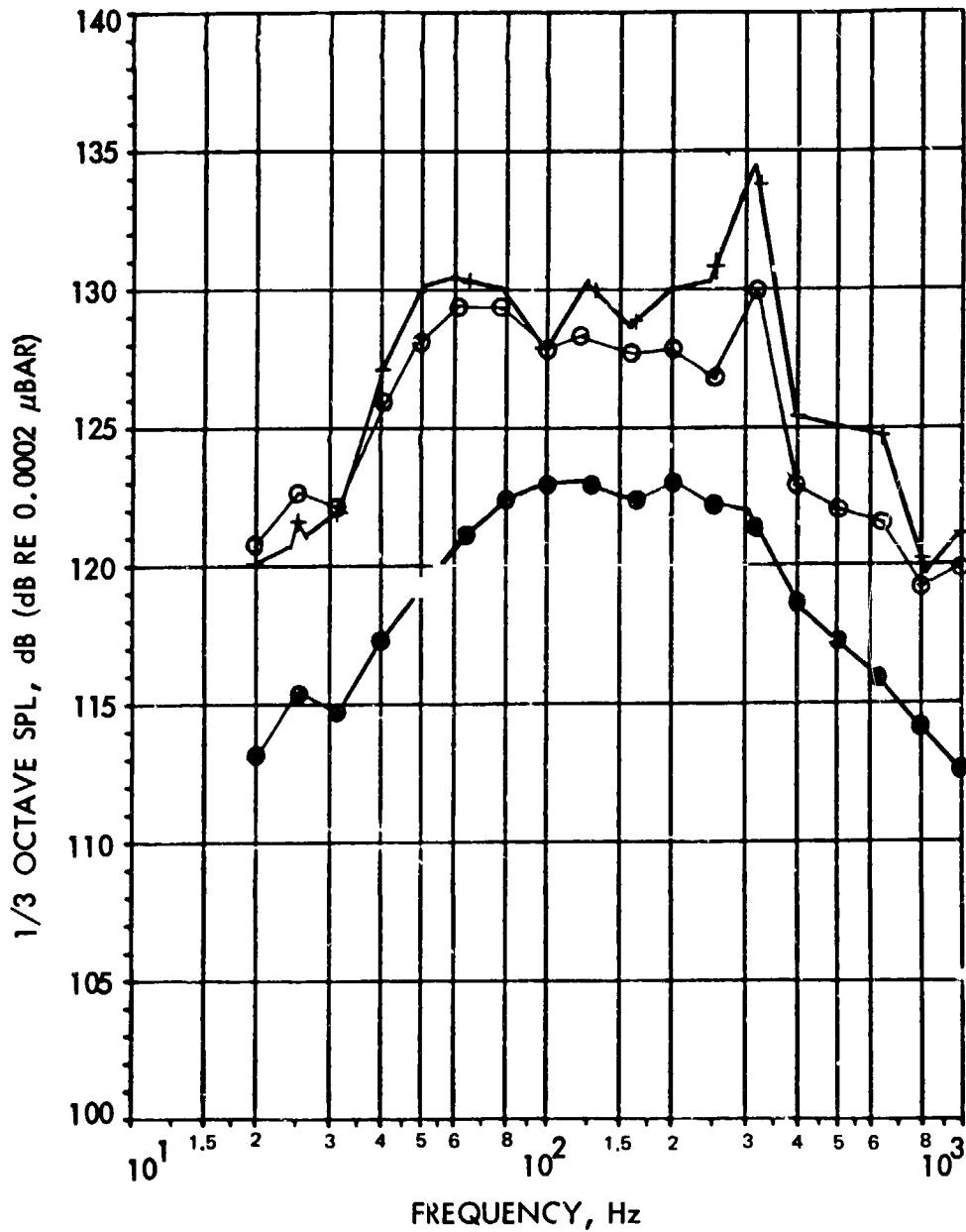
Payload mean levels for each flight are seen in Figure 5-18. Payload levels were derived using only the microphones in the payload region defined in Table 5-1. Flight to flight variation of the acoustic environment at the pallet payloads is apparent in this plot. The scatter about the flight ensemble mean level was ± 1.5 dB below 80 Hz and ± 1 dB or less above 80 Hz. Scatter in the composite maximum levels anywhere in the payload bay was ± 1.5 dB to ± 2 dB (Figure 5-19). The mean, 97% probability and maximum payload levels for all payload flight data combined are given in Figure 5-20. Mean and various probability levels (90, 95, 97.5%) of each flight are given singularly in Figures 5-21 through 5-24. Figure 5-25 shows the same probability curves for all the payload flight data.

5.1.3 Aft Flight Deck Acoustics

The measured acoustic data in the aft flight deck, the cargo area of the crew cabin, were low and were not evaluated in detail for this report. For the readers' convenience, the acoustic interface environment specified in Reference 13 for the aft flight deck is shown in Table 5-2. These specified levels envelope the measured flight data.

Table 5-2. Aft Flight Deck Acoustic Environment

| 1/3 Octave Band Center Frequency (Hz) | Sound Pressure Level (dB re $2 \times 10^{-5} \text{N/m}^2$) | |
|--|--|-------------------|
| | Lift-Off | Aeronoise |
| | 5 Seconds/Flight | 10 seconds/Flight |
| 31.5 | 107 | 99 |
| 40.0 | 108 | 100 |
| 50.0 | 109 | 100 |
| 63.0 | 109 | 100 |
| 80.0 | 108 | 100 |
| 100.0 | 107 | 100 |
| 125.0 | 106 | 100 |
| 160.0 | 105 | 99 |
| 200.0 | 104 | 99 |
| 250.0 | 103 | 99 |
| 315.0 | 102 | 98 |
| 400.0 | 101 | 98 |
| 500.0 | 100 | 97 |
| 630.0 | 99 | 97 |
| 800.0 | 98 | 96 |
| 1000.0 | 97 | 95 |
| 1250.0 | 96 | 94 |
| 1600.0 | 95 | 93 |
| 2000.0 | 94 | 92 |
| 2500.0 | 93 | 91 |
| OVERALL | 117.5 | 111 |



| | |
|--------------------|-------------|
| ● AVERAGE | 132.9 dB OA |
| + MAXIMUM | 139.0 dB OA |
| ○ 0.97 PROBABILITY | 141.0 dB OA |

Figure 5-1. Payload Bay Acoustic Level Statistics for All Bay Microphones, STS-1 Through STS-5

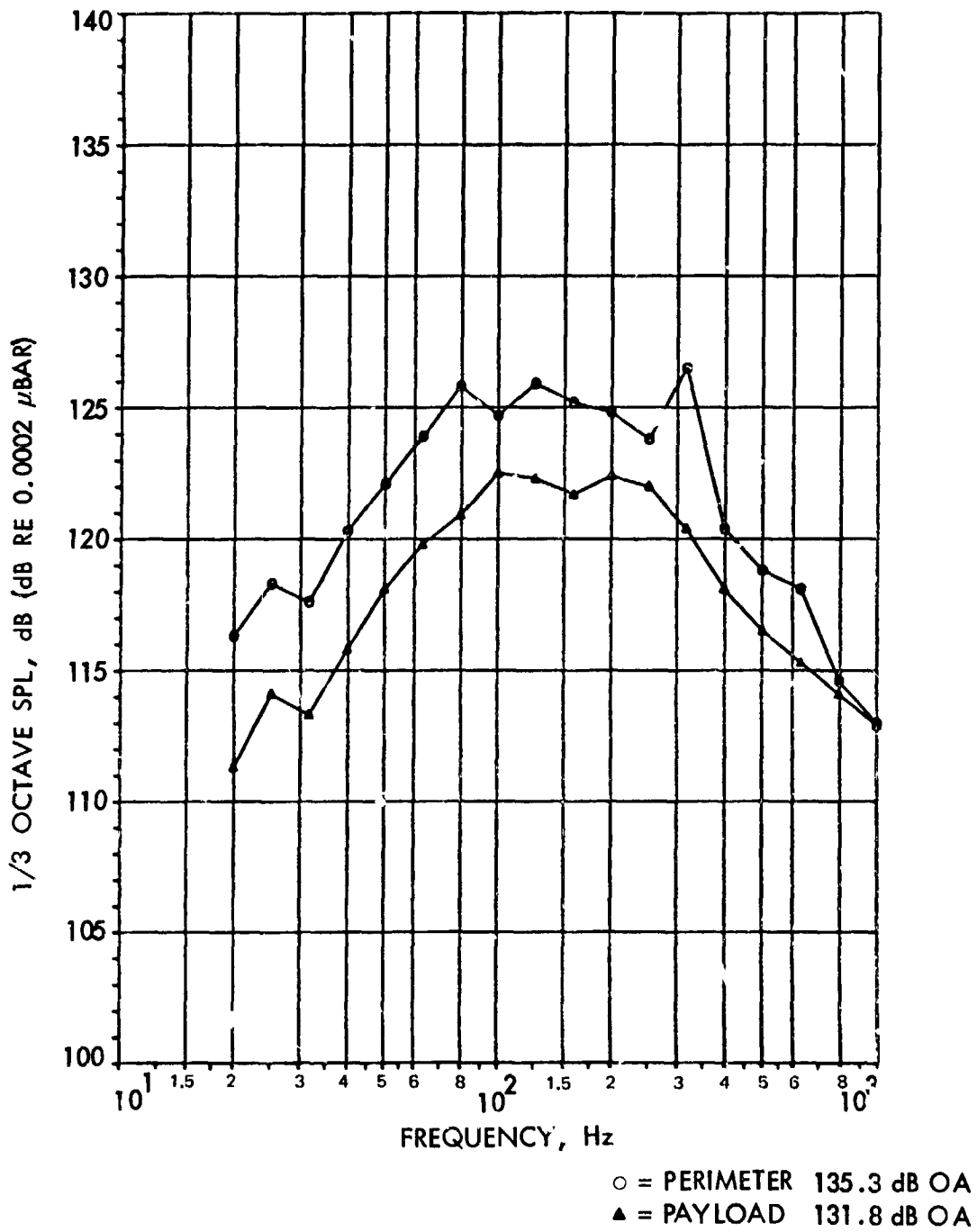


Figure 5-2. Perimeter and Payload Region Average Level Comparison Average of Maximum Time Envelope Levels for Each Microphone

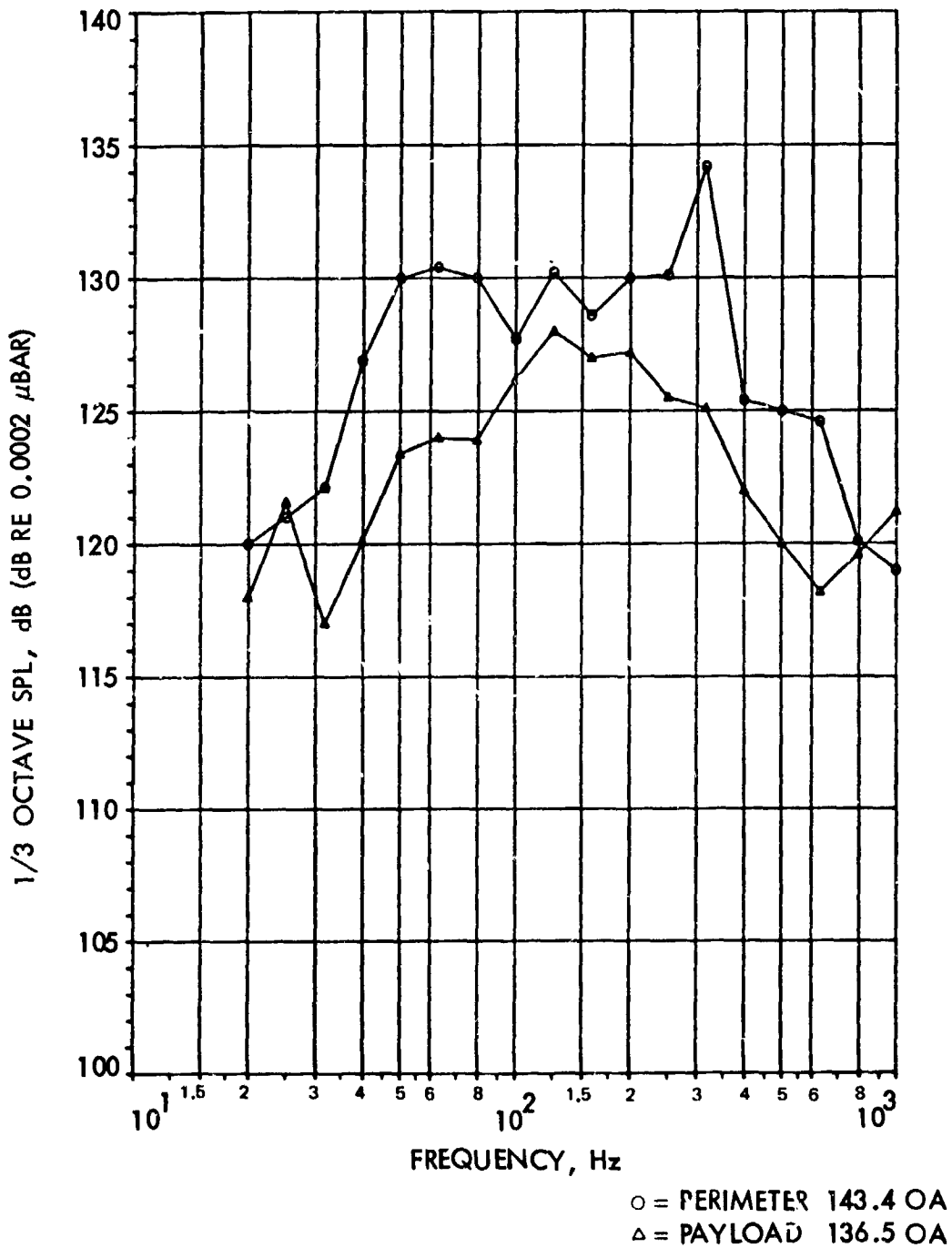


Figure 5-3. Perimeter and Payload Region Maximum Acoustic Levels

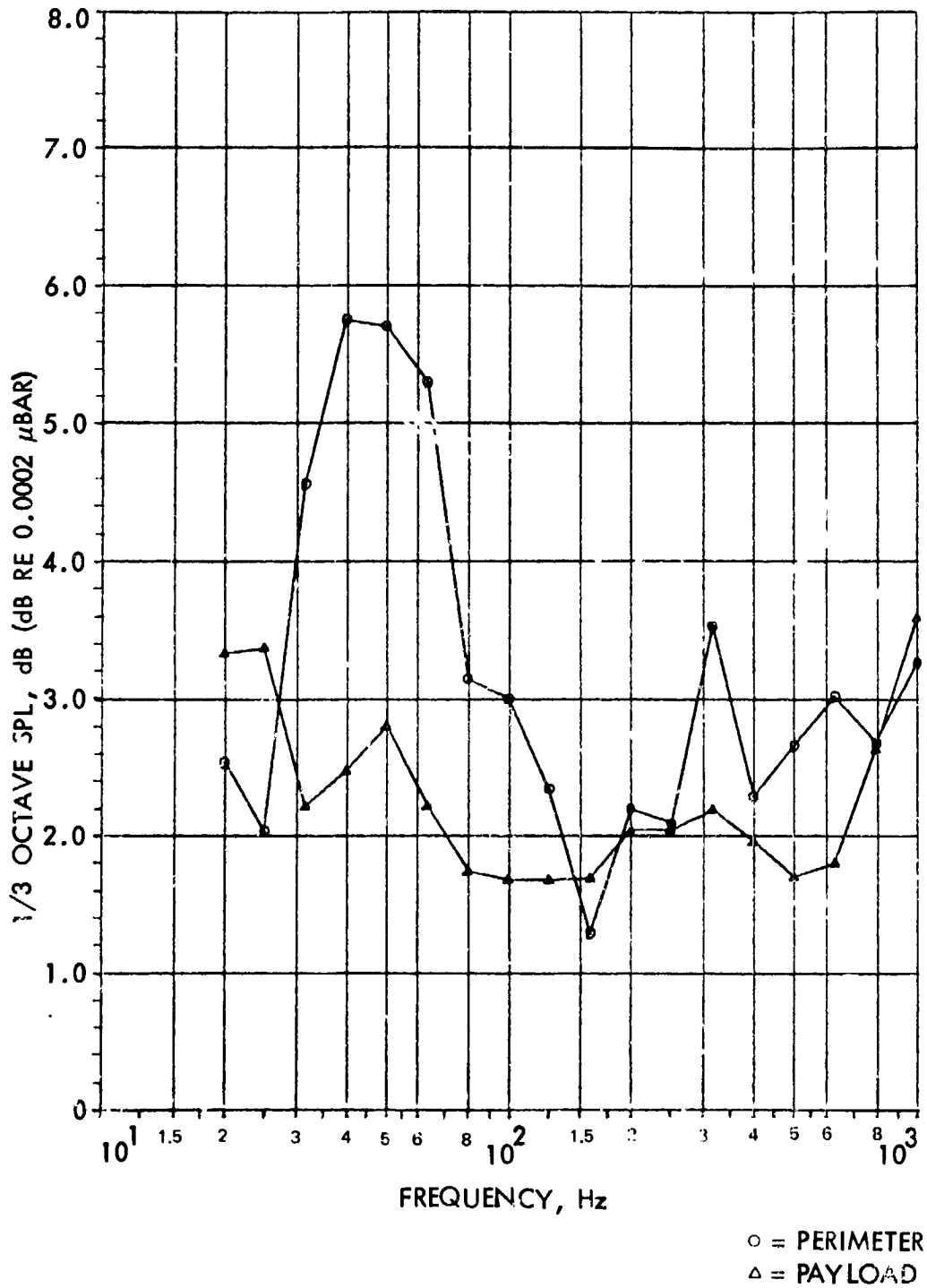
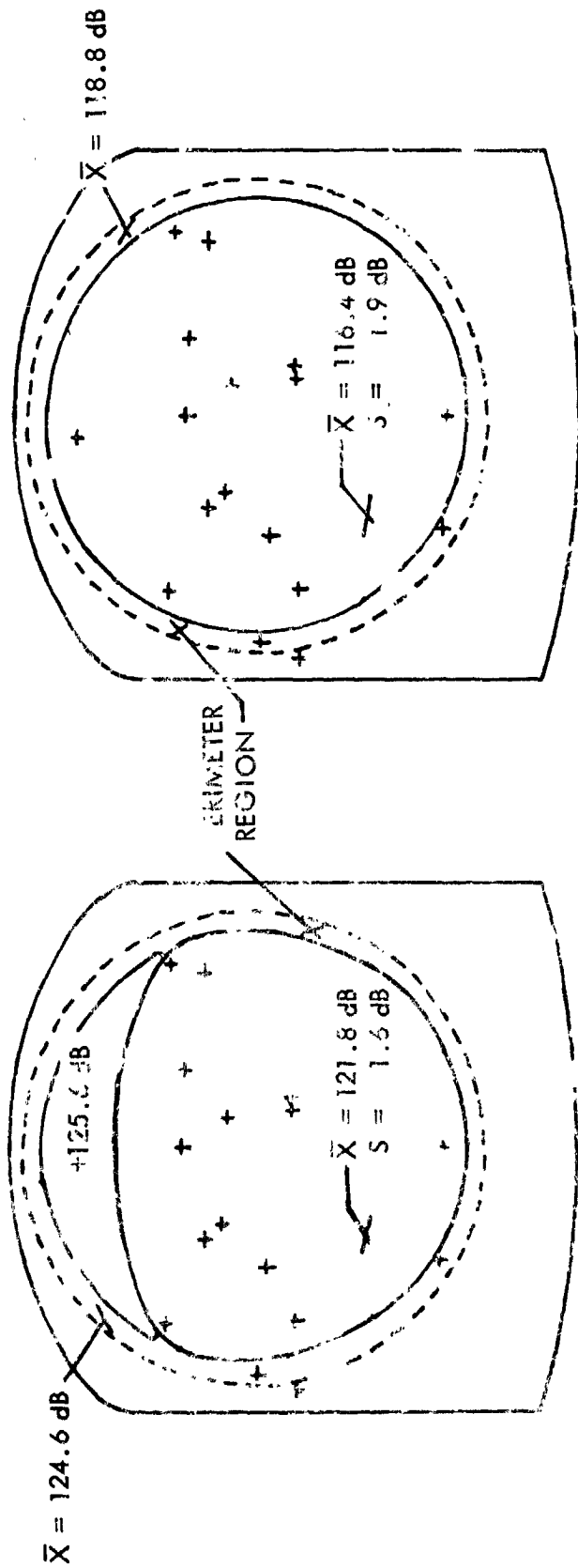


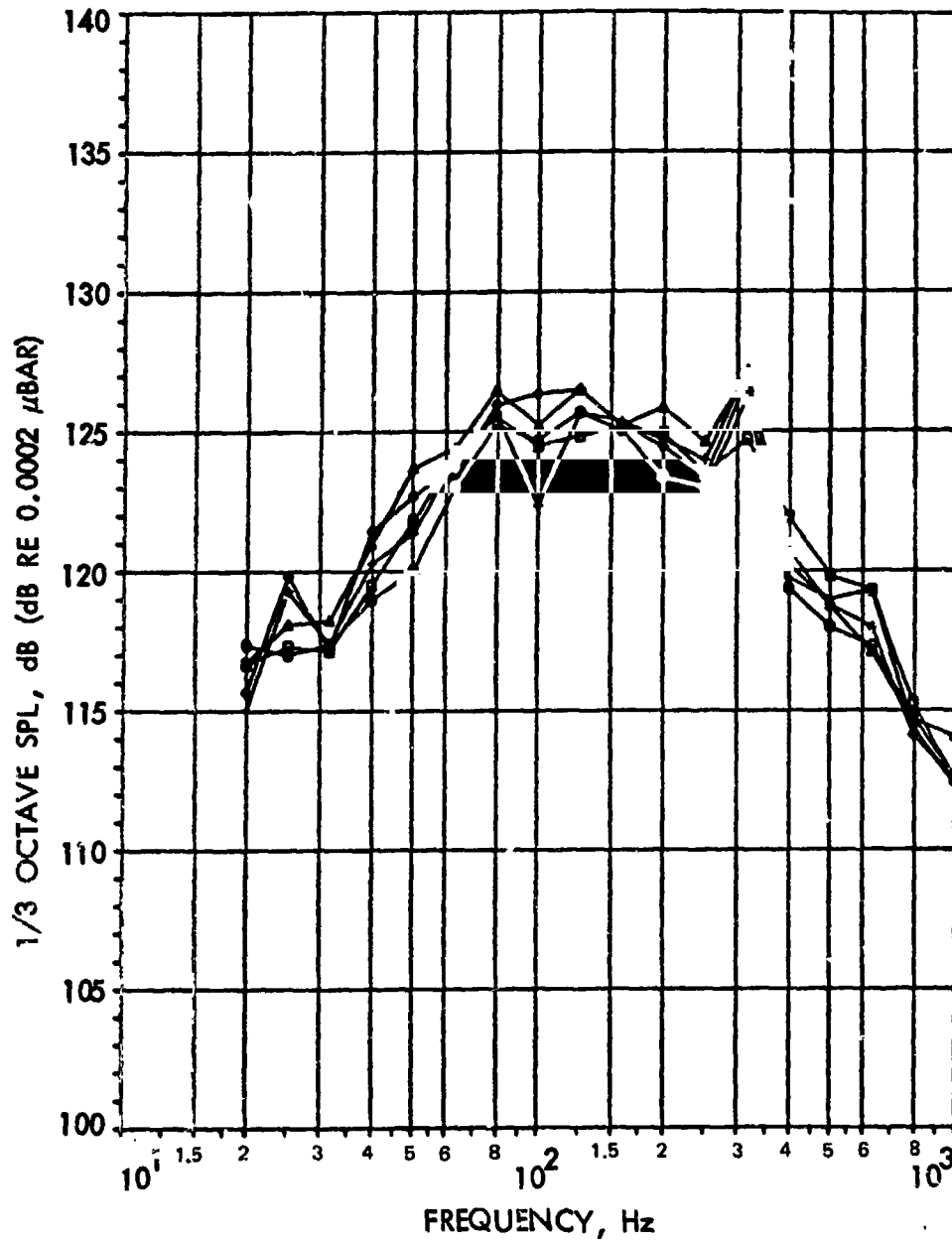
Figure 5-4. Perimeter and Payload Acoustic Level Standard Deviation



ACOUSTIC CONTOUR AT 250 Hz
 CONTOUR SHAPE TYPICAL FOR
 LIFTOFF FROM 50 Hz TO 400 Hz

ACOUSTIC CONTOUR AT 500 Hz
 TYPICAL FOR ALL FLIGHT CONDITIONS
 EXCEPT LIFTOFF FROM 50 Hz TO 400 Hz

Figure 5-5. Shuttle Payload Bay Acoustic Contours for Small Payloads/Empty Bay



- = STS-1 134.7 dB OA
- △ = STS-2 135.8 dB OA
- ◆ = STS-3 135.6 dB OA
- = STS-4 135.0 dB OA
- + = STS-5 135.2 dB OA

Figure 5-6. Mean of Acoustic Time Envelopes for Each Flight's Perimeter Microphones

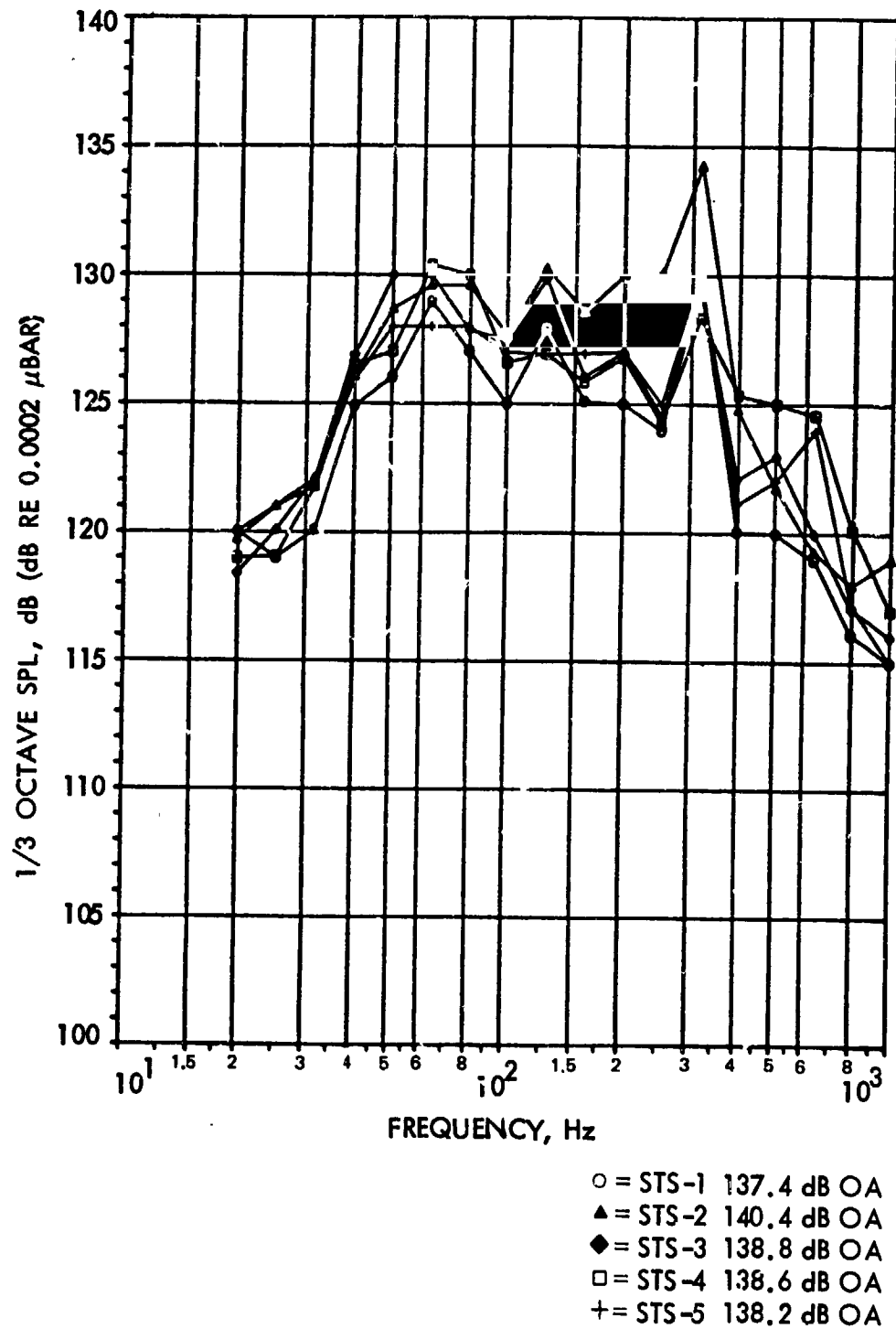
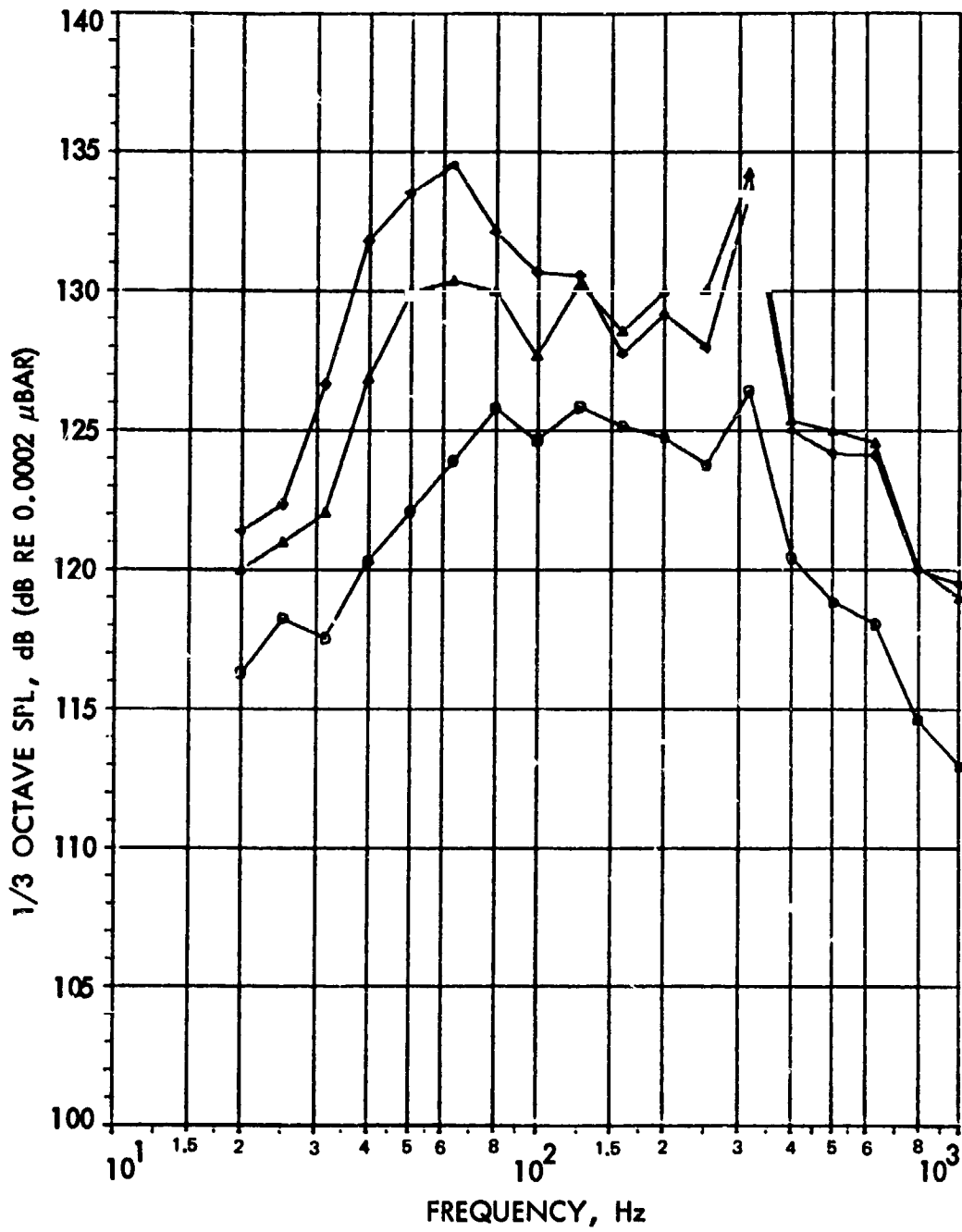


Figure 5-7. Maximum of Acoustic Time Envelopes for Each Flight's Perimeter Microphones



○ = AVERAGE 135.3 dB OA
 ◇ = 0.97 PROBABILITY 142.2 dB OA
 △ = MAXIMUM 143.4 dB OA

Figure 5-8. Acoustic Envelope Statistics for Perimeter Microphones

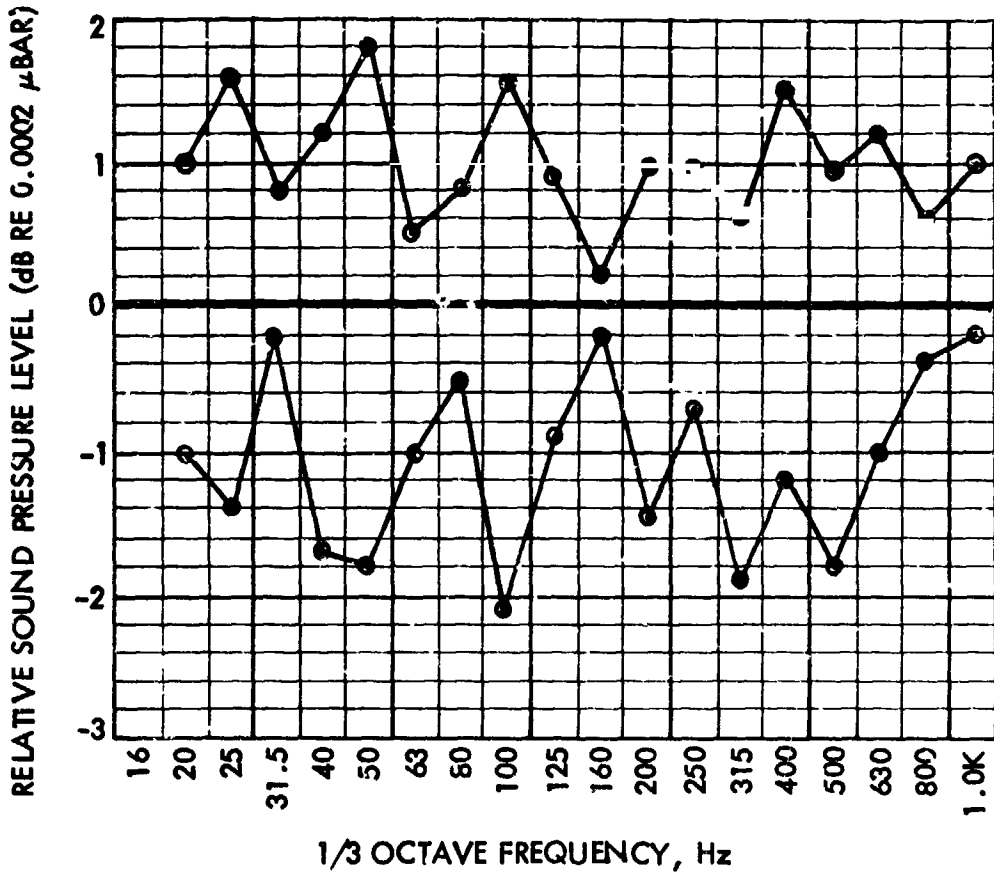
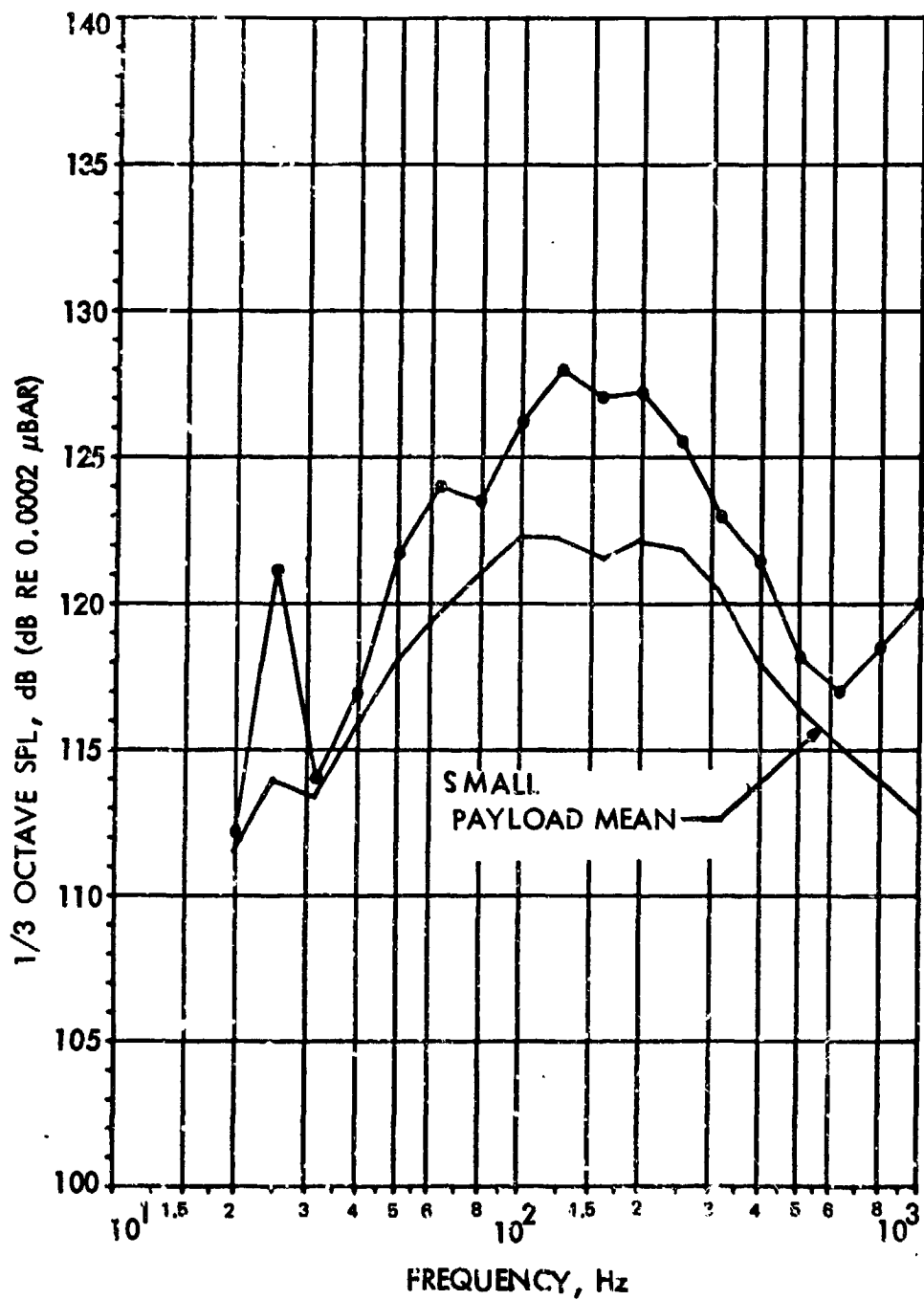
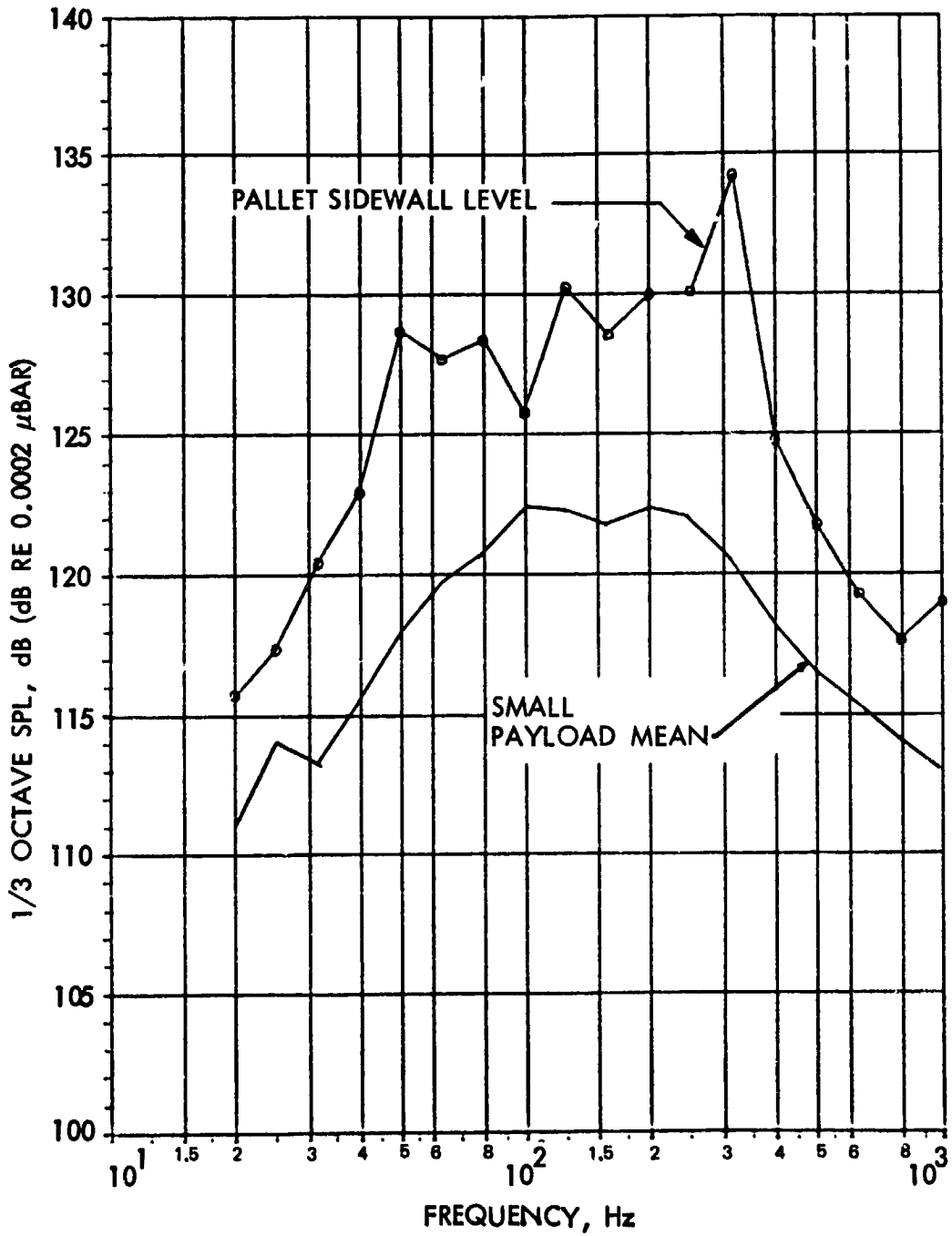


Figure 5-9. Flight-to-Flight Variation and Scatter of Each Flight's Perimeter Acoustic Mean Levels From Overall Perimeter Mean, STS-1 Through STS-5



○ = STS-3 136.4 OA

Figure 5-10. Maximum Time Envelope Acoustic Level 6 Feet From Payload Bay Centerline Near Payload Doors, Microphone S231, STS-3



o = STS-2 140.0 OA

Figure 5-11. Maximum Time Envelope Acoustic Level Between Pallet and Sidewall, Microphone 9256, STS-2

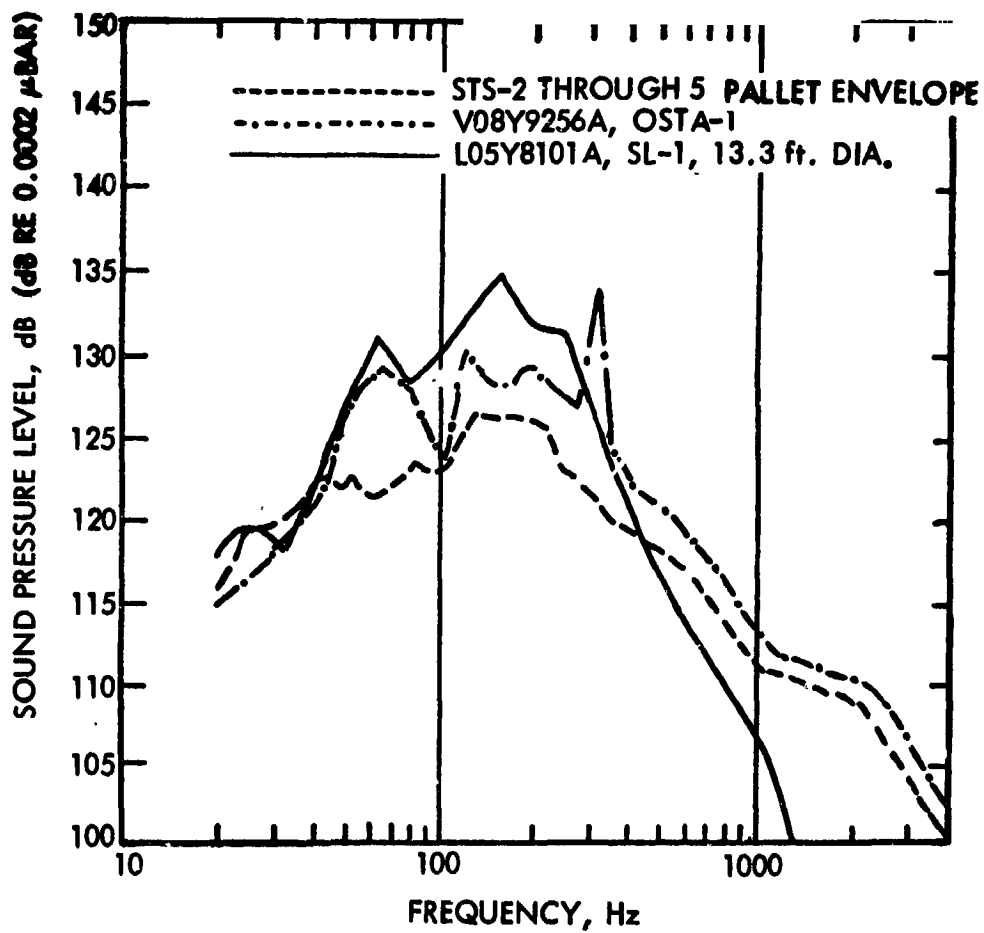
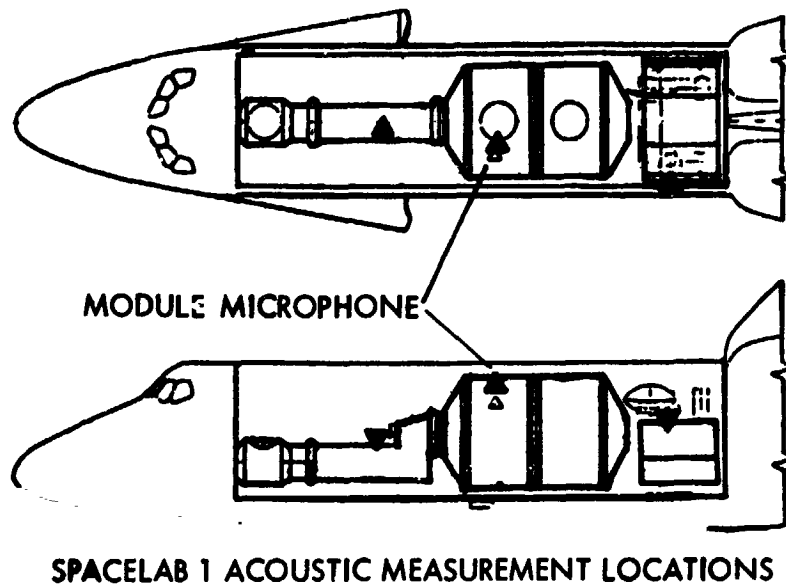
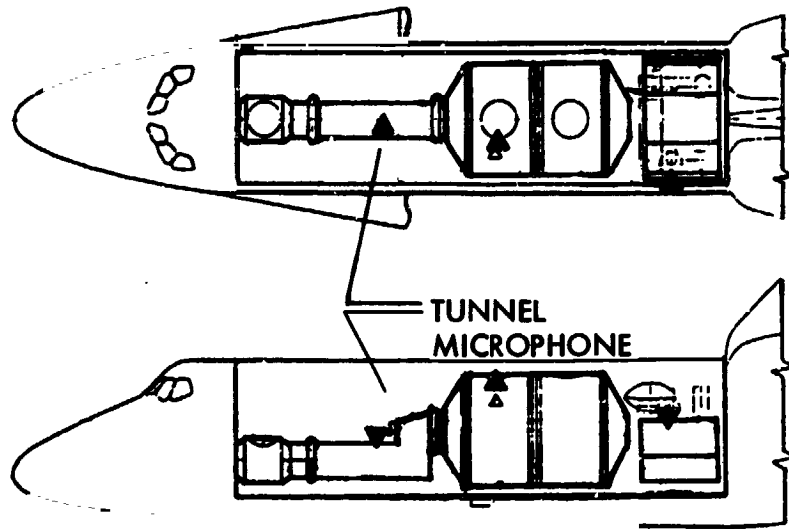


Figure 5-12. Spacelab Module External Acoustics vs. STS-2 Through STS-5 Pallet Envelope and STS-2 Pallet Side Levels



SPACELAB 1 ACOUSTIC MEASUREMENT LOCATIONS

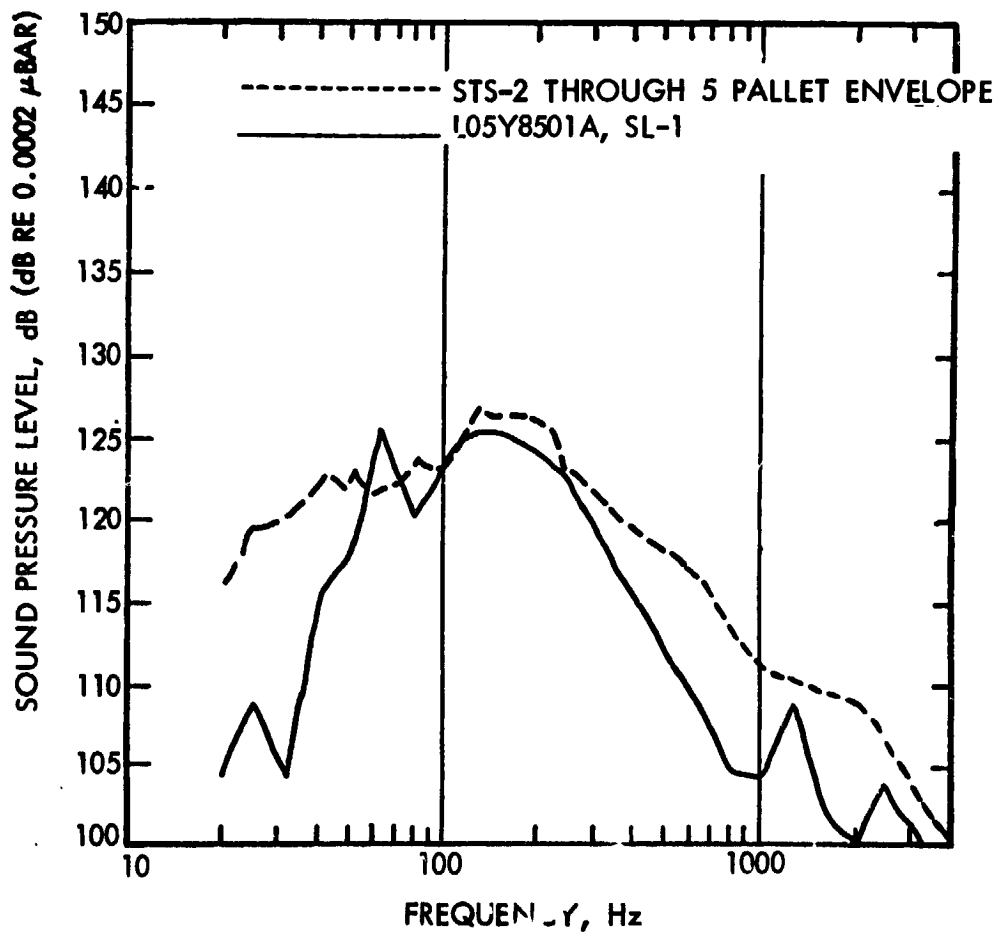
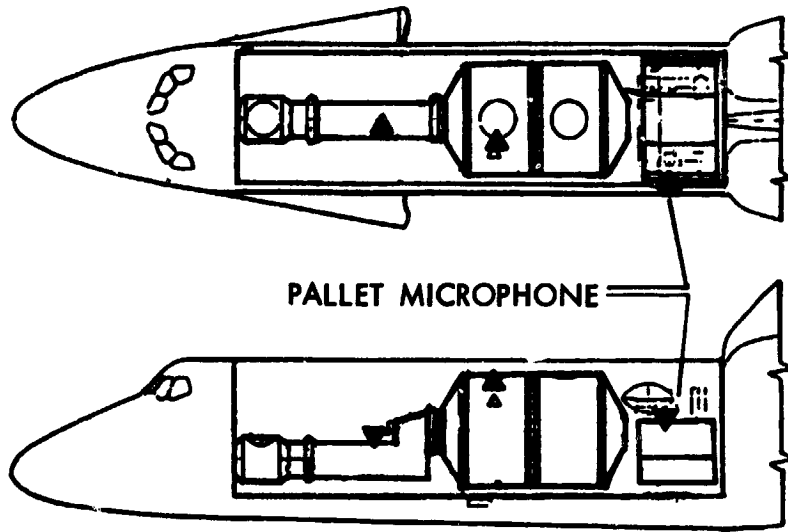


Figure 5-13. Spacelab Tunnel Acoustics vs. STS-2 Through STS-5 Envelope



SPACELAB 1 ACOUSTIC MEASUREMENT LOCATIONS

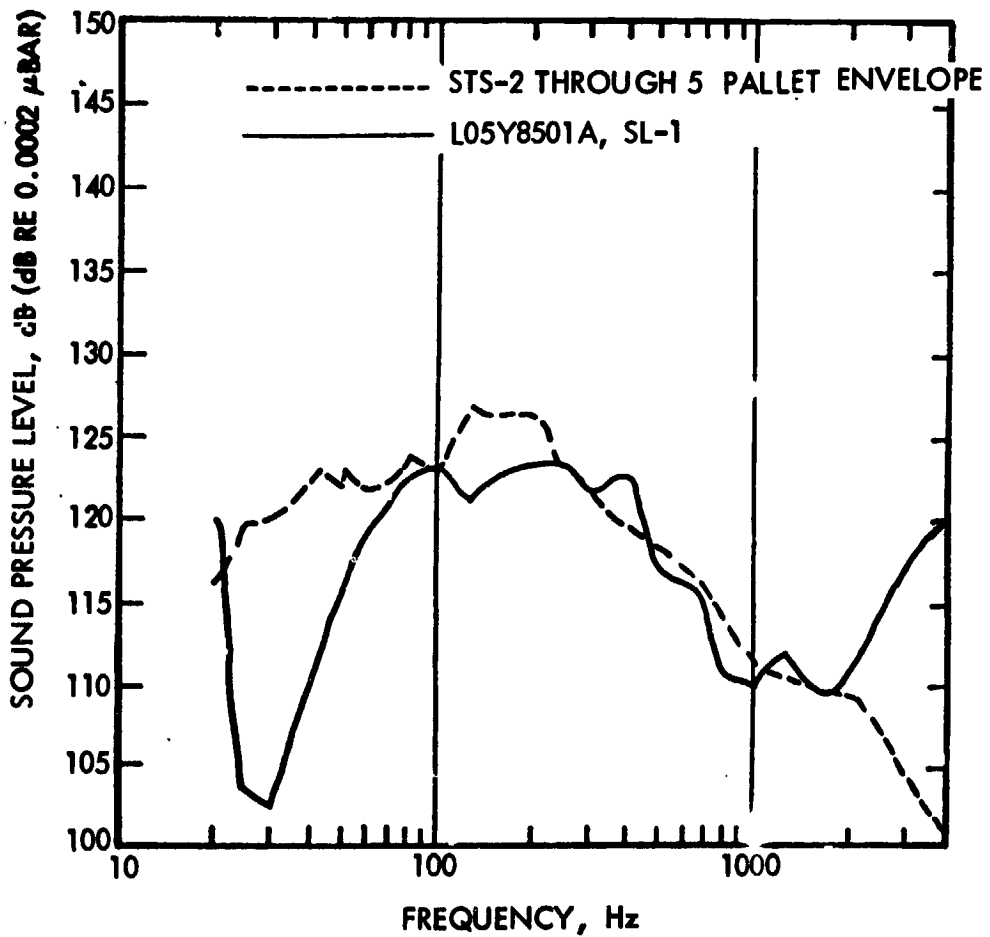


Figure 5-14. Spacelab STS-9 Pallet Acoustics

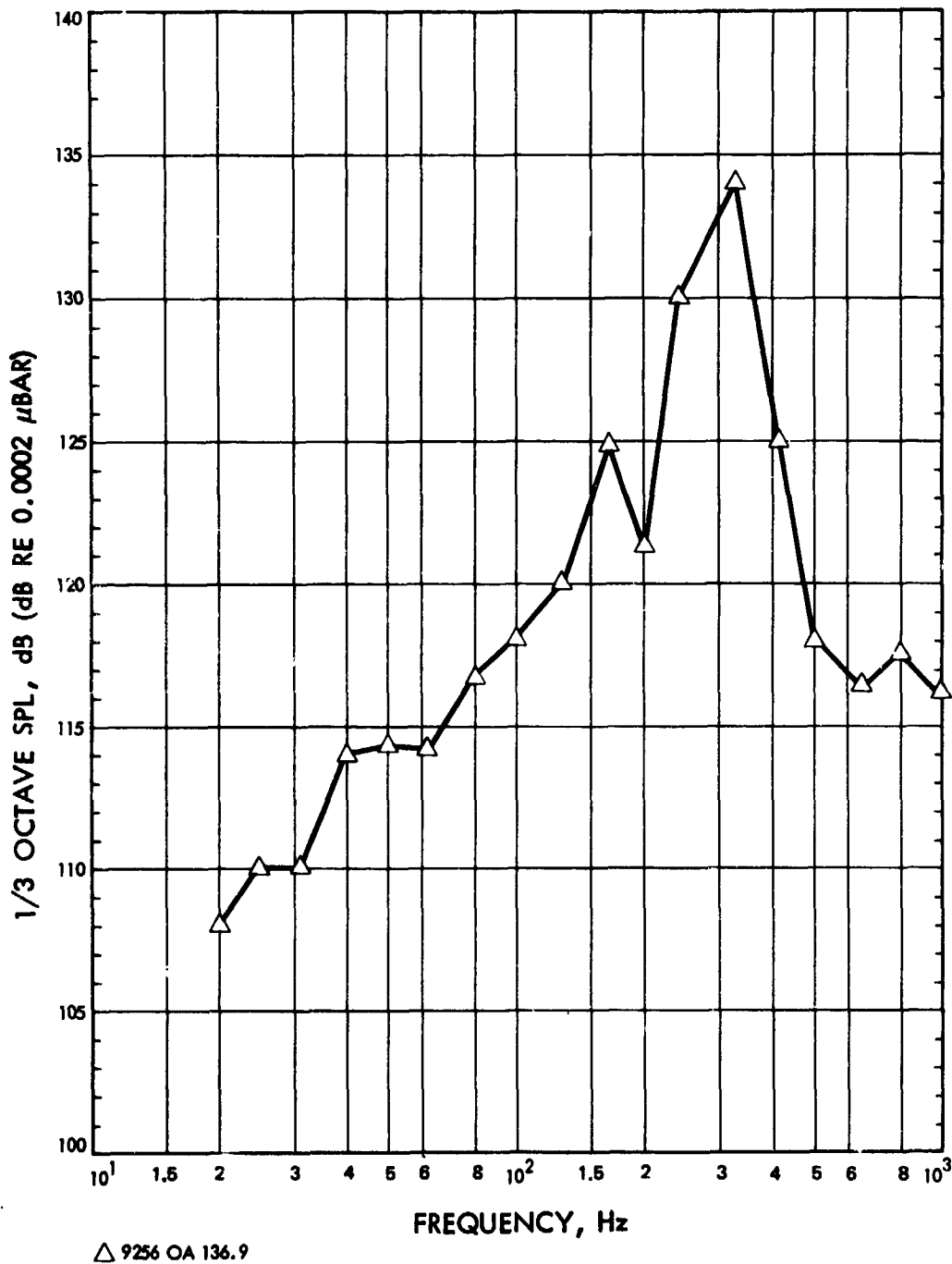
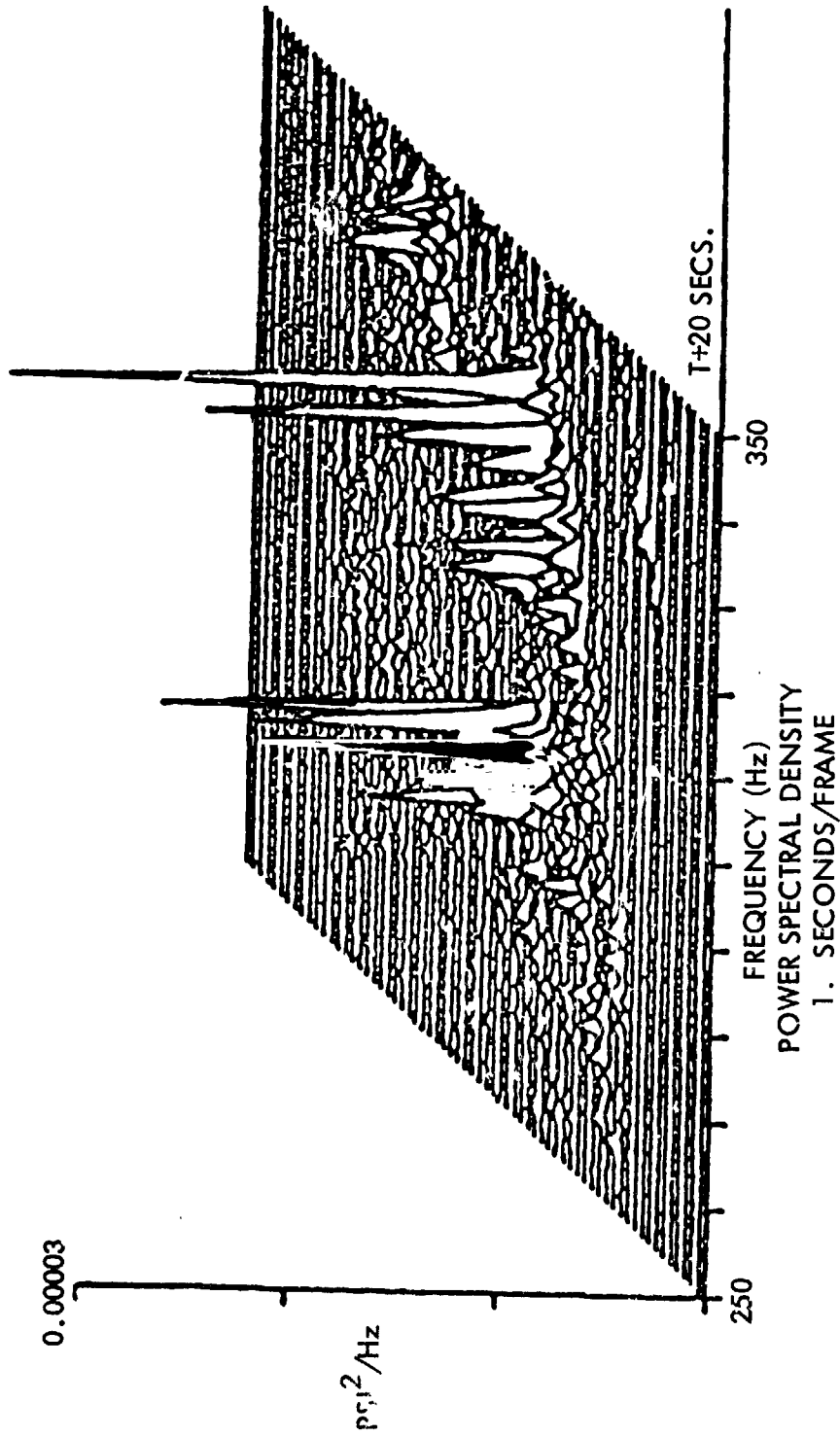


Figure 5-15. Discrete Tone, 315 Hz, During Transonic Flight, Microphone 9256, STS-2

STS-1 LA J.NCH
MICROPHONE V08Y9219A



ORIGINAL PAGE IS
OF POOR QUALITY

Figure 5-16. Power Spectral Density of Transonic Flight Acoustic Measurements, STS-1, Cargo Bay Internal (250-350 Hz from T+20 to T-85 seconds)

ORIGINAL PAGE IS
OF POOR QUALITY

STS-2 LAUNCH
MICROPHONE VP8Y9256A

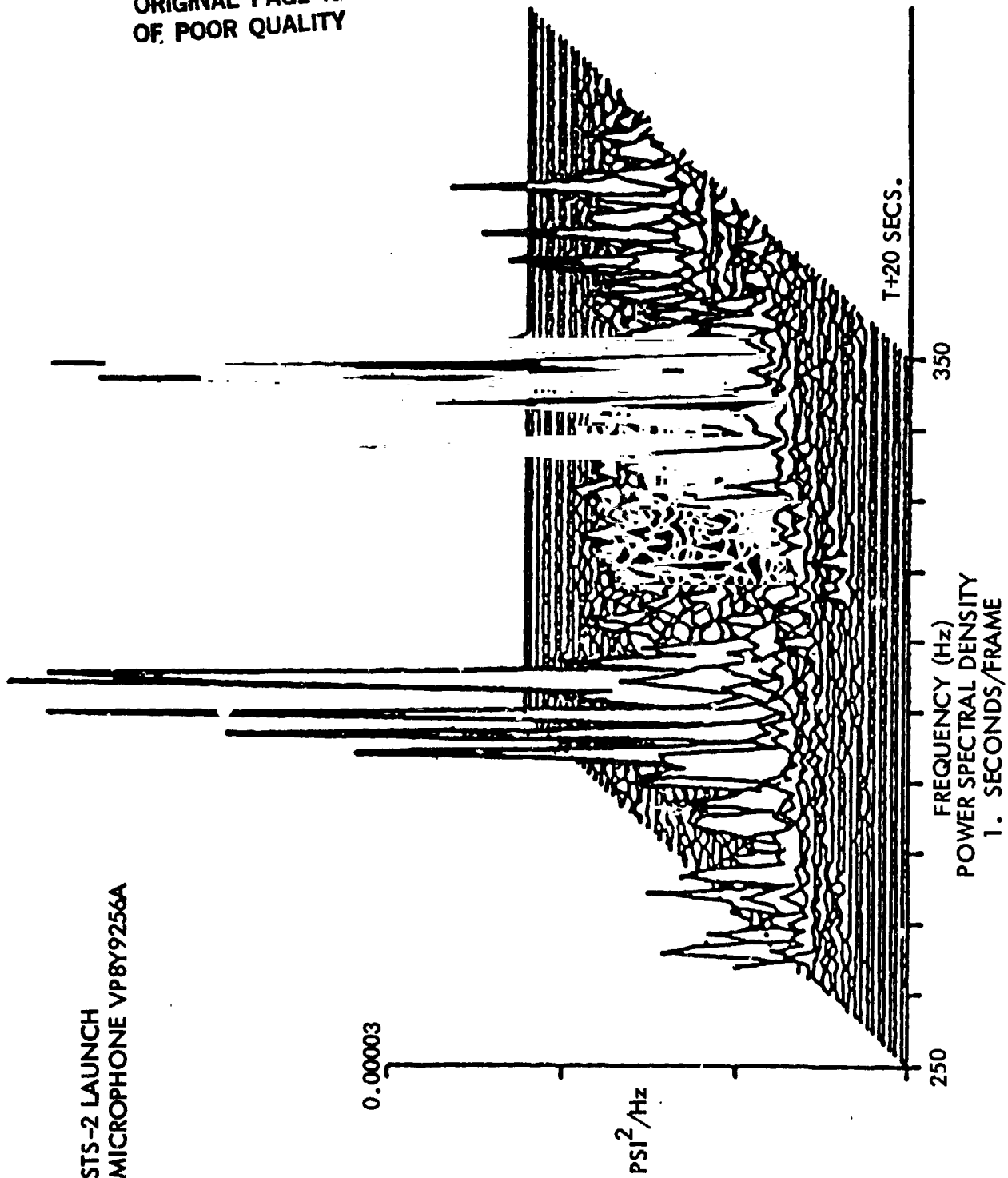
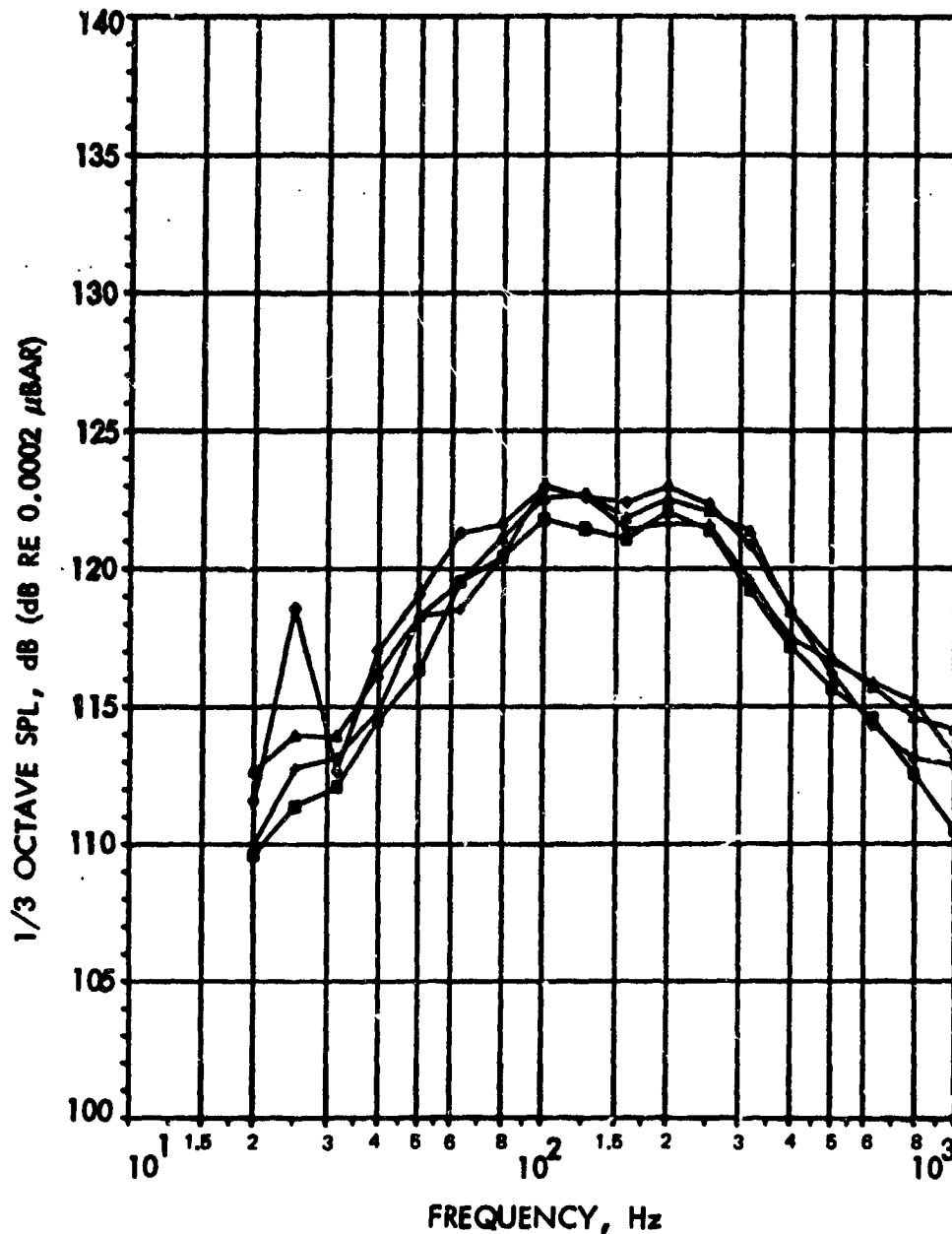
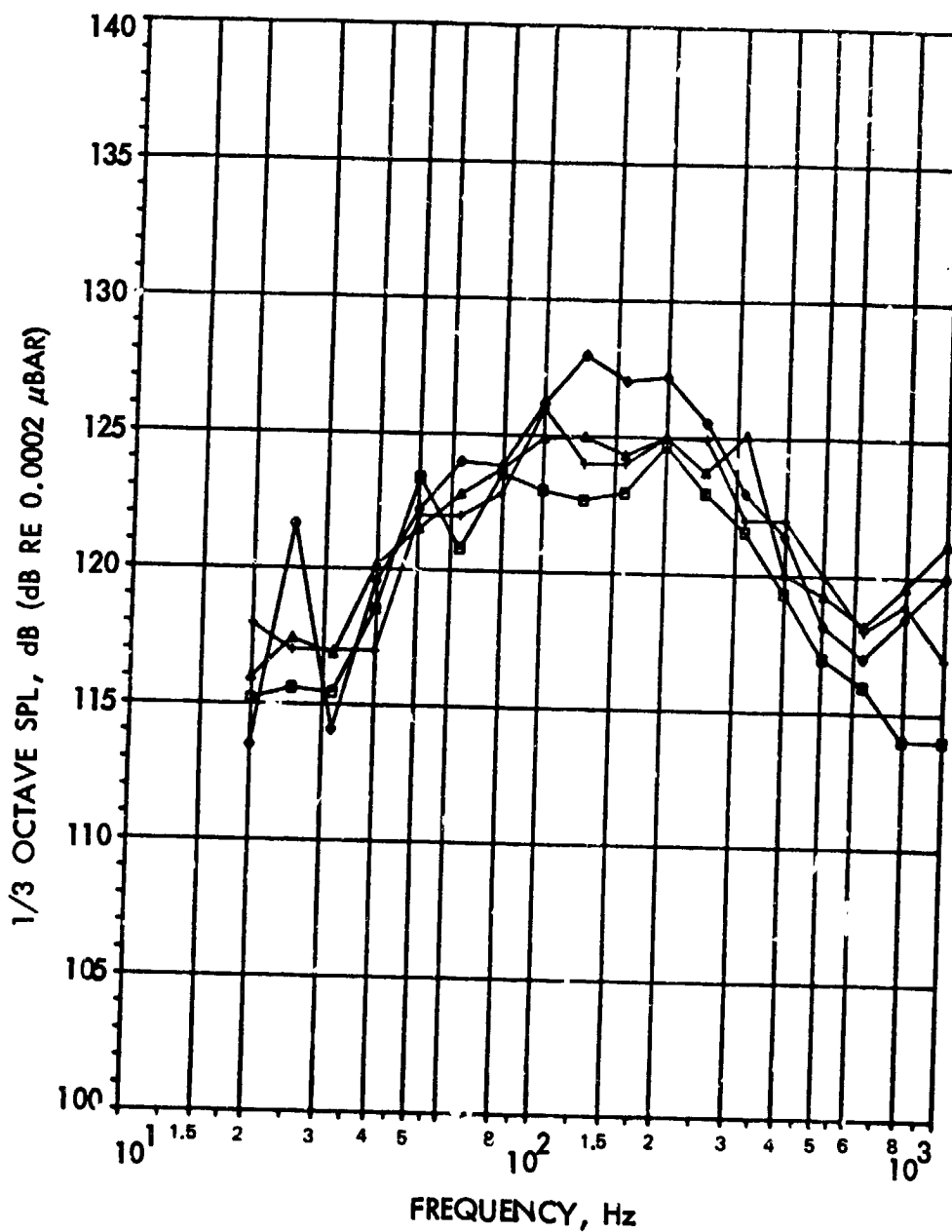


Figure 5-17. Power Spectral Density of Transonic Flight Acoustic Measurements, STS-2, OSTA-1 Pallet (250-350 Hz from T+20 to T-85 seconds)



Δ = STS-2 132.2 dB OA
 ○ = STS-3 132.4 dB OA
 □ = STS-4 131.0 dB OA
 + = STS-5 131.5 dB OA

Figure 5-18. Mean of Acoustic Time Envelopes for Each Flight's Payload Microphones



Δ = STS-2 134.9 OA
 ◇ = STS-3 136.0 OA
 □ = STS-4 133.4 OA
 + = STS-5 134.6 OA

Figure 5-19. Maximum Envelope of Acoustic Time Envelopes for Payload Microphones

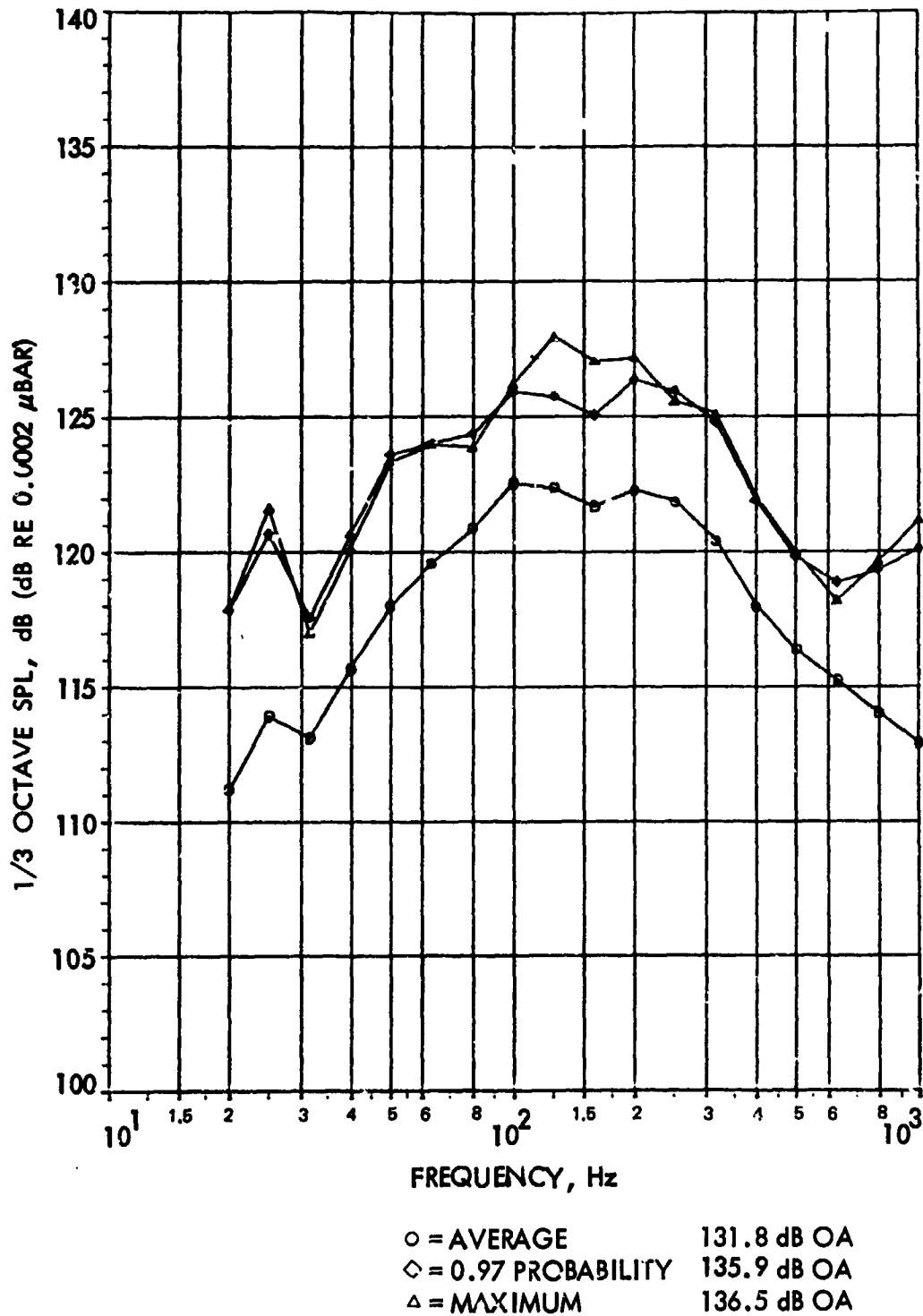
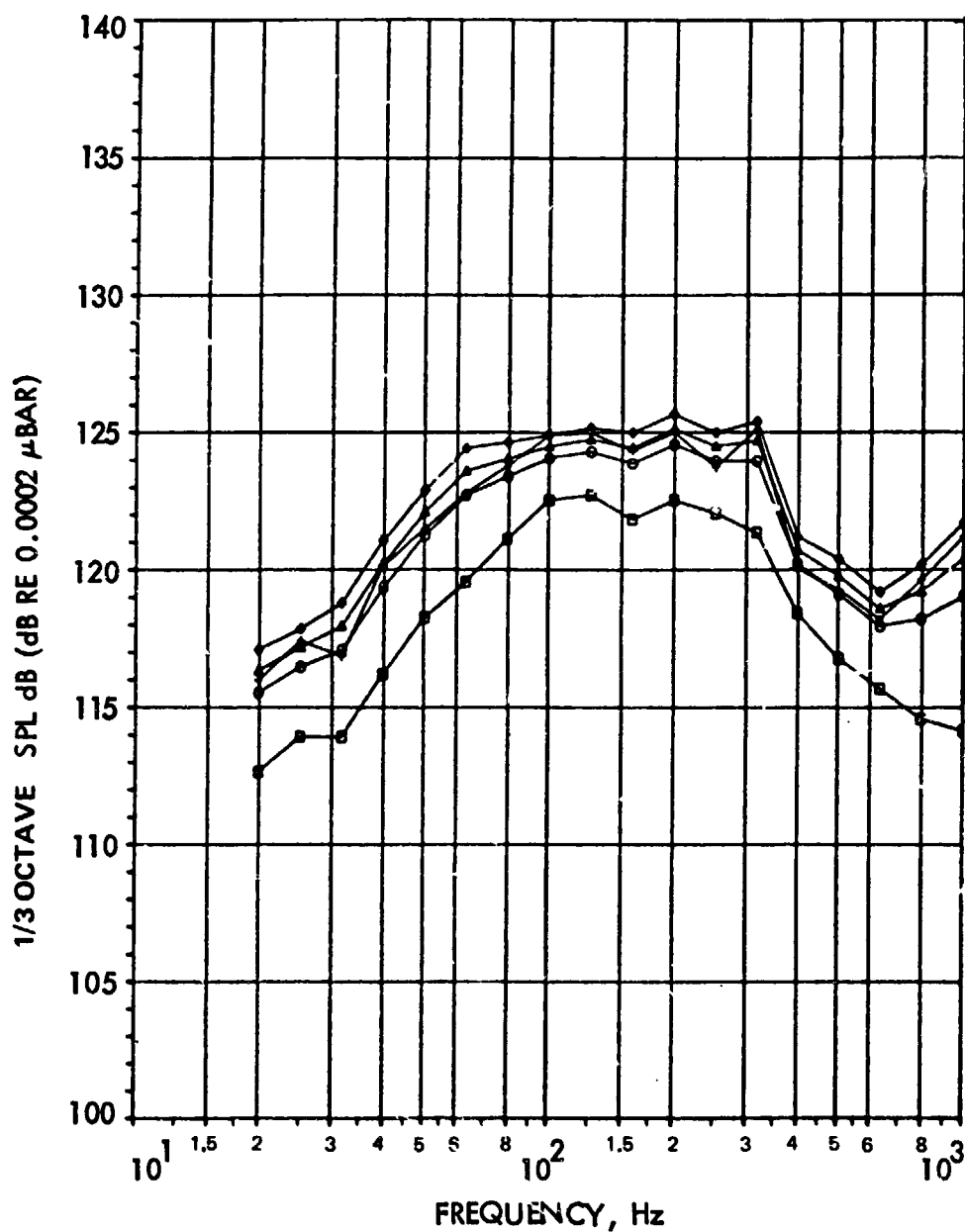


Figure 5-20. Acoustic Data Time Envelope Statistics for Payload Microphones, All Flights



◇ = 97.5 PROBABILITY 135.6 dB OA
 △ = 95 PROBABILITY 134.9 dB OA
 ○ = 90 PROBABILITY 134.4 dB OA
 □ = AVERAGE 132.0 dB OA
 + = MAXIMUM 134.8 dB OA

Figure 5-21. Acoustic Data Time Envelope Statistics for Payload Microphones, STS-2

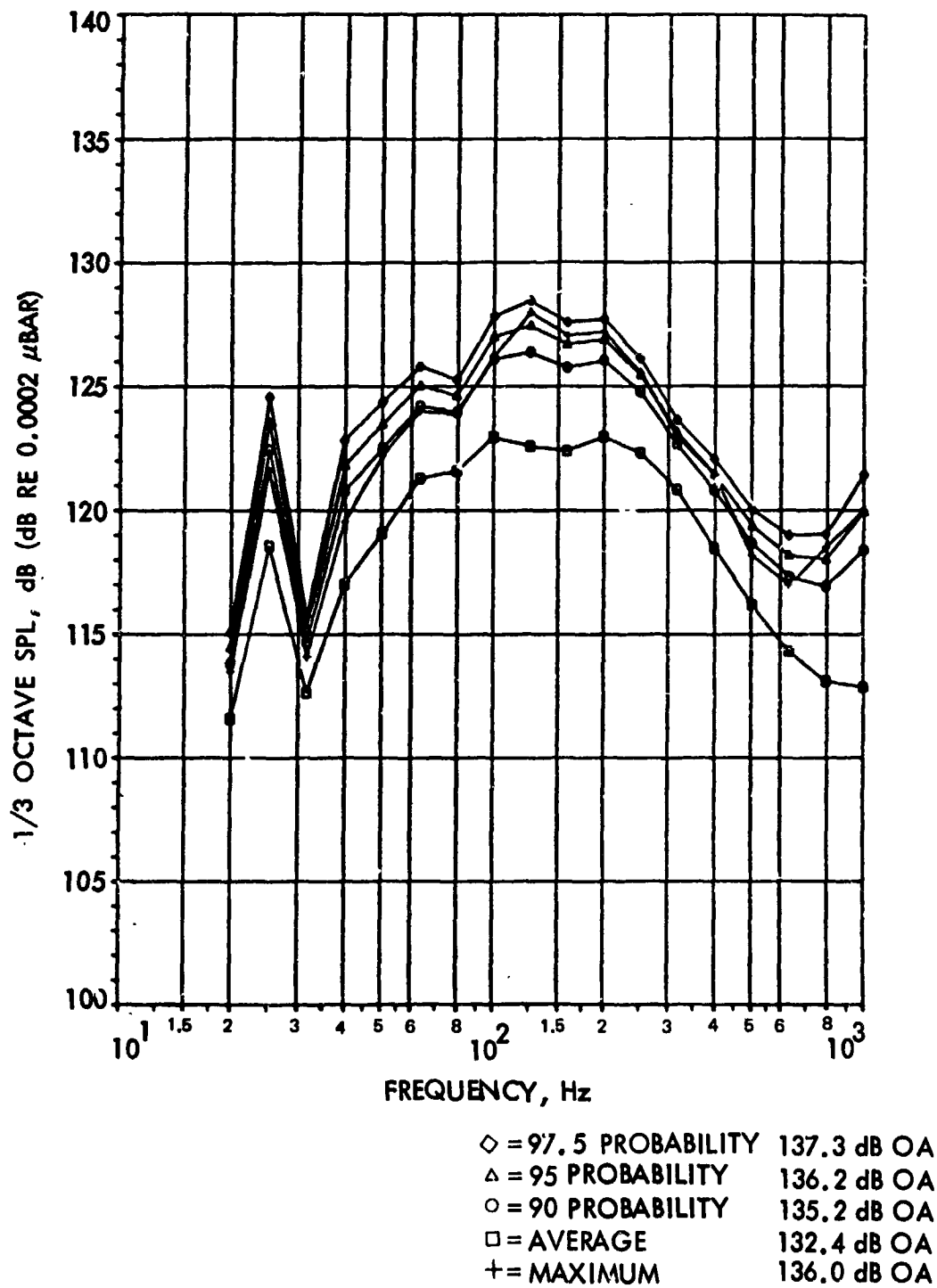


Figure 5-22. Acoustic Data Time Envelope Statistics for Payload Microphones, STS-3

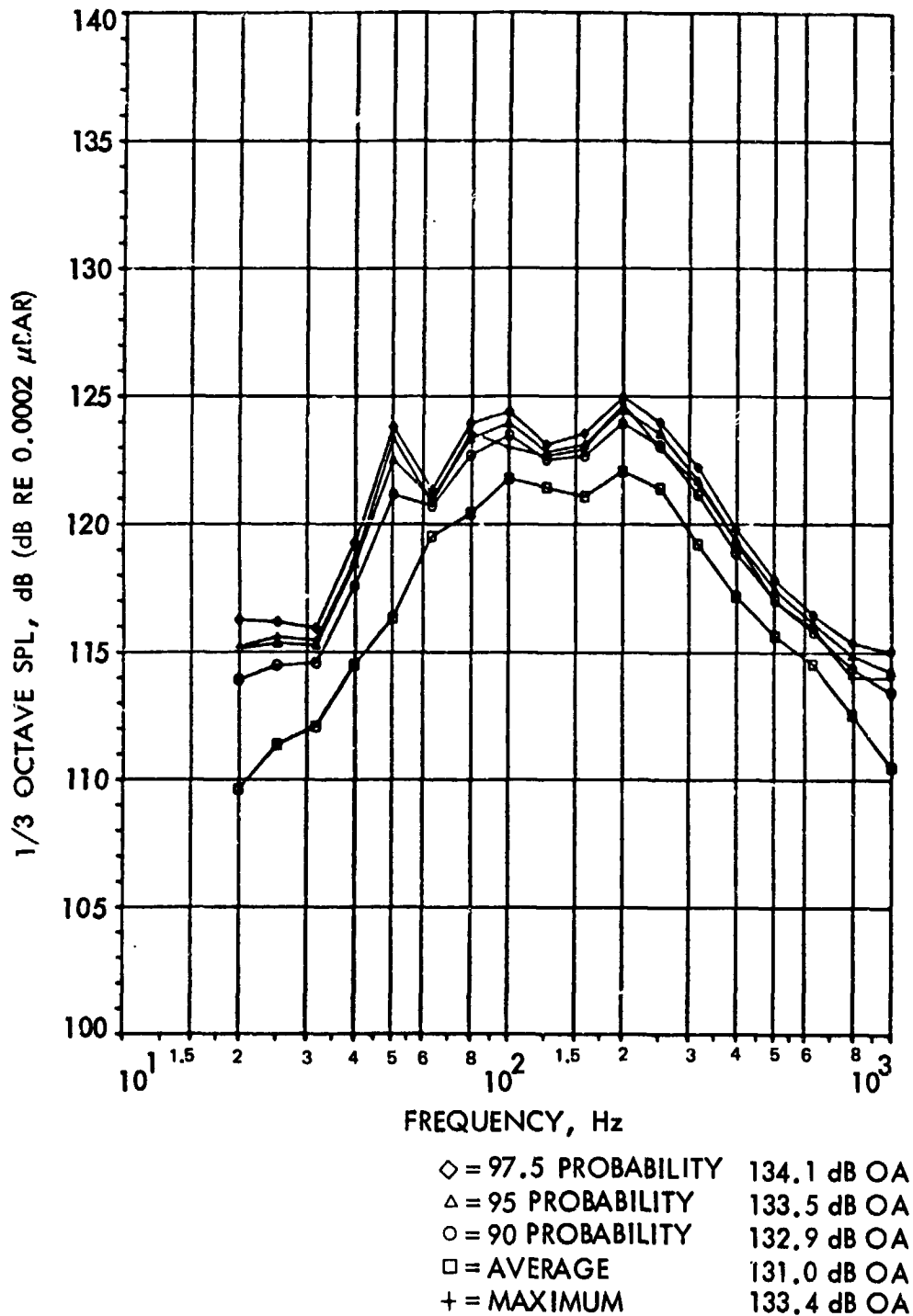


Figure 5-23. Acoustic Data Time Envelope Statistics for Payload Microphones, STS-4

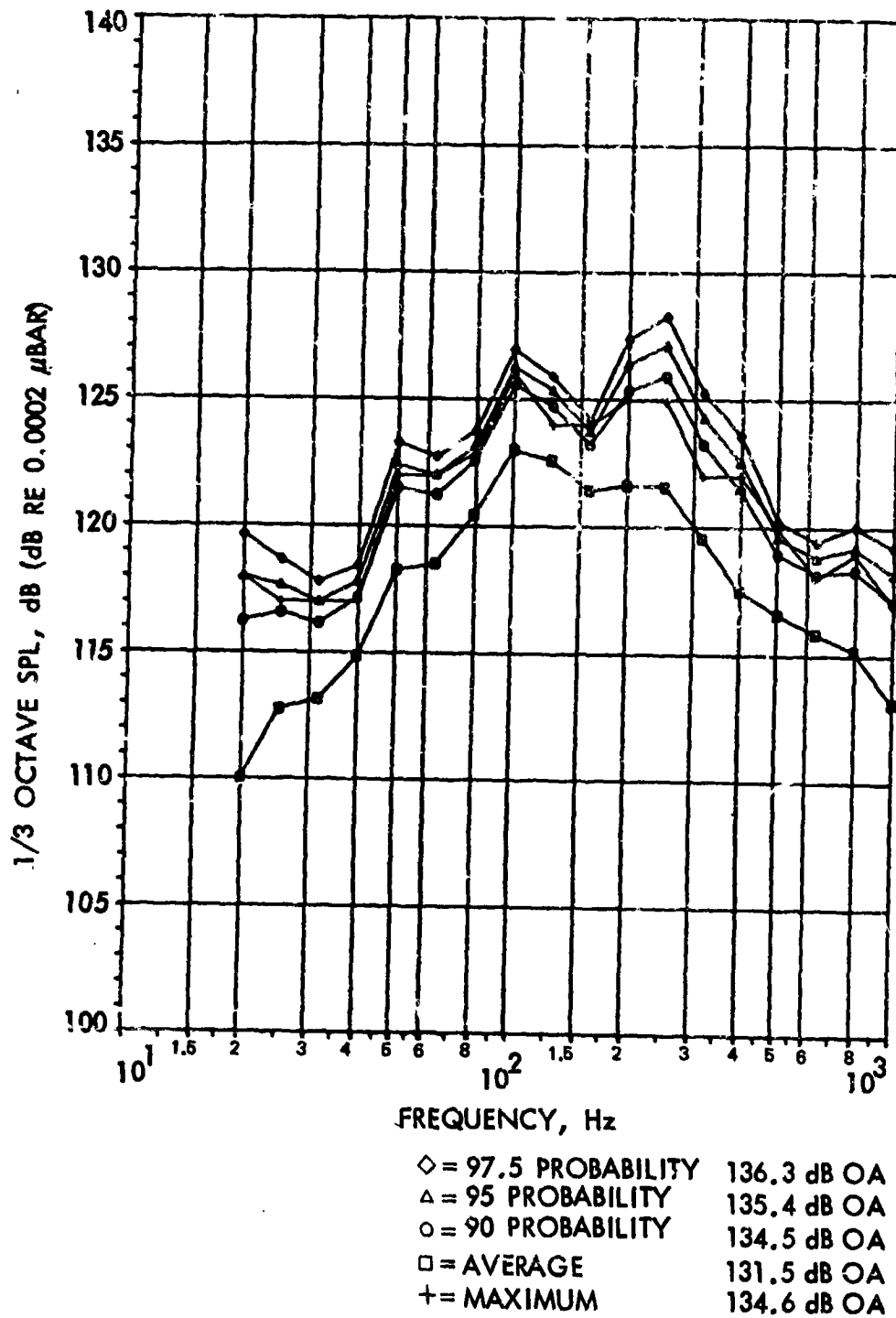
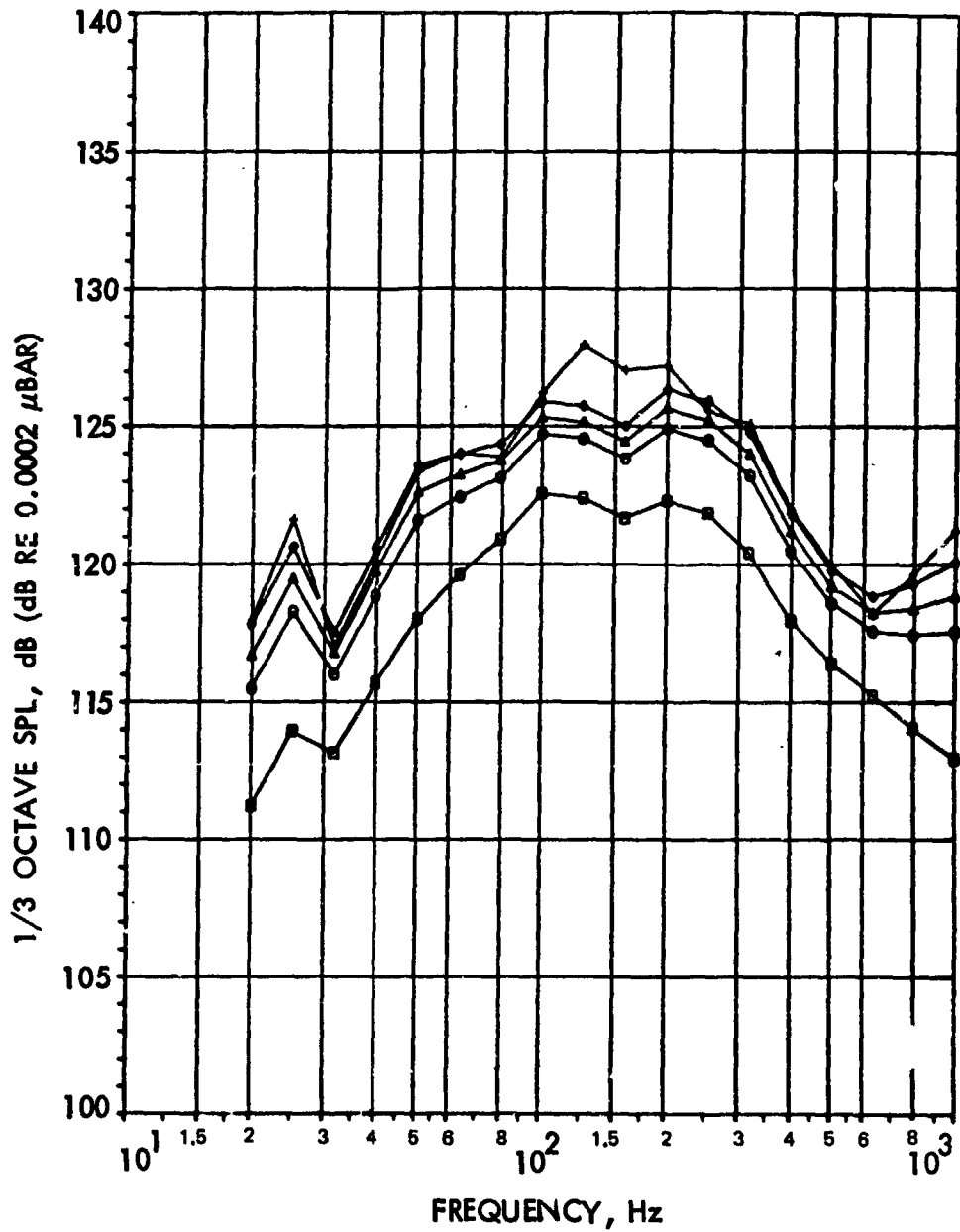


Figure 5-24. Acoustic Data Time Envelope Statistics for Payload Microphones, STS-5



| | |
|----------------------|-------------|
| ◇ = 97.5 PROBABILITY | 135.9 dB OA |
| △ = 95 PROBABILITY | 135.3 dB OA |
| ○ = 90 PROBABILITY | 134.5 dB OA |
| □ = AVERAGE | 131.8 dB OA |
| + = MAXIMUM | 136.4 dB OA |

Figure 5-25. Expanded Acoustic Data Time Envelope Statistics for Payload Microphones, All Flights

5.2 Vibration Data Summary

5.2.1 Payload Bay Vibration

High frequency vibration data was obtained on the orbiter longeron pallet trunnions, pallet shelves and pallet hard points (References 2, 3 and 14). Open dissemination of this data was confined to STS-2 and 3. Because of the small size of the data base, the vibration data for the various types of STS and payload structure were enveloped for presentation. Vibration data plots and accelerometer locations from Reference 14 are shown in Figures 5-26 through 5-38. Accelerometer locations were classified on STS-4 and were not available. Also, no high frequency DATE accelerometers were on STS-5. A filter bandwidth of 10 Hz was used for the accelerometer spectral density data reduction. Consequently, data below 80 Hz is subject to errors caused by small numbers of data samples.

Vibration for small longeron-mounted payloads, such as the Get Away Special cannisters, is shown in Figure 5-26. These levels exceeded the preflight prediction level for the longeron vibration criteria. The maximum measured levels from 3 directions are shown on the same plot, along with the preflight longeron criteria. As a result, the criteria of the payload criteria Interface Control Document (ICD) were revised to those in Figure 5-27. Vibration levels across the DFI trunnions were attenuated 10 dB or more at most frequencies compared to the longeron vibration. Three axis levels at the DFI trunnion are shown in Figure 5-28. Figures 5-29, 5-30, and 5-31, respectively, compare the longeron vibration in the x, y, and z axes to trunnion vibration on the payload side. The x direction vibration at the pallet trunnion was nearly identical to the longeron levels between 100 Hz and 400 Hz (Figure 5-29). Two high-energy modes appear at the trunnion in the x axis at 140 Hz and 300 Hz. Below 100 Hz and above 400 Hz longeron levels were much attenuated at the pallet trunnion. The same 140 Hz and 300 Hz modes that appeared in the x axis also appear in the y axis, with vibration at other frequencies being highly attenuated. In the z axis the attenuation is similar except that modes centered at 90 Hz and 180 Hz appear at the trunnion. Vibration at the DFI pallet center (Figure 5-32) is about 10 dB below the levels at the pallet trunnions. The pallet center is about 7 feet from the DFI trunnions.

Keel vibration is shown in Figure 5-33 for the y axis. Vibration was only measured in the y axis because it was the primary axis of constraint and due to instrumentation limitations. Levels in the y axis are well below the current keel vibration requirements. Keel levels in the z direction are expected to be greater than for the y direction (Reference 14).

Vibration levels on the OSTA-1 and OSS-1 experiment pallets were measured at experiment interfaces and shelves. Figure 5-34 shows the envelope of vibration levels at pallet hard point/experiment interfaces were generally below $.005 G^2/Hz$. The data of Figure 5-34 is an envelope of experiment interface vibration measured on the OSTA-1 Materials Experiment Assembly (MEA) shelf interface, the OSS-1 Thermal Can Base and the Spacelab Cold Plate Support Structure (CPSS) component interface.

Figure 5-35 shows a vibration peak level on the OSTA-1 pallet shelf that reached $0.2 G^2/Hz$ at 300 Hz during transonic flight. This shelf response coincides with the vent acoustic excitation frequency. The response was also present at lift off with a broader frequency range of response (100 - 400 Hz).

Vibration on the OSS-1 cold plate edge (Figure 5-36) was as high as $0.04 \text{ G}^2/\text{Hz}$ for a peak at 170 Hz but was generally below $.01 \text{ G}^2/\text{Hz}$. Bracket vibration ($0.01 \text{ G}^2/\text{Hz}$) on an OSS-1 experiment support is seen in Figure 5-37. All of these pallet levels are payload peculiar and depend on the design and mass of the pallet experiments.

Most flight vibration data indicated that payloads are responding more in flight than in acoustic tests (Reference 15). OSS-1 data shows more vibration response in flight below 125 Hz for most accelerometers. Figure 5-38 shows the difference between flight and test response at the OSS-1 Spherical Retarding Potential Analyzer (SRPA) support bracket and is typical of the difference seen at the other accelerometers. However, the effect is seen all across the frequency range on the side of the cold plate (Figure 5-39). Figure 5-40 shows the amount of extrapolation used to normalize the acoustic test data to flight levels. Note that there is a 2 dB difference in the extrapolation depending on if the test acoustic level is taken from the pallet microphones instead of the test control microphones. The pallet microphones are in the same location in the ground acoustic test and in flight.

Lockheed Missiles and Space Company (LMSC) data on a Department of Defense (DOD) payload shows the same trend of higher vibration responses in flight than in acoustic tests (Reference 16). The LMSC analysis shows higher levels throughout the frequency spectrum but the effect is accentuated below 100 Hz (Figure 5-41). The difference in ground and test flight levels for the DOD payload is shown in Figure 5-42.

The dark datum line at 0 dB (Figure 5-41) represents the normalized ground test vibration response. The two lines of in-flight response correspond to extrapolations of the ground response data based on the flight average Sound Pressure Level (SPL) and then the envelope of the flight SPL. A similar LMSC analysis of the OSS-1 data shows that in-flight vibration exceeded ground test vibration more than in the GSFC analysis for the same payload (Figure 5-43).

Some data from Spacelab have the reverse of the trend of the OSS-1 and DOD payload data (Reference 17). The flight response versus acoustic test response comparison from the Spacelab pallet (STS-9) in Figure 5-44 indicates that ground test responses were higher for all frequencies (Reference 17). Acoustic test response was extrapolated to a 139 dB acoustic input. The plot of Figure 5-44 is typical of the other Spacelab data (Reference 17). However, the flight levels at the 1.3 meter ring (Figure 5-45) and the tunnel fan housing interface (Figure 5-46), exceeded acoustic test levels significantly, as the OSS-1 and DOD pallet data did. These excesses were all below 100 Hz and were only 20-30 Hz wide. It should be noted that ground test accelerometer locations were not duplicated exactly in flight but comparisons were made between accelerometers that were "generally" in the same location. Also, thermal insulation blankets were not present during the ground acoustic tests but were present in flight. Data at JPL indicate that the absence of thermal blankets should have little effect on the vibration response of a large test item.

The higher than expected flight vibration environment in the lower frequencies (below approximately 125 Hz) is likely to have been transmitted from the orbiter itself, but the transfer function is still being investigated. The cause of the discrepancy between the OSS-1 and DOD data set and the Spacelab

vibration response may be related to differences in the amount of extrapolation applied to the ground vibration data. Also, differences in the Spacelab accelerometer locations during its ground acoustic tests and flight could have caused significantly different trends in the ground/flight response comparison. For this reason in particular, the Spacelab data probably should not be used in a rigorous study of the payload response during flight versus ground acoustic test.

Shock response spectra with dynamic amplifications of 10, 20 and 50 are given for pallet payload structure in Figures 5-47 through 5-53. These spectra are time envelopes of the shock response spectra of References 2 and 3. Launch events included in the envelopes are Space Shuttle Main Engine (SSME) ignition, Solid Rocket Booster (SRB) ignition, SRB separation and External Tank (ET) separation.

Shock response on pallets from the SSME and SRB ignition events do not seem to be severe for typical space hardware. Reference 2 states, "While the low frequency responses (below 50 Hz), particularly at liftoff, are characterized as responses to transient inputs, the high frequency responses would be best characterized as responses to a relatively broadband and reasonably stationary excitation. This conclusion is based on the fact that the difference between the spectra for different damping values is rather constant as a function of frequency and on the observed ratio of the peak spectral values to the peak value of the time history." The shock spectra from the SRB and ET separation indicate that the shock levels during these events were negligible at pallets (Reference 2).

5.2.2 Aft Flight Data Vibration

The measured vibration data in the aft flight deck, the cargo area of the crew compartment, were low and were not evaluated in detail for this report. For the readers' convenience, the vibration interface environment specified in Reference 13 for the aft flight deck is shown in Table 5-3. These specified levels very conservatively envelope the measured flight data.

Table 5-3. Aft Flight Deck Vibration

| Frequency | Level |
|-----------|------------------------|
| 20 - 150 | +6 dB/octave |
| 150 - 1K | .03 G ² /Hz |
| 1K - 2K | -6 dB/octave |
| Overall | 6.5 Grms |

Duration: 10 seconds/per axis per mission

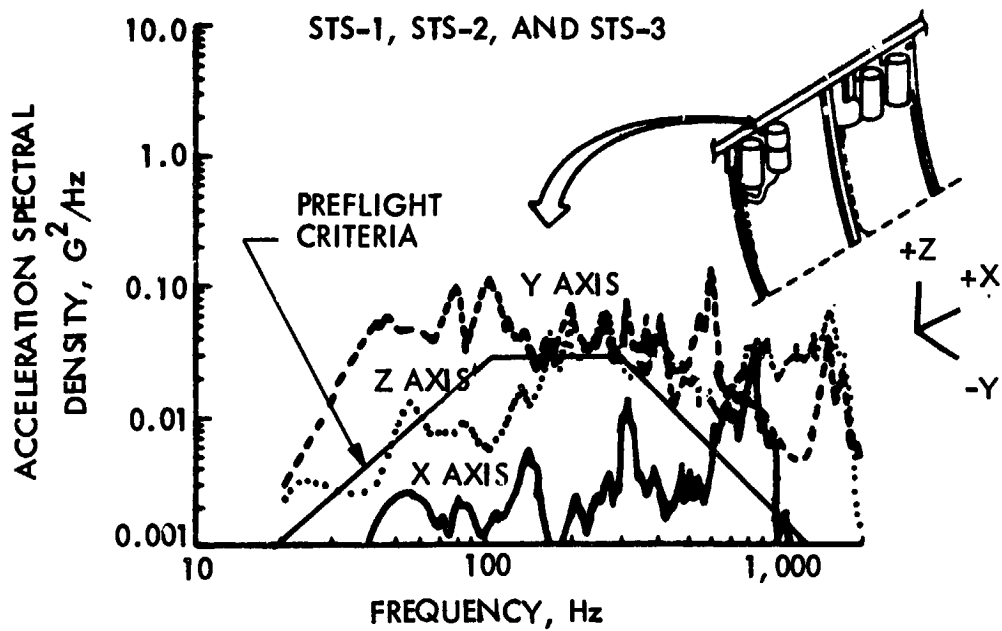


Figure 5-26. Vibration Data for Longeron Bridge Fitting Mounted Payload

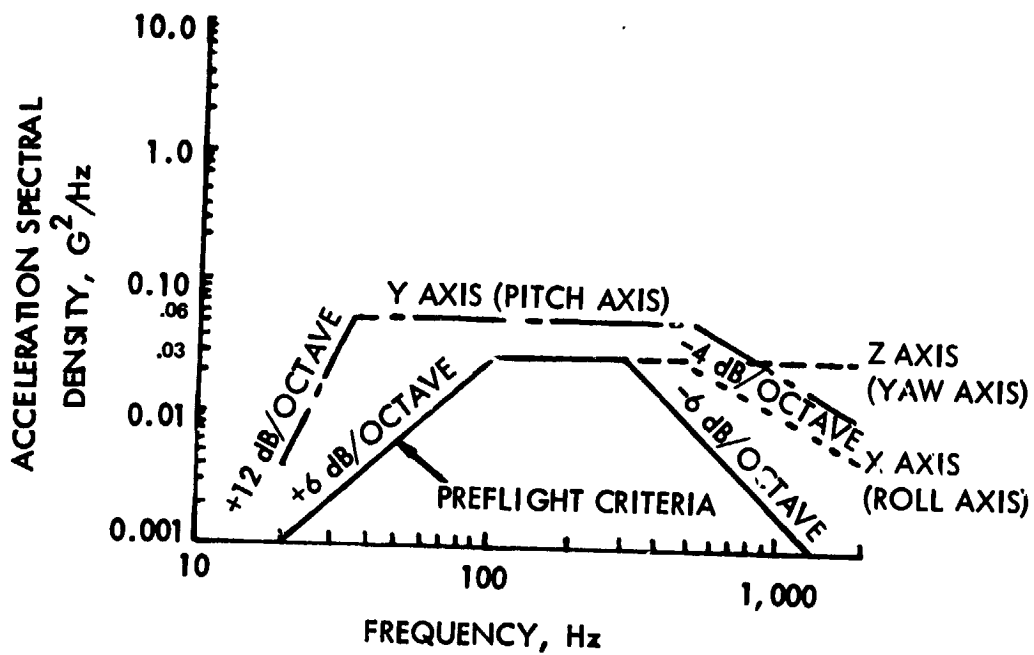


Figure 5-27. Orbiter Longeron Vibration Criteria Derived From Flight Data

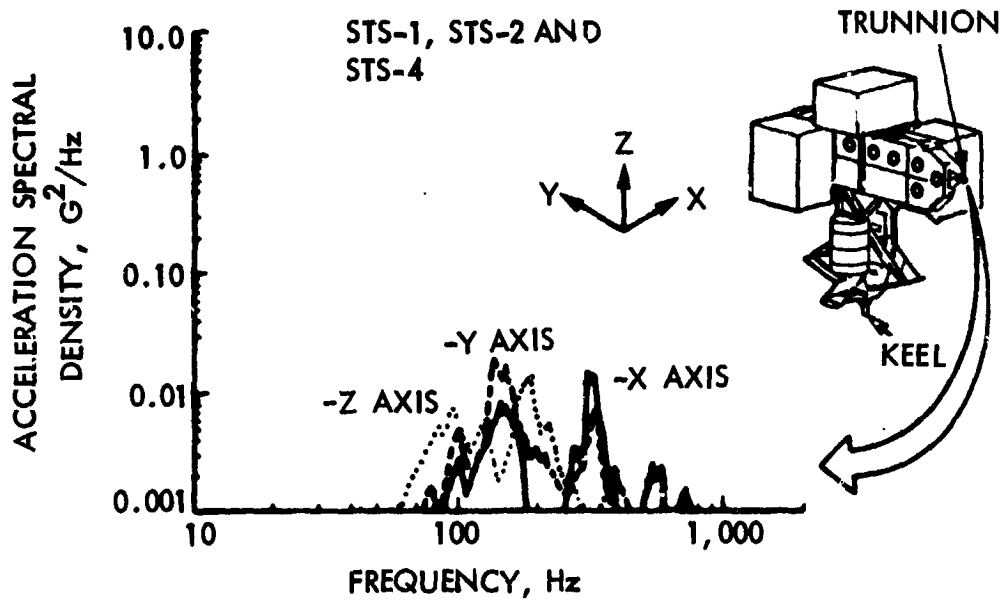


Figure 5-28. DFI Payload Trunnion Vibration

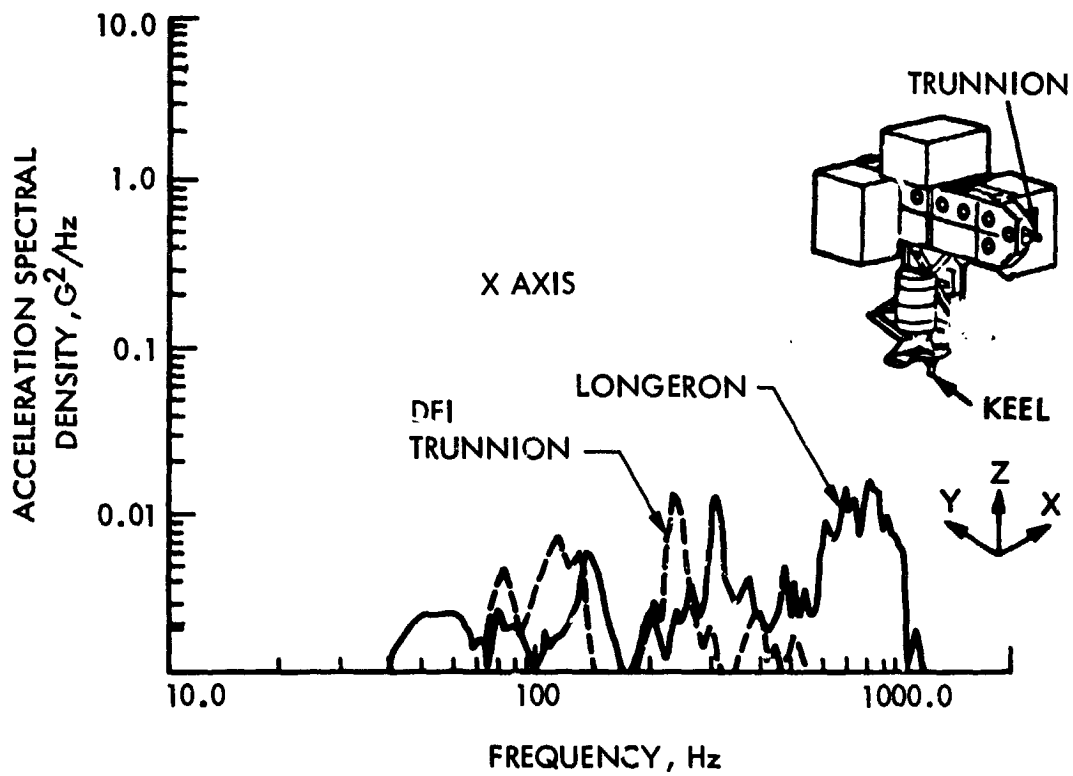


Figure 5-29. DFI Payload Longeron and Trunnion Vibration Comparison in X-Axis, STS-1 Through STS-3

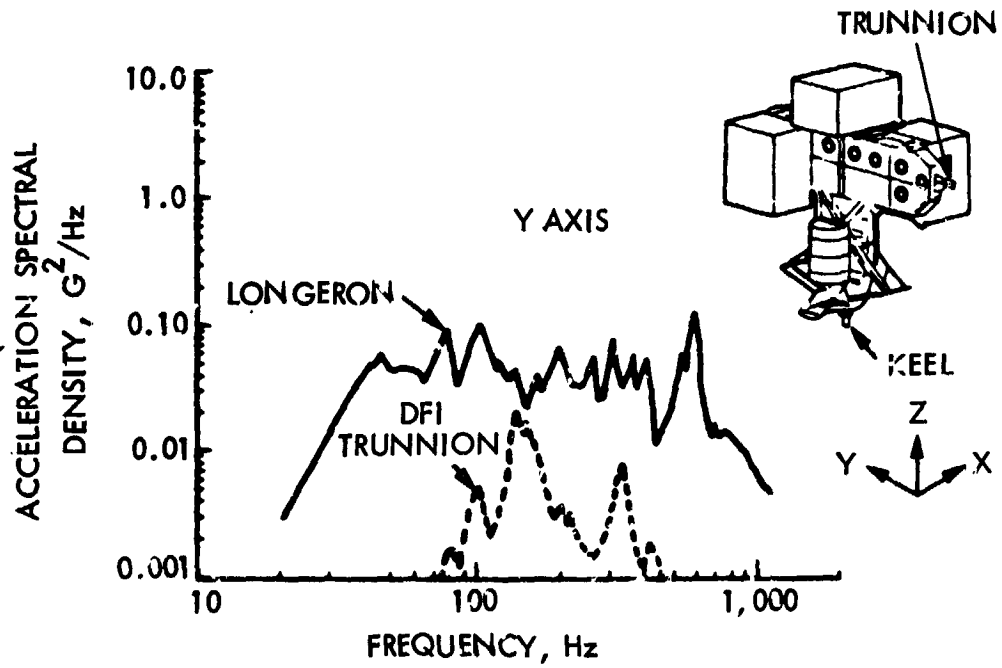


Figure 5-30. DFI Payload Longeron and Trunnion Vibration Comparison in Y-Axis, STS-1 Through STS-3

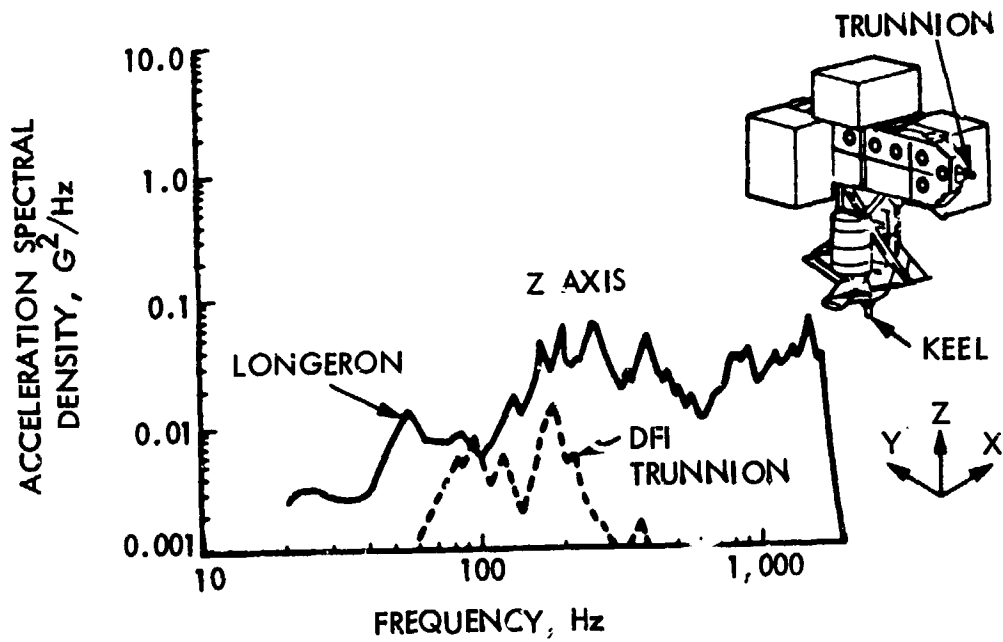


Figure 5-31. DFI Payload Longeron and Trunnion Vibration Comparison in Z-Axis, STS-1 Through STS-3

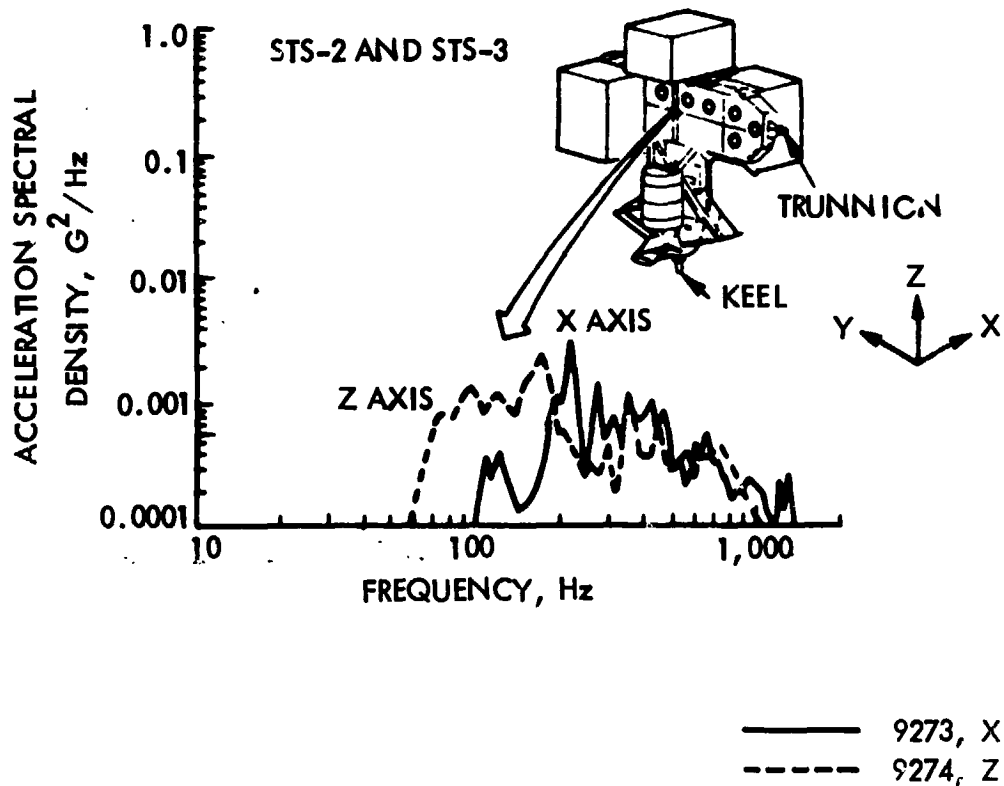


Figure 5-32. DFI Payload Pallet Center Vibration

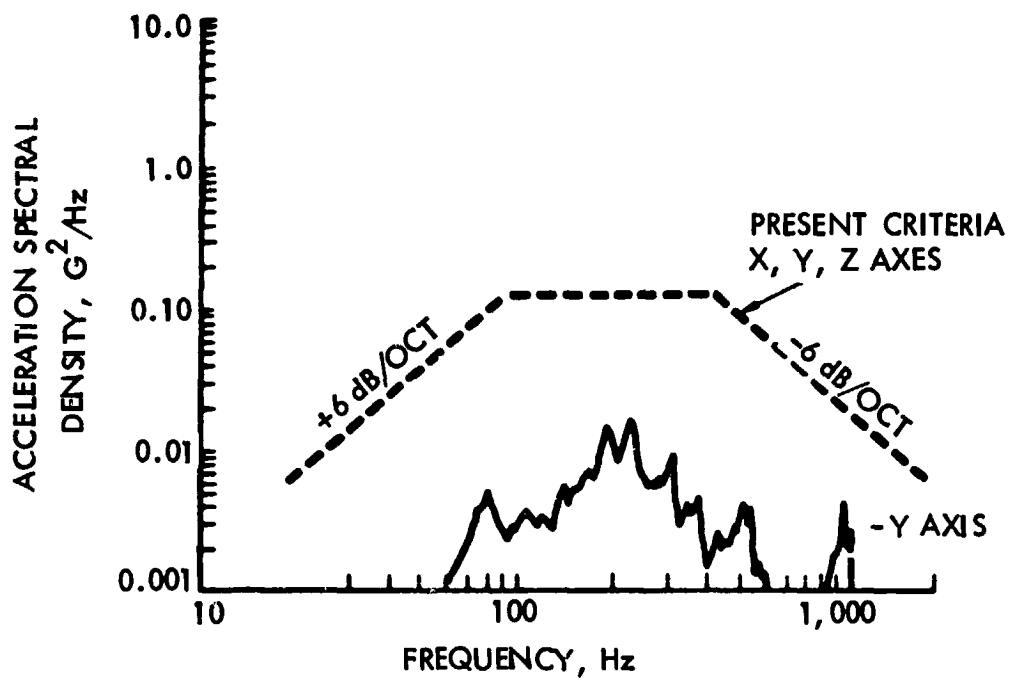


Figure 5-33. Orbiter Keel Fitting Flight Vibration Data

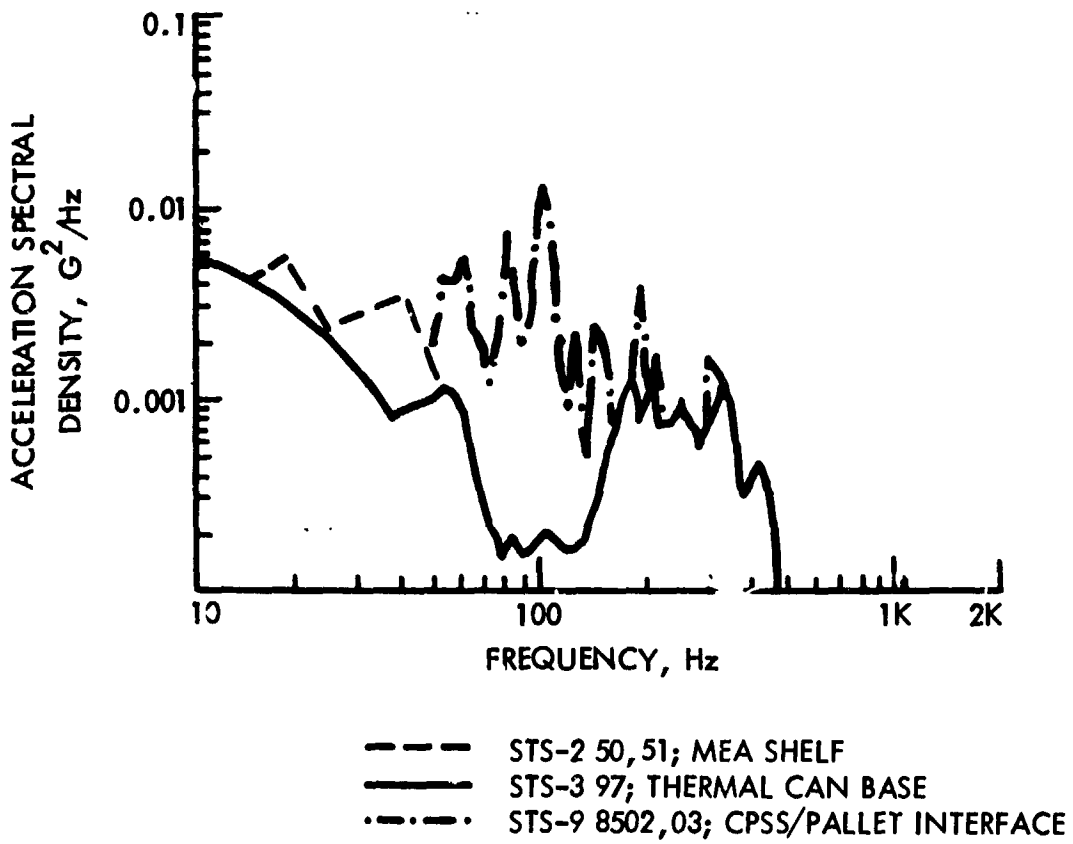


Figure 5-34. Pallet Hardpoint/Experiment Interface Vibration

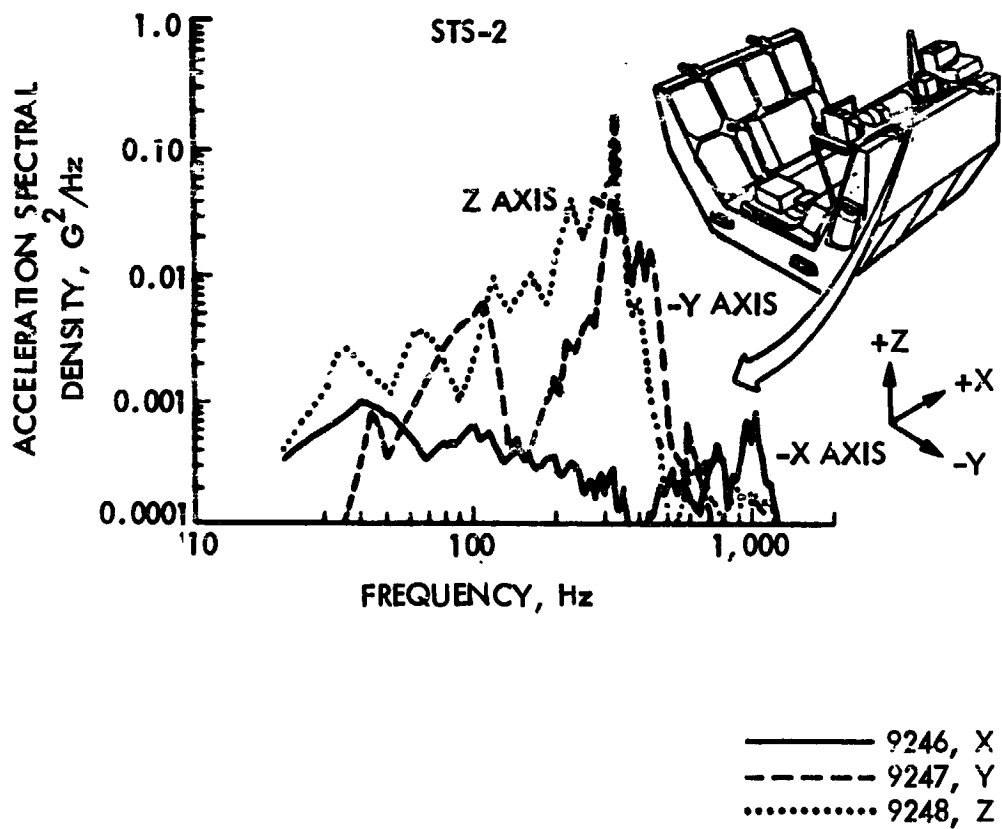


Figure 5-35. OSTA-1 Payload Shelf Vibration

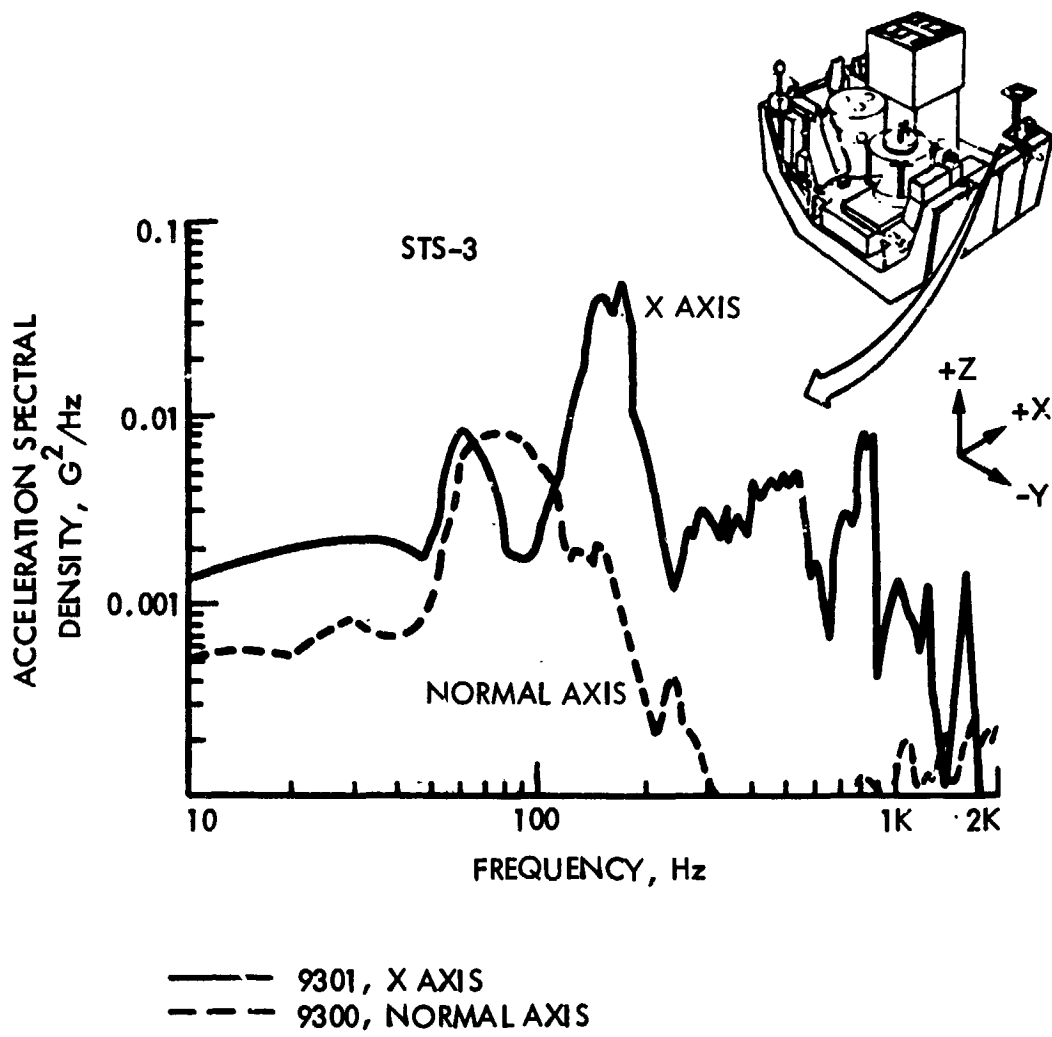


Figure 5-36. OSS-1 Cold Plate Edge Vibration

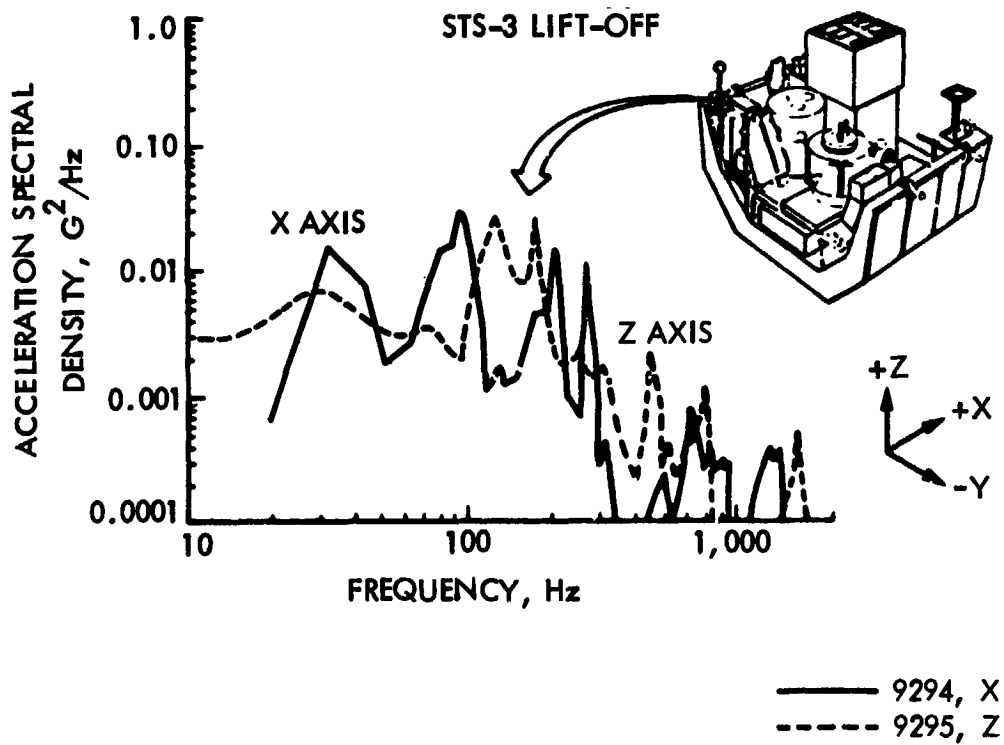


Figure 5-37. OSS-1 Experiment Support Bracket Vibration (Mounted on Small Shelf)

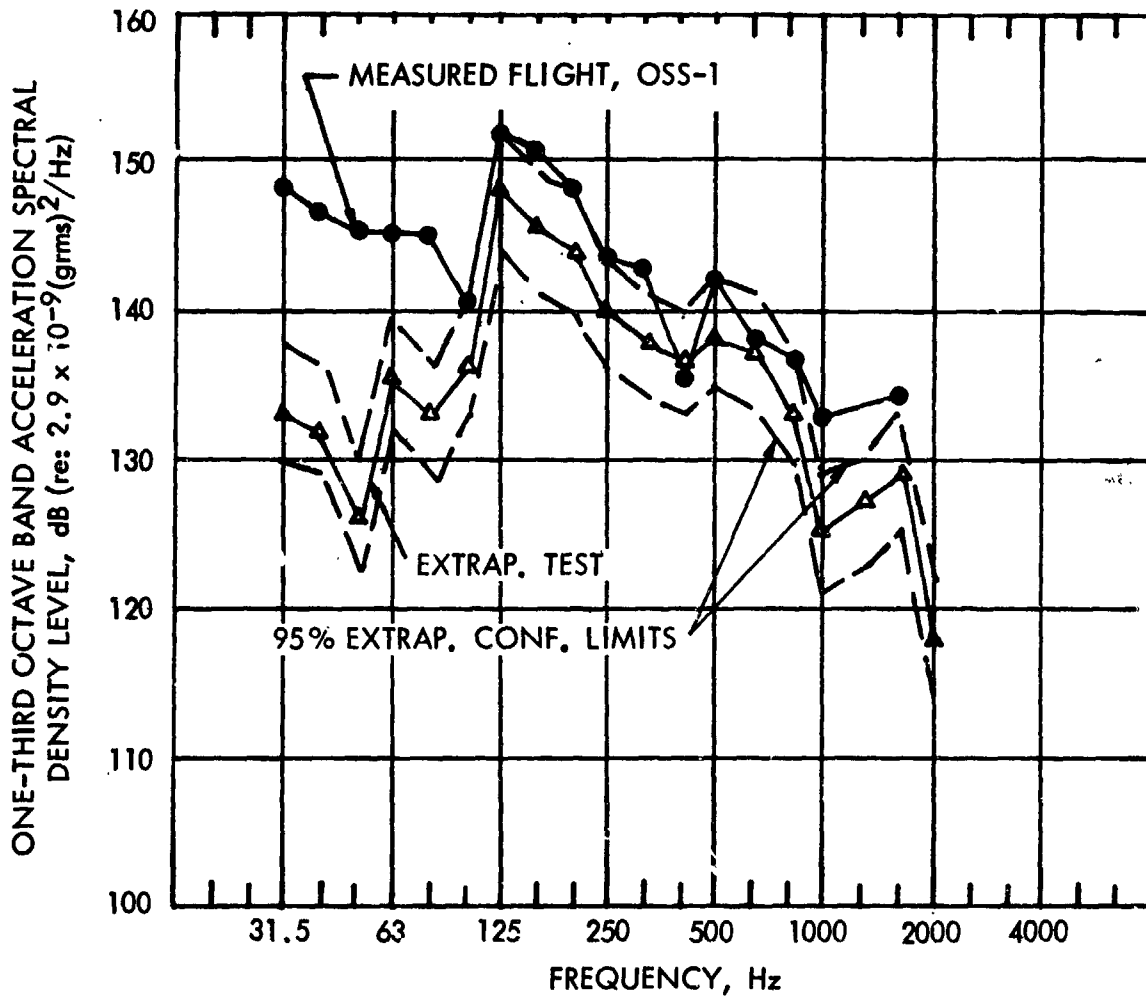


Figure 5-38. Measured STS and Extrapolated Test Acceleration Spectral Density for OSS-1 Shelf, Experiment Support Bracket, Accelerometer 9295

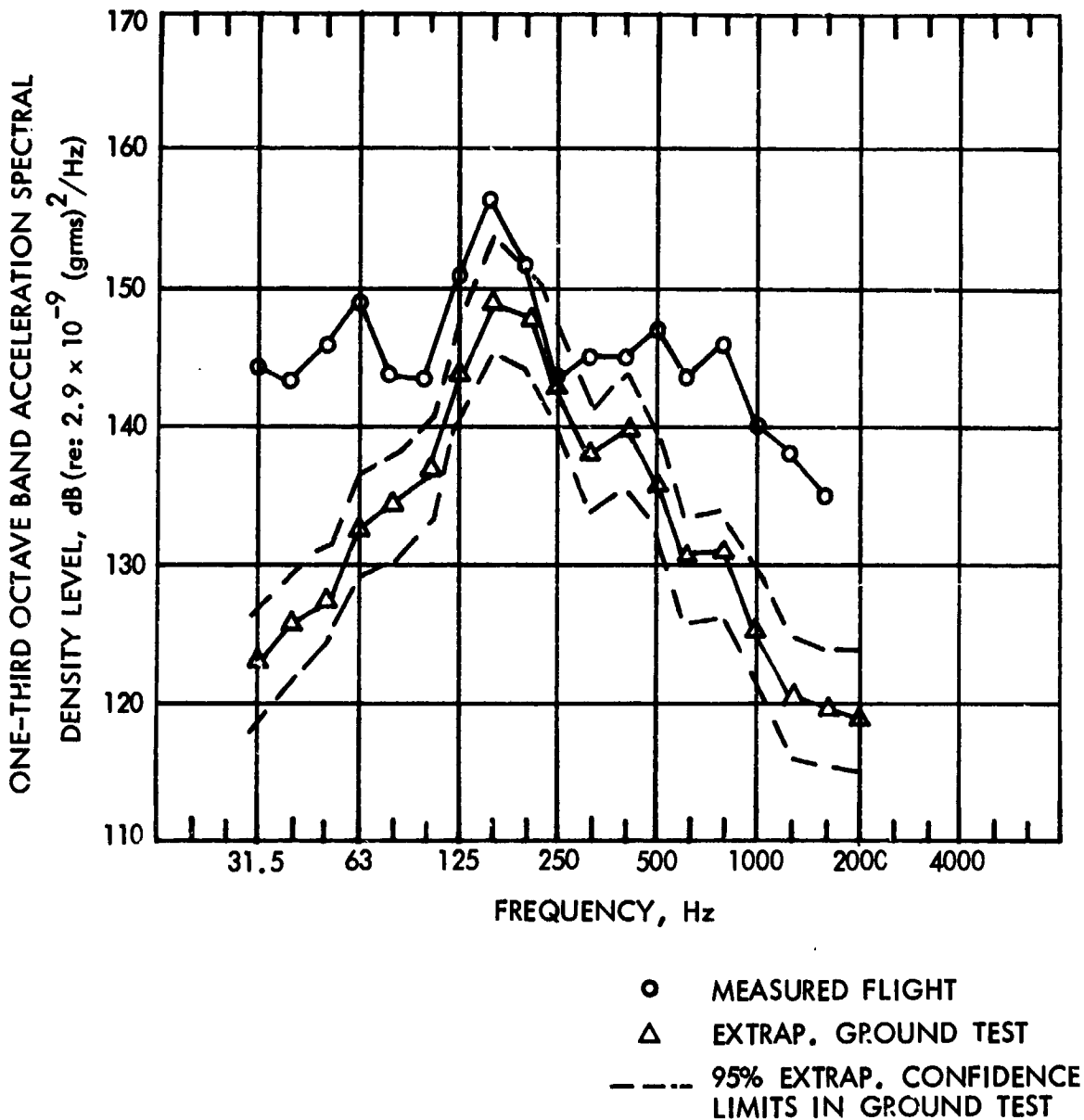


Figure 5-39. Measured and Extrapolated Test Acceleration Spectral Density Level for OSS-1, Cold Plate Edge, Accelerometer 9301, Normal to Plate

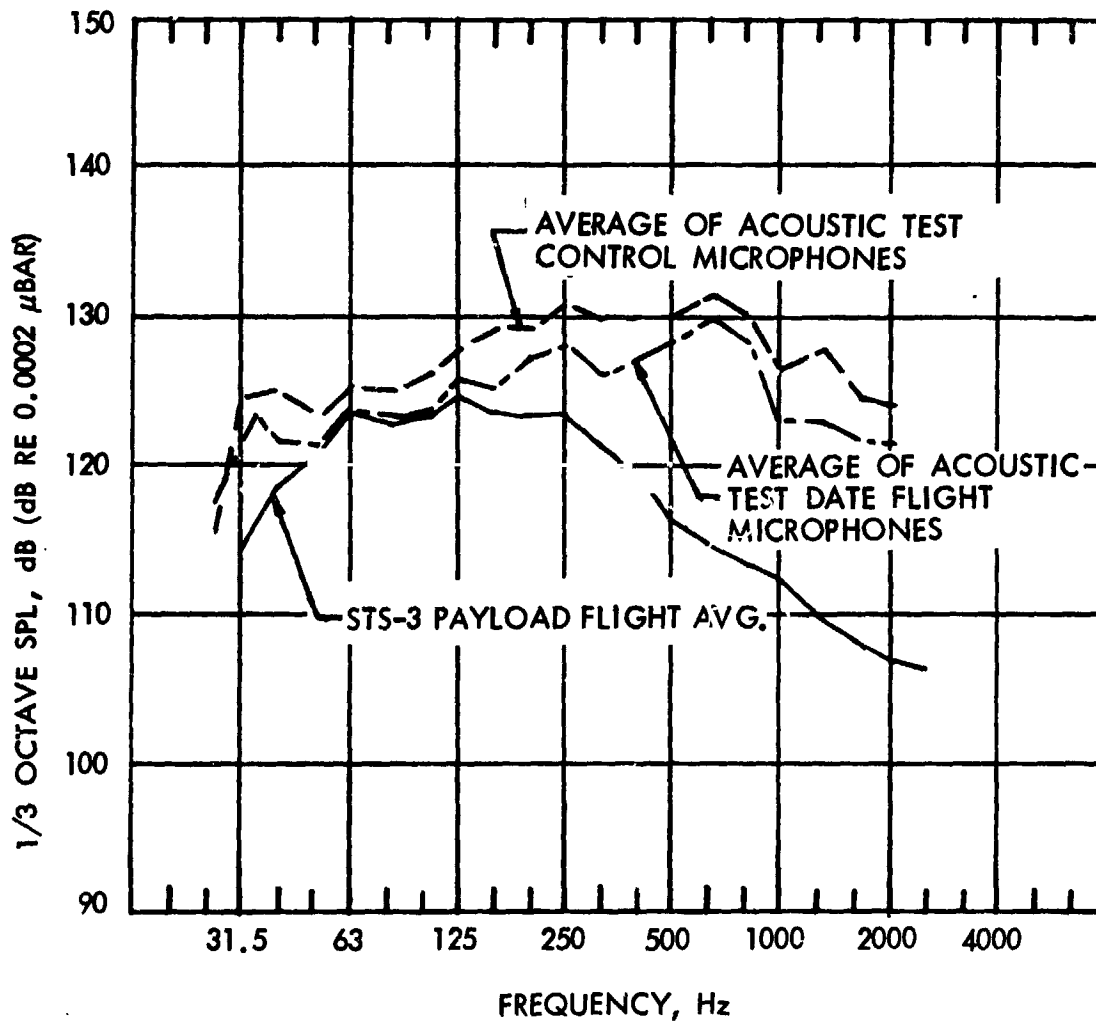


Figure 5-40. STS-3/OSS-1 vs. Acoustic Ground Test Payload Acoustic Environment

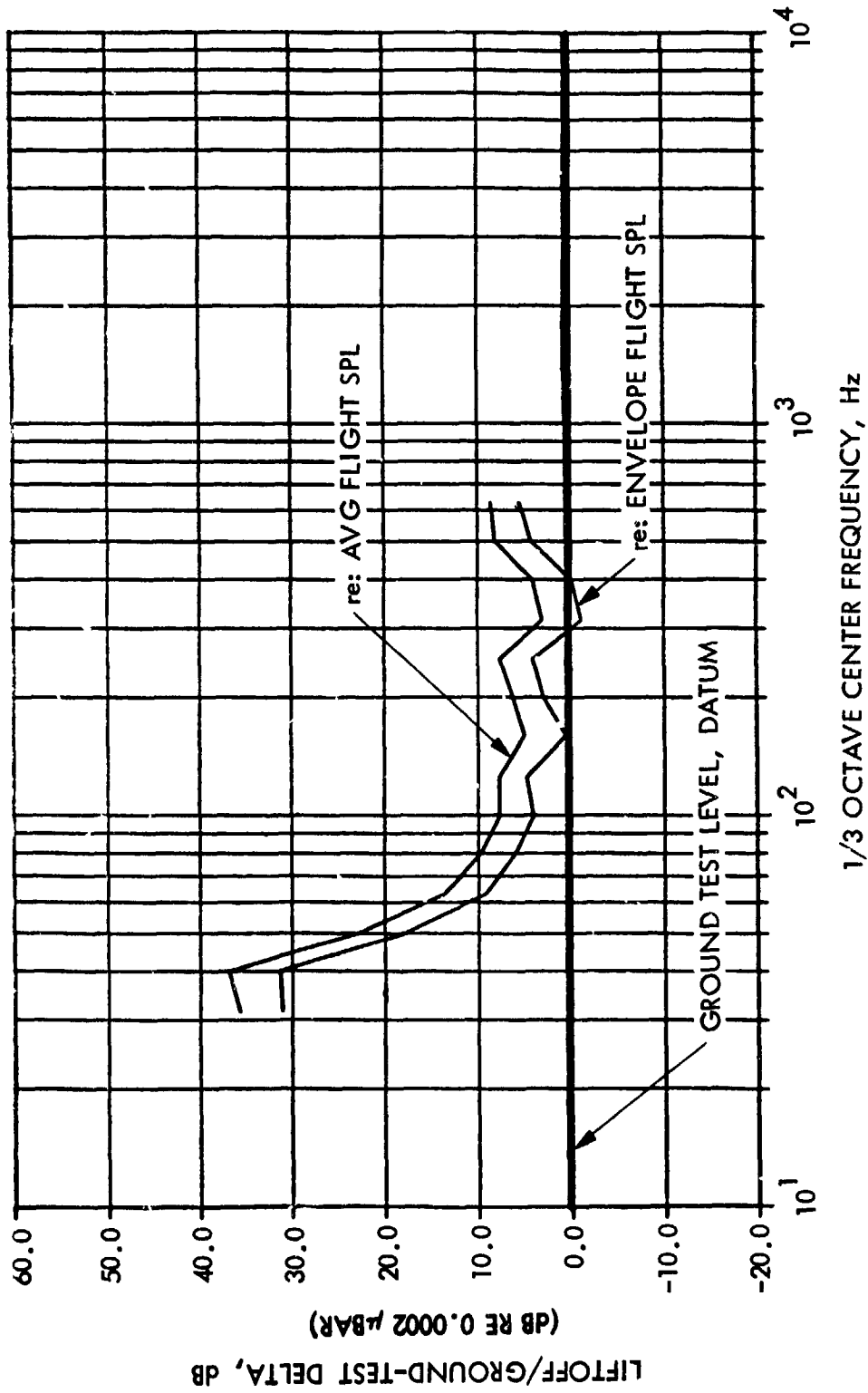
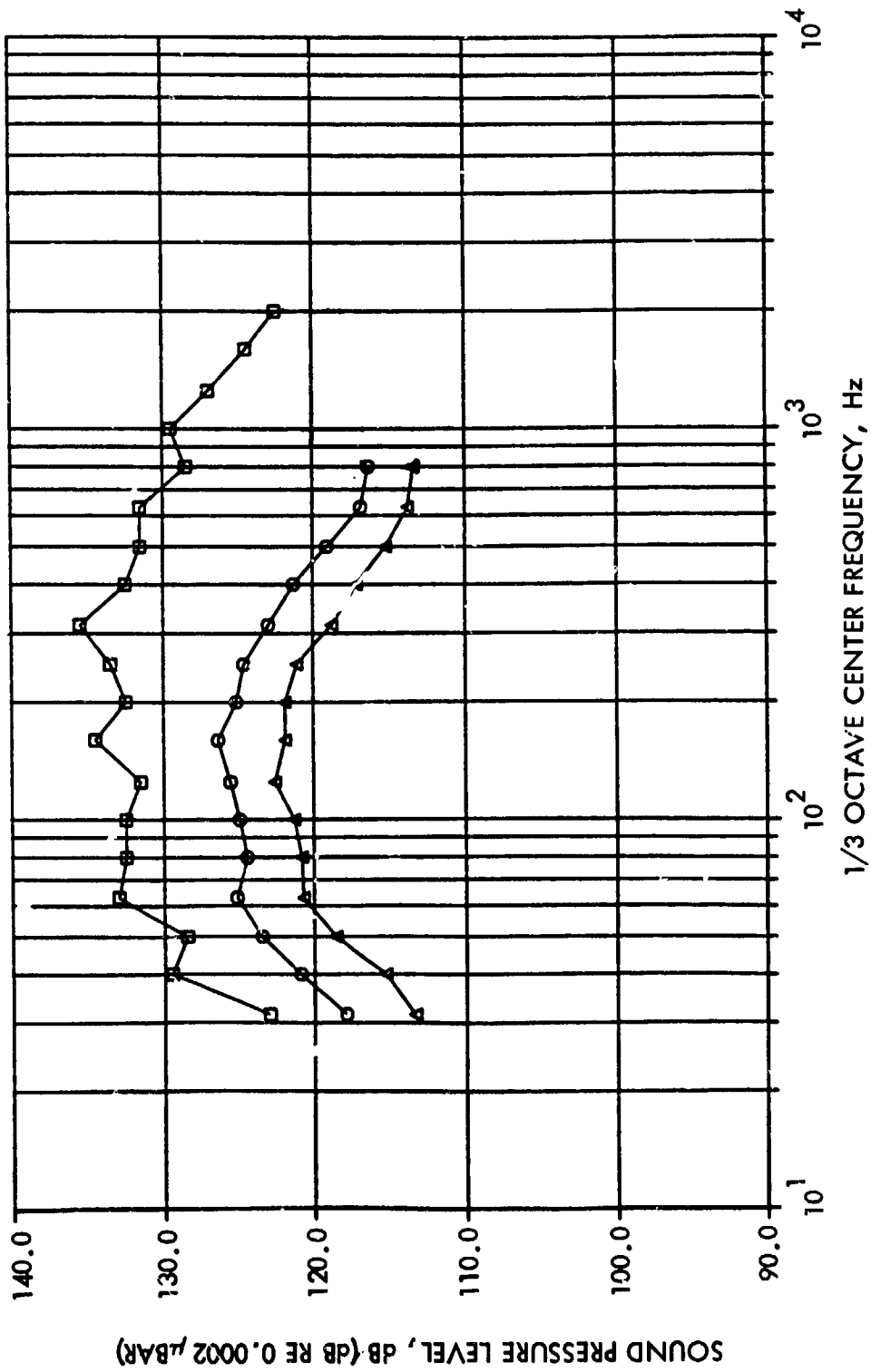


Figure 1. Comparison of STS-4 Flight and Ground Test Vibration Data, DOD Pallet, Normalized to Extrapolated Ground Vibration Data.



- = GROUND TEST
- = ENVELOPE OF FLIGHT
- ▲ = AVERAGE OF FLIGHT

Figure 5-42. Ground Test and STS Liftoff Acoustic Comparisons

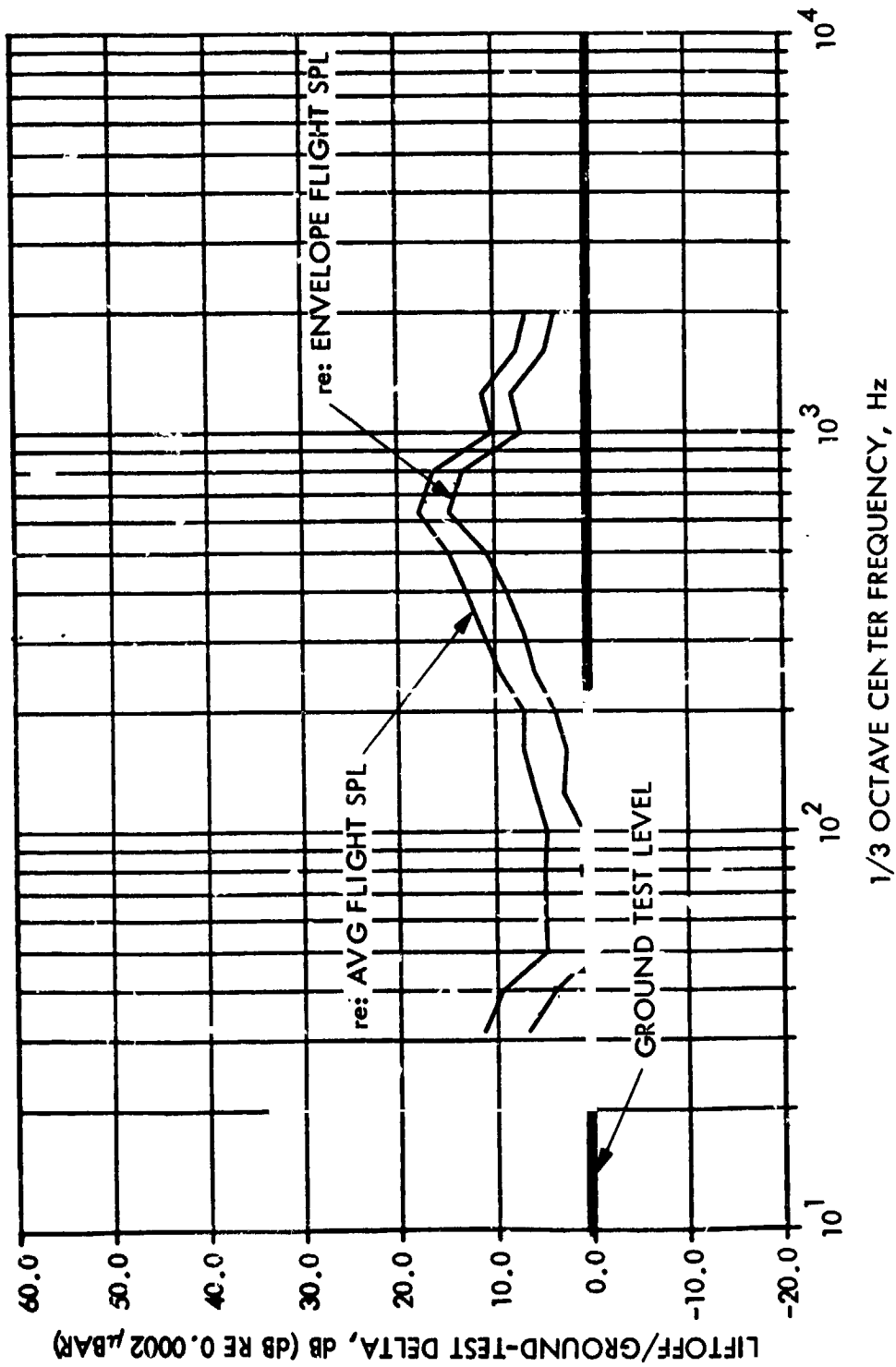
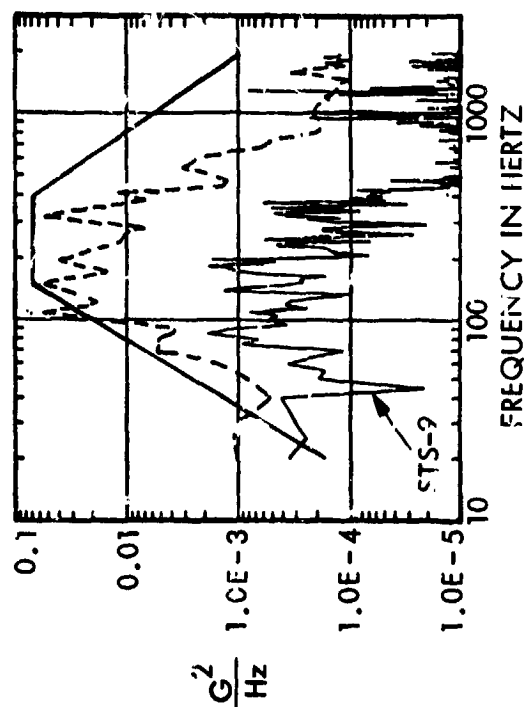
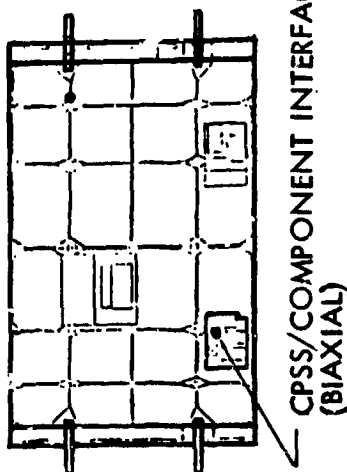
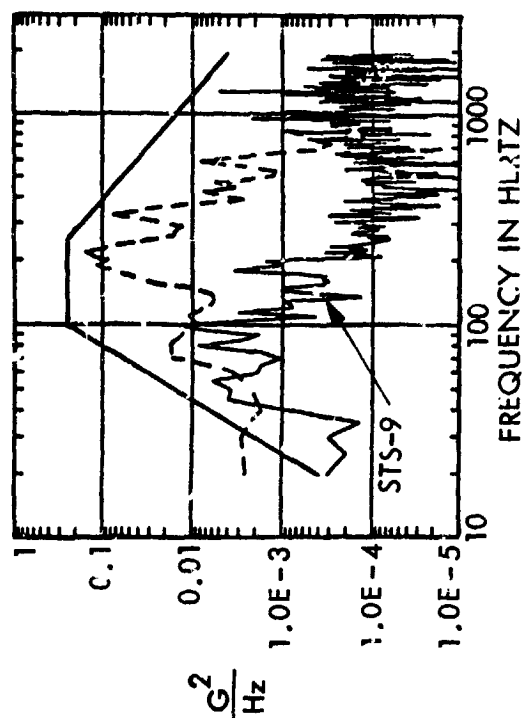


Figure 5-43. Comparison of SFS-3 Flight and Ground Test Vibration Data, OSS-1 Pallet, Normalized to Extrapolated Ground Vibration Data



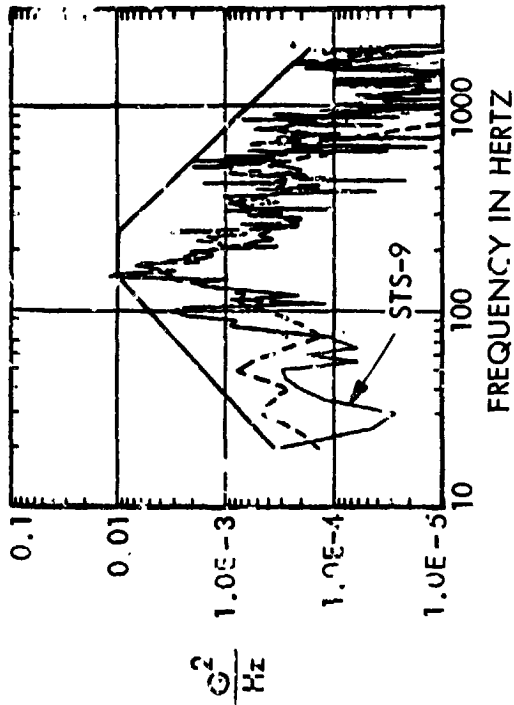
L05D8503A/TP04 OVERALL = 0.42 grms
 ACUSTIC TEST DATA OVERALL = 2.89 grms
 CRITERIA OVERALL = 5.98 grms



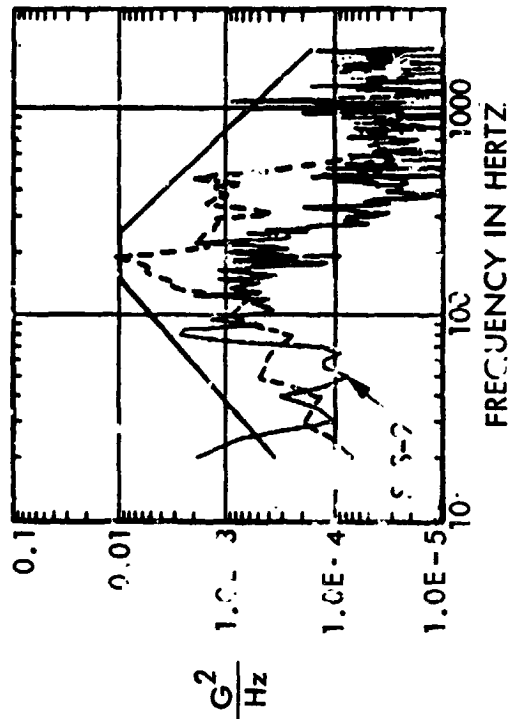
L05D8503A/TP00 OVERALL = 0.85 grms
 ACUSTIC TEST DATA OVERALL = 2.70 grms
 CRITERIA OVERALL = 9.88 grms

NOTE: GROUND TEST VIBRATION DATA NORMALIZED TO 139 JB ACOUSTIC SPECTRUM

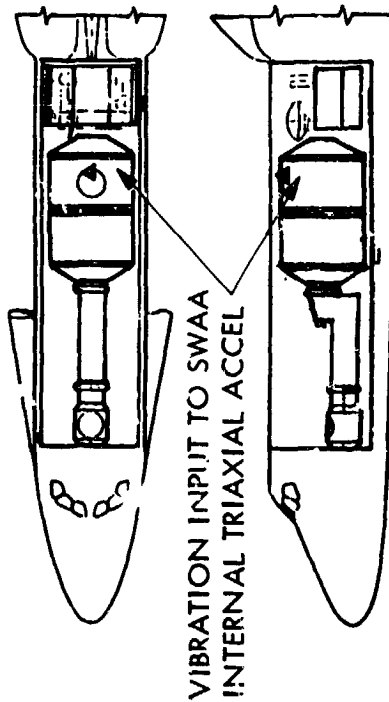
Figure 5-44. STS-9 Pallet CPSS/Component Interface Vibration, Ground Acoustic Test vs. Flight Vibration



L05D8802A/TP04 ——— OVERALL = 0.85 grms
 ACOUSTIC TEST DATA - - - - OVERALL = 0.65 grms
 CRITERIA ——— OVERALL = 1.94 grms



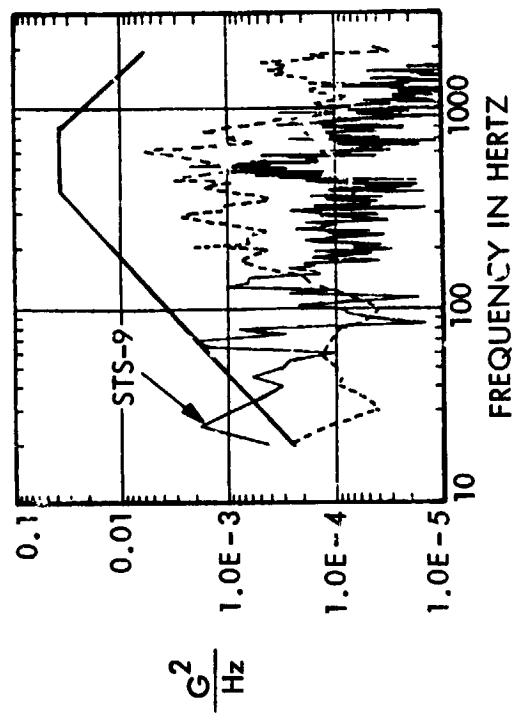
L05D8802A/TP04 ——— OVERALL = 0.50 grms
 ACOUSTIC TEST DATA - - - - OVERALL = 0.94 grms
 CRITERIA ——— OVERALL = 1.94 grms



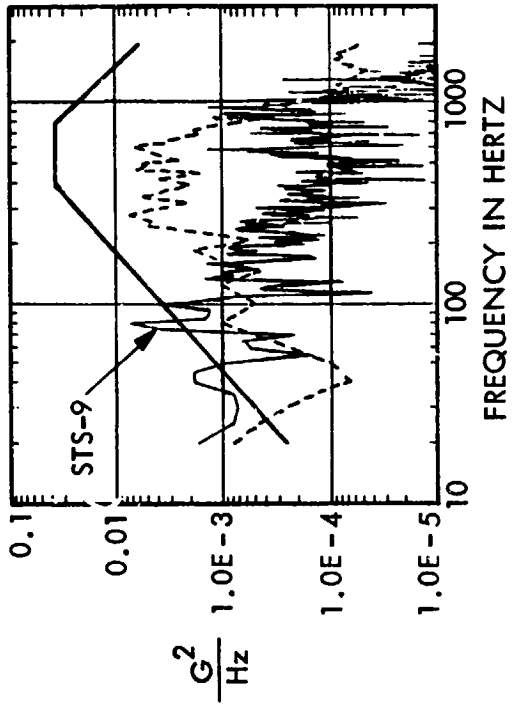
VIBRATION INPUT TO SWAA
 INTERNAL TRIAXIAL ACCEL

NOTE: GROUND TEST VIBRATION DATA
 NORMALIZED TO 139 dB
 ACOUSTIC SPECTRUM

Figure 5-45. STS-9 Vibration Input to SWAA at 1.3-m Ring, Ground Acoustic Test vs. Flight Vibration



L05D0010A/TP04 ——— OVERALL = 3.47 grms
 ACOUSTIC TEST DATA - - - - OVERALL = 1.10 grms
 CRITERIA ——— OVERALL = 6.17 grms



L05D0011A/TP04 ——— OVERALL = 3.67 grms
 ACOUSTIC TEST DATA - - - - OVERALL = 1.49 grms
 CRITERIA ——— OVERALL = 6.17 grms

NOTE: GROUND TEST VIBRATION DATA
 NORMALIZED TO 139 dB
 ACOUSTIC SPECTRUM

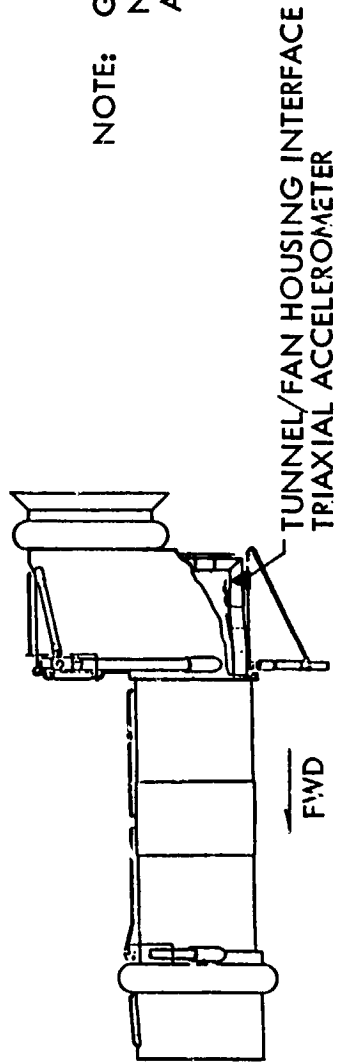


Figure 5-46. STP-9 Spacelab Fan Housing Interface Vibration, Ground Acoustic Test vs. Flight Vibration

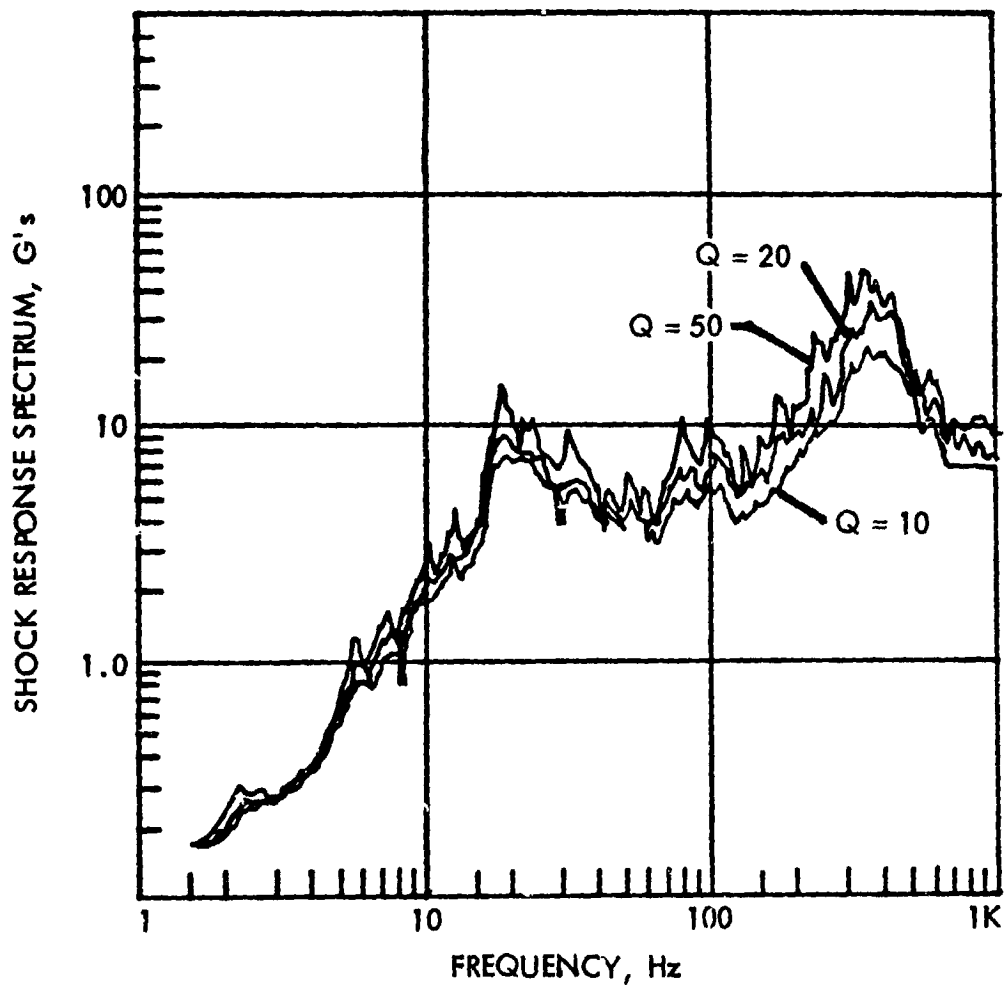


Figure 5-47. OCE Shelf Shock Response Spectrum Time Envelope, Accelerometer 9247, STS-2

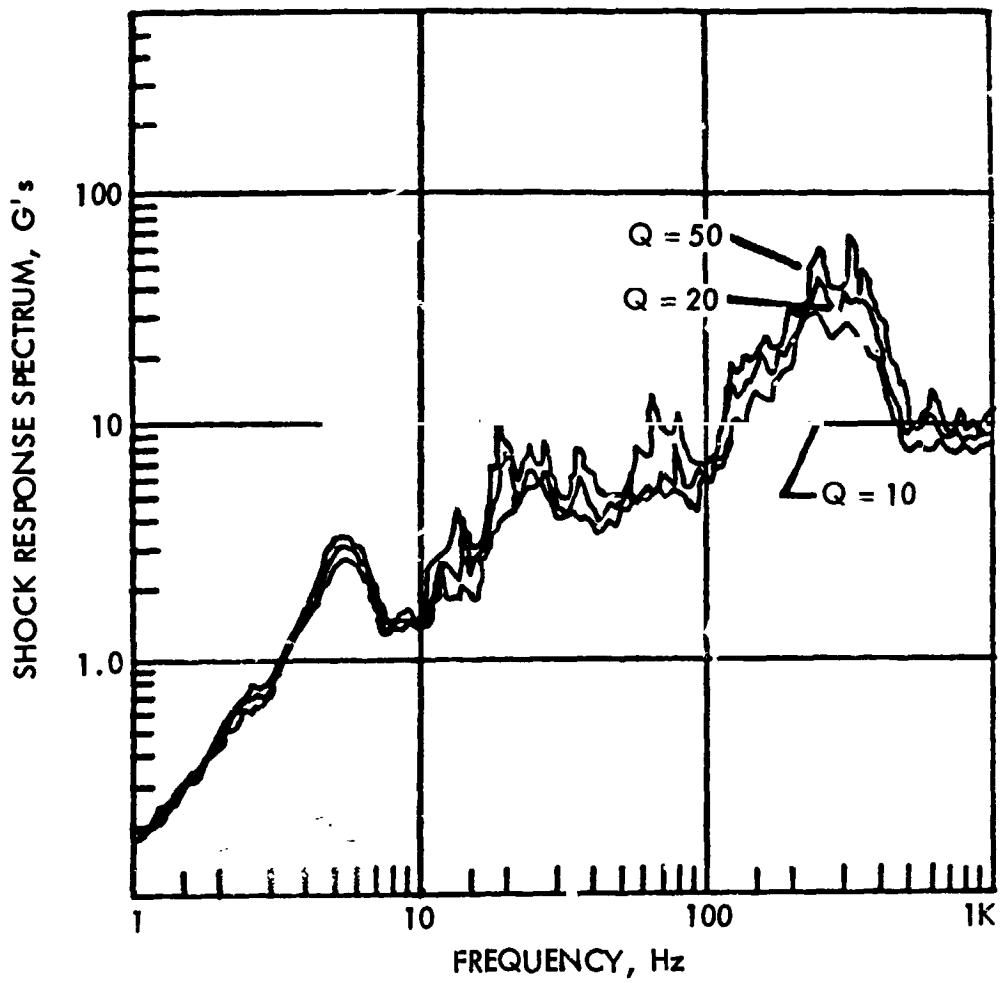


Figure 5-48. OCE Shelf Shock Response Spectrum Time Envelope, Accelerometer 9048, STS-2

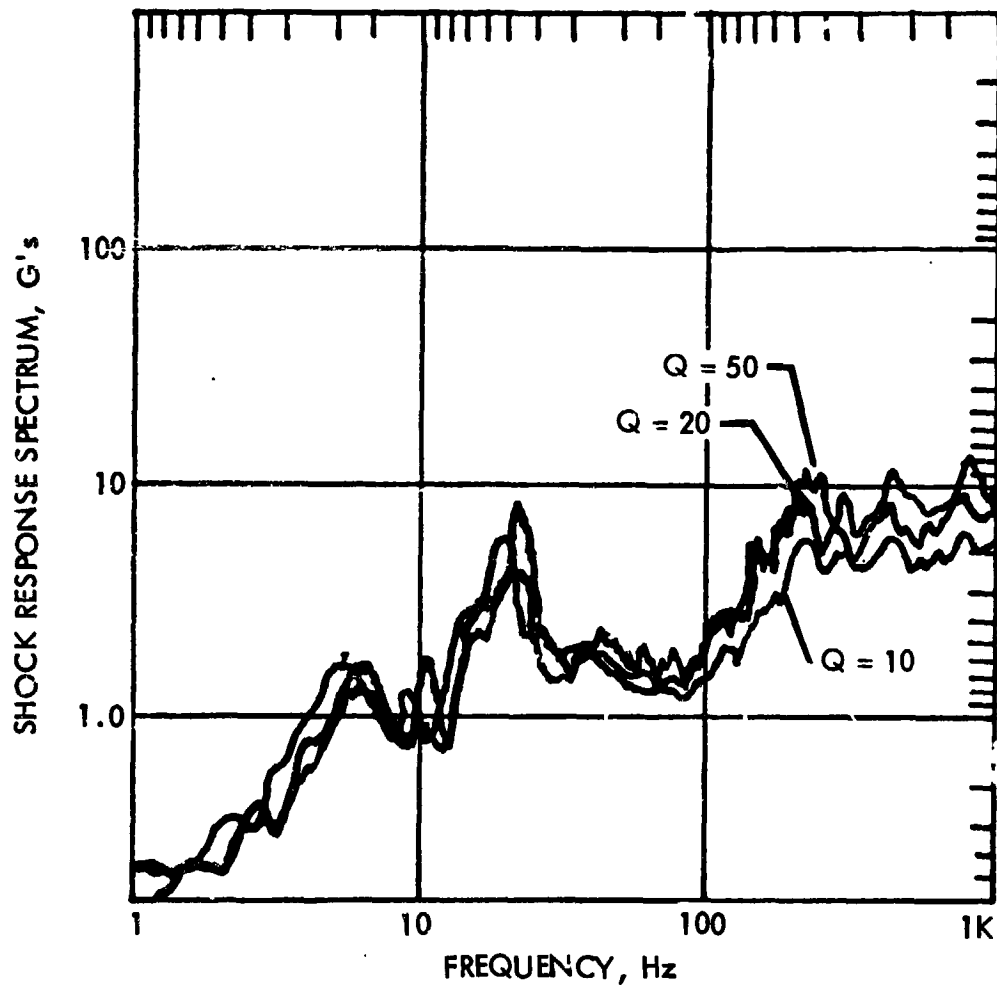


Figure 5-49. DFI Pallet Beam Shock Response Spectrum Time Envelope, Accelerometer 9273, STS-3

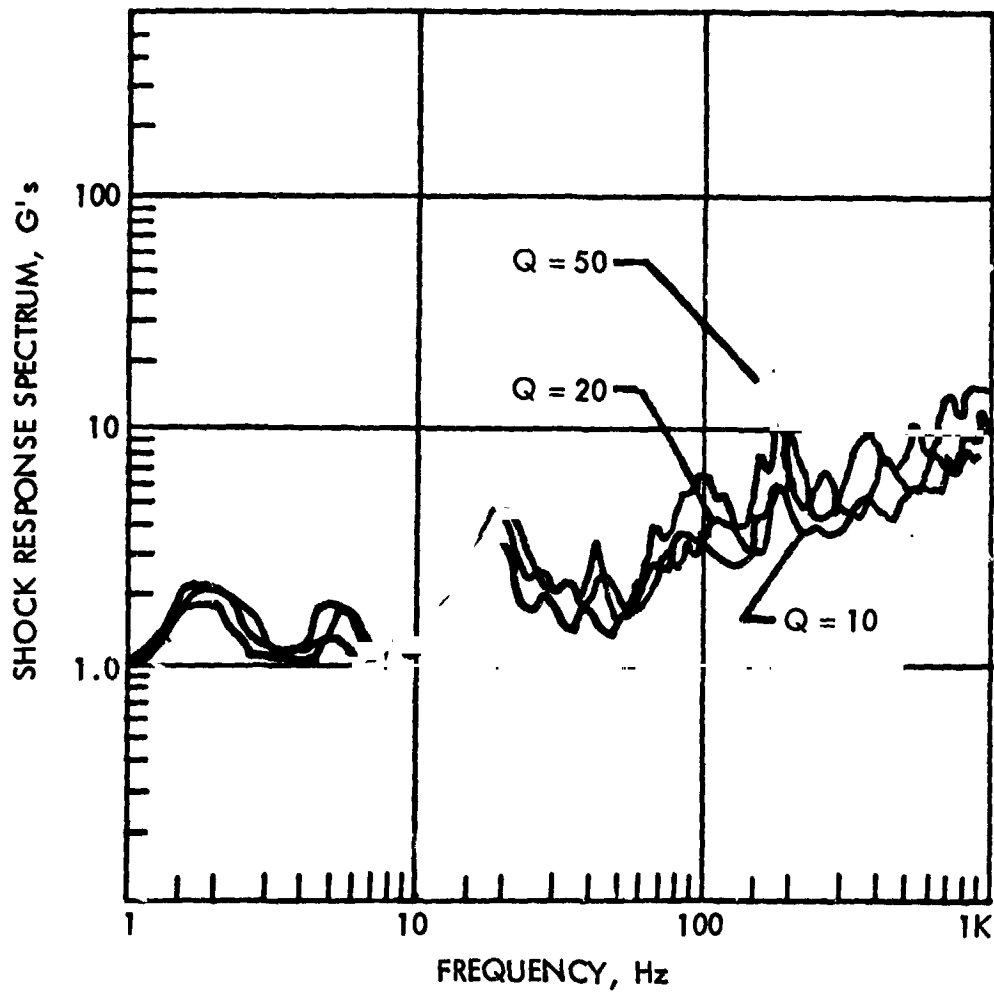


Figure 5-50. DFI Pallet Beam Shock Response Spectrum Time Envelope, Accelerometer 9274, STS-3

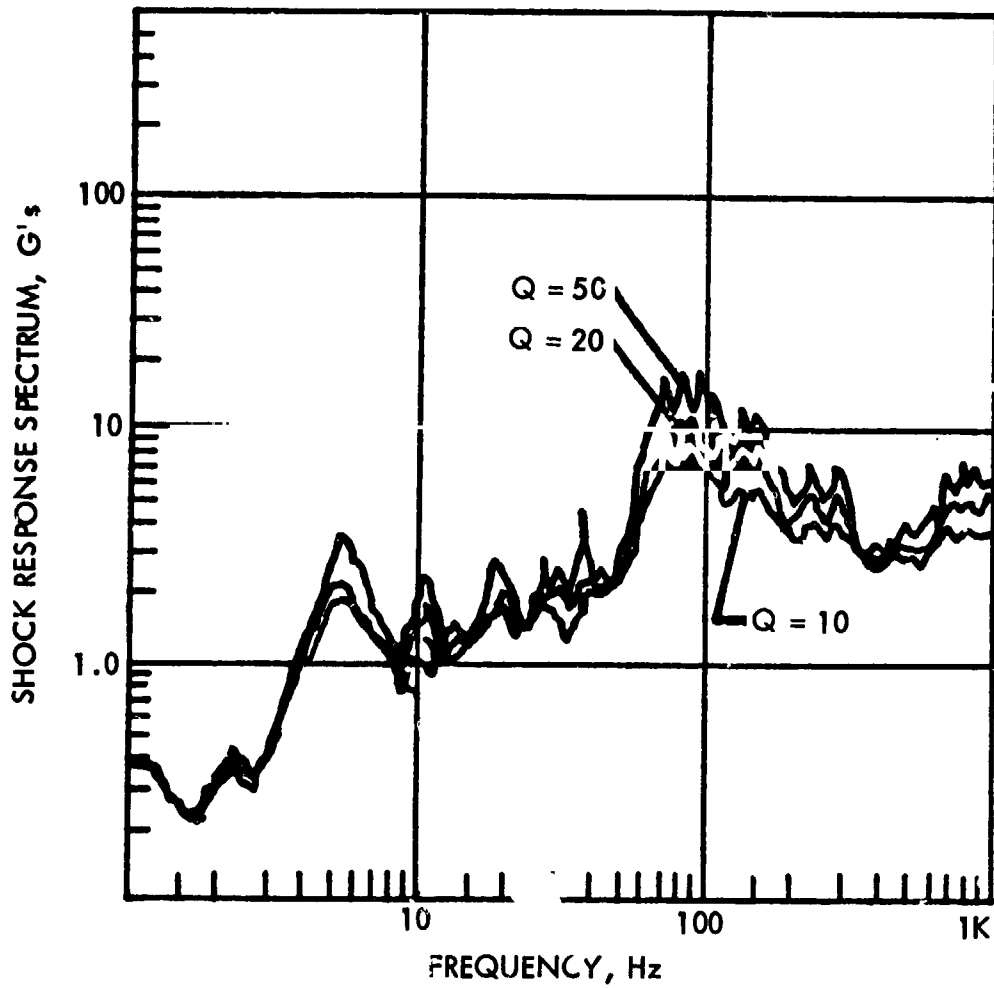


Figure 5-51. Cold Plate Side, Shock Response Spectrum Time Envelope, Accelerometer 9300, STS-3

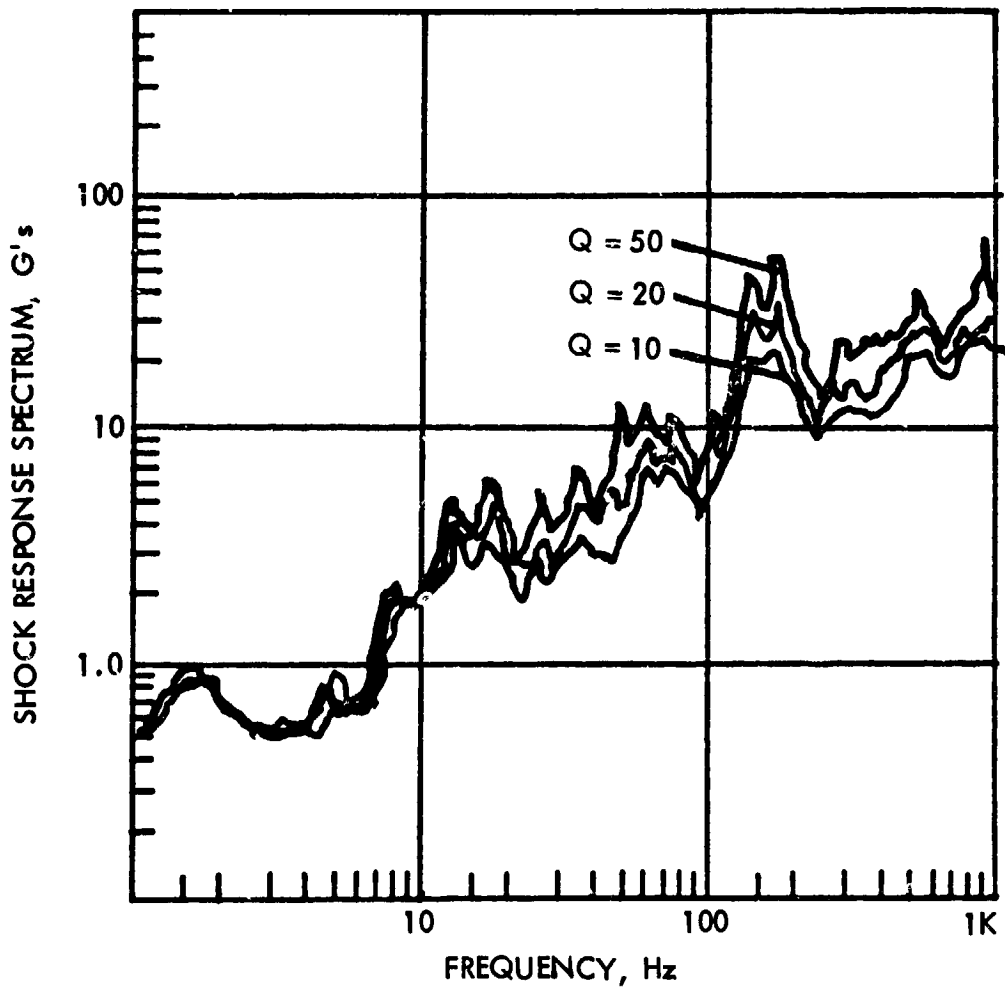


Figure 5-52. Cold Plate Side, Shock Response Spectrum Time Envelope, Accelerometer 9301 STS-3

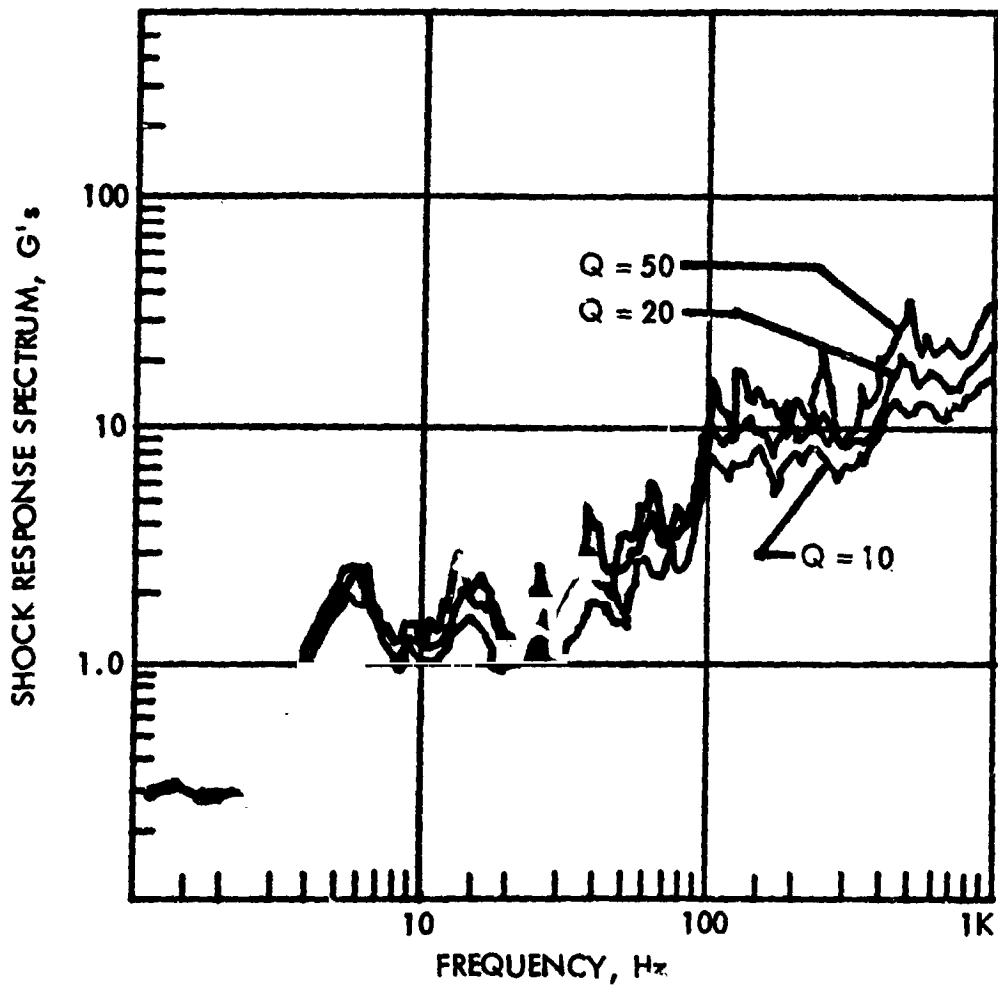


Figure 5-53. Thermal Can Base Shock Response Spectrum Time Envelope, Accelerometer 9292, STS-3

5.3 Low Frequency Vibration

The definition of the loads or low frequency environment is required for the design of the main load carrying payload structures. In general, the frequency regime which is of concern for primary structure is 0 to 50 Hz and the methodology for obtaining design loads is deterministic rather than statistical. The loads environment is, in general, dependent on the dynamic characteristics of the coupled payload/launch vehicle system and the frequency content of the external forcing functions. The objectives of flight response measurements in the low frequency or loads regime differ from the objectives of measurements in the vibroacoustic regime in that the latter aims to define the flight environment statistically while the former requires instrumentation for the verification of methodology. The low frequency data evaluation is summarized in Reference 31.

On STS-2 through STS-5 the payloads were relatively lightweight and several dynamic response measurements were made in identical locations on all five flights of the Orbiter Vehicle (OV) 102 launch vehicle. The location of the DFI accelerometers is shown in Figure A-6 and Table A-2. Of the DFI accelerometers, the two in the crew cabin and the three on the aft bulkhead are considered to be physically far enough removed from the payloads to provide meaningful comparisons for flight-to-flight variations. Of the DATE supplied instrumentation, four 0-50 Hz measurements were common on STS-2 and STS-3. These measured the input to the DFI pallet on the Orbiter side and will be used for an assessment of variations of the responses for these two flights. The DFI pallet beam centerline carried identical 1.5 to 50 Hz accelerometers on STS-2, STS-4, and STS-5. Data from these measurements will be used to assess the variations in response for those three flights. The DATE sensor locations at the DFI pallet which are used to study flight-to-flight variation are shown in Figures A-6 and A-7 and Table A-1.

Flight-to-flight variations can be assessed for only four flights, STS-2 through STS-5. The STS-1 data must be excluded as being not representative because, subsequent to the STS-1 flight, the launch pad was modified to alleviate the vehicle response due to overpressure. Some measurements from the STS-2 through STS-5 flights cannot be used for such a flight-to-flight comparison because of the effect of payload impedance.

5.3.1 Low Frequency Response During Ascent

For purposes of analytical predictions the ascent event is considered to be one event encompassing the Space Shuttle Main Engine (SSME) ignition and the Solid Rocket Booster (SRB) ignition. For purposes of assessing flight-to-flight variations these two events will be examined separately.

5.3.1.1 Low Frequency Response During Main Engine Ignition

Variations in the response spectra for the crew cabin y and z directions for STS-2 through STS-5 are shown in Figures 5-54 and 5-55, respectively. Similar data for the aft bulkhead response in the x, y, and z directions are shown in Figures 5-56 through 5-58. The above data has been derived from the DFI accelerometers and is valid in the frequency range 0-14 Hz. The duration of the event analyzed has been chosen to cover any appreciable dynamic response. The time interval bounded varied from 2.8 seconds for STS-2, 4.0 seconds for STS-3, to 5.0 seconds for STS-4 and STS-5.

5.3.1.2 Low Frequency Response During Solid Rocket Booster Ignition

The response data from the Orbiter crew cabin and the aft bulkhead is repeated for the SRB ignition in Figures 5-59 through 5-63. Variations of response measurements for STS-2 and STS-3 at the interface of the DFI pallet on the Orbiter side are shown in Figures 5-64 through 5-67. These data have been derived from the DATE accelerometers and are valid in the frequency range 0-50 Hz. Note that the data shown in Figures 5-65 and 5-66 represent z direction responses at the right- and left-hand side of the vehicle, respectively. These data are an indication of the symmetry of the responses. Figures 5-68 through 5-70 show the variation of the responses of the DFI pallet beam centerline for STS-2, STS-4 and STS-5 in the x, y, and z directions. The latter data is obtained from DATE accelerometers and is valid from 1.5 to 50 Hz. All SRB ignition has been derived from 9 second intervals.

5.3.2 Low Frequency Response During Landing

For purposes of analytical prediction, the landing event is considered to be one event encompassing the main landing gear touchdown and the nose gear touchdown. For purposes of assessing flight-to-flight variations, these two events are examined separately. In general, the landing event seems to have more dispersion than ascent. Of the five landings, STS-3 had by far the highest response. It was a near limit design load condition. Only a few representative response spectra are shown. The landing data from STS-4 was reduced treating both the main gear touchdown and the nose gear touchdown as one event and hence is not directly comparable with the other flights.

In general, all the landing events have been quite symmetrical, that is, the z-responses on the right- and left-hand side of the Orbiter were comparable.

5.3.2.1 Low Frequency Response During Main Landing Gear Touchdown

Response spectra plots for the bulkhead accelerometer in the z-direction for STS-2, STS-3, and STS-5 are shown in Figure 5-71. These data are valid for the 0-14 Hz region. The time interval used was 4.0 seconds for STS-2 and STS-3 and 6.0 seconds for STS-5.

5.3.2.2 Low Frequency Response During Nose Gear Touchdown

Response spectra plots of the crew cabin accelerometer in the z-direction for STS-2, STS-3, and STS-5 are shown in Figure 5-72. These data are valid for the 0-14 Hz region. The time interval used was 4.0 seconds for STS-2 and STS-3 and 6.0 seconds for STS-5.

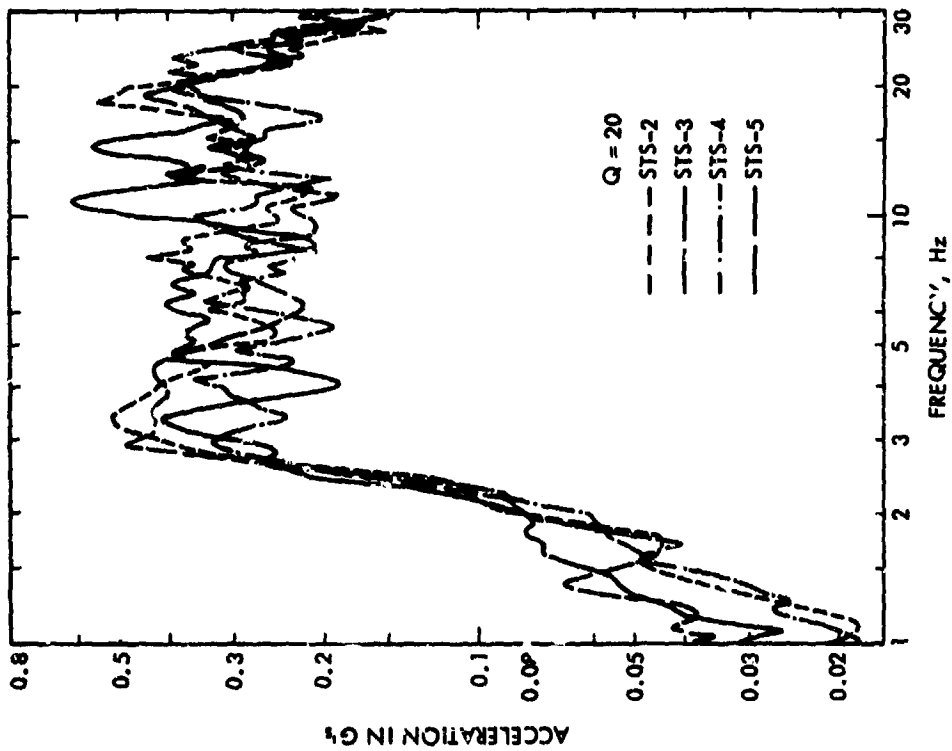


Figure 5-54. Response Spectra, Main Engine Ignition, Crew Cabin, Y Direction, Accelerometer V33A9215A

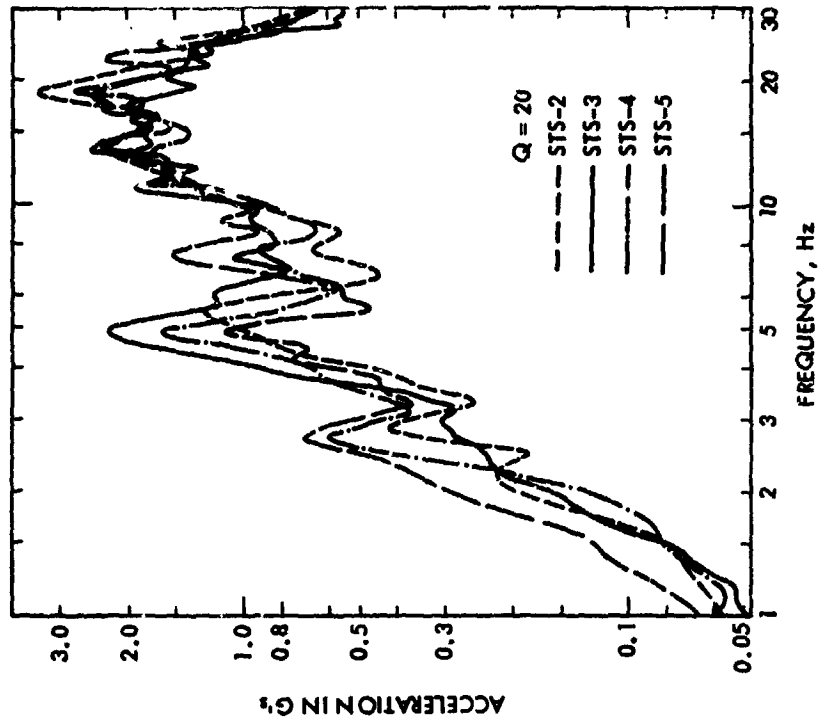


Figure 5-55. Response Spectra, Main Engine Ignition, Crew Cabin, Z Direction, Accelerometer V33A9216A

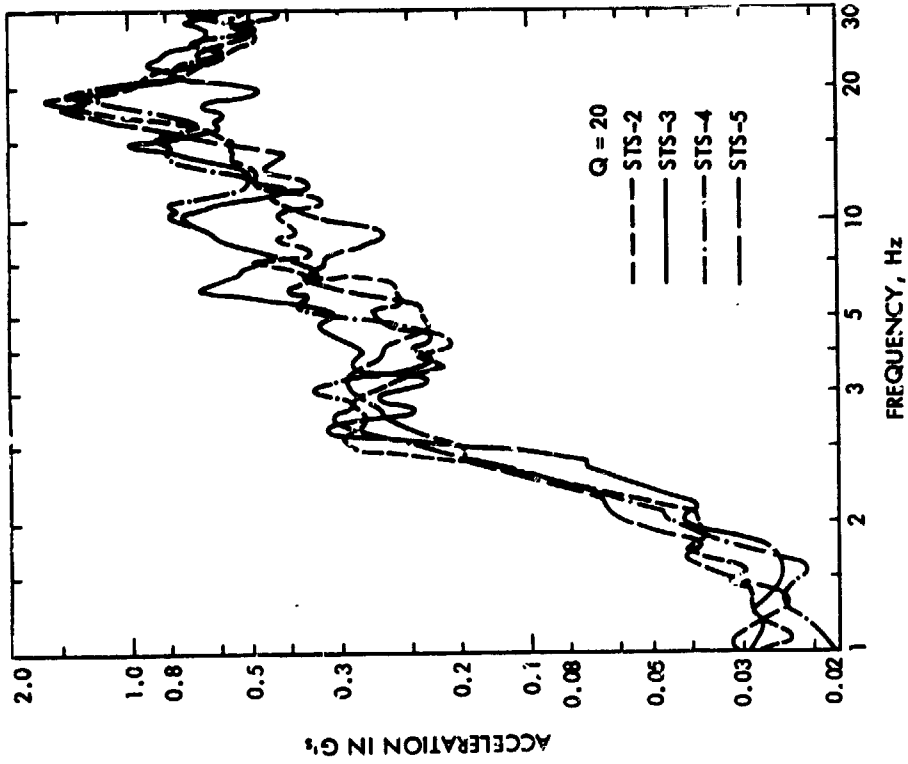


Figure 5-57. Response Spectra, Main Engine Ignition, Aft Bulkhead, Y Direction, Accelerometer V34A9435A

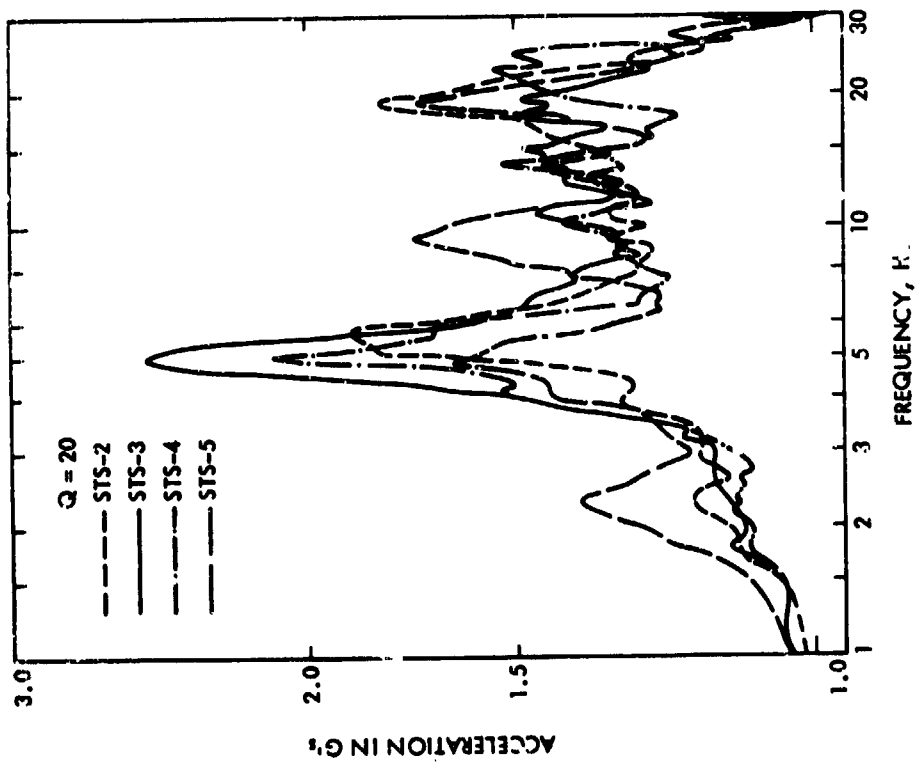


Figure 5-56. Response Spectra, Main Engine Ignition, Aft Bulkhead, X Direction, Accelerometer V34A9434A

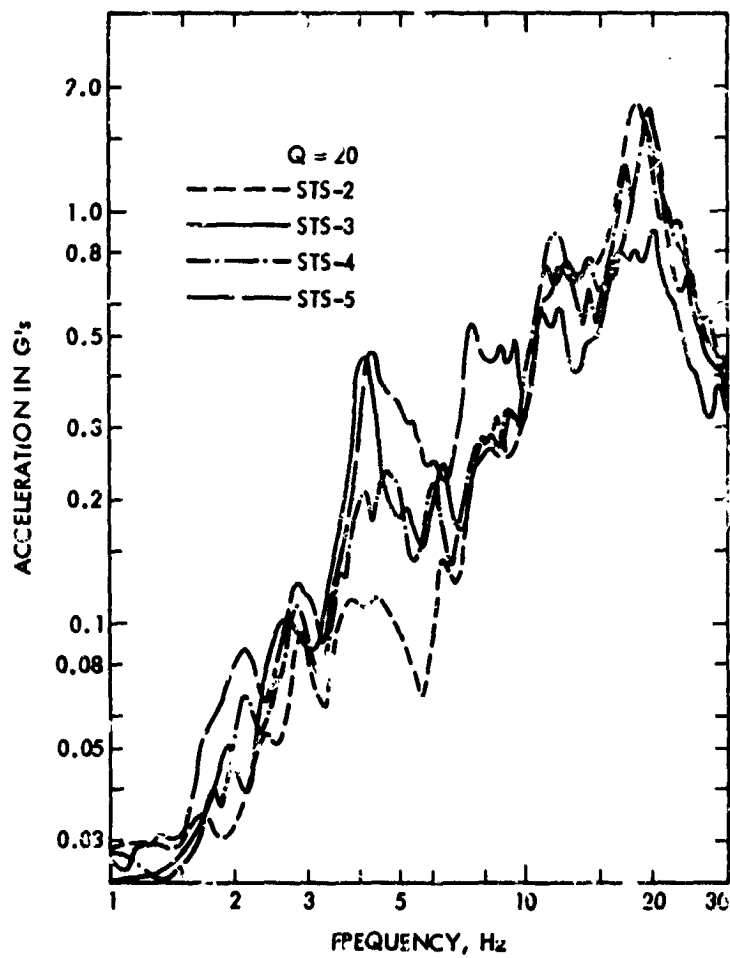


Figure 5-58. Response Spectra, Main Engine Ignition, Aft Bulkhead, Z Direction, Accelerometer V34A9436A



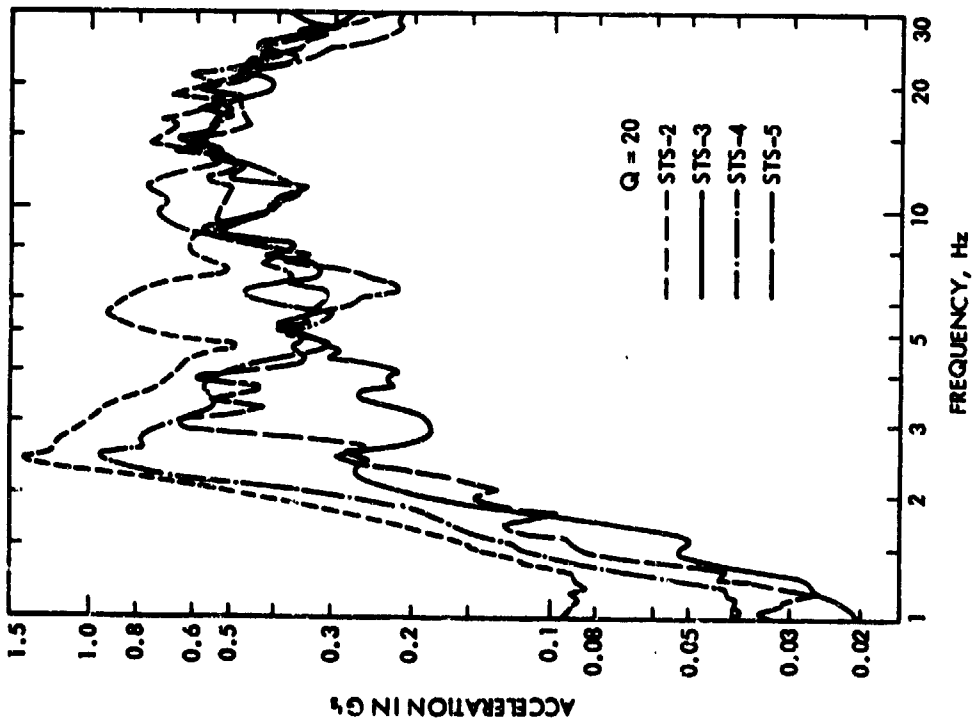


Figure 5-59. Response Spectra, Solid Rocket Booster Ignition, Crew Cabin, Z Direction, Accelerometer V33A9215A

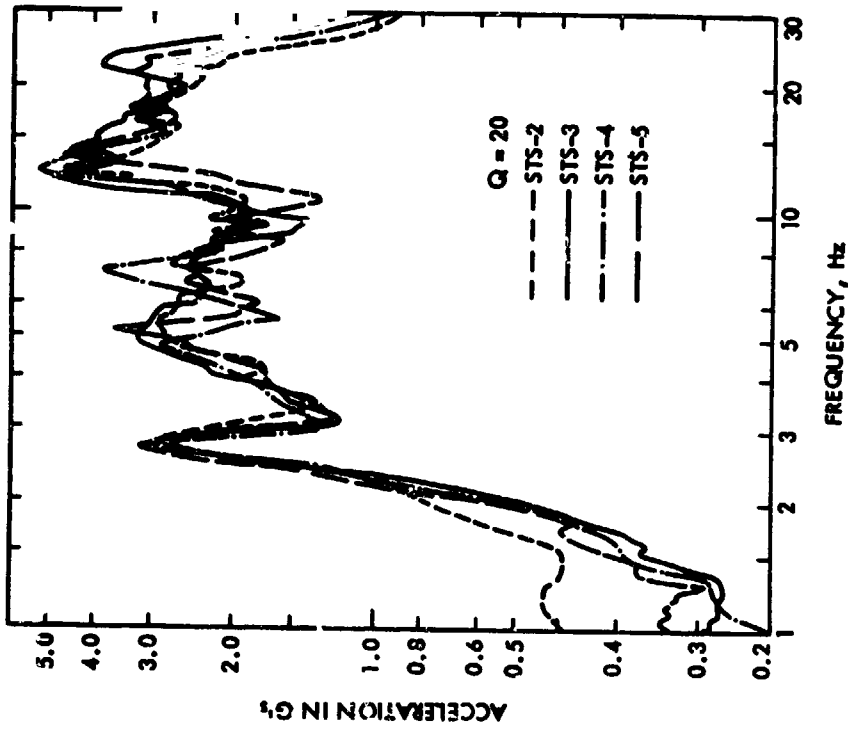


Figure 5-60. Response Spectra, Solid Rocket Booster Ignition, Crew Cabin, Z Direction, Accelerometer V33A9216A

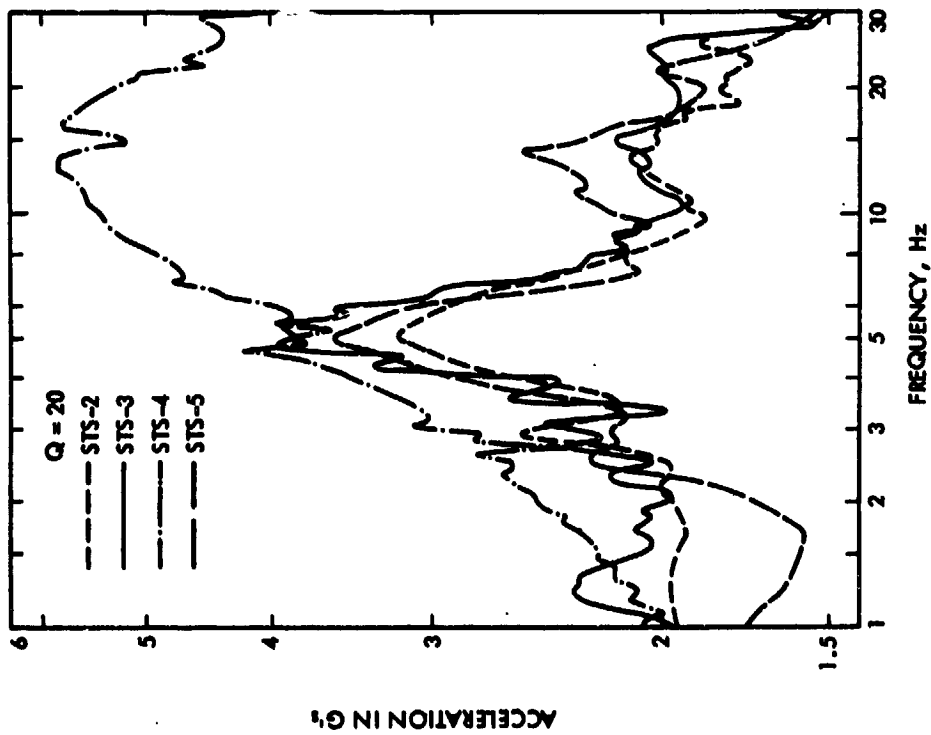


Figure 5-61. Response Spectra, Solid Rocket Booster Ignition, Aft Bulkhead, X Direction, Accelerometer V34A9434A

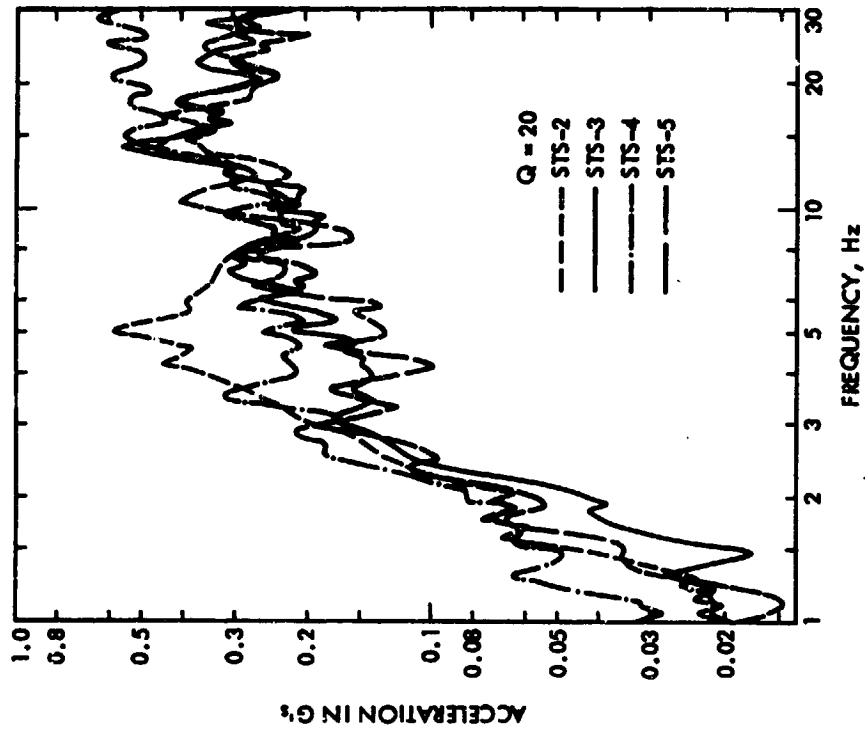


Figure 5-62. Response Spectra, Solid Rocket Booster Ignition, Aft Bulkhead, Y Direction, Accelerometer V34A9435A

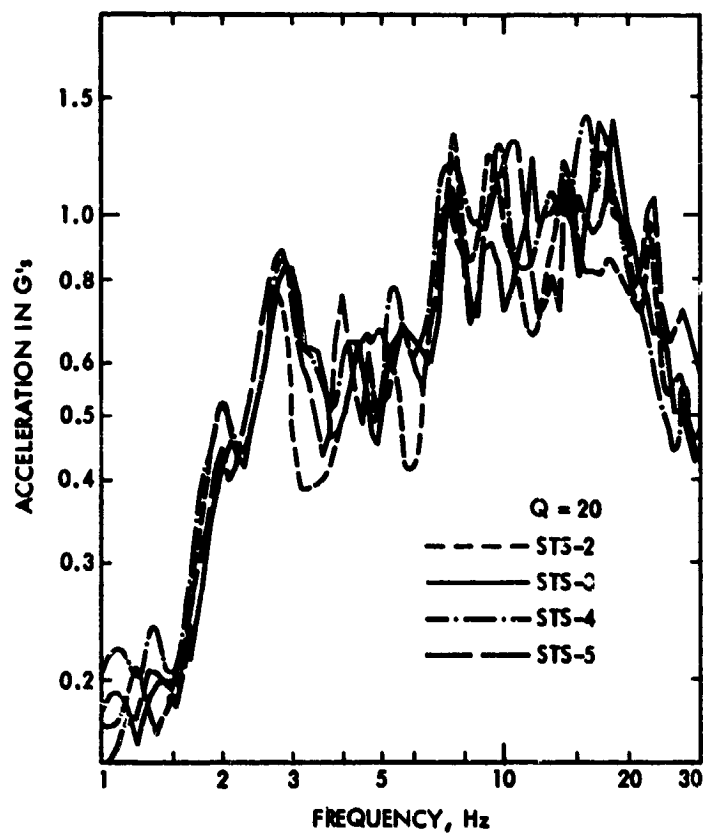


Figure 5-63. Response Spectra, Solid Rocket Booster Ignition, Aft Bulkhead, Z Direction, Accelerometer V3/A9436A

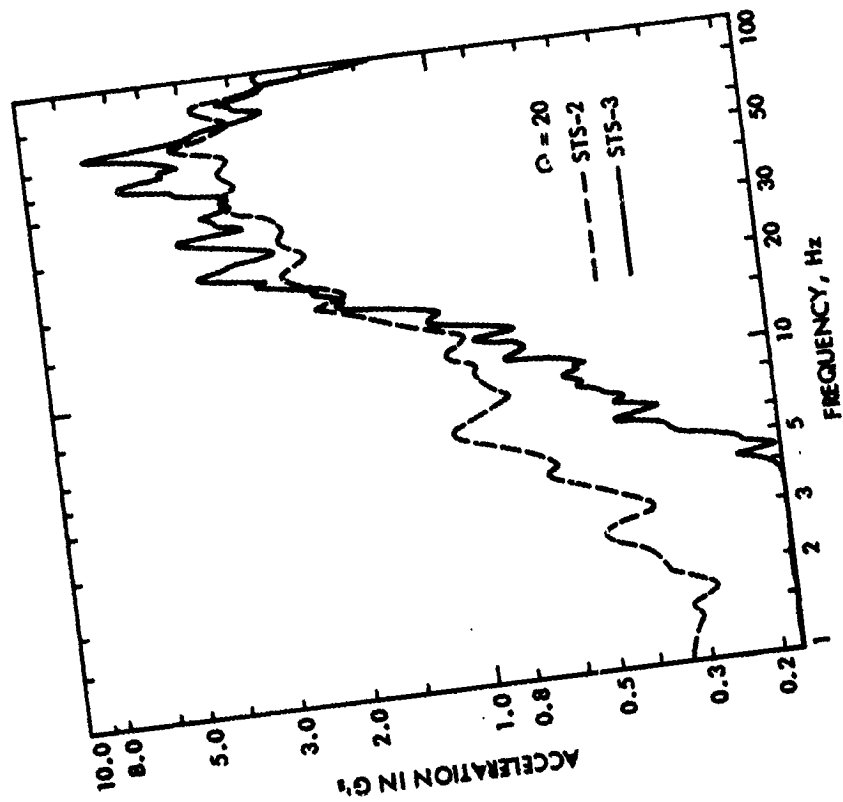


Figure 5-64. Response Spectra, Solid Rocket
Booster Ignition, Input to DFI
Pallet, Z Direction, Right-Hand
Bridge Fitting, Accelerometer
V08D9261A

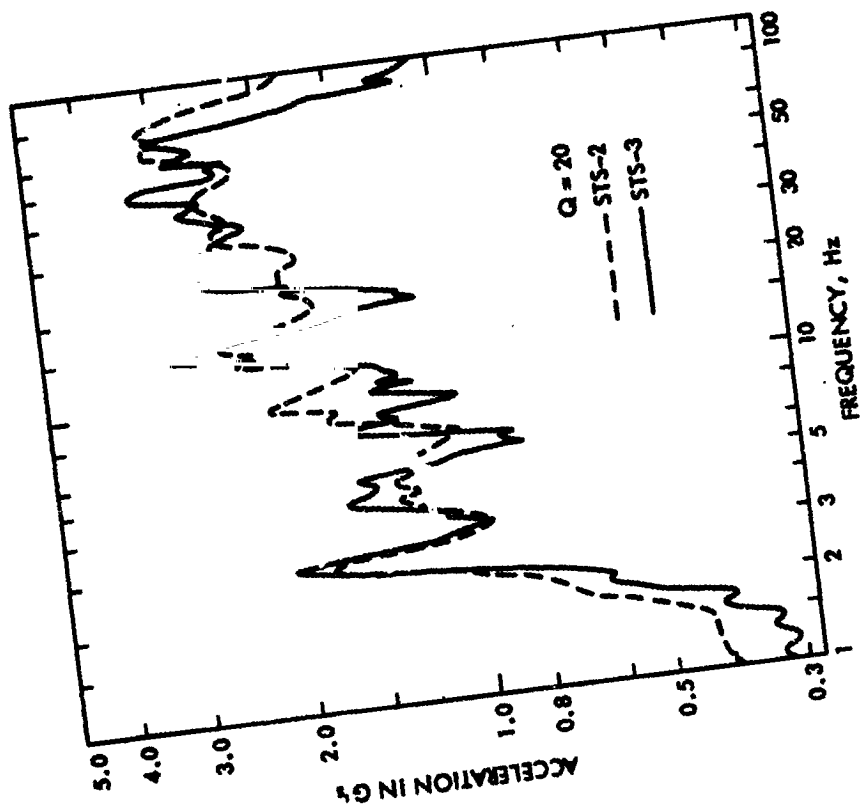


Figure 5-65. Response Spectra, Solid Rocket
Booster Ignition, Input to DFI
Pallet, Z Direction, Right-Hand
Bridge Fitting, Accelerometer
V08D9262A

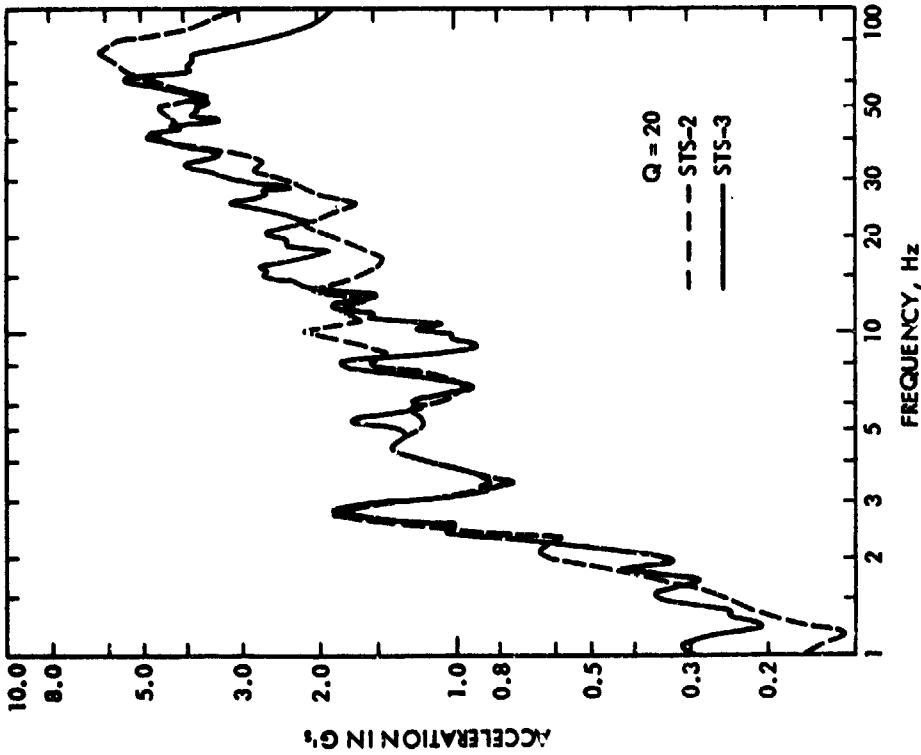


Figure 5-66. Response Spectra, Solid Rocket Booster Ignition, Input to DFI Pallet, Z Direction, Left-Hand Bridge Fitting, Accelerometer V08D9264A

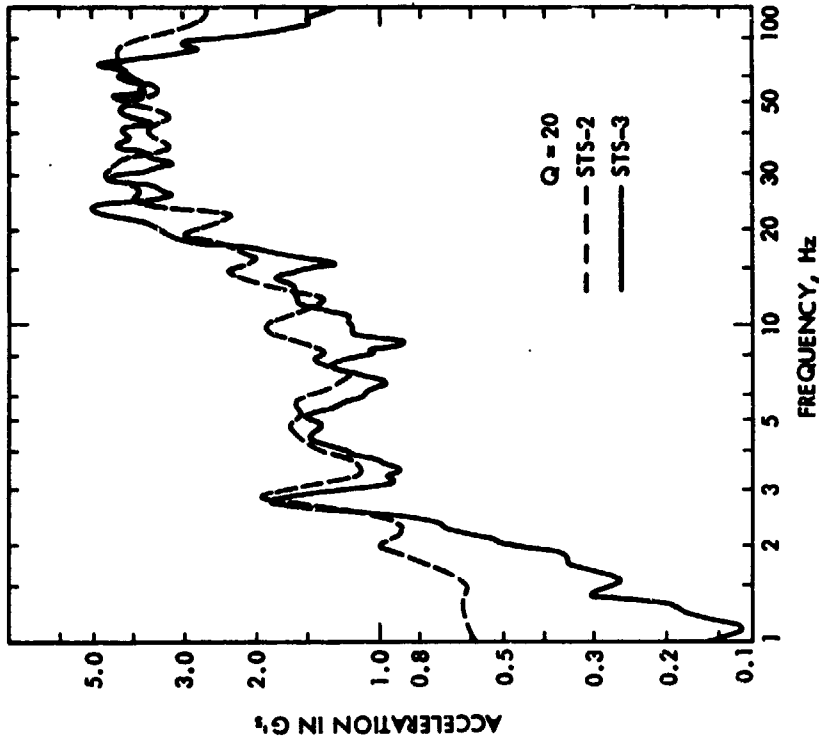


Figure 5-67. Response Spectra, Solid Rocket Booster Ignition, Input to DFI Pallet, Z Direction, Keel Bridge Fitting, Accelerometer V08D9265A

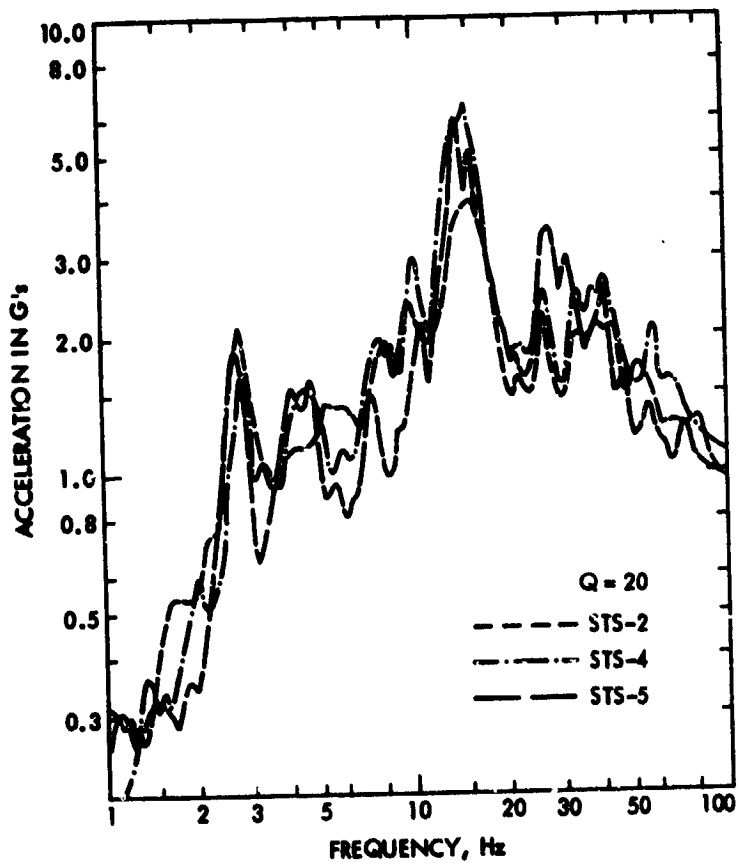


Figure 5-70. Response Spectra, Solid Rocket Booster Ignition, DFI Pallet Beam, Z Axis, Accelerometer V08D9269A

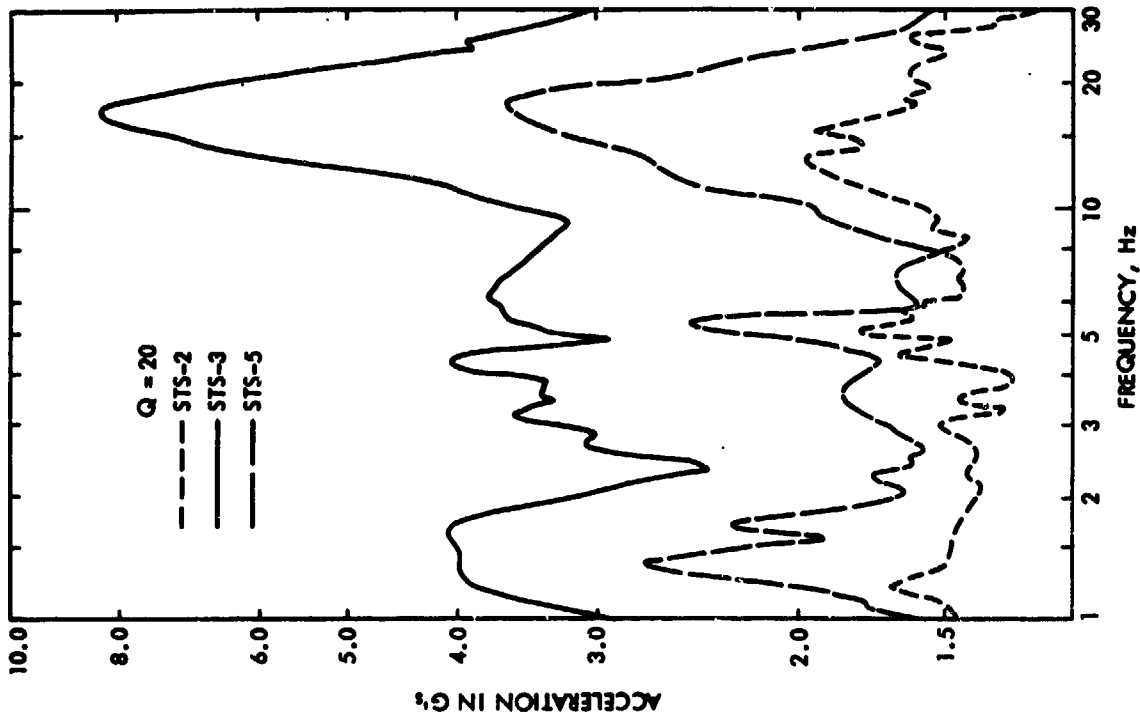


Figure 5-72. Response Spectra, Landing, Nose Landing Gear Contact, Crew Cabin, Z Direction, Accelerometer V33A9216A

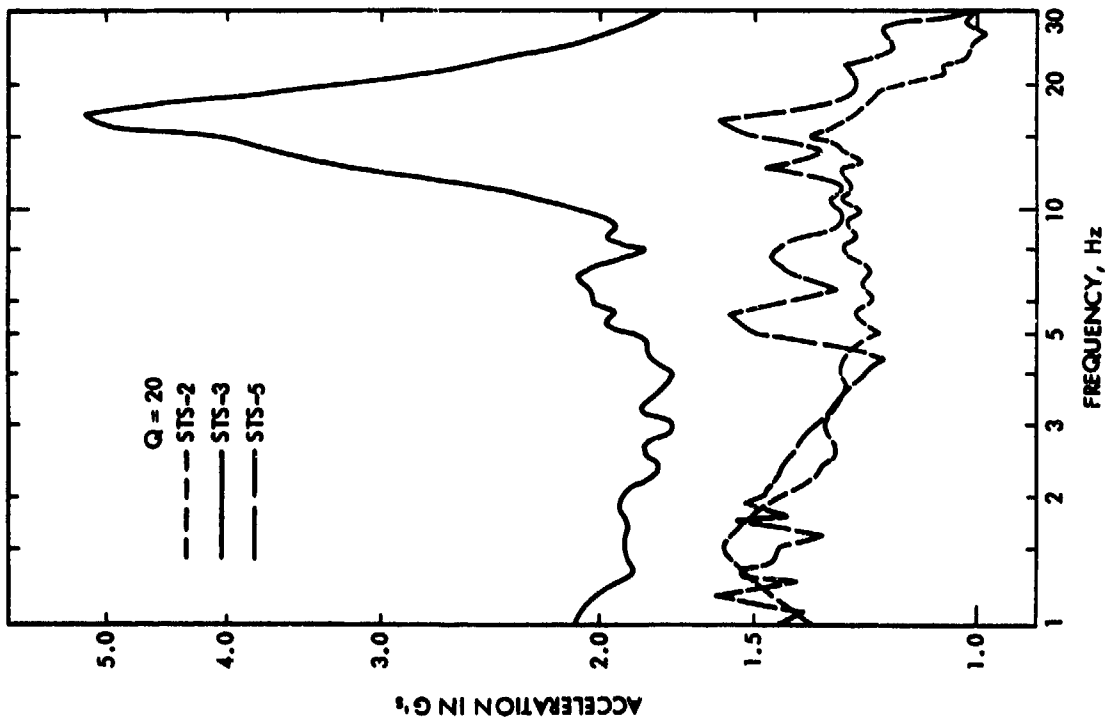


Figure 5-71. Response Spectra, Landing, Main Landing Gear Contact, Aft Bulkhead, Z Direction, Accelerometer V34A9436A

6.0 ENVIRONMENTAL UNCERTAINTIES

Assessment of the uncertainties in the shuttle dynamic environment is an important factor in predicting the environments for a payload. These uncertainties fall into two categories: bias errors or effects which may be predicted deterministically, and statistically independent random variables. Bias corrections, such as payload effects, are added directly to the mean bay environment. Spatial variations and flight-to-flight variations are statistically independent random variables important to STS acoustic environments. The root sum of the squares of these independent variations is added to the mean envelope. The errors in the data reduction and acquisition are not known for the particular data reduction facilities that reduced the DATE flight data and the errors may not be constant for each set of reduced data. Therefore, data reduction errors for the DATE data should be also treated as statistically independent.

6.1 Spatial Bias Errors

Spatial bias errors arise from the positioning of microphones in the non-diffuse bay perimeter or small numbers of microphones in the payload bay. The effect of the non-diffuse bay perimeter can be eliminated from the data set by only considering the payload microphones. When this is done, the standard deviation from the STS payload means are relatively small, indicating a uniform acoustic field for pallet payloads. Therefore, no spatial bias error corrections are necessary when the payload microphones are considered by themselves. When the perimeter microphones are included in an evaluation of the acoustic environment, the bias errors may become important. Bias error predictions were made for STS-1 through STS-3 by Bolt, Beranek and Newman (BB&N) in Reference 19. Flight data (Figure 5-2) shows that the mean level of the payload microphones is 3.5 dB lower overall than those located in the bay perimeter. This indicates that spatial bias errors can be significant in making payload predictions if the microphone data is not carefully chosen.

Some centers include the perimeter microphones with the payload microphones in acoustic predictions to add conservativeness to their environmental estimates.

6.2 Payload Effects

Model data and some flight data (Figures 5-11 and 5-12) indicate that large payloads can have a significant effect on local acoustic levels. The effect is seen especially on the Spacelab module (4.05 m (13.3 ft.) dia.) in Figure 5-12. A large payload is a high volume payload whose boundary extends into the near perimeter acoustic effects. Studies by BB&N (Reference 10) show that payloads with a diameter greater than 60% of the payload envelope can be described as a large payload. For small payloads, the payload effect is negligible except where a large payload surface is close to the payload bay perimeter. The pallet payloads on STS-1 through 5 did not exhibit any detectable payload effects on the payload bay mean sound pressure level except between the outer pallet wall and the orbiter longeron bridge fitting.

In the low frequency (0-50 Hz) regime the payload impedance has a strong influence on the dynamic response. In examining repeatability the approach taken was to compare responses that were either (1) physically far removed from the payloads, thus minimizing the effect of payload impedance, or (2) located on an identical payload structure, such as the DFI package.

6.3 Spatial Variation

Spatial variation in the acoustic environment can be calculated directly from the data from each flight. Probability levels for the bay payload acoustic environment are given for each of the first five flights in Figures 5-21 through 5-24. These were calculated by adding the standard deviation (times the appropriate constant) to the mean bay level. A Gaussian distribution of the acoustic levels in the bay was assumed for the probability levels. Localized areas, such as near the payload bay doors or near the pressure equalization vents, may be higher than can be expected from assuming a strictly Gaussian distribution of acoustic levels. When the mean and probability levels are calculated by combining the data from the first 5 flights, flight-to-flight variation of the first five flights is implicit in the standard deviation. This has been done for the mean and probability levels in Figure 5-25.

6.4 Flight-To-Flight Variation

6.4.1 Acoustic Environment

Based on the perimeter microphone mean levels, variations from Flights 1 through 5 were within ± 1.5 dB for each one-third octave band (Figure 5-9). Flight-to-flight variation is affected by launch drift from the launch pad exhaust ports and vehicle/pad configuration changes. However, these effects are likely to be small. Since the STS weighs approximately 4.5 million pounds and has a thrust to weight ratio of approximately 1.4:1, the inclusion of a heavy payload (65,000 lbs) will not appreciably change the vehicle thrust to weight ratio or launch rise time. Wind induced drift increases due to increased launch weight/rise time will probably also be negligible.

Acoustic environments generated at the Vandenberg Launch Site (VLS) are estimated to be slightly less than Kennedy Space Center (Reference 20). Later shuttles will also have main engines uprated to 109% thrust. Current STS data shows that the solid rockets dominate the launch acoustic environment. Consequently, uprated main shuttle engines will only increase the total launch thrust a few percent and will not significantly affect the total launch acoustic power.

Although shuttle vehicle to vehicle differences and other launch configuration changes are not anticipated to significantly increase flight to flight acoustic environments variations, this needs to be verified.

6.4.2 Low Frequency Vibration

By examining Figures 5-54 through 5-70, an estimate of the bounds of repeatability can be established for OV-102. For the main engine ignition, Figure 5-56 shows appreciable variation from flight-to-flight in the x direction at practically all the system resonances, 2.5 Hz, 5 Hz, 10 Hz, and 20 Hz. For the y direction (Figure 5-54 and 5-57) the variations are also appreciable. The z direction responses (Figures 5-55 and 5-58) show somewhat better correlation, although even here at the aft bulkhead the response spectra differs by a factor of 2 to 3 at 5 Hz.

For SRB ignition in the x direction (Figures 5-61 and 5-68), the repeatability is reasonable up to 5 Hz, but seems to diverge above that, even as one discounts the questionable spectral response for STS-4 of Figure 5-61. For the y direction (Figures 5-59, 5-62, and 5-69) the variation between flights at 3 Hz and 5 Hz is appreciable, on the order of factors of 3 to 5. The z direction (Figures 5-60, 5-63, and 5-70) shows the same trend, namely, good repeatability for the z direction but not as good repeatability for the y direction.

It can be concluded that in general the repeatability for the SRB ignition is better than for the SSME ignition and that the y direction had the worst repeatability of the three directions. The response in the y axis is the lowest of the three directions. The repeatability for the landing event (Figures 5-71 and 5-72) is not very good in amplitude but is quite good in frequency content.

In any event, these data form a good basis for the start of a data base and can be used, within the bounds of the frequency limitations of the measurements, to determine statistical variables for the derivation of design forcing function.

7.0 DYNAMIC ENVIRONMENT AND LOADS PREDICTIONS

Vibration and acoustic predictions for payloads are discussed in Sections 7.1 through 7.3 below. STS flight loads data is compared to analytical loads predictions in Section 7.4.

7.1 Acoustic Predictions

Different methodologies were employed by the DATE Working Group contributing centers in predicting acoustic environments for payloads. Though prediction methods differ, environmental predictions from the various NASA, Air Force and industrial centers for small payloads are very similar. However, there is a greater divergence of opinion on how to predict the effect of a large payload on the shuttle acoustic environment.

Prediction methods from some centers participating in DATE do not include large payload effects at all. The Lockheed Missiles and Space Company (LMSC), Aerospace Corporation and Jet Propulsion Laboratory (JPL) have made predictions for the same DOD payload that do agree within ± 1.5 dB though they were derived by different methods. The predictions and methodologies employed by the centers participating in the DATE Working Group are summarized in the following sections along with the methodology used to derive the prediction. Current predictions are also compared to the recently revised levels specified in the Shuttle Payload Accommodations document (Reference 13).

7.1.1 Jet Propulsion Laboratory Acoustic Prediction

The method used by JPL to predict shuttle payload acoustic levels can be summarized in the equation below (Reference 21). The JPL acoustic environmental prediction of Figure 7-1 for small payloads (with the large payload effect, $P_p = 0$ dB) is the basis for this prediction. The small payload level was based on the space dB average of payload microphones for all flights. This is because a dB average is more nearly log normal. Other values for the variables in the equation are noted below. Values for the uncertainties were conservatively estimated using the available STS data and engineering judgement. Flight to flight variation was estimated from the scatter of the perimeter levels about the "all flights" perimeter mean levels. Probability levels for the uncertainties were not estimated, except for the spatial variation, because the STS data base was too small. Microphones in the bay perimeter were excluded to calculate the payload bay mean level, P_m , for a small payload or empty bay. Two times the standard deviation from P_m was calculated and the root sum of the squares was added to the mean along with the flight-to-flight variation and data reduction errors. Large payload effects, P_p , were predicted by a combination of the results from PACES (Reference 10) and perimeter flight data. PACES is a computer code that is intended to predict the effect of large payloads on the local acoustic environment. The same value of P_m is used for large and small payloads in the prediction calculations. P_{max} , the maximum expected acoustic environment, is loosely based on the .97 probability level of the spatial deviation from the mean, P_m . P_{max} is thought to be conservative. However, since the probability level of the other acoustic environment uncertainties could not be derived from the STS data, a probability level could not be estimated for P_{max} .

$$P_{\max} = P_M + P_b + P_p + [P_e^2 + P_s^2 + P_f^2 + P_v^2]^{1/2}$$

where

- P_{\max} = Maximum expected acoustic environment.
- P_M = Mean envelope acoustic environment for small payloads from STS-2 through STS-5 flight data, average in dB.
- P_e = Data reduction errors; 1 dB.
- P_b = Spatial bias error arising from non-representative positioning or small number of microphones; 0 dB.
- P_p = Large payload diameter effect; PACES plus perimeter and or/vent noise data (Figure 7-2).
- P_s = Spatial variation uncertainty within the payload bay; 2 sigma of 20 payload microphones, 97% probability (Figure 7-3).
- P_f = Flight-to-flight uncertainty; 1.5 dB (Figure 5-10).
- P_v = Vehicle-to-vehicle variation; 1 dB.

Vent noise for small payloads is accounted for in P_M , the mean small payload 1/3 octave band level.

A prediction for a payload with a large surface near the payload bay doors is shown in Figure 7-4. Predictions for the same payload are also presented from Lockheed and the Aerospace Corporation. The payload effect, P_p , was found by enveloping the results of a PACES computer analysis and the perimeter data from microphone 9256 (Figure 7-2). Microphone 9256 was between the pallet and the orbiter sidewall. Vent noise was not added to the JPL prediction because surfaces of concern were not near vents.

7.1.2 Lockheed Missiles and Space Company Acoustic Predictions

The Lockheed Missiles and Space Company (LMSC) approach is to derive an average small payload level and add to it various factors to account for uncertainties and payload effects. LMSC acoustic predictions for small payloads are shown in Figure 7-1, reproduced from Reference 22. The small payload level is derived by averaging all STS-2 and STS-3 data separately and then averaging the two sets of data. The level of 95% probability was found and then various uncertainty factors were added. The uncertainty factors included flight-to-flight variation (3 dB), a correction for removal of the aft thermal radiators (1 dB), and a forward to aft gradient correction. A prediction for a large DOD payload was made with an addition to account for an accompanying payload. Payload effects are based on 1/4 scale model acoustic tests which were performed by BB&N (Reference 10). The resulting predicted level was specified without any smoothing of the spectrum (Figure 7-4). The prediction calculations are summarized in Table 7-1. The prediction algorithms of the Vibroacoustic Payload Environment Prediction System (VAPEPS) program (Reference 23) are also used extensively in LMSC vibration and acoustic predictions.

Table 7-1. LMSC Acoustic Prediction Factors
for Large DOD Payload

| 1/3 OCTAVE FREQUENCY | STS-2/STS-3 ENVP. (AVG) | AVG TO 95X CORRECTION | FLI-TO-FLT VARIATIONS | OTHER RAD AFFECT | FWD-AFT GRADIENT | MAX ACOMP. P/L AFFECT | MAX EXPECTED |
|-------------------------|----------------------------|--------------------------|--------------------------|---------------------|---------------------|--------------------------|-----------------|
| 25.0 | 117.0 | 3.9 | 3.0 | .1 | .0 | 5.6 | 128.6 |
| 31.5 | 113.3 | 4.6 | 3.0 | .5 | 1.5 | 6.4 | 129.3 |
| 40.0 | 115.3 | 5.5 | 3.0 | .3 | 3.0 | 4.0 | 131.2 |
| 50.0 | 118.6 | 4.9 | 3.0 | .7 | 2.5 | 5.3 | 135.0 |
| 63.0 | 120.7 | 4.5 | 3.0 | 1.8 | .5 | 2.9 | 132.9 |
| 80.0 | 120.8 | 3.7 | 3.0 | 1.6 | .5 | 3.7 | 133.3 |
| 100.0 | 121.3 | 3.7 | 3.0 | 1.5 | .5 | 4.4 | 134.4 |
| 125.0 | 122.6 | 3.0 | 3.0 | 1.0 | 1.0 | 3.5 | 134.7 |
| 160.0 | 121.9 | 4.5 | 3.0 | .9 | .5 | 5.2 | 136.0 |
| 200.0 | 121.9 | 3.3 | 3.0 | 1.0 | .0 | 2.1 | 131.3 |
| 250.0 | 121.1 | 3.6 | 3.0 | 2.1 | .0 | 2.6 | 132.4 |
| 315.0 | 118.8 | 4.2 | 3.0 | 1.5 | .0 | 1.5 | 128.2 |
| 400.0 | 117.1 | 4.2 | 3.0 | 1.1 | .0 | 1.5 | 126.9 |
| 500.0 | 115.2 | 3.9 | 3.0 | 1.1 | .0 | 2.8 | 126.0 |
| 630.0 | 115.4 | 3.1 | 3.0 | 1.2 | .0 | 2.4 | 125.1 |
| 800.0 | 114.0 | 3.0 | 3.0 | 2.0 | .0 | 2.6 | 124.6 |
| 1000.0 | 110.7 | 3.0 | 3.0 | 1.7 | .0 | 4.3 | 122.3 |
| 1250.0 | 110.0 | 3.0 | 3.0 | 1.2 | .0 | 4.4 | 121.6 |
| 1600.0 | 107.9 | 3.0 | 3.0 | 1.4 | .0 | 4.5 | 118.8 |
| 2000.0 | 107.5 | 3.0 | 3.0 | 1.0 | .0 | 3.4 | 117.9 |
| OVERALL | 131.5 | | | | | | 144.1 |

7.1.3 Aerospace Corporation Acoustic Predictions

The current Aerospace acoustic requirement for DOD payloads is shown in Figure 7-1 (References 24 and 25). It was developed by enveloping all flight data (STS-1 through 5) for microphones located within a 9 foot diameter. Three dB's were added to account for flight-to-flight variations and the resulting curve was smoothed. A correction is added if the aft thermal radiators are not present (± 1.5 dB). A prediction for a large payload includes a payload effect added to this small payload level. The large payload effect correction factor which Aerospace uses is given in Figure 7-5. The aerodynamically induced discrete tone noise was adjusted for payload effects. Finally, a best fit curve was used to describe the specification level for the large payload (Figure 7-4). Figure 7-4 also shows the JPL and LMSC predictions for the same large payload.

7.1.4 Rockwell International/Johnson Space Center Acoustic Predictions

An enveloping technique was applied to arrive at the empty bay liftoff and aeronoise environments from STS-1 through 4, seen in Figure 7-6 (Reference 14). No other factors were added to the levels. The lift off levels were smoothed to obtain the specification level of Figure 7-1. This level has been adopted as a minimum safety requirement in the Shuttle Interface Control Document (ICD 2-19001) by JSC (Reference 13).

7.1.5 Goddard Space Flight Center Acoustic Predictions

The Goddard Space Flight Center (GSFC) small payload level (Figure 7-1) was based on a smoothed envelope of the 97.73 percent probability acoustic level and the worst case average of the maximum levels during transonic flight (Reference 7). In the 315 Hz 1/3 octave band, the worst case average of the maximum levels was used. Payload effects for large payloads are based on smoothing and applying the general trend predicted by the PACES program (Reference 10). This usually means adding 2-4 dB to the entire spectrum, depending on the characteristics of the large payload in question.

7.2 Computerized Acoustic and Vibration Predictions

7.2.1 PACES

The Payload Acoustic Environment for Shuttle (PACES) is a computer code which predicts the influence of large payloads on the local shuttle cargo bay acoustic environment (Reference 10). The program was developed by BB&N (under contract to GSFC) by using 1/4 scale model test results and computerized prediction techniques. PACES predicts the payload induced changes in the acoustic environment in the air space around payloads. The average change within each subvolume surrounding the payload from the empty bay mean level is computed by PACES. PACES is limited to seven air space volumes or subvolumes so that results are obtained for gross areas of payload. PACES takes into account payload size, the exterior acoustic environment and the anticipated acoustic absorptivity. It is relatively easy to use and can be a useful guide in trying to account for large payload influences on payload bay acoustic environments. PACES has been validated based on small payload shuttle flight data only. A capability to estimate the variance of the predicted acoustic levels was recently added to PACES.

7.2.2 VAPEPS

VAPEPS (Vibroacoustic Payload Environment Prediction System) is a data base management and vibroacoustic prediction program developed by LMSC under contract to GSFC (Reference 23). It is capable of storing large amounts of dynamic test and flight data along with the attending structural characteristics. Data is stored with labels and parameterized structural information. Algebraic operations may be performed on the data as well as making vibration predictions for new payload configurations. VAPEPS can predict acoustic and vibration environments for payloads on the STS or other launch vehicles. Vibration predictions for structures can be made with VAPEPS using classical analysis methods, statistical energy methods or extrapolations by structural similiarity.

Proposals are being developed that will establish centralized data base management for VAPEPS. A center is also proposed to coordinate program maintenance and improvements. Recently, a plotting capability has been added to VAPEPS, though its documentation is not yet complete. Other improvements to enhance VAPEPS utility and ease of use are being planned.

7.3 Vibration Predictions

7.3.1 Rockwell Vibration Prediction

The Rockwell International high frequency vibration environments were developed by enveloping the lift off flight data (Reference 14). Revised levels for small longeron-mounted payloads are shown in Figure 5-27 (Reference 13). Keel levels (Figure 5-33) remain unchanged though existing keel vibration data is well below the criteria (References 13 and 14).

7.3.2 Aerospace Corporation Vibration Prediction

The Aerospace Corporation high frequency vibration environments were developed by enveloping vibration during all flight conditions.

Figure 7-7 shows the payload vibration levels for the longeron and bridge fitting.

7.3.3 GSFC Vibration Prediction

Baseline pallet payload vibration has been predicted by GSFC by extrapolating the ground acoustic test vibration data based on flight-measured acoustic environments (Reference 26). Predictions (Table 7-2) have been made for type of structure with general characteristics as outlined below.

Table 7-2. BASELINE RANDOM VIBRATION ENVIRONMENT CRITERIA
FOR SHUTTLE PALLET PAYLOAD SUBSYSTEMS FLIGHT LEVELS

| ZONE | FREQUENCY HZ | ACCELERATION SPECTRAL DENSITY G ² /Hz |
|--------------------|-----------------|---|
| Near P/L Trunnion: | | |
| 1 (All Axes)* | 20 - 125 | +9 dB/oct |
| | 125 - 315 | 0.025 <10,000 lb P/L |
| | 315 - 2000 | -9 dB/oct |
| | OA grms | 3.1 |
| Near P/L Keel: | | |
| 1 (All Axes) | 20 - 100 | +9 dB/oct |
| | 100 - 315 | 0.01 <10,000 lb P/L |
| | 315 - 2000 | -9 dB/oct |
| | OA grms | 2.0 |
| 2 (All Axes) | 20 - 40 | +12 dB/oct |
| | 40 - 800 | 0.002 |
| | 800 - 2000 | -12 dB/oct |
| | OA grms | 1.4 |
| 3 (All Axes) | 20 - 40 | +12 dB/oct |
| | 40 - 250 | 0.002 |
| | 250 - 2000 | -12 dB/oct |
| | OA grms | 0.8 |
| 4* (Normal) | 20 - 125 | +9 dB/oct |
| | 125 - 200 | 0.10 |
| | 200 - 2000 | -12 dB/oct |
| | OA grms | 4.2 |
| 4 (in-plane) | 20 - 63 | +12 dB/oct |
| | 63 - 200 | 0.001 |
| | 200 - 2000 | -9 dB/oct |
| | OA grms | 0.5 |

* Surface Weight Density: 0.02 to 0.1 psi.

Zone Definition

A zone is defined as a major area of the OSS-1 payload in which subsystems can be mounted. For the OSS-1 payload, the determination of a particular zone in which a subsystem was mounted is based on the following descriptions:

Zone 1 -- Payload primary structure within proximity of the payload--orbiter vehicle separation plane.

Zone 2 -- Payload primary and secondary structure (exclusive of mounting brackets) not included in Zone 1.

Zone 3 -- Payload structures specifically designed for mounting of subsystems such as shelving, platforms, or brackets.

Zone 4 -- Payload large surface area lightweight structures at outboard areas which respond primarily to acoustic pressure forces.

7.4 Flight Data and Analytical Loads Predictions

There are two different objectives for comparing the flight data to analytical predictions. One is to assure that the flight responses are below the design conditions and to assess the margin of the design load to the flight load. The other objective aims at the reconstruction of the flight conditions to verify the methodology for the prediction of the dynamic responses. The first objective is primarily the concern of the engineers responsible for the launch vehicle performance. While the payload engineer is also concerned about assuring that the design conditions envelope the actual expected flight responses, the payload designer is also weight limited and hence is trying to reduce the design margins, yet retaining a high confidence in these margins. Both objectives require a statistical data base. The payload designer, facing more stringent constraints than the launch vehicle designer, seeks a larger data base in order to reduce the design margins and increase the statistical confidence level. Since payload instrumentation is usually flown only for diagnostic purposes, and many programs consist of only one flight vehicle, project offices lack the interest in post-flight data reduction on successful flights. The NASA Dynamic, Acoustic and Thermal Environments (DATE) program provides a focal point for a well-coordinated research program. DATE-type instrumentation has been flown on STS-2 through STS-5 and these data have been disseminated (Ref. 1 through 5), but very little has been done in the verification of loads methodology. The available flight data will be compared to pre-flight design type levels as well as to post-flight reconstruction analyses.

7.4.1 Comparison of Flight Data With Design Conditions

The primary objective of such a comparison is to insure that the flight levels are below the design conditions in order to verify the validity and the adequacy of the launch vehicle model and the set of design forcing functions. The subject of flight responses versus design load factors is discussed extensively in References 27 through 29. Only a few representative examples will be included here. These are obtained from References 8, 29 and 30. For the liftoff analyses Reference 29 uses design cases L0933 through L0943, which have been updated using a 4 cycle overpressure wave. Figure 7-8 shows a

comparison of the response spectra for the design cases with those obtained from STS-2 through STS-5 for the x direction as measured on the aft bulkhead. It should be noted that the location of the analytical predictions ($x = 1307.0$, $y = 0.0$, $z = 261.0$) differs somewhat from the locations of the flight measurement ($x = 1294.0$, $y = 3.0$, $z = 296.0$). Data obtained from a 10 second liftoff time interval for the keel y response is shown in Figure 7-9. The analytical prediction for these data are at Orbiter location ($x = 979.0$, $y = 0$, $z = 305.0$). Flight data was recorded at ($x = 979.0$, $y = 9.0$, $z = 305.0$). Design levels for the z-direction are compared to flight responses in Figure 7-10. These data are for the Orbiter left longeron during liftoff. The analytical predictions are for a point at ($x = 863.0$, $y = -94.0$, $z = 401.8$), while the flight responses were measured at ($x = 823.0$, $y = -100$, $z = 407.0$). All above response spectrum data was calculated with a gain of $Q = 25$.

Additional data comparing design levels to flight data for STS-5 at the PAM-TELESAT/Orbiter interface and the PAM/SBS interface are contained in Reference 29.

For STS-3 the correlation comparison is based on the data provided by the Goddard Space Flight Center (References 8 and 30). These references summarize the comparison for 8 accelerometer locations on the OSS-1 payload. For liftoff the analysis utilized the Shuttle Model M6.0 with nominal forcing function L09093. For the landing the prediction used the same Shuttle model with design maximum landing forcing function LB4070 for nose gear landing contact at 11.0 feet per second and LB4071 for symmetric main landing gear contact at 6.0 feet per second sink rate. These response spectra were generated using a gain factor of $Q = 20$.

The locations of the eight GSFC accelerometers are shown in Figure 7-11. Typical accelerometer responses, each one in the x, y, and z directions for points on the payload, have been selected for the comparison of the response spectra for liftoff. These comparisons are shown in Figures 7-12 through 7-14. All response spectra have been calculated for a gain of $Q = 20$. Figure 7-15 compares results of post-flight reconstruction analysis to flight data for the main landing gear contact. Similar data is shown in Figure 7-16 for nose landing gear contact.

The adequacy of the design forcing functions can only be grossly assessed by examining Figures 7-8 through 7-10, which have been derived from Reference 29 and compare the flight responses from STS-2 through STS-5 with those obtained using design forcing functions L0933 through L0943. These figures show that, in general, for the present data base, flight data and analysis, the design forcing function appears to be conservative for all directions, especially above 15 Hz. The exception is for the z direction (pitch) at 3 Hz where the design forcing function is underpredicting the response.

However, no conclusion can be drawn for the conservativeness above 15 Hz because the apparently low level flight data in Figures 7-8 through 7-10 above 12.5 Hz is beyond the practical digitizing limit (8 points per cycle) imposed by the PCM sample rate (100 samples per second) of the DFI System. To amplify this remark it should be noted that the OSS-1 data (Figures 7-12 through 7-14) show significant response above 12 Hz.

The underprediction of the z response is of concern to some payloads, particularly those utilizing large transfer stages which have resonances in this region.

For STS-3 the nominal forcing function, L09C93, was used in the reconstruction analysis. Typical results are shown in Figures 7-12 through 7-15 for SRB ignition (taken from Reference 30). These figures show that the analysis somewhat overpredicted the responses for all directions. The overprediction is more pronounced for the landing event, as shown in Figures 7-15 and 7-16.

7.4.2 Comparison of Flight Data With Post-Flight Correlation Analyses

The objective of such comparisons is to evaluate the load prediction methodology. Such evaluation addresses mainly the fidelity of the launch vehicle and payload models as well as the forcing function. The forcing function is reconstructed from flight measurements such as pressure transducers. In contrast to comparing flight data to design levels, this comparison does not account for any dispersions in the forcing functions. The post-flight correlation analyses aims at reconstructing the flight levels using the best available data for a particular flight. Post-flight correlation analyses have been performed for STS-5; these are documented in Reference 29. Only representative examples will be presented here. These are the data from the three accelerometers mounted at the SBS/PAM-D interface as shown in Figure 7-17. For the correlation analysis the analytical forcing function was based on measured STS-5 thrust buildup of both the Space Shuttle Main Engines (SSME) and the Solid Rocket Boosters (SRB). These reconstructed forces used a 4 cycle overpressure wave which is also used for design forcing functions L0933 and L0943. The amplitude of the nominal overpressure was reduced by a factor of 0.71 to discount for the dispersions of the design cases.

Response spectra data is shown in Figures 7-18 through 7-20 for SRB ignition. The comparison shows that there is severe underprediction at 3 Hz for both the x and z directions as well as severe underprediction of the response in the 20 to 30 Hz region for the y direction. The response in the x and z directions above 10 Hz is predicted reasonably well.

Based on the data available at the time of this report, it is concluded that the forcing function and/or the structural model might be conservative between 15 and 30 Hz. However, a larger data base is necessary for a further assessment of this potential conservativeness.

The underpredicted response near 3 Hz seems to be real, but it could be attributed to either the forcing function or the structure model.

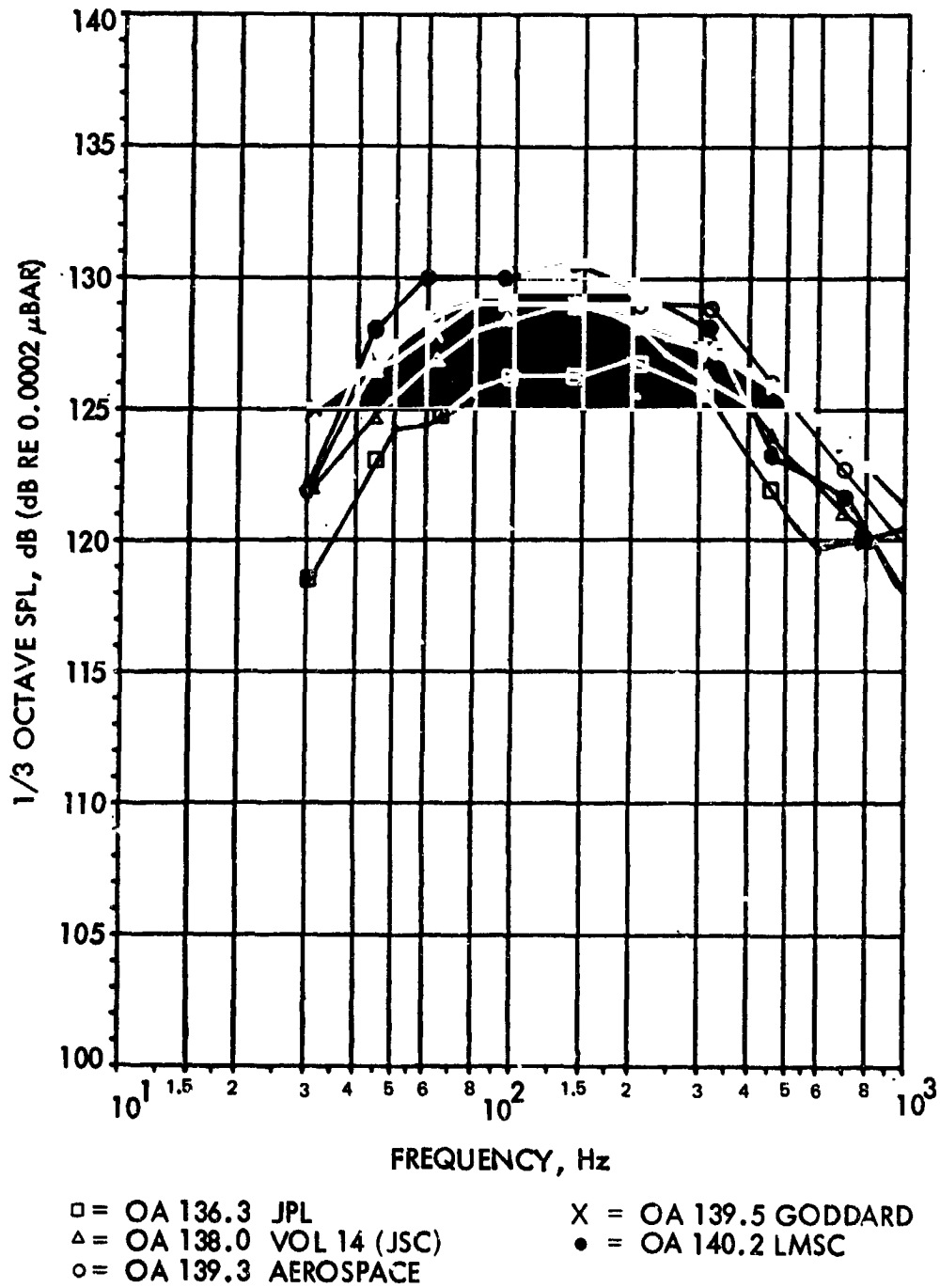


Figure 7-1. Small Payload/Empty Bay Acoustic Prediction Comparison

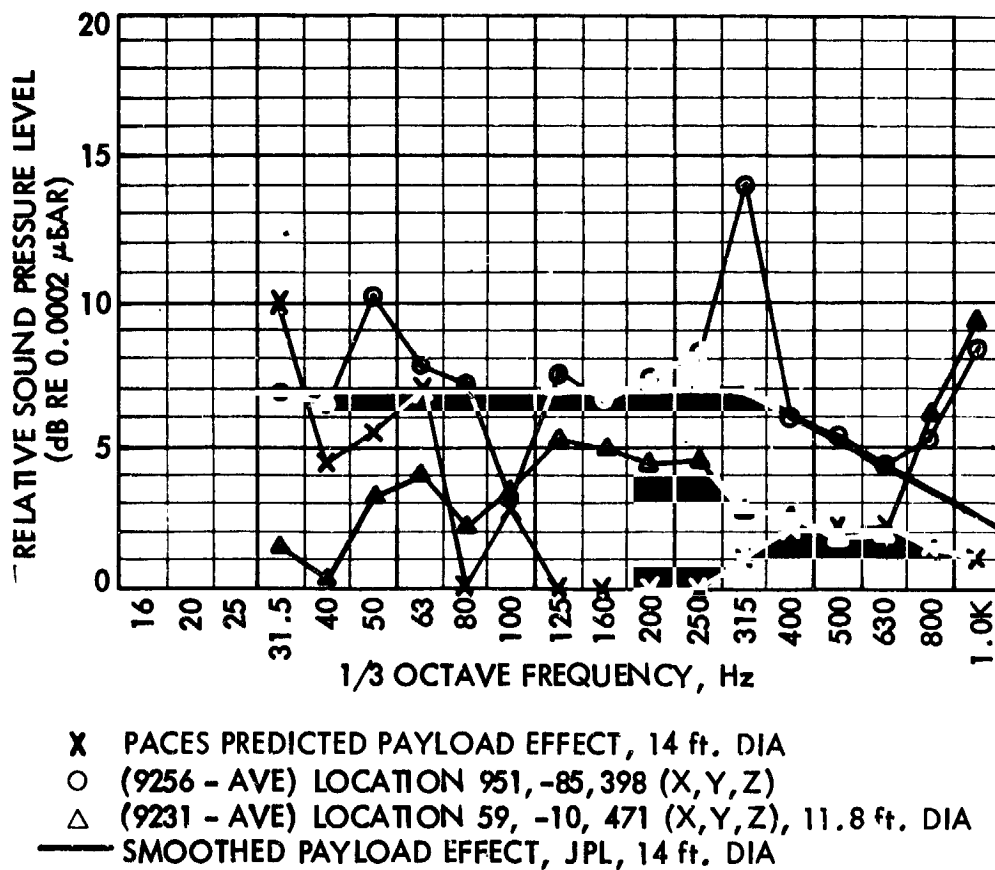


Figure 7-2. JPL STS Large Payload Acoustic Prediction

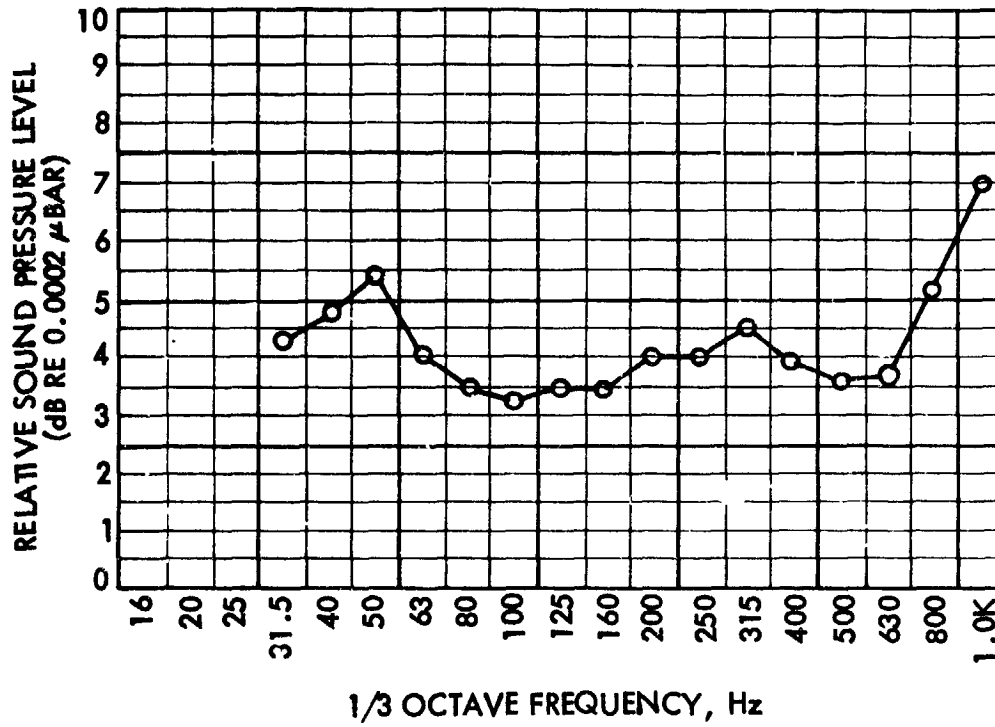


Figure 7-3. 2 Sigma of Payload Acoustic Data, All Payload Mics, Flights 1-5, JPL

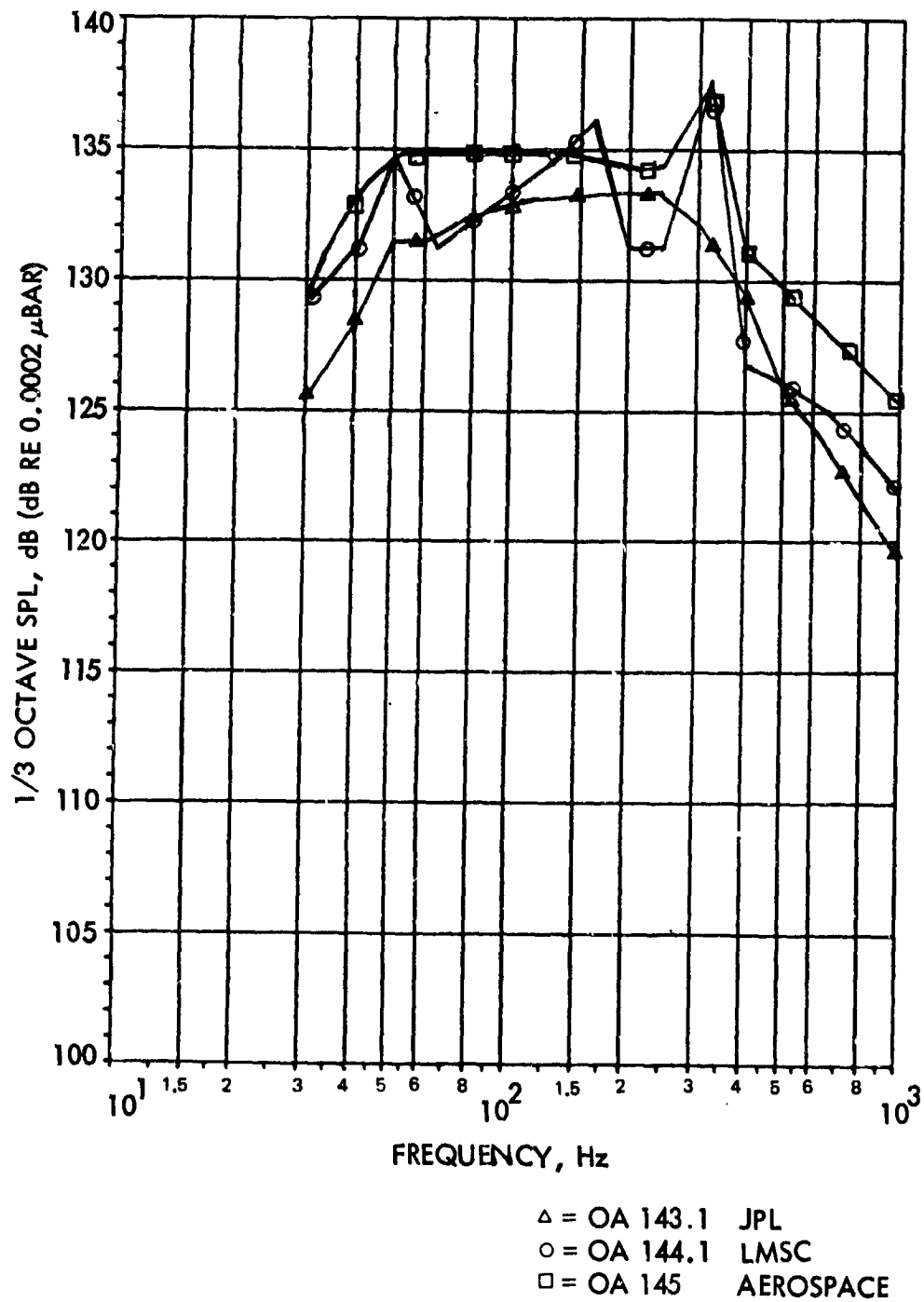


Figure 7-4. Large Payload Acoustic Prediction Comparison

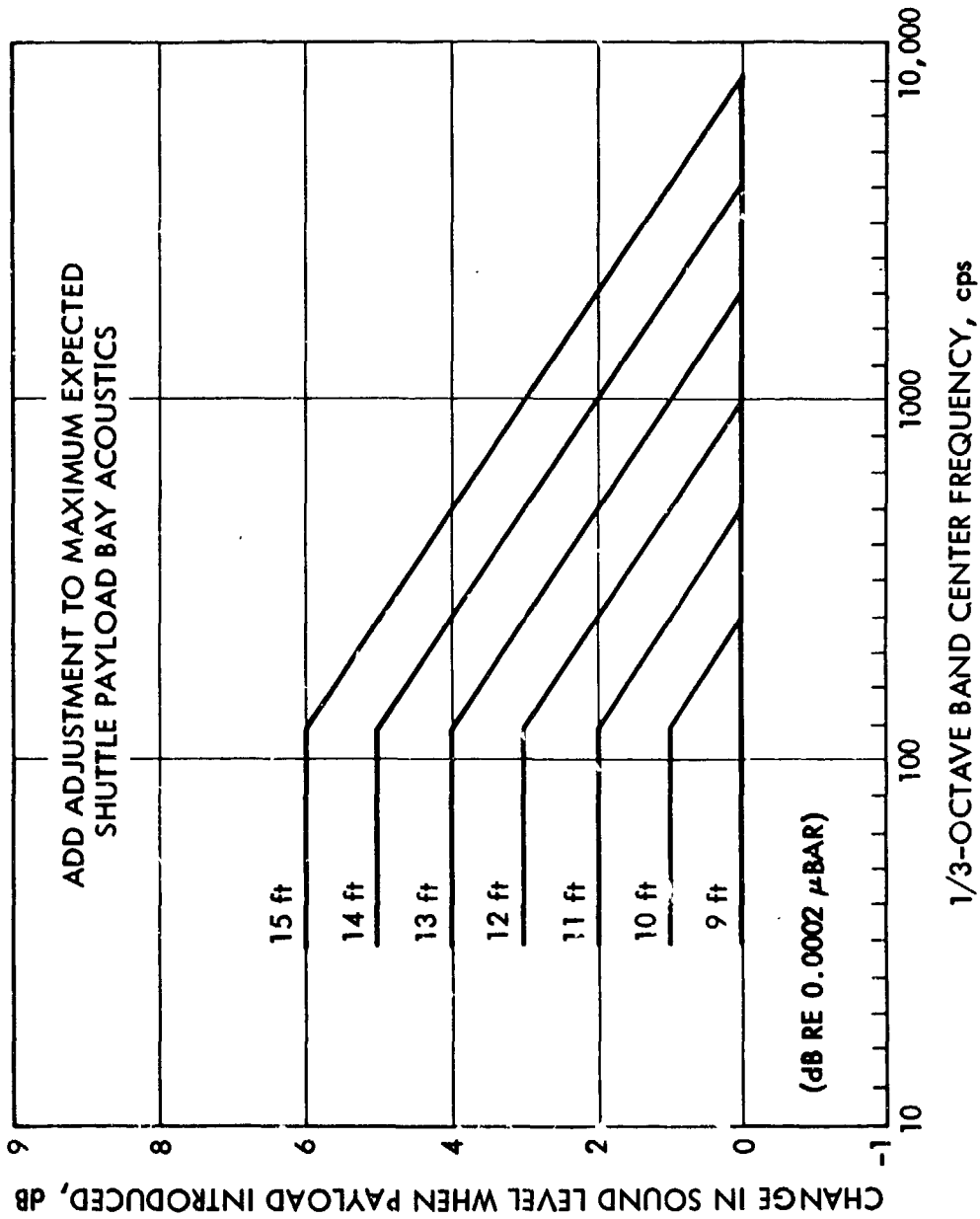


Figure 7-5. Aerospace Corporation Adjustment for Large Payloads

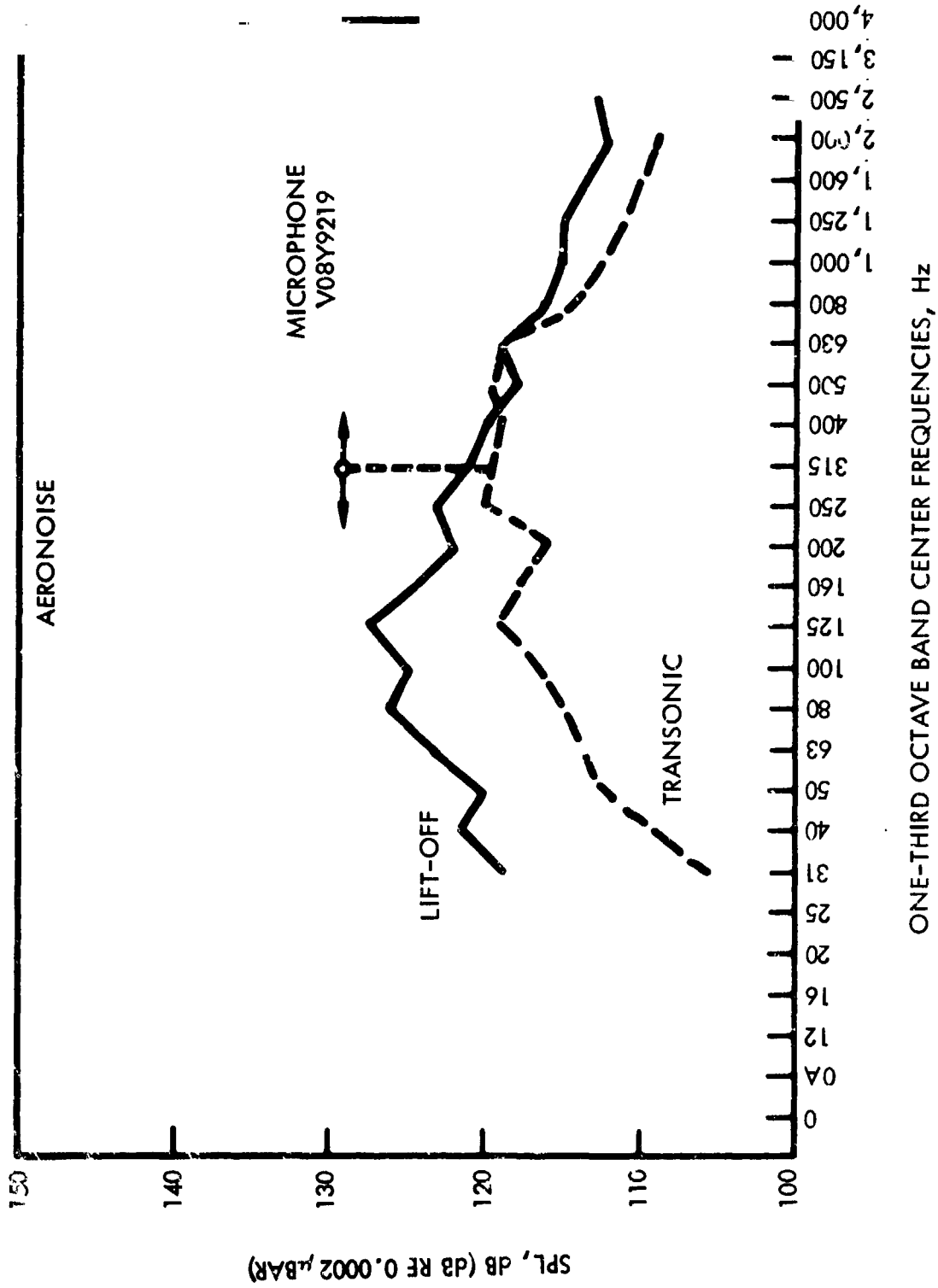


Figure 7-6. Rockwell. International Comparison of Transonic Flight and Lift-off Payload Bay Noise

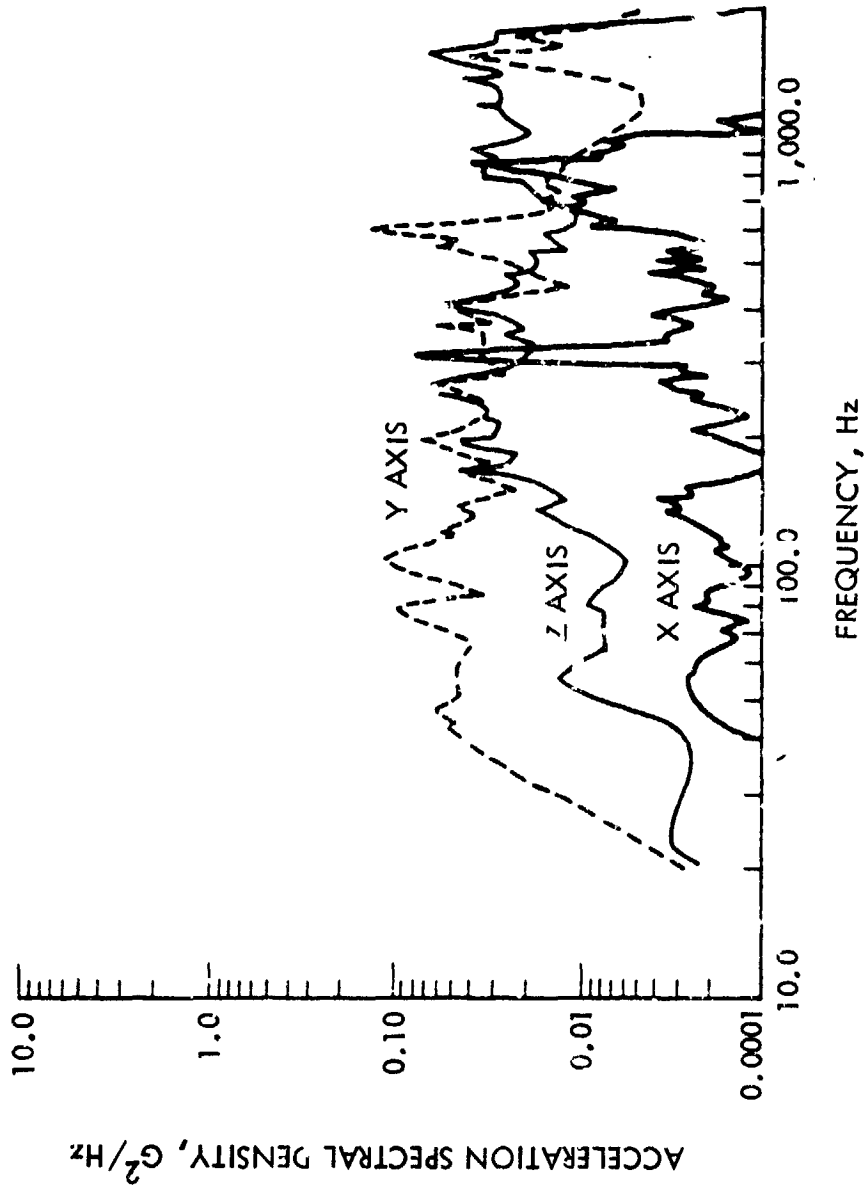


Figure 7-7. Aerospace Corporation L-angeron/Bridge Fitting Payload Vibrat on for STS-1 Through STS-3 Liftoif

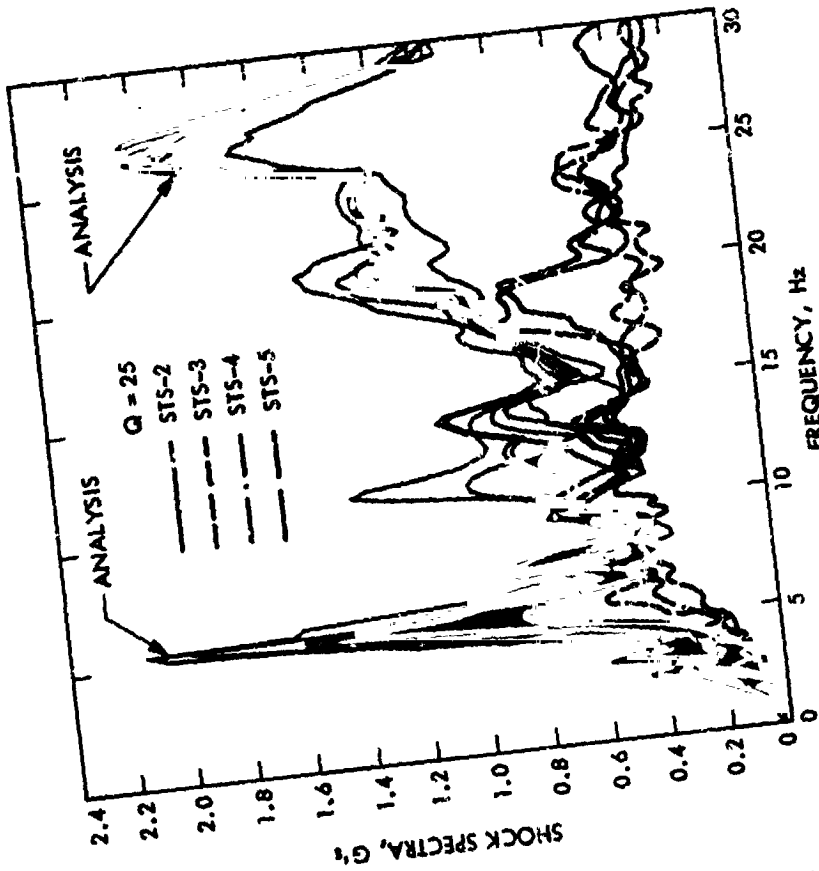


Figure 7-8. Response Spectra, Comparison of Design Conditions With Flight Data, Liftoff, SSME Ignition +10 Seconds, Aft Bulkhead, X Direction

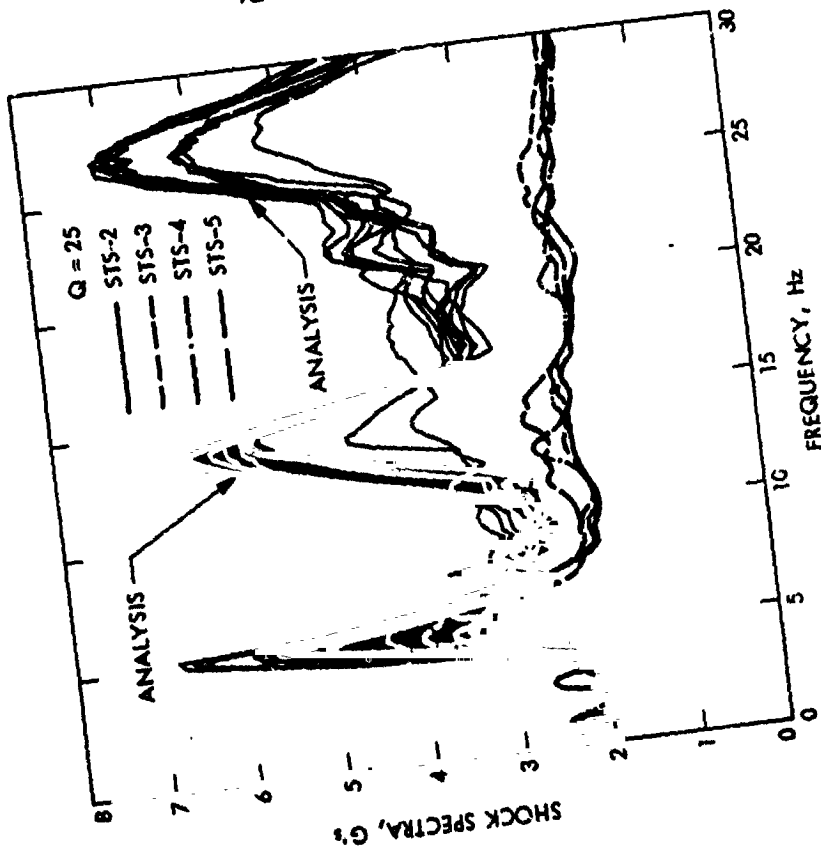


Figure 7-9. Response Spectra, Comparison of Design Conditions With Flight Data, Liftoff, SSME Ignition +10 Seconds, Keel, Y Direction

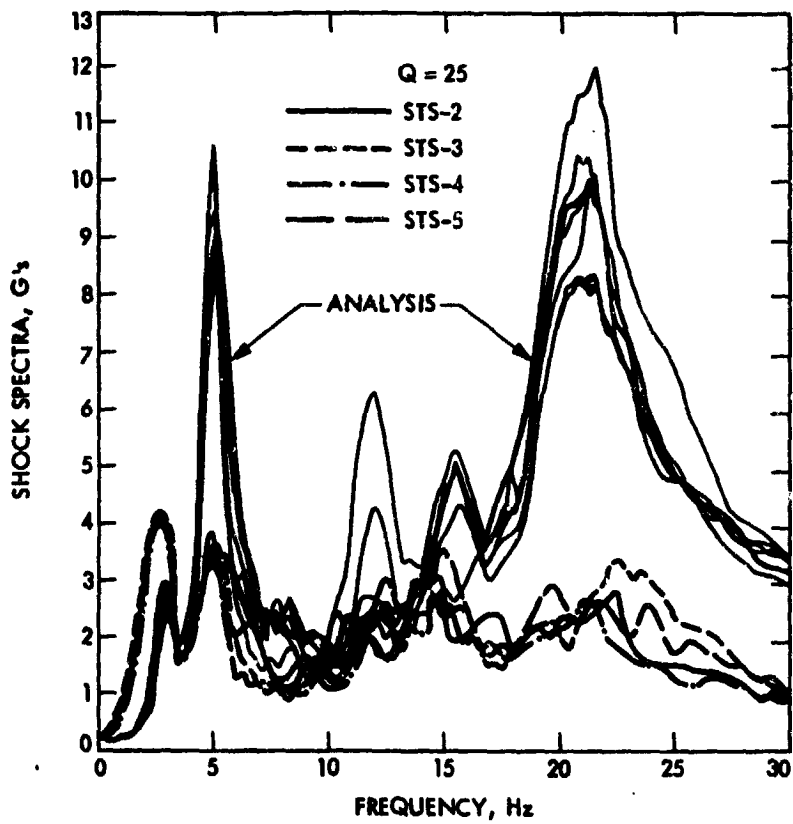


Figure 7-10. Response Spectra, Comparison of Design Conditions With Flight Data, Liftoff, SSME Ignition +10 Seconds, Left Longeron, Z Direction

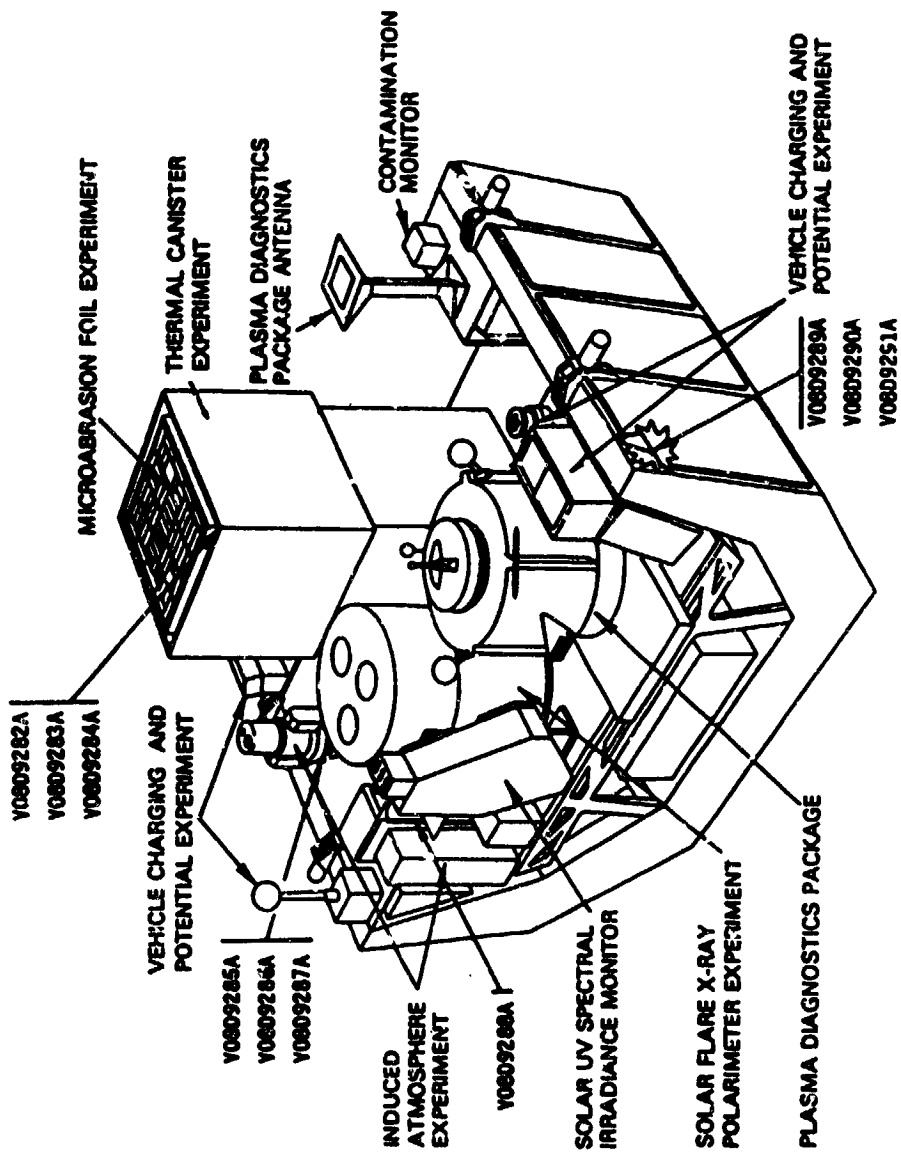


Figure 7-11. GSFC-Installed Measurement Locations on OSS-1

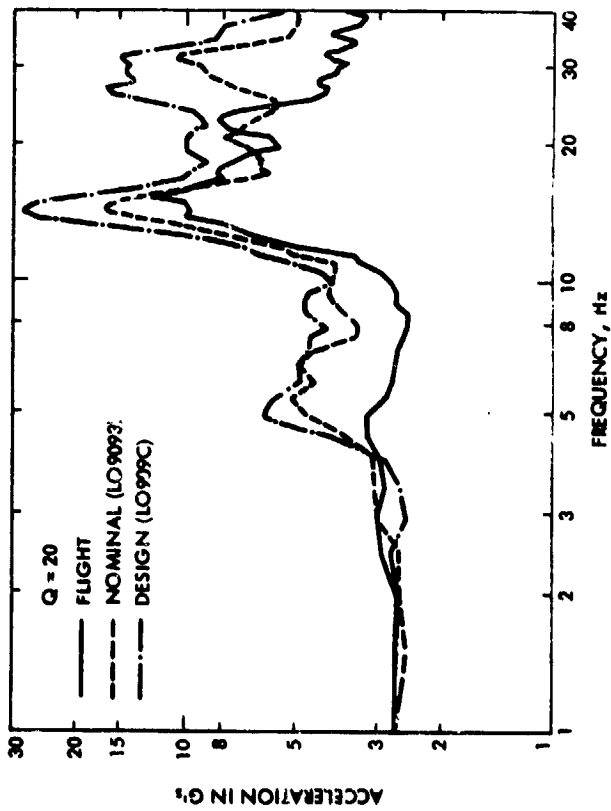


Figure 7-12. Response Spectra, Post Liftoff, SRB Ignition +4 Seconds, OSS-1 Experiment, X Direction, Ac-celerometer V08D9285A

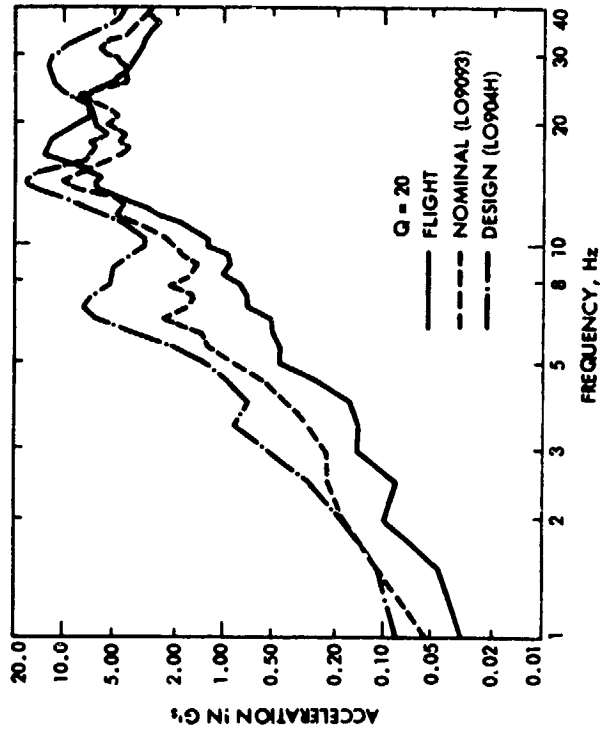


Figure 7-13. Response Spectra, Post Liftoff, SRB Ignition +4 Seconds, OSS-1 Experiment, Y Direction, Ac-celerometer V08D9286A

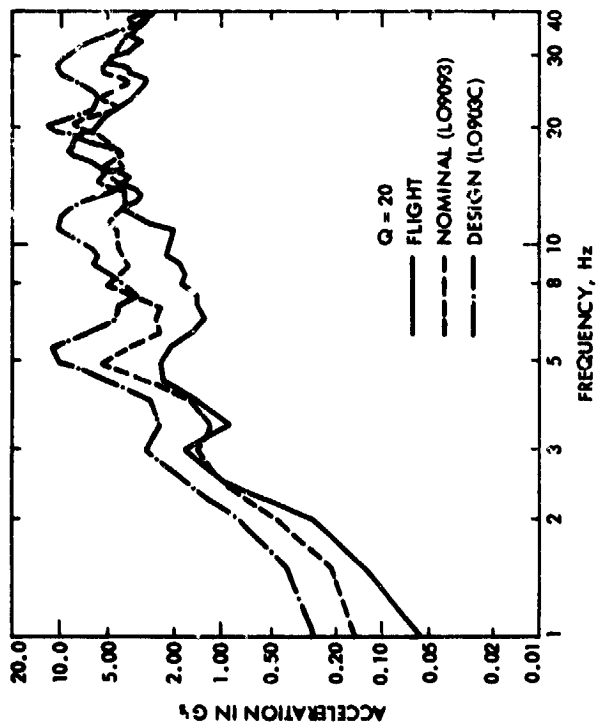


Figure 7-14. Response Spectra, Post Liftoff, SRB Ignition +4 Seconds, OSS-1 Experiment, Z Direction, Accelerometer V08D9287A

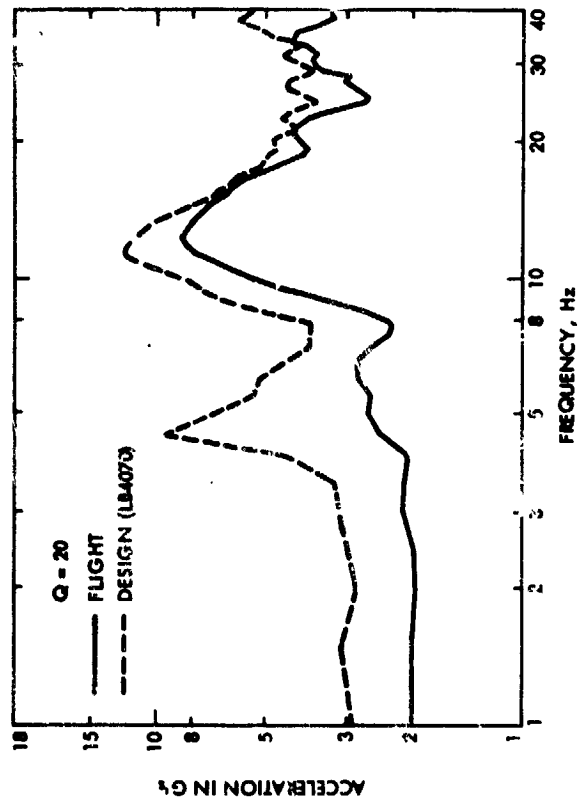


Figure 7-15. Response Spectra, Landing, Main Gear Contact +2 Seconds, OSS-1 Experiment, Z Direction, Accelerometer V08D9284A

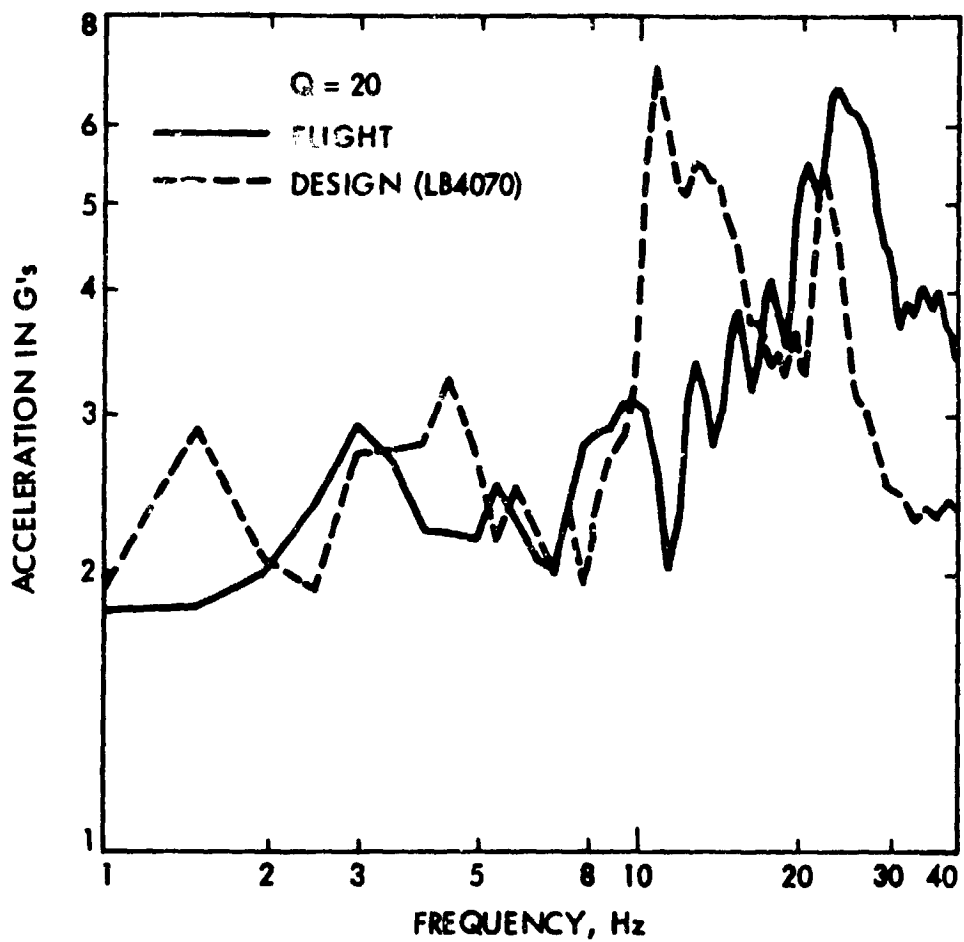
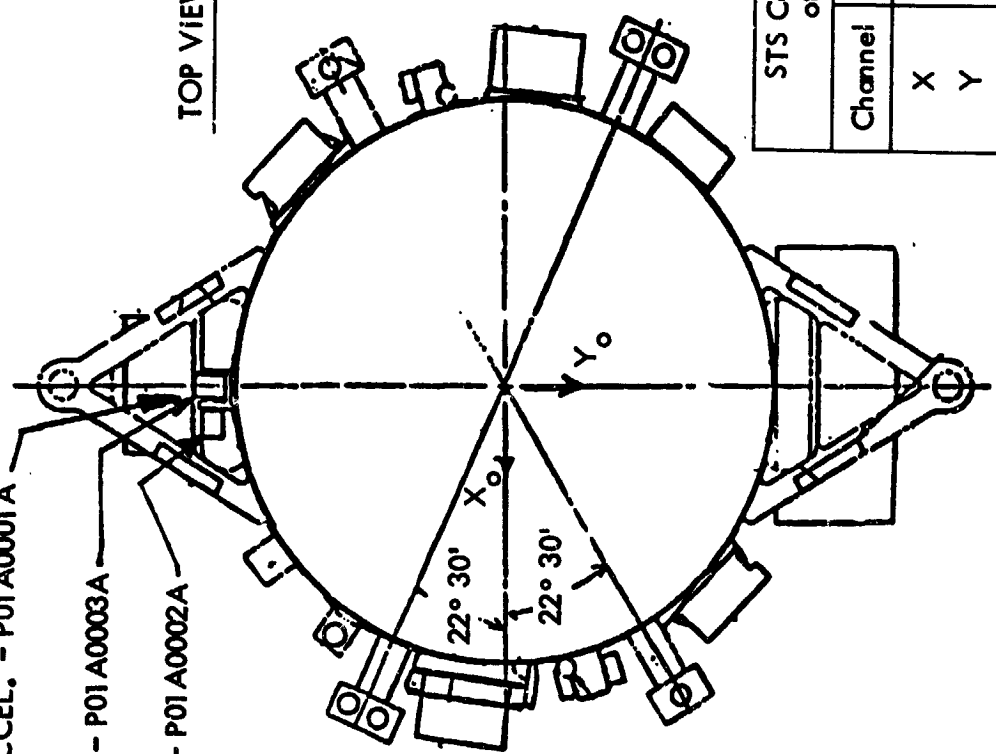


Figure 7-16. Response Spectra, Landing, Nose Gear Contact +2 Seconds, OSS-1 Experiment, Z Direction, Accelerometer V08D9284A

Z AXIS ACCEL. - P01A0001A
 Y AXIS ACCEL. - P01A0003A
 X AXIS ACCEL. - P01A0002A

TOP VIEW OF SBS/PAM-D INTERFACE AREA



| STS Co-ordinates for Mounting Location of SBS/PAM-D Accelerometers | | | |
|--|------------|------------|------------|
| Channel | X Location | Y Location | Z Location |
| X | 937.8 | -20 | 384.9 |
| Y | 935.3 | -20 | 384.9 |
| Z | 935.3 | -20 | 382.6 |

Figure 7-17. Location of SBS/PAM-D Accelerometers, STS-5

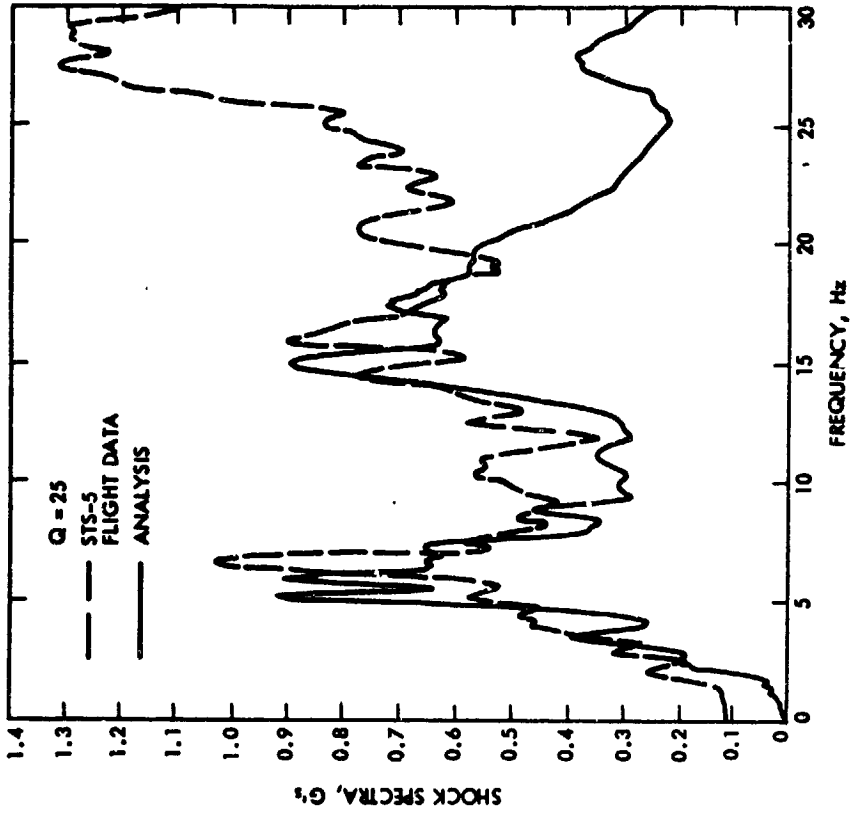


Figure 7-18. Response Spectra, Comparison of Reconstructed Liftoff Analysis to STS-5 Flight Data, SRB Ignition +3 Seconds, PAM-D/SBS Interface, X Direction, Accelerometer P01A0002A

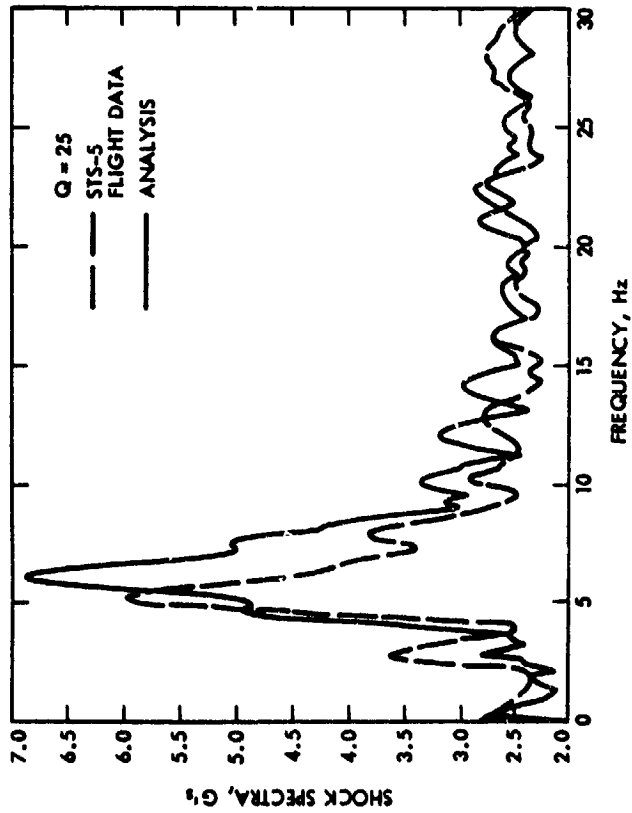


Figure 7-19. Response Spectra, Comparison of Reconstructed Liftoff Analysis to STS-5 Flight Data, SRB Ignition +3 Seconds, PAM-D/SBS Interface, Y Direction, Accelerometer P01A0003A

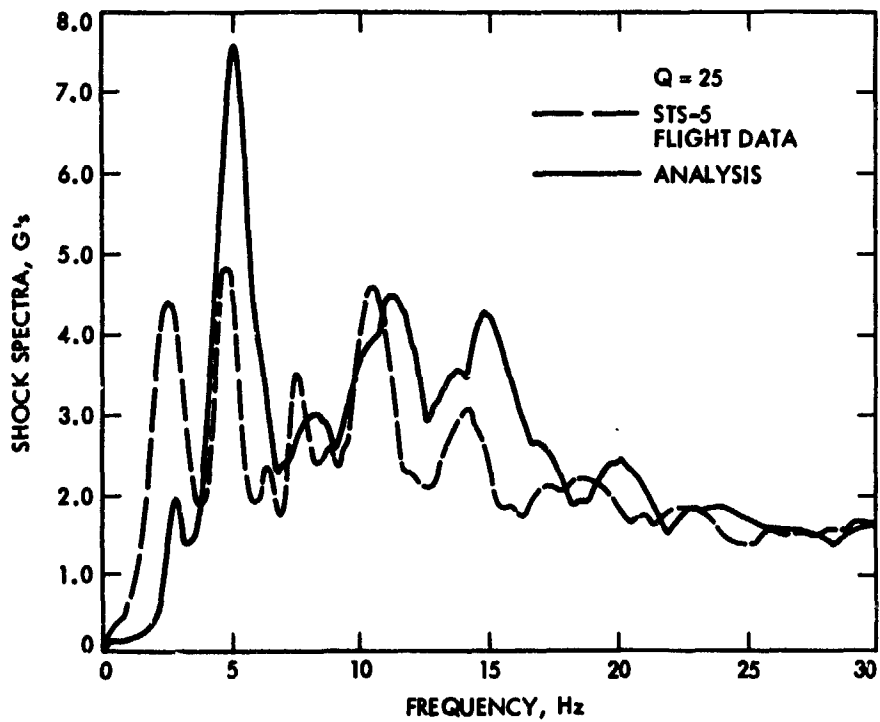


Figure 7-20. Response Spectra, Comparison of Reconstructed Liftoff Analysis to STS-5 Flight Data, SRB Ignition +3 Second, PAM-D/SBS Interface, Z Direction, Accelerometer P01A0001A

8.0 RELATED ACTIVITIES

Several studies related to shuttle dynamic environments are proceeding or are being proposed to study aspects of the shuttle environments that are not well understood. Studies are under way at GSFC, Rockwell International and the Aerospace Corporation to determine the relative influence of the payload bay acoustic environment and the orbiter payload bay structural vibration. Loads and random vibration criteria will be updated as a result of these efforts. Data from STS-2 and STS-4 indicates that low frequency inputs (below 125 Hz) to payloads from the orbiter are higher than expected. This was determined by comparing flight pallet responses to ground acoustic test response. Lockheed and Rockwell are also studying the frictional forces at payload trunnions. This will indicate how much vibration is transmitted through the trunnion in non-load bearing directions.

Studies of the payload bay pressure equalization vent noise are being planned by the Aerospace Corporation. A vent may be tested in a wind tunnel to study the cavity resonance characteristics of the vents. Currently, Rockwell International is studying the feasibility of closing vents during liftoff but there are no definite plans to develop a fix for quieting the vent discrete tones.

Hughes has tested a spacecraft in a reverberation chamber with localized discrete tones and assessed the impact on a spacecraft structure. Lockheed and the Aerospace Corporation are contemplating this type of simulation of the vent discrete tones for future tests of the Space Telescope and Air Force payloads.

Instrumentation for payloads is being planned at a number of centers. GSFC plans to take measurements on several NASA pallet-mounted payloads. The Centaur upper stage will be extensively instrumented on its first flight by the Lewis Research Center (LeRC). Galileo will have some instrumentation added by JPL and the Ulysses Project (formerly the International Solar Polar Mission) is being instrumented by LeRC. The Air Force plans measurements on several of its payloads. To facilitate these measurements the Air Force is developing a data recording system, the Orbiter Experiment Autonomous Supporting Instrumentation System (OASIS). The Air Force has also proposed a new data acquisition system that will not require STS power. Payload bay data recorded on OASIS will be documented in post flight reports and in summary and conclusion reports by JPL.

There are plans to update the VAPEPS program by adding a data dictionary and verifying its dynamic environment prediction methods. LMSC plans more elaborate modeling of payloads, similar to that in VAPEPS, for vibroacoustic predictions.

Forcing functions for the transient loads analyses for both the liftoff and landing event are being reviewed by both NASA JSC and Rockwell International using flight data obtained to date. Revised forcing functions for liftoff will be released to the payload community in the near future.

9.0 CONCLUSIONS

9.1 Acoustic Data

The results from the acoustic data are summarized below:

1. The maximum overall mean acoustic environment for small payloads, 132 dB, occurred at liftoff. A few frequencies are dominated by transonic aerodynamic noise.
2. The acoustic environment overall mean level at pallet payloads was 13 dB below the preflight JSC Volume 14 requirements. Measured levels below 125 Hz were nearly the same as the original requirement. The JSC Volume 14 requirement has been revised on the basis of flight data to 138 dB overall.
3. The acoustic environment is relatively uniform for small payloads except near the payload bay perimeter. In particular, there seem to be higher levels near the payload bay doors.
4. The small pallet payloads flown on STS-1 through STS-5 have negligible effect on the local acoustic environment. The exception is that higher acoustic levels will exist where a payload surface is near the bay longeron bridge fitting plates or payload bay doors.
5. Large payloads may have a significant effect on local acoustic and vibration levels. Data from ESA pallet outer side walls and the Spacelab show local increases in environments due to large payloads. Model data and analytical predictions support the conclusion that large payloads can increase local acoustic environments.
6. The payload bay acoustic environments may be divided into two characteristic regions at the bay perimeter and the bay "core" region or at small payloads. For small payloads or empty bay the payload region extends nearly to the bay sidewalls. Mean levels at the bay perimeter were 3.5 dB higher than at pallet payloads for Flights 1 through 5 and exhibited a greater variance.
7. There are high intensity discrete tones emanating from the payload bay pressure equalization vents during transonic flight. Multiple discrete tones are centered in the 315 Hz 1/3 octave band. In general, these discrete tones will only influence payloads in the vicinity of the vents. The intensity at each vent depends on the direction of air flow through it during transonic flight. Some vents ingest air while others expel it from the bay.

8. Flight-to-flight variation was approximately ± 1.5 dB in each $1/3$ octave band for the first 5 flights. Configuration and launch site changes could influence flight-to-flight variations, but these effects should be small. Model tests performed by the Aerospace Corporation show that launch pad effects at Vandenberg should not be significant.
9. Other uncertainties have been determined for the vibroacoustic data base. These uncertainties include:
 - a. Spatial variation, calculated as probability levels.
 - b. Spatial bias errors, negligible for payload microphones.
 - c. Data system/reduction errors, ± 1 dB overall.
10. There is not total agreement among DATE Working Group members on whether or not to make large payload acoustic environment corrections. However, among 3 centers that do account for payload effects, prediction results agree well for a DOD large payload.

9.2 High Frequency Vibration Data

1. The most severe vibration environment occurred during liftoff in general, although in some cases the vibration environment was dominated by transonic flight for certain frequencies.
2. Vibrations at pallet trunnions are well below those seen at the payload bay longeron. Levels on the pallet experiment support bracket or hard structure were attenuated more than 10 dB below pallet trunnion levels.
3. Requirements for small payloads mounted to the payload bay longeron have been increased because of higher than expected vibration.
4. Vibration at the pallet shelves was the most severe measured on the pallet payloads for STS-2 and 3.
5. High frequency shock responses were not severe on the first five flights.
6. Orbiter structure induced vibration may be higher at payloads than anticipated below 125 Hz. The acoustic transfer function for STS payload vibration is not well understood at this time.

9.3 Low Frequency Vibration Data

In the loads or low frequency (0-50Hz) regime the worst levels were observed during liftoff and landing.

Generally, the responses during liftoff were well below those of the design load factors, as shown in Table 9-1, from Reference 31. A comparison of the composite shock spectra of the flight data for STS-2 through STS-5 (Figure 9-1) to the composite of the analytical cases shows that the excitation at the higher frequencies is over-predicted and there is underprediction at the low frequencies, specifically at 3 Hz. The comparison in the x direction is somewhat better than in the y and z directions. A comparison of the quasi-static load factors measured in the first five flights with payload design requirements is shown in Table 9-2. The landing conditions, shown in Table 9-3, are all below the design requirements. On STS-3 the landing conditions were near the limit. The landing load factors (Table 9-4) were also generally below design values. There was a y response on the keel which exceeded the design condition. The discrepancy between the flight data and the analytical predictions at 3 Hz and in the 12-50 Hz region is of concern to many payloads.

Repeatability for liftoff appears reasonable in the x direction up to 5 Hz, but seems to diverge above that. For the y direction the variation is appreciable. The z direction shows the best correlation for liftoff. In general, for the liftoff event, it can be stated that the repeatability for the SRB Ignition is better than for the SSME Ignition.

The repeatability for the landing event is not very good in amplitude but is quite consistent in frequency content.

Table 9-1. Maximum Load Factors for STS Lift-Off from the Orbiter Low-Frequency Accelerometers

| MEASURE POINT NUMBER | X ₀ LOCATION DESCRIPTION | DIRECTION | FLIGHT DATA, g | | | | | PRELIMINARY DESIGN LOAD FACTORS |
|----------------------|-------------------------------------|-----------|----------------|-------|-------|-------|-------|---------------------------------|
| | | | STS-1 | STS-2 | STS-3 | STS-4 | STS-5 | |
| V34A9434A | 1294, BULKHEAD | NX | -2.10 | -1.79 | -1.91 | -1.82 | -1.87 | -0.2/-3.2 |
| V34A9433A | 979, KEEL | NY | 0.40 | 0.18 | 0.18 | 0.14 | 0.15 | ±1.4 |
| V34A9435A | 1294, BULKHEAD | NY | 0.25 | 0.13 | 0.19 | 0.08 | 0.13 | ±1.4 |
| V34A9430A | 823, LEFT LONGERON | NZ | 2.8* | 2.74 | 0.72 | 0.94 | 0.77 | ±2.5 |
| V34A9431A | 973, RIGHT LONGERON | NZ | 2.9* | 0.80 | 0.98 | 0.70 | 0.88 | ±2.5 |
| V34A9432A | 973, LEFT LONGERON | NZ | 2.9* | 1.52 | 0.68 | 0.72 | 0.88 | ±2.5 |
| V34A9436A | 1294, BULKHEAD | NZ | 1.25* | 0.25 | 0.25 | 0.35 | 0.32 | ±2.5 |

*HIGH Z₀ ACCELERATIONS ON STS-1 CAUSED BY SRB IGNITION OVERPRESSURE. LAUNCH PAD MODIFICATIONS WERE MADE PRIOR TO STS-2.

Table 9-2. Shuttle Quasi-Static Load Factors on STS-1 Through STS-5

| DIRECTION | LOAD FACTOR | | | | | PAYLOAD REQUIREMENTS |
|----------------|-------------|-------|-------|-------|-------|----------------------|
| | STS-1 | STS-2 | STS-3 | STS-4 | STS-5 | |
| ASCENT | | | | | | |
| NX | -2.92 | -2.99 | -2.92 | -2.93 | -2.95 | -3.17 |
| NY | 0.1 | 0.2 | 0.1 | 0.2 | 0.2 | ±0.4 |
| NZ | -0.6 | -0.6 | -0.6 | -0.6 | -0.6 | -0.9 |
| DESCENT | | | | | | |
| NX | 0.4 | 0.4 | 0.3 | 0.3 | 0.4 | 1.01 |
| NY | 0.2 | 0.2 | 0.3 | 0.3 | 0.1 | ±0.85 |
| NZ | 1.6 | 1.9 | 1.6 | 1.6 | 1.7 | 2.5 |

Table 9-3. Landing Touchdown Conditions in Shuttle Test Flights

| CONDITION | FLIGHT DATA | | | | |
|--|-------------|-------|-------|-------|-------|
| | STS-1 | STS-2 | STS-3 | STS-4 | STS-5 |
| HORIZONTAL VELOCITY AT MAIN IMPACT, KNOTS | 189 | 196 | 233 | 199 | 202 |
| MAIN GEAR SINK RATE, FPS | 1 | <1 | 5.7 | 1 | <1 |
| NOSE GEAR SINK RATE, FPS | 5.7 | 5.1 | 8.8 | 5.4 | 4.7 |

Table 9-4. Maximum Load Factors for STS Landing from the Orbiter Low-Frequency Accelerometers

| MEASUREMENT NUMBER | X ₀ LOCATION, DESCRIPTION | DIRECTION | FLIGHT DATA, g | | | | | PRELIMINARY DESIGN LOAD FACTORS |
|-----------------------|---|-----------|----------------|-------|-------|-------|-------|---------------------------------------|
| | | | STS-1 | STS-2 | STS-3 | STS-4 | STS-5 | |
| V34A9434A | 1204, BULKHEAD | NX | 0.6 | 0.5 | 0.6 | 0.3 | 0.3 | 1.5/-1.7 |
| V34A9433A | 878, KEEL | NY | 0.2 | 0.2 | 0.9 | 0.1 | 0.1 | ±0.8 |
| V34A9435A | 1204, BULKHEAD | NY | 0.2 | 0.1 | 0.5 | 0.1 | 0.1 | ±0.8 |
| V34A9430A | 823, LEFT LONGERON | NZ | 1.6 | 1.3 | 2.8 | 1.4 | 1.4 | 0.2/3.0 |
| V34A9431A | 873, RIGHT LONGERON | NZ | 1.4 | 1.8 | 2.3 | 1.4 | 1.3 | 0.2/3.0 |
| V34A9432A | 873, LEFT LONGERON | NZ | 1.4 | 1.2 | 2.3 | 1.4 | 1.4 | 0.2/3.0 |
| V34A9433A | 1204, BULKHEAD | NZ | 1.4 | 1.2 | 2.2 | 1.3 | 1.2 | 0.2/3.0 |

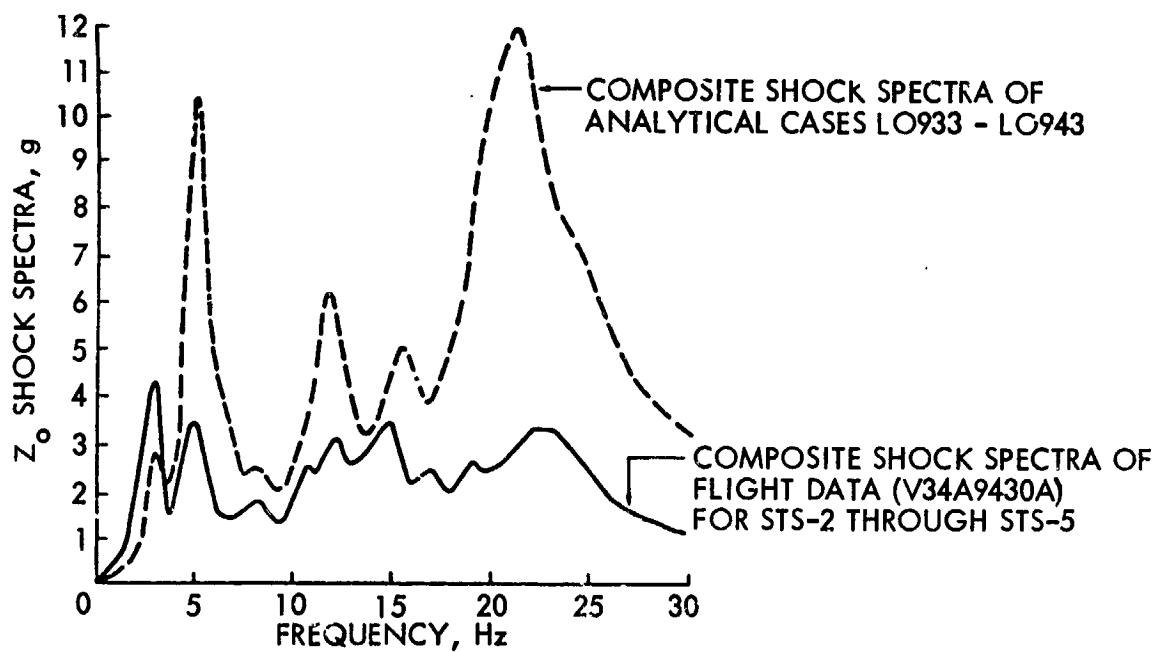


Figure 9-1. Shock Spectra of Left Longeron Z₀ Load Factor at X₀ 823 for Flight Data and Analytical Design Cases, SRB Ignition to +3 Seconds

9.4 Data Deficiencies

9.4.1 Acoustics and High Frequency Vibration

There is generally good agreement among the NASA and industrial centers in defining the acoustic environment for pallet payloads and the vibration environment at the orbiter pallet attachment structure. However, there are still significant uncertainties in the definition of these environments. The data deficiencies are divided into five major areas of concern: a) the acoustic environment at liftoff, which is the highest broad-band noise event in the payload bay, b) the acoustic environment during transonic flight, which is characterized by higher level discrete noise emanating from the pressure equalization vents, c) structure-borne vibration induced from the orbiter into payloads, d) the effects of launch vehicle configuration differences or changes on the payload bay environments, and e) the effects of the difference between the KSC and VLS pad and terrain on the environments.

The deficiencies in the liftoff acoustics data result from the lack of measurements in the forward one-third of the cargo bay, no definition of the effect of large payloads on the bay environment, and the low signal to noise ratio which compromised the validity of the high frequency data. The greatest concern is centered on the effects of large payloads on the environment. Model data and limited flight data indicate that large payloads can have a significant effect on the local acoustic environment. The lack of data for the forward one-third of the bay was also a concern, particularly in view of the high-level microphone measurement on the forward bulkhead. The lack of valid high frequency data is due to the relatively benign levels measured; however, this environment remains undefined.

The inadequate definition of the higher-level discrete noise emanating from the pressure equalization vents has been identified as the major data deficiency for transonic flight. Based on the limited data available near the aft vents, transonic flight vent noise would be a significant acoustic event for payloads located in the vicinity of the vents. However, the trend of the data measured near the vents is inconsistent, the forward vent environment is unknown, and the effects of large payloads on the localized acoustic environment near the vents are also unknown.

Comparing flight vibration measurements on the OSS-1 pallet payload to vibration response measurements obtained from the pallet ground acoustic test showed that the orbiter may induce significant mechanically transmitted vibration in the lower frequencies (below 125 Hz). A similar effect was observed on the STS-4 pallet payload. A major flaw in payload design and test requirements may exist and an adequate data base is required to characterize the mechanically transmitted vibration for the range of anticipated STS payload masses and structural configurations.

Other areas of flight data deficiencies are the effects of vehicle configuration changes and launch sites on the payload environment. The differences between the KSC and VLS launch pads have a great potential for causing major differences in the payload environments; a data base for VLS launches will be required to define the differences. Other areas that can affect payload environments are STS engine upratings and changes in the STS configuration.

9.4.2 Low Frequency Vibration

Deficiencies in the low frequency data base are discussed by the subheading below.

Frequency Response

The DFI accelerometers had a response limitation of 20 Hz (or more accurately, a flat response spectra to 14 Hz) while the DATE accelerometer measurements were good to 50 Hz (or more accurately, a flat response spectra to 18 Hz). The usefulness of the DFI data was further limited by a sampling rate of 100 samples/second. Some of the DATE accelerometers did not measure the DC component, responding only above 1.5 Hz. This makes correlation of the loads data difficult since such instruments produce erroneous data at the initiation of transients. For purposes of loads verification, instrumentation with a flat frequency response from 0 to 50 Hz is required.

Measurement Locations

Some measurements were not suitable for a systematic analysis verification. This is especially true where the input to a payload was not completely defined, that is, where not all pertinent input degrees of freedom were measured. This is further complicated by the friction found in the trunnions. Measurements on both side of the payload/Shuttle interface are desirable but were not always implemented.

Model Fidelity

Some of the payload dynamic models for STS-2 through STS-5 were not adequately test verified. Hence, it is not known if the noted discrepancies between analysis and flight responses are attributable to the Shuttle model, payload model, or forcing function inadequacies.

Data Base

Although the low frequency acceleration measurements from STS-2 through STS-5 have produced valuable data, there are limitations which make the data base incomplete. First, the data is valid for Orbiter Vehicle (OV) 102 only. Structural differences between this vehicle and other Orbiter vehicles limit the validity for the extrapolation of payload loads for the other Orbiter vehicles. Furthermore, the data obtained was for light-weight payloads only and there were no alleviated elements. Data for crosswind and high sink rate landings is also lacking. STS-3 did have a high sink rate but constitutes only one data point. Finally, four flights are too limited in number for a representative data base. Other considerations for a complete data base are launches from VLS and anticipated changes in the launch vehicle such as engine characteristics and structural changes in the SRB's and the ET.

10.0 RECOMMENDATIONS

A number of tasks are recommended as follow-on activities to the current DATE effort. Improving the data base and analysis methods will lead to lower margins and project costs. In general these tasks include:

1. Establish an expanded STS loads and vibroacoustic data base.
2. Improve large payload and payload proximity effect methodologies.
3. Refine characterization of the pressure equalization vent noise.
4. Determine payload vibration transfer functions from the STS acoustic and vibration environment.
5. Develop a transient loads and acoustically induced environmental criteria.
6. Refine the VAPEPS program and its payload prediction methods.
7. Define the launch environments at the VLS.

10.1 STS Dynamic Data Base

10.1.1 Vibration and Acoustic Data Base

A data base should be established that includes data taken on non-DATE payloads. The data should be documented in post flight reports and in Summary and Conclusion reports similar to this report. It is recommended that the STS vibroacoustic data base be expanded in the following specific areas:

Include available vibration and acoustic data from all instrumented STS payloads in the STS data base.

The STS data signal to noise ratio should be improved so that high frequency acoustics and pallet hard points vibration may be measured.

The recording of vibroacoustic data at common points in the bay for each flight should continue. Acoustic measurement locations should include the bay sidewall and bulkhead locations identical to those in STS 1-5. Vibration measurements should include data taken on either side of pallet trunnions, the orbiter bay trunnion support structure. Ground acoustic tests should be planned to supplement the orbiter flight data. This will allow further study of the vibroacoustic transfer functions of payload vibration responses.

Instrumentation of future payloads should be carefully planned, particularly for large payloads. Transducer locations should be planned to include measurement of the discrete tones near the pressure equalization vents, as well as the environment at the forward 1/3 of the payload bay, and the airspace near the bay doors. Measurements should be devised to define large payload mass attenuation factors.

Both the orbiter and the launch facility should be instrumented for VLS launches.

10.1.2 Low Frequency Data Base

Future data acquisition should be directed mainly towards verifying basic loads methodology and towards providing an adequate statistical data base to provide the desired level of confidence, that is, a methodology which would predict payload loads to acceptable but not excessive levels of conservativeness. It is generally agreed (Refs. 17 and 30) that improved correlation is required between analytical predictions and flight data.

To this end additional effort should be directed towards analyzing data and analysis/flight data correlation. Future data acquisitions should be directed towards the original objectives of the NASA DATE Program. Well planned and analyzed experiments should be flown, completely characterizing the input and responses of the payloads. To implement this, supporting technology for the application of flight data for the design of payloads is required.

In building a data base for loads prediction purposes, special attention should be paid to account for all the variables such as structural variations in the launch vehicle and payloads. It is important that data be obtained for a variety of payloads, specifically heavy payloads and payloads utilizing load alleviation. Data from STS-2 through STS-5 and only for OV-102 is not considered a satisfactory data base. Flight response measurements in the low frequency regime must be made on both sides of the payload/Shuttle interface and must completely define the input to the payload. Such instrumentation must be phase correlated, and have a flat frequency response in the 0-50 Hz region. A sampling rate of no less than 500 samples/second is desirable. The instrumentation should be well planned using preflight analyses. Typically, such instrumentation should measure the responses of the major payload masses. Ideally, such measurements should consist of a combination of DC accelerometers, strain gauges, and deflection transducers.

A representative statistical data base is desired for the development of design forcing functions. Factors in the development of such forcing functions are: repeatability of data, adequacy of the current design forcing functions, and the adequacy of the current methodology, that is, how well can the responses be reproduced by post-flight analysis using forcing functions derived from flight measurements.

Other recommendations include the acquisition of data for crosswind and high sink rate landings, data for the Western Test Range (WTR), expected to be different from Eastern Test Range (ETR) data due to launch stand differences, and a minimum level of data for all future flights to evaluate flight-to-flight variations. Special attention should be directed to the acquisition of

flight data for the verification of the effect of trunnion friction on payload loads. This will require measurements on both the payload and Orbiter side of the interface.

The benefits of flight instrumentation are cost-effective analysis techniques leading to increased reliability, lower structural design margins, lower structural weight, and lower cost for analysis and test.

10.2 Large Payload Methodology

Empirical methodologies should be developed to account for payload position and large payload effects in the payload bay. Payload effect prediction curves should be developed for various large payload configurations and payload/orbiter proximities. Data from model tests on large payloads should be included in the development of these methodologies where appropriate. The PACES code should be revised on the basis of acoustic data taken on large payloads.

Low Frequency (0-50 Hz) flight response data should be obtained for large, heavy payloads, preferably payloads utilizing an upper stage such as IUS or Centaur. These data should be compared to analytical predictions. Such a comparison should include a study of the effect of trunnion friction.

10.3 Vent Tone Definition

The bay pressure equalization vent discrete tone environment should be defined with sound power levels and sound pressure levels versus distance for each of the 8 bay vents. The feasibility of performing wind tunnel tests to characterize this noise source should be determined. A vent tone model should be developed that will predict tone intensities at payloads, and the effect of the vent discrete noise on spacecraft structures should also be studied.

10.4 Vibroacoustic Transfer Functions

Payload response vibroacoustic transfer functions response need to be developed. Current vibration specifications may be deficient for frequencies below 125 Hz. In addition, the difference in acoustic efficiency (of vibration excitation in payloads) between STS flight and acoustic tests should be defined.

10.5 Loads Combination Methodology

A methodology for combining transient loads and acoustically induced loads at payloads should be developed. This problem is currently under study at Rockwell International, GSFC, and Aerospace Corporation.

Additional flight data should be obtained to resolve the discrepancy between the flight responses and the analysis in the 12-50 Hz region. To accomplish this, instrumentation and a data acquisition system are required which guarantee a phase correlated frequency response flat to 50 Hz. ●

10.6 VAPEPS Improvement

Proposals are being prepared that will create a center for centralized VAPEPS data base management. Eventually, it is hoped that this data base will be accessible to users by remote site computer terminals. This center will also coordinate program maintenance and improvements. An independent validation of VAPEPS modeling and prediction methods is also being proposed.

The data management portion of VAPEPS should also be revised to include a data dictionary that will make the program easier to use.

10.7 Western Test Range Environment and Forcing Functions for Loads Analysis

The acoustic environment at the Western Test Range should be defined and compared to scale model test results and to the Kennedy Space Center launch levels.

11.0 REFERENCES AND BIBLIOGRAPHY

11.1 References

1. "Payload Bay Acoustic and Vibration Data from STS-1 Flight," DATE Report 002, NASA GSFC, Greenbelt, MD, June 1981.
2. "Payload Bay Acoustic and Vibration Data from STS-2 Flight," DATE Report 003, NASA GSFC, Greenbelt, MD, January 1982.
3. "Payload Bay Acoustic and Vibration Data from STS-3 Flight," DATE Report 004, NASA GSFC, Greenbelt, MD, June 1982.
4. "Payload Bay Acoustic and Vibration Data from STS-4 Flight," DATE Report 005, NASA GSFC, Greenbelt, MD, December 1982.
5. "Payload Bay Acoustic and Vibration Data from STS-5 Flight," DATE Report 006, NASA GSFC, Greenbelt, MD, May 1983.
6. On, F., "Power Spectral Density Evaluation of Space Transportation System (STS) Transonic Flight Acoustic Measurements (250-350 Hz)," Internal NASA GSFC Memorandum, Greenbelt, MD, December 1982.
7. On, F., "Update to Acoustic Environment for Space Transportation System (STS) Payloads," Internal NASA GSFC Document, GSFC, Greenbelt, MD, September 1982.
8. Brodeur, Stephen J., "Detailed Data for Measured and Predicted Accelerations for Goddard Space Flight Center Accelerometer Locations During STS-3/OSS-1 Lift-Off and Landing," Internal NASA GSFC Document, GSFC, Greenbelt, MD, May 1982.
9. Wise, J., "DATE Dynamic Data Error Analysis," in "Proceedings of the NASA OAST Shuttle Payload Environments and Loads Prediction Workshop," JPL D-1347 (internal JPL document), Jet Propulsion Laboratory, Pasadena, CA, January 1984.
10. Piersol, A.G., "Space Shuttle Payloads Acoustic Predictions Study," NASA CR-159956 (5 volumes), NASA GSFC, Greenbelt, MD, March 1980.
11. Cho, A.C., "Sound Transmission Loss of the Mid-Fuselage/Payload Bay of the Orbiter," SSP/V&A: 74-25, Rockwell International, Downey, CA, April 1974.
12. Cho, A.C., "Orbiter Payload Bay Acoustic Attenuation," SSP/V&A: 75-44, Rockwell International, Downey, CA, May 1975.
13. "Shuttle Orbiter/Cargo Standard Interfaces," JSC 07700 Volume XIV, Attachment 1 (ICD 2-19001), Revision G, NASA JSC, Houston, TX, September 1980.
14. Hill, R.E., and Coody, M.C., "Vibratio. and Acoustic Environments for Payload/Cargo Integration," AIAA Paper, 21st AIAA Aerospace Sciences Meeting, Reno, NV, January 1983.

15. On, Frank J., "OSS-1 Payload - DATE Vibroacoustic Data From the GSFC System Level Acoustic Test," Memorandum Report 731-0001-82, GSFC, Greenbelt, MD, 1982.
16. LMSC unpublished viewgraphs.
17. McBride, J., and Harrison, P., "Spacelab-1, Vibroacoustics," in "Proceedings of the NASA OAST Shuttle Payload Dynamic Environments and Loads Prediction Workshop," JPL D-1347 (internal JPL document), Jet Propulsion Laboratory, Pasadena, CA, January 1984.
18. "Summary Report on Air Force Workshop on STS Payloads Environmental Data," JPL D-828 (internal JPL document), Jet Propulsion Laboratory, Pasadena, CA, October 1983.
19. Piersol, A.G., "Bias Error Corrections for Acoustic Data from Space Shuttle FRF and STS-1 through STS-3," Report 4547, Bolt, Beranek, and Newman, Inc., Canoga Park, CA, 1981.
20. Cho, A.C., Dougherty, N.S., and Guest, S.H., "Scale Model Acoustic Test of SSV for VAFB," in "Proceedings of the NASA OAST Shuttle Payload Dynamic Environments and Loads Prediction Workshop," JPL D-1347 (internal JPL document), Jet Propulsion Laboratory, Pasadena, CA, January 1984.
21. O'Connell, M.R., "Shuttle Payload Dynamic Environments - Update," presented at the 8th IES Aerospace Testing Seminar, Los Angeles, CA 1984.
22. "Technical Operating Report, Talon Gold Vibroacoustic Data Analysis," LMSC D-985437, LMSC, Sunnyvale, CA, February 1984.
23. Henricks, W., Davis, B.K., Russell, D.W., and Schafer, J.E., "Vibroacoustic Payload Environment Predictor System (VAPEPS)," NASA CR-166822, Volumes II through IV, LMSC, Sunnyvale, CA, December 1982.
24. Tanner, C., "Acoustic Environments for DOD Payloads on Shuttle," in "Proceedings of the NASA OAST Shuttle Payload Dynamic Environments and Loads Prediction Workshop," JPL D-1347 (internal JPL document), Jet Propulsion Laboratory, Pasadena, CA, January 1984.
25. "Acoustic Requirements for DOD Shuttle Payloads Launched from KSC," Document SD-YV-0093, Aerospace Corporation, El Segundo, CA, June 1982.
26. On, F., "Development of Baseline Random Vibration Environment Criteria for Shuttle Pallet Payload Subsystems," NASA TM 86087, NASA GSFC, Greenbelt, MD, April 1984.
27. Hamilton, D.A., and Rocha, R., "An Overview of Shuttle Payload Bay Structural Response for STS-1," Report JSC - 17769, NASA JSC, Houston, TX, 1981.
28. Hamilton, D.A., and Rocha, R., "An Overview of Shuttle Payload Bay Structural Response for STS-2 and STS-3," Report JSC-18371, NASA Johnson Space Center, Houston, TX, June 1982.

29. Hamilton, D.A., "A Review of Shuttle Payload Bay Low Frequency Structural Response for STS-1 through STS-5," Report JSC-18870, NASA Johnson Space Center, Houston, TX, April 1983.
30. Brodeur, S.J., "Comparison of Flight Data Versus Predictions for Low Frequency Acceleration Loads on STS-3/OSS-1 Instruments," in "Proceedings of the NASA OAST Shuttle Payload Dynamic Environments and Loads Prediction Workshop," JPL D-1347 (internal JPL document), Jet Propulsion Laboratory, Pasadena, CA, January 1984.
31. "Proceedings of the NASA OAST Shuttle Payload Environments and Loads Prediction Workshop," JPL D-1347 (internal JPL document), Jet Propulsion Laboratory, Pasadena, CA, January 1984.

11.2 Bibliography

32. "Summary of Loads and Low Frequency Dynamics Panel Presentations," in "Proceedings of the Air Force Workshop on STS Payloads Environmental Data," JPL D-947 (internal JPL document), Jet Propulsion Laboratory, Pasadena, CA, June 1983.
33. O'Connell, M.R. and Kern, D.L., "Acoustic Environments for JPL Payloads Based on Early Flight Data," The Shock and Vibration Bulletin, No. 53, Naval Research Laboratory, Washington D. C., May 1983.
34. Young, J.P., "Payload Environments and Dynamics," AIAA Paper 82-1778, Washington, D.C., October 1982.
35. Divita, R.L. (JPL), and Bangs, W.F. (GSFC), "The Shuttle Environment from a Payload Viewpoint," AIAA Paper 81-0268, 19th AIAA Aerospace Sciences Meeting, St. Louis, MO, January, 1981.
36. Kern, D.L., and O'Connell, M.R., "Dynamic Environments for Space Shuttle Payload," N82-2591, 12th IES Space Simulation Conference, Pasadena, CA, May 1982.
37. On, F.J., "Evaluation of Space Transportation System (STS) OV-102, Orbiter Payload Bay Acoustic Environment," NASA TM 84958, NASA Goddard Space Flight Center, Greenbelt, MD, 1982.
38. Wilby, J.F., Piersol, A.G., and Wilby, E.G., "An Evaluation of Space Shuttle STS-1 Payload Bay Acoustic Data and Comparison with Predictions," BBN Report 4738, Bolt, Beranek, and Newman, Inc., Canoga Park, CA, February 1982.
39. Chen, J.C., and Garba, J.A., "Survey of Load Methodologies for Shuttle Orbiter Payloads," JPL Publication 80-37, Jet Propulsion Laboratory, Pasadena, CA, June 1980.
40. Keegan, W.B., "Vibration and Acoustic Environments of Early Payloads," in "Proceedings of the 7th IES Aerospace Testing Seminar," Los Angeles, CA, October 1982.
41. "An Interim Report on Shuttle Vibroacoustics," Shock and Vibration Bulletin, No. 47, Vibration and Acoustic Unit, Space Division, Rockwell, International Corporation, Downey, CA, 1977.

42. "Detailed Data for Measured and Predicted Accelerations for Goddard Space Flight Center (GSFC) Accelerometer Locations During Space Transportation System-3 (STS-3)/Office of Space Science - 1 (OSS-1) Lift-Off and Landing," Internal GSFC Document 731.1, Structural Loads and Analysis Section, GSFC, Greenbelt, MD, 1982.
43. Clauser, R.E., and Wong, D.M., "Acoustic Requirements for DOD Shuttle Payload Launched From KSC," Document 83-3493.17029, Aerospace Corporation, El Segundo, CA, February 1983.
44. "The Shuttle Environment Workshop," NAS5-27362, NASA Office of Space Science and Applications, Calverton, MD, February 1983.
45. Pratt, H.K., "Space Shuttle System Acoustic And Shock Data Book," SD 74-SH-00824A, Shuttle Vibration and Acoustic Unit, Space Division, Rockwell International, Downey, CA, December 1976.
46. On, F.J., "Evaluation of STS Payload Bay Acoustic Environment Based on STS-1 Flight Measurements," Memorandum for the Record (internal GSFC document), GSFC, Greenbelt, MD, August 1981.
47. "Space Shuttle Orbiter Vibration Data Book," SD 76-SH-0203A, Space Division, Rockwell International, Downey, CA, November 1978.
48. "Details Concerning SSV Acoustic Model Testing at AMTF (Stand 116)," Internal NASA-MSFC Memorandum S&E-Aero-AU-73-55, From S&E-Aero-AU to S&E-ASTN-T, NASA MSFC, Marshall Space Flight Center, AL, April 1973.
49. "Environmental Requirements and Test Criteria for the Orbiter Vehicle," MF0004-014, Space Division, Rockwell International, Downey, CA, March 1978.
50. "Shuttle Orbiter/Cargo Standard Interfaces," NASA-JSC Interface Control Document 2-19001, NASA JSC, Houston, TX, Revised February 1978.
51. Cho, A.C., "Sound Transmission Loss of the Mid-Fuselage/Payload Bay of the Orbiter," SSP/V&A: 74-25, Rockwell International, Downey, CA, April 1974.
52. Cho, A.C., "Orbiter Payload Bay Acoustic Attenuation," SSP/V&A: 75-44, Rockwell International, Downey, CA, May 1975.
53. "Correlation of Model and Full Scale Acoustic Data Measured on the STS Program," MDC G8427, McDonnell Douglas Astronautics Company, Huntington Beach, CA, December 1979.
54. Coody, M.C., and Pratt, H.K., "The Development and Verification of Shuttle Orbiter Random Vibration Test Requirements," Shock and Vibration Bulletin No. 52, Rockwell International, Downey, CA, May 1982.

Summary and Conclusion Report

STS Flight 1-5, and 9

APPENDIX

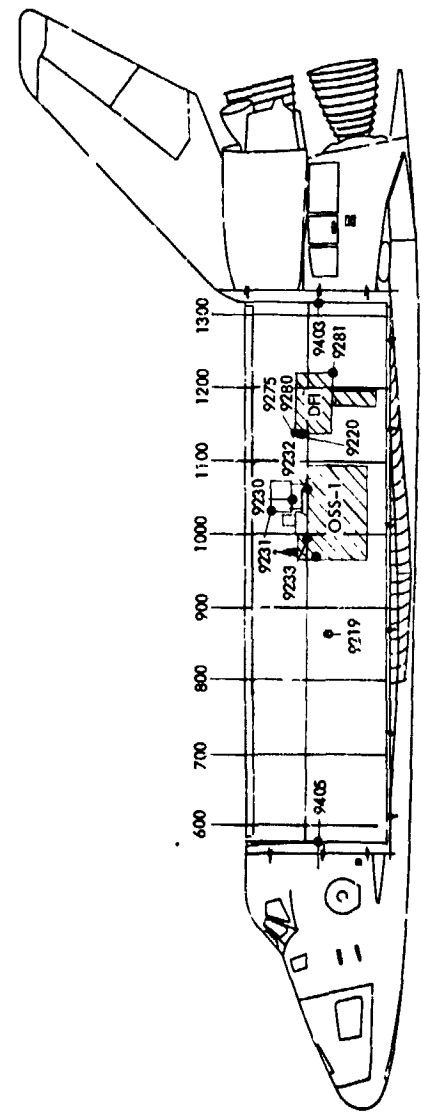
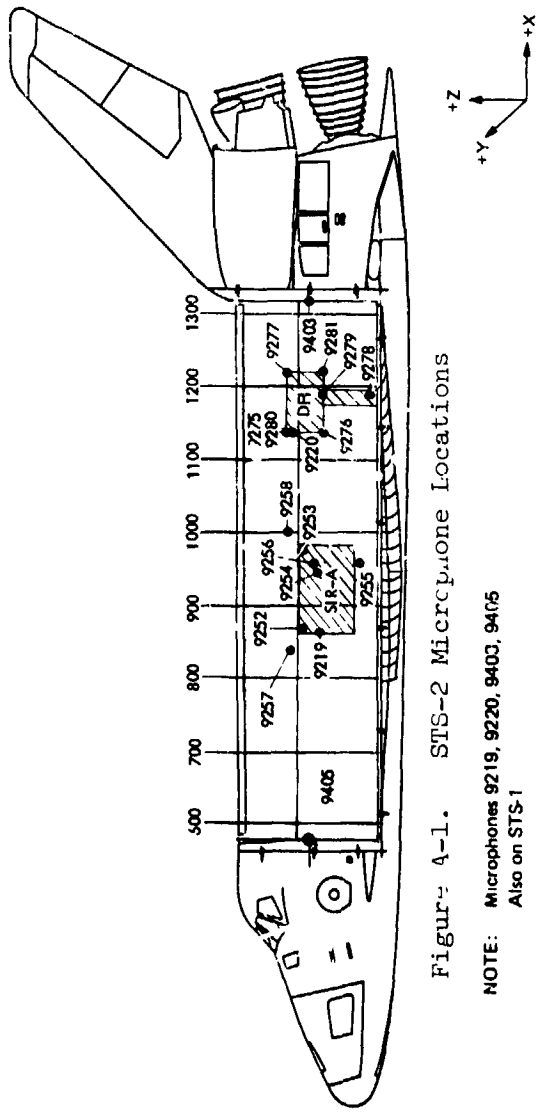
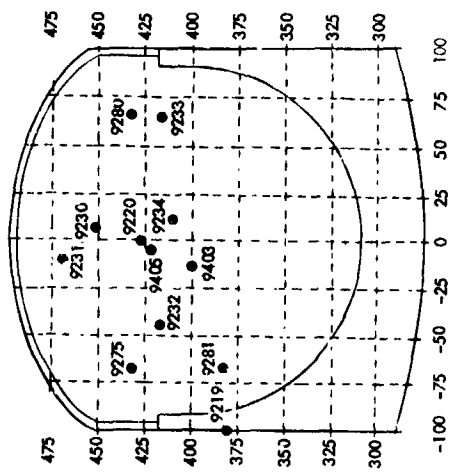
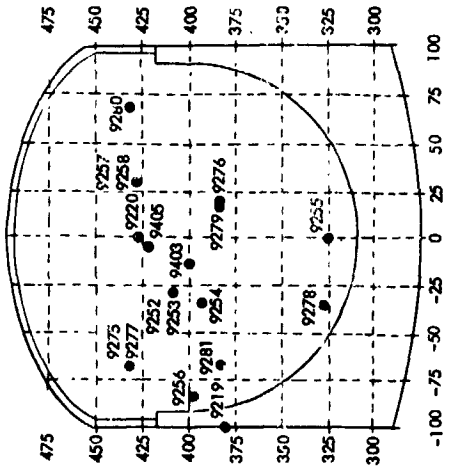


Figure A-1. STS-2 Microphone Locations

NOTE: Microphones 9219, 9220, 9403, 9405
Also on STS-1

Figure A-2. STS-3 Microphone Locations

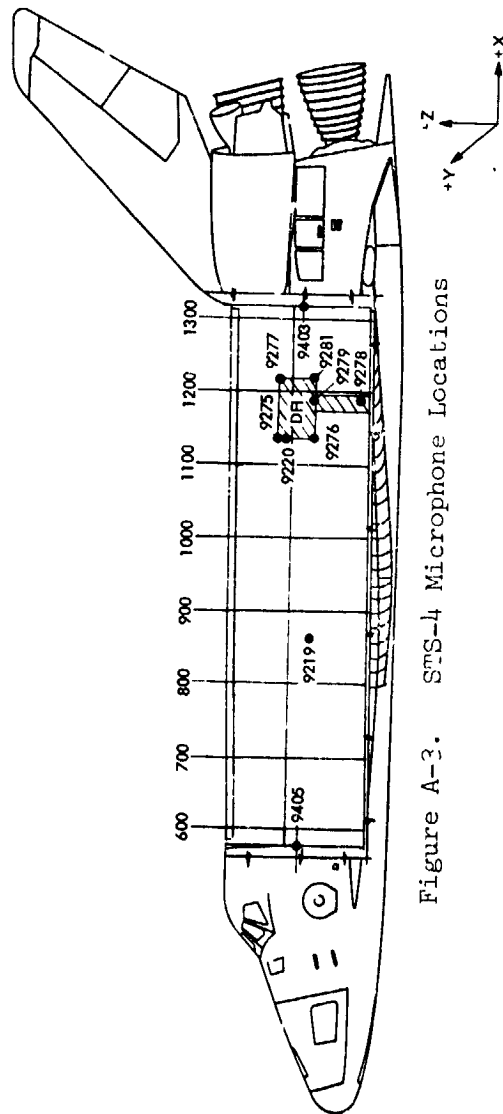
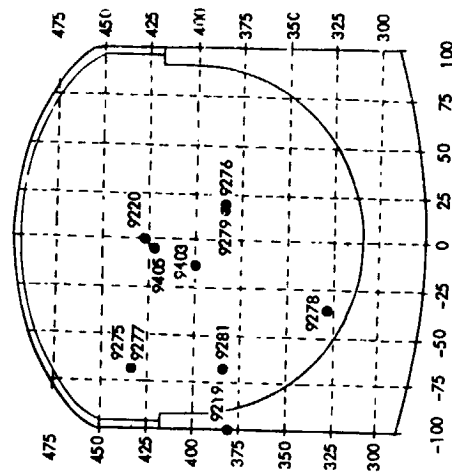
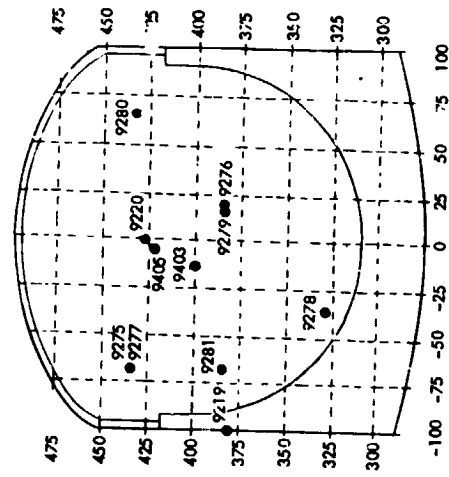


Figure A-3. STS-4 Microphone Locations

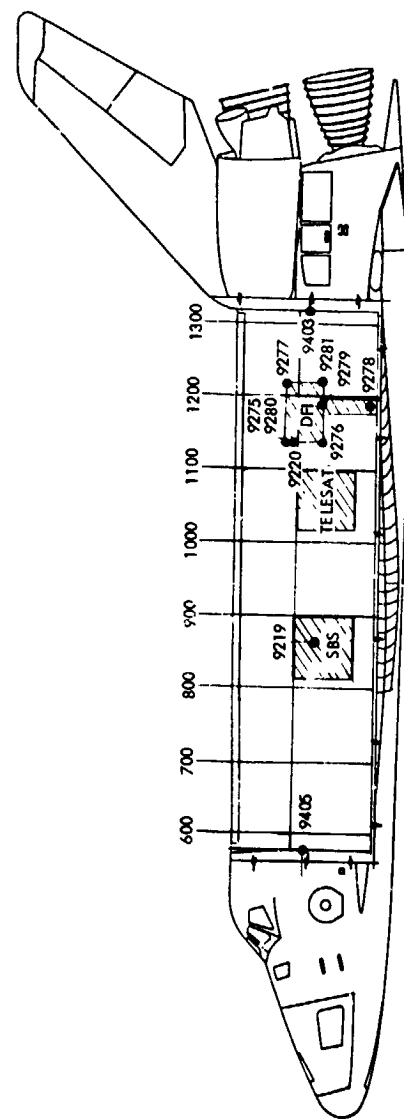
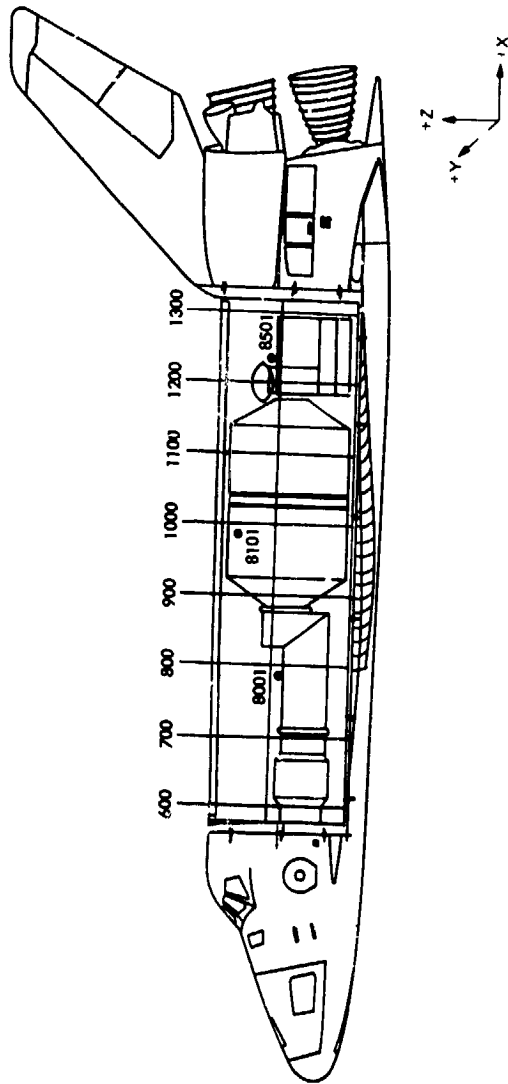
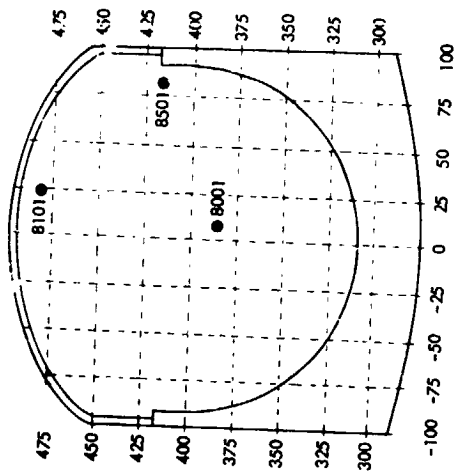


Figure A-4. STS-5 Microphone Locations



A-4

Figure A-5. STS-9 Microphone Locations

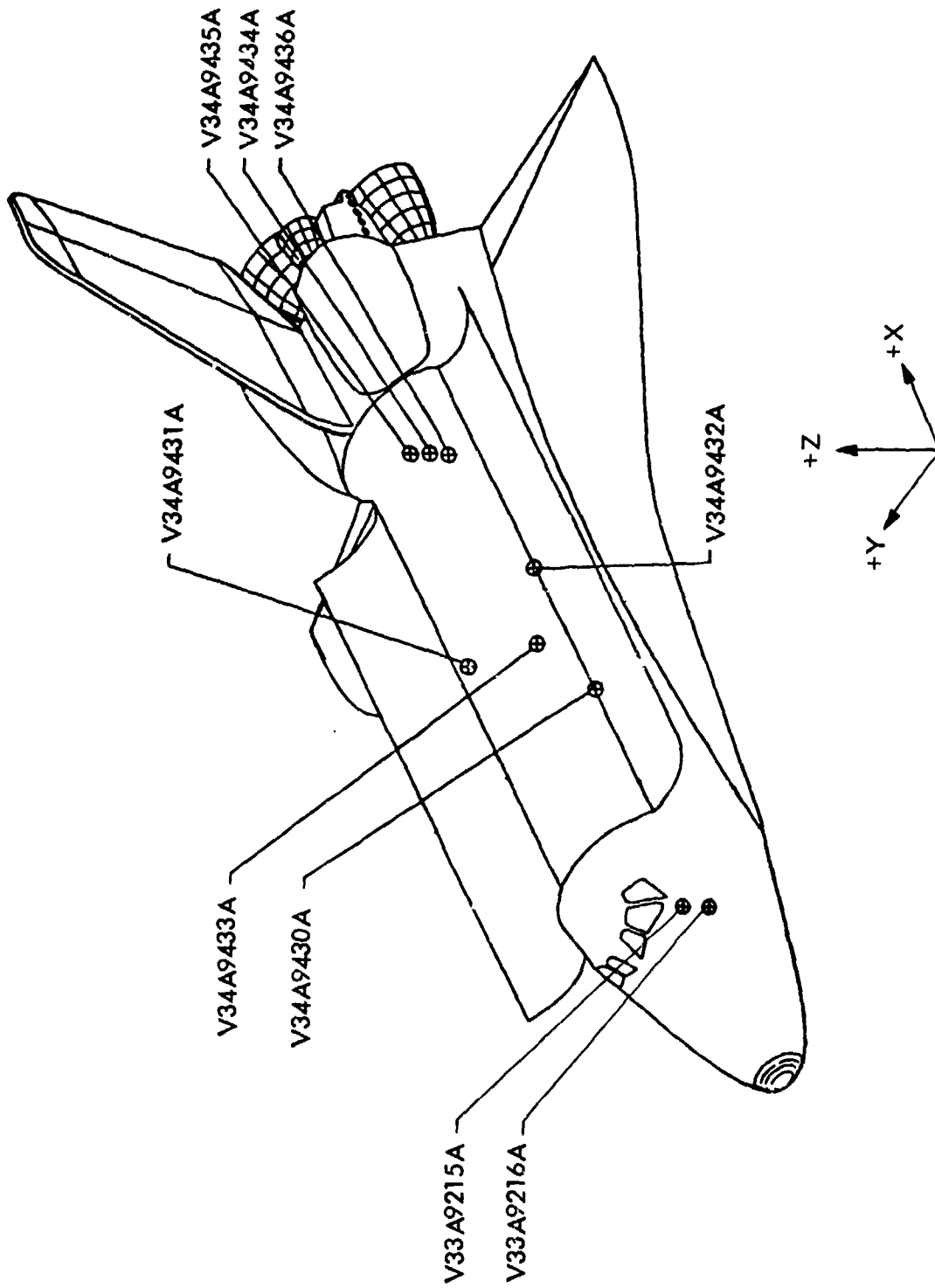


Figure A-6. DFBI Acceleration Measurement Locations

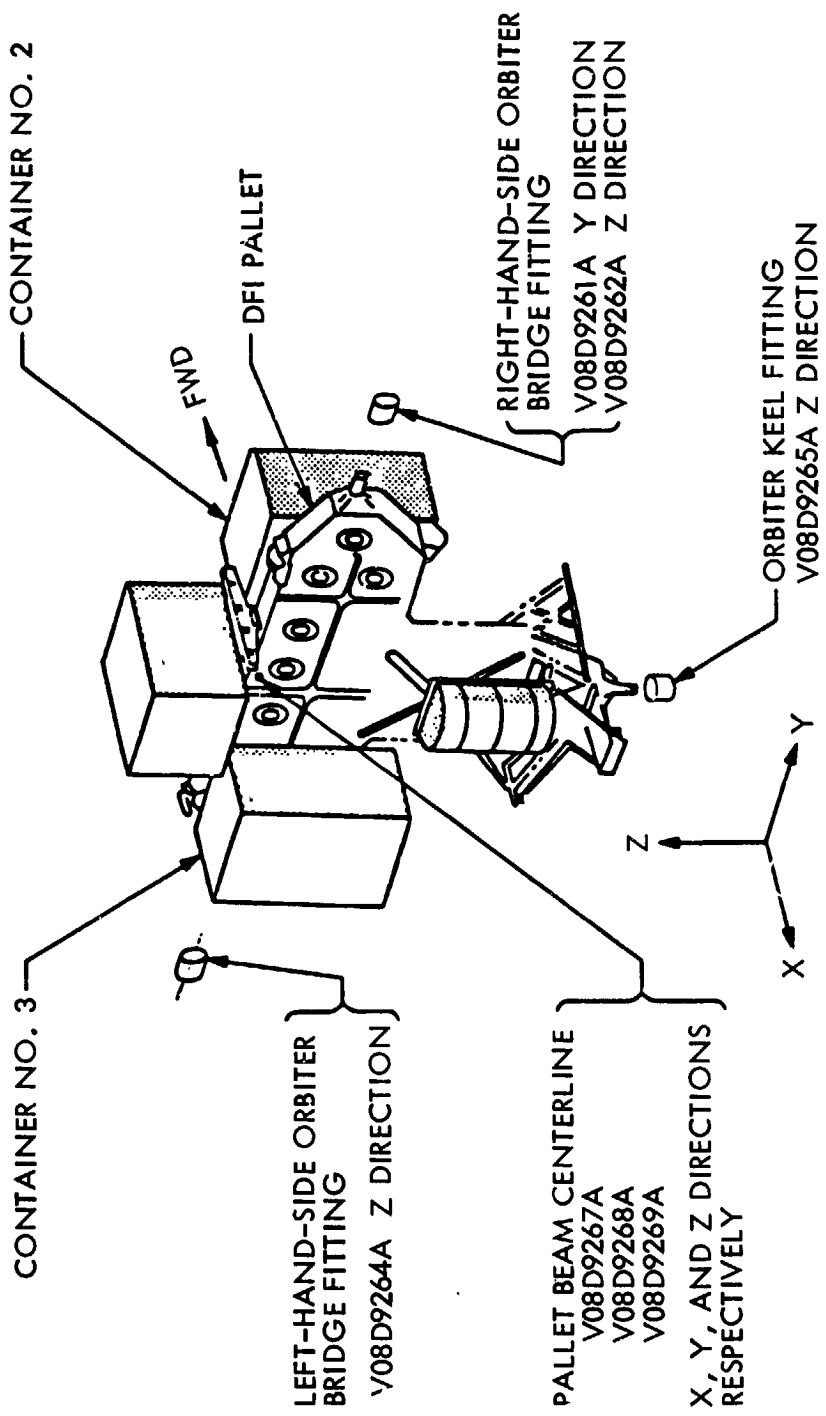


Figure A-7. DATE Low Frequency Accelerometers at DFII Pallet in Identical Locations for Multiple Flights

Table A-1.

DATE ACCELEROMETERS AT DFI PALLET IN IDENTICAL LOCATIONS FOR MULTIPLE FLIGHTS

| Measurement No. | Type | Exp. | Location Description | Axis | Range | Frequency Response | Orbiter Station Location | | |
|-----------------|------|------|----------------------|------|-------|--------------------|--------------------------|-----|-----|
| | | | | | | | X | Y | Z |
| V08D9261A* | LFA | DFI | Bridge Ftg R.H. | LONG | ±10 G | 0-50 Hz | 1171 | +98 | 414 |
| V09D9262A* | LFA | DFI | Bridge Ftg R.H. | LONG | ±10 G | 0-50 Hz | 1171 | +96 | 414 |
| V09D9264A* | LFA | DFI | Bridge Ftg L.H. | LONG | ±10 G | 0-50 Hz | 1171 | -90 | 414 |
| V09D9265A* | LFA | DFI | Bridge Ftg Keel | LONG | ±10 G | 0-50 Hz | 1171 | +4 | 308 |
| V08D9267A** | LFA | DFI | Pallet Beam C.L. | X | ±16 G | 1.5-50 Hz | 1167 | +4 | 428 |
| V08D9268A** | LFA | DFI | Pallet Beam C.L. | Y | ±16 G | 1.5-50 Hz | 1187 | +4 | 428 |
| V08D9269A** | LFA | DFI | Pallet Beam C.L. | Z | ±16 G | 1.5-50 Hz | 1187 | +4 | 428 |

*On STS-2 and STS-3 only

**On STS-2, STS-4, and STS-5 only

Table A-2.

DFI ACCELERATION MEASUREMENT INFORMATION

| Measurement No. | Sensing Axis | Range (G) | Location Description | Orbital Station Location | | |
|-----------------|--------------|-----------|------------------------------|--------------------------|------|-----|
| | | | | X | Y | Z |
| V33A9215A | Z | -2,+2 | Crew Cabin | 513 | -3 | 422 |
| V33A9216A | Z | -2,+6 | Crew Cabin | 513 | -3 | 422 |
| V34A930A | Z | -2,+5 | Cargo Bay, Sill Longeron | 823 | -100 | 407 |
| V34A931A | Z | -2,+5 | Cargo Bay, Sill Longeron | 973 | 100 | 407 |
| V34A932A | Z | -2,+5 | Cargo Bay, Sill Longeron | 973 | -100 | 407 |
| V34A933A | Y | -2,+2 | Cargo Bay near Keel Longeron | 979 | +9 | 305 |
| V34A934A | X | +3.4,-2.5 | Cargo Bay, Aft Bulkhead | 1294 | +3 | 296 |
| V34A935A | Y | -2,+2 | Cargo Bay, Aft Bulkhead | 1294 | +3 | 300 |
| V34A936A | Z | -1.5,+5 | Cargo Bay, Aft Bulkhead | 1294 | +3 | 290 |

Table A-3.

DFI ACOUSTIC MEASUREMENT INFORMATION

| Measurement No. | Range (dB) | Frequency | Location Description | Orbiter Station Location | | |
|--------------------|------------|--------------------|----------------------------|--------------------------|------|-----|
| | | | | X | Y | Z |
| V08Y9219A | 110-150 | Wide Band 20-8KHz | Cargo Bay, Internal | 863 | -100 | 381 |
| V08Y9220A | 110-150 | Wide Band 20-8KHz | Cargo Bay, Internal | 1190 | 0 | 427 |
| V08Y9401A | 130-170 | Wide Band 20-8KHz | Cargo Bay Door, External | 639 | 3.5 | 500 |
| V08Y9402A | 130-170 | Wide Band 20-8KHz | Cargo Bay Door, External | 1281 | 4.2 | 500 |
| V08Y9403A | 110-150 | Wide Band 20-8KHz | Cargo Bay, Internal | 1306 | 12.0 | 400 |
| V08Y9404A | 130-170 | Wide Band 20-80KHz | Cargo Bay Bottom, External | 1296 | 0 | 300 |
| V08Y9405A | 110-150 | Wide Band 20-8KHz | Cargo Bay, Internal | 640 | 4 | 423 |

Table A-4.

STS-2 DATE MEASUREMENT INFORMATION ON DFI PALLET

| Measurement No. | Type | Exp. | Location | | Frequency Response | Orbiter Station Location | | | |
|-----------------|-------|------|--------------|-------------|--------------------|--------------------------|------|------|-----|
| | | | Description | Axis | | Range | X | Y | Z |
| V08D9260A | LFA | DFI | BRIDGE FTG | R.H. LONG X | + 10 G | 0 - 50 Hz | 1171 | + 96 | 414 |
| V08D9261A | LFA | DFI | BRIDGE FTG | R.H. LONG Y | + 10 G | 0 - 50 Hz | 1171 | + 98 | 414 |
| V08D9262A | LFA | DFI | BRIDGE FTG | R.H. LONG Z | + 10 G | 0 - 50 Hz | 1171 | + 96 | 414 |
| V08D9263A | LFA | DFI | BRIDGE FTG | L.H. LONG Y | + 10 G | 0 - 50 Hz | 1171 | - 90 | 414 |
| V08D9264A | LFA | DFI | BRIDGE FTG | L.H. LONG Z | + 10 G | 0 - 50 Hz | 1171 | - 90 | 414 |
| V08D9265A | LFA | DFI | BRIDGE FTG | KEEL LONG Z | + 10 G | 0 - 50 Hz | 1171 | + 4 | 308 |
| V08D9266A | LFA | DFI | BRIDGE FTG | KEEL LONG X | + 16 G | 1.5 - 50 Hz | 1179 | + 4 | 306 |
| V08D9267A | LFA | DFI | PALLET BEAM | C.L. X | + 16 G | 1.5 - 50 Hz | 1187 | + 4 | 428 |
| V08D9268A | LFA | DFI | PALLET BEAM | C.L. Y | + 16 G | 1.5 - 50 Hz | 1187 | + 4 | 428 |
| V08D9269A | LFA | DFI | PALLET BEAM | C.L. Z | + 16 G | 1.5 - 50 Hz | 1187 | + 4 | 428 |
| V08D9273A | HFA | DFI | PALLET BEAM | L.H. X | + 40 G | 5 - 2 KHz | 1187 | - 14 | 428 |
| V08D9274A | HFA | DFI | PALLET BEAM | L.H. Z | + 40 G | 5 - 2 KHz | 1187 | - 14 | 428 |
| V08Y9275A | AM LF | DFI | No 1 UPR FWD | OUTBD COR | + .4101 PSI | 5 - 2 KHz | 1139 | - 68 | 432 |
| V08Y9276A | AM LF | DFI | No 2 LWR FWD | INBD COR | + .4101 PSI | 5 - 2 KHz | 1139 | + 20 | 384 |
| V08Y9277A | AM LF | DFI | No 3 UPR AFT | OUTBD COR | + .4101 PSI | 5 - 2 KHz | 1219 | - 68 | 432 |
| V08Y9278A | AM LF | DFI | PALLET CONN | PL L.H. | + .4101 PSI | 5 - 2 KHz | 1194 | - 44 | 328 |
| V08Y9279A | AM LF | DFI | PALLET COOL | PUMP BRACE | + .4101 PSI | 5 - 2 KHz | 1192 | + 15 | 384 |
| V08Y9280A | AM HF | DFI | No 2 UPR FWD | OUTBD COR | + .4101 PSI | 20 - 8 KHz | 1139 | + 68 | 432 |
| V08Y9281A | AM HF | DFI | No 3 LWR AFT | | + .4101 PSI | 22 - 8 KHz | 1219 | - 68 | 384 |

Table A-5.

STS-2 DATE MEASUREMENT INFORMATION ON OSTA PALLET

| Measurement No. | Type | Exp. | Location | | | Frequency Response | Orbiter Station Location | | |
|-----------------|-------|--------|----------------|-----------|-------------|--------------------|--------------------------|------|-----|
| | | | Description | Axis | Range | | X | Y | Z |
| V08D9240A | LFA | OSTA-1 | BRIDGE FLT LH | LONG X | + 16 G | 1.5 - 50 Hz | 892 | -100 | 414 |
| V08D9241A | LFA | OSTA-1 | BRIDGE FLT LH | LONG Y | + 16 G | 1.5 - 50 Hz | 890 | -100 | 414 |
| V08D9242A | LFA | OSTA-1 | BRIDGE FLT LH | LONG Z | + 16 G | 1.5 - 50 Hz | 890 | -100 | 414 |
| V08D9243A | LFA | OSTA-1 | FLOOR UPR SURF | LONG X | + 16 G | 1.5 - 50 Hz | 895 | 0 | 344 |
| V08D9244A | LFA | OSTA-1 | FLOOR UPR SURF | LONG Y | + 16 G | 1.5 - 50 Hz | 895 | 0 | 344 |
| V08D9245A | LFA | OSTA-1 | FLOOR UPR SURF | LONG Z | + 16 G | 1.5 - 50 Hz | 895 | 0 | 349 |
| V08D9246A | HFA | OSTA-1 | OCG SHELF L.H. | SIDE X | + 40 G | 5 - 2 KHz | 920 | - 73 | 413 |
| V08D9247A | HFA | OSTA-1 | OCG SHELF L.H. | SIDE Y | + 40 G | 5 - 2 KHz | 920 | - 73 | 413 |
| V08D9248A | HFA | OSTA-1 | OCG SHELF L.H. | SIDE Z | + 40 G | 5 - 2 KHz | 920 | - 73 | 413 |
| V08D9249A | HFA | OSTA-1 | MEA SHELF L.H. | SIDE X | + 40 G | 5 - 2 KHz | 868 | - 35 | 357 |
| V08D9250A | HFA | OSTA-1 | MEA SHELF L.H. | SIDE Y | + 40 G | 5 - 2 KHz | 868 | - 35 | 357 |
| V08D9251A | HFA | OSTA-1 | MEA SHELF L.H. | SIDE Z | + 40 G | 5 - 2 KHz | 868 | - 35 | 357 |
| V08Y9252A | AM LF | OSTA-1 | OCE SHELF FWD | INBD COR | + .4101 PSI | 5 - 2 KHz | 864 | - 29 | 410 |
| V08Y9253A | AM LF | OSTA-1 | OCE SHELF AFT | INBD COR | + .4101 PSI | 5 - 2 KHz | 978 | - 29 | 410 |
| V08Y9254A | AM LF | OSTA-1 | OCE SHELF MID | TRUSS | + .4101 PSI | 5 - 2 KHz | 951 | - 45 | 394 |
| V08Y9255A | AM LF | OSTA-1 | PALLET FLOOR | LWR SURF | + .4101 PSI | 5 - 2 KHz | 951 | 0 | 326 |
| V08Y9256A | AM LF | OSTA-1 | PALLET L.H. | SIDE | + .4101 PSI | 5 - 2 KHz | 951 | - 85 | 398 |
| V08Y9257A | AM HF | OSTA-1 | FWD SIR-A | ANT TRUSS | + .4101 PSI | 20 - 8 KHz | 832 | + 29 | 427 |
| V08Y9258A | AM HF | OSTA-1 | AFT SIR-A | ANT TRUSS | + .4101 PSI | 20 - 8 KHz | 1001 | + 29 | 427 |

Table A-6.

STS-3 DATE MEASUREMENT INFORMATION ON DFI PALLET

| Measurement No. | Type | Exp. | Location Description | Axis | EMRC | Frequency Response | Orbiter X | Station Y | Location Z |
|-----------------|-------|------|------------------------|--------|------------|--------------------|-----------|-----------|------------|
| V08D9260A | LFA | DFI | Bridge FTC R.H. | Long X | ±100 | 0 - 50 Hz | 1171 | +96 | 414 |
| V08D9261A | LFA | DFI | Bridge FTC R.H. | Long Y | ±100 | 0 - 50 Hz | 1171 | +98 | 414 |
| V08D9262A | LFA | DFI | Bridge FTC R.H. | Long Z | ±100 | 0 - 50 Hz | 1171 | +96 | 414 |
| V08D9263A | LFA | DFI | Bridge FTG L.H. | Long X | ±100 | 0 - 50 Hz | 1171 | -90 | 414 |
| V08D9264A | LFA | DFI | Bridge FTG L.H. | Long Z | ±100 | 0 - 50 Hz | 1171 | -90 | 414 |
| V08D9265A | LFA | DFI | Bridge FTG Keel | Long Z | ±100 | 0 - 50 Hz | 1171 | +4 | 308 |
| V08D9273A | HFA | DFI | Pallet Beam L.H. | X | ±200 | 5 - 2 KHz | 1187 | -14 | 428 |
| V08D9274A | HFA | DFI | Pallet Beam L.H. | Z | ±200 | 5 - 2 KHz | 1187 | -14 | 428 |
| V08Y9275A | AM LF | DFI | No 1 Upr Fwd Outbd Cor | | ±.2306 PSI | 5 - 2 KHz | 1139 | -58 | 432 |
| V08Y9280A | AM LF | DFI | No 2 Upr Fwd Outbd Cor | | ±.2306 PSI | 20 - 8 KHz | 1139 | +68 | 432 |
| V08Y9281A | AM LF | DFI | No 3 Lwr Aft | | ±.2306 PSI | 22 - 8 KHz | 1219 | -68 | 384 |

Table A-7.

STS-3 DATE MEASUREMENT INFORMATION ON OSS-1

| Measurement No. | TYPE | Measurement Description | AXIS | RANGE | Frequency Response | Pallet Location | | |
|-----------------|-------|------------------------------------|----------|-------------|--------------------|-----------------|-----|-----|
| | | | | | | X | Y | Z |
| V08Y9230A | AM LF | Ibercal Cannister Inside | OMNI | ±0.0918 PSI | 5-2 KHz | 78 | 7 | 452 |
| V08Y9231A | AM LF | Thermal Can Outd Inbd Fwd Cor | OMNI | ±0.2306 PSI | 5-2 KHz | 59 | -10 | 471 |
| V08Y9232A | AM LF | End Long Boom Plat 6 Facing Aft | OMNI | ±0.2306 PSI | 5-2 KHz | 87 | -35 | 419 |
| V08Y9233A | AM HF | Plat 4 Aft Inbd Cor Facing Aft | OMNI | ±0.2306 PSI | 20-8 KHz | 32 | 66 | 417 |
| V08Y9234A | AM HF | End Sht Boom Vert Plat Facing Fwd | OMNI | ±0.2306 PSI | 20-8 KHz | 3 | 11 | 409 |
| V08D9282A | LFA | Therm Can X Axis Fwd Inbd Cor | X | ±8 G | 1.5-50 Hz | 61 | -7 | 470 |
| V08D9283A | LFA | Therm Can Y Axis Fwd Inbd Cor | Y | ±8 G | 1.5-50 Hz | 61 | -7 | 470 |
| V08D9284A | LFA | Therm Can Z Axis Fwd Inbd Cor | Z | ±8 G | 1.5-50 Hz | 61 | -7 | 470 |
| V08D9285A | LFA | Sunys Instr Ped X Axis Facing Aft | +X | ±6 G | 1.5-50 Hz | 53 | 63 | 414 |
| V08D9286A | LFA | Sunys Instr Ped Y Axis Facing | -Y | ±8 G | 1.5-50 Hz | 53 | 63 | 414 |
| V08D9287A | LFA | Sunys Instr Ped Z Axis Facing | -Z | ±8 G | 1.5-50 Hz | 53 | 63 | 414 |
| V08D9288A | LFA | Intersect Stiff Fwd Side Vert Plat | -X | ±8 G | 1.5-50 Hz | 1 | 40 | 408 |
| V08D9289A | LFA | Plat #3 Ctr Upper Side | -X | ±8 G | 1.5-50 Hz | 29 | -62 | 393 |
| V08D9290A | LFA | Plat #3 Ctr Upper Side | Normal | ±8 G | 1.5-50 Hz | 29 | -62 | 393 |
| V08D9291A | LFA | Plat #3 Ctr Upper Side | In Plane | ±8 G | 1.5-50 Hz | 29 | -62 | 393 |
| V08D9292A | HFA | Panel #4 Ctrl Insert | X | ±40 G | 5-2 KHz | 101 | 65 | 392 |
| V08D9300A | HFA | Side of Cold Plat X Axis | In Plane | ±20 G | 5-2 KHz | 84 | -61 | 390 |
| V08D9294A | HFA | On Supt Bracket for Srpa Inst | -X | ±20 G | 5-2 KHz | 11 | 52 | 433 |
| V08D9302A | HFA | Aft Side Vert Platform | X | ±20 G | 5-2 KHz | 4 | 51 | 409 |
| V08D9296A | HFA | Aft Side Therm Cann Base | X | ±20 G | 5-2 KHz | 108 | -7 | 352 |
| V08D9298A | HFA | Insd Therm Cann Fwd Inbd Corner | X | ±20 G | 5-2 KHz | 72 | -5 | 446 |
| V08D9297A | HFA | Aft Side Therm Cann Base | Z | ±20 G | 5-2 KHz | 108 | -7 | 352 |
| V08D9299A | HFA | Aft Inside Therm Cann | Y | ±40 G | 5-2 KHz | 72 | -5 | 446 |
| V08D9293A | HFA | Panel #4 Central Insert | Normal | ±40 G | 5-2 KHz | 101 | 65 | 392 |
| V08D9301A | HFA | Side of Cold Plate | Normal | ±20 G | 5-2 KHz | 84 | -61 | 390 |
| V08D9295A | HFA | On Support Bracket for Srpa Inst | -Z | ±20 G | 5-2 KHz | 11 | 52 | 433 |
| V08D9303A | HFA | Aft Side Vert Platform | Z | ±20 G | 5-2 KHz | 4 | 51 | 409 |

Table A-8.

STS-4 DATE MEASUREMENT INFORMATION

| Sensor Number | Description | Orientation Axis | | | Location | | | RANGE | FREQUENCY RESPONSE |
|---------------|---------------------------------------|------------------|-----|-----|----------|---|---|-------------|--------------------|
| | | X | Y | Z | X | Y | Z | | |
| V08Y9276A | AM LF DFI NO. 2 LWR FWD INBD. CORNER | 1139 | +20 | 384 | | | | +0.2306 PSI | 5 to 8 KHZ |
| V08Y9277A | AM LF DFI NO. 3 UPR AFT OUTBD. CORNER | 1219 | -68 | 432 | | | | +0.2306 PSI | 5 to 8 KHZ |
| V08Y9278A | AM LFA DFI PALLET CONN. PL. L. H. | 1194 | -44 | 328 | | | | +0.2306 PSI | 5 to 2 KHZ |
| V08Y9279A | AM LF DFI PALLET COOL PUMP BRACE | 1192 | +5 | 384 | | | | +0.2306 PSI | 5 to 2 KHZ |
| V08Y9275A | AM LF DFI NO. 1 UPR FWD OUTBD COR | 1139 | -68 | 432 | | | | +0.2306 PSI | 5 to 2 KHZ |
| V08Y9280 | AM HF DFI NO. 2 UPR FWD OUTBD COR | 1139 | +68 | 432 | | | | +0.2306 PSI | 5 to 8 KHZ |
| V08Y9281A | AM HF DFI NO. 3 LWD AFT OUTBD COR | 1219 | -68 | 384 | | | | +0.2306 PSI | 5 to 8 KHZ |
| V08D9647A | LFA P/L BRIDGE FTG KEEL | 947 | +6 | 307 | | | | +10G | 0 to 50 HZ |
| V08D9648A | LFA P/L BRIDGE FTG RT FWD LONGA | 905 | +96 | 416 | | | | +10G | 0 to 50 HZ |
| V08D9649A | LFA P/L BRIDGE FTG RT AFT LONGN | 1088 | +95 | 415 | | | | +10G | 0 to 50 HZ |
| V08D9650A | LFA P/L BRIDGE FTG LFT FWD LONGN | 955 | -96 | 416 | | | | +10G | 0 to 50 HZ |
| V08D9651A | LFA P/L BRIDGE FTG LFT AFT LONGN | 1086 | -95 | 415 | | | | +10G | 0 to 50 HZ |
| V08D9652A | FLA P/L BRIDGE FTG LFT AFT LONGN | 1086 | -96 | 414 | | | | +10G | 0 to 50 HZ |
| V08D9653A | FLA P/L BRIDGE FTG LFT AFT LONGN | 1086 | -97 | 412 | | | | +8G | 1.5 to 50 HZ |
| V08D9654A | LFA DFI BRIDGE FTG RT LONGN | 1171 | +95 | 413 | | | | +8G | 1.5 to 50 HZ |
| V08D9655A | LFA DFI BRIDGE FTG RT LONGN | 1171 | +95 | 414 | | | | +8G | 1.5 to 50 HZ |
| V08D9656A | LFA DFI BRIDGE FTG LFT LONGN | 1171 | -95 | 414 | | | | +8G | 1.5 to 50 HZ |
| V08D9657A | LFA DFI BRIDGE FTG LFT LONGN | 1171 | -95 | 414 | | | | +8G | 1.5 to 50 HZ |



Table A-8. (continued)

| Sensor Number | Description | Orientation Axis | Location X | Location Y | Location Z | Range | Frequency Response |
|---------------|-------------------------|------------------|--------------------|------------|------------|-----------|--------------------|
| V08D9658A | LFA DFI BRIDGE FTG KEEL | Y | 1179 | +4 | 306 | +85 | 1.5 to 50 Hz |
| V08D96266A | LFA DFI BRIDGE FTG KEEL | X | 1179 | +4 | 306 | +86 | 1.5 to 50 Hz |
| V08D96267A | LFA DFI PALLET BEAM C/L | X | 1187 | +4 | 428 | +86 | 1.5 to 50 Hz |
| V08D96268A | LFA DFI PALLET BEAM C/C | Y | 1187 | +4 | 428 | +86 | 1.5 to 50 Hz |
| V08D96269A | LFA DFI PALLET BEAM C/L | Z | 1187 | +4 | 428 | +86 | 1.5 to 50 Hz |
| V08D9632A | PAYLOAD ACCELEROMETER | X | PURPOSELY LEFT OUT | | | +20G | 5 to 2 kHz |
| V08D9633A | PAYLOAD ACCELEROMETER | Z | " | | | +20G | 5 to 2 kHz |
| V08D9634A | PAYLOAD ACCELEROMETER | Y | " | | | +20G | 5 to 2 kHz |
| V08D9635A | PAYLOAD ACCELEROMETER | X | " | | | +20G | 5 to 2 kHz |
| V08D9636A | PAYLOAD ACCELEROMETER | X | " | | | +20G | 5 to 2 kHz |
| V08D9637A | PAYLOAD ACCELEROMETER | Y | " | | | +20G | 5 to 2 kHz |
| V08D9638A | PAYLOAD ACCELEROMETER | Y | " | | | +20G | 5 to 2 kHz |
| V08D9639A | PAYLOAD ACCELEROMETER | X | " | | | +20G | 5 to 2 kHz |
| V08D9640A | PAYLOAD ACCELEROMETER | Z | " | | | +20G | 5 to 2 kHz |
| V08D9641A | PAYLOAD ACCELEROMETER | Y | " | | | +20G | 5 to 2 kHz |
| V08D9642A | PAYLOAD MICROPHONE 1 | OMNI | " | | | +2306 PSI | 5 to 2 kHz |
| V08D9643A | PAYLOAD ACCELEROMETER | X | " | | | +20G | 5 to 2 kHz |
| V08D9644A | PAYLOAD ACCELEROMETER | X | " | | | +20G | 5 to 2 kHz |
| V08D9645A | PAYLOAD ACCELEROMETER | X | " | | | +20G | 5 to 2 kHz |
| V08D9646A | PAYLOAD ACCELEROMETER | Y | " | | | +20G | 5 to 2 kHz |

Table A-9.

STS-5 DATE MEASUREMENT INFORMATION

| MEAS. NO. | Meas. TYPE | Loca- tion | LOCATION DESCRIPTION | AXIS | FREQUENCY RESPONSE | RANGE | COORDINATES | |
|-----------|------------------------------|---------------------------------|---------------------------------|----------|--------------------|--------|-------------|-----|
| | | | | | | | X | Y |
| V0809266A | LOW-FREQUENCY ACCELEROMETERS | DFI | BRIDGE FTG KEEL X-AXIS | X | 1.5 - 50 | +8G | 1179 | +4 |
| V0809267A | | DFI | PALLET BEAM C/L X-AXIS | X | 1.5 - 50 | +8G | 1187 | +4 |
| V0809268A | | DFI | PALLET BEAM C/L Y-AXIS | Y | 1.5 - 50 | +8G | 1187 | +4 |
| V0809269A | | DFI | PALLET BEAM C/L Z-AXIS | Z | 1.5 - 50 | +8G | 1187 | +4 |
| V0809654A | | DFI | BRIDGE FTG RT LONGN X-AXIS | X | 1.5 - 50 | +8G | 1171 | +95 |
| V0809655A | | DFI | BRIDGE FTG RT LONGN Z-AXIS | Z | 1.5 - 50 | +8G | 1171 | +95 |
| V0809656A | | DFI | BRIDGE FTG LFT LONGN X-AXIS | X | 1.5 - 50 | +8G | 1171 | -95 |
| V0809657A | | DFI | BRIDGE FTG LFT LONGN Z-AXIS | Z | 1.5 - 50 | +8G | 1171 | -95 |
| V0809658A | | DFI | BRIDGE FTG KEEL Y-AXIS | Y | 1.5 - 50 | +8G | 1179 | +4 |
| V0809801A | | TELESAT | BRIDGE FTG RT FWD LONGN Y-AXIS | X | 0 - 50 | +10G | 1030 | +95 |
| V0809802A | | TELESAT | BRIDGE FTG RT FWD LONGN Z-AXIS | Z | 0 - 50 | +10G | 1030 | +95 |
| V0809803A | | TELESAT | BRIDGE FTG RT APT LONGN Z-AXIS | Z | 0 - 50 | +10G | 1108 | +95 |
| V0809804A | | TELESAT | BRIDGE FTG LFT FWD LONGN X-AXIS | X | 0 - 50 | +10G | 1030 | -95 |
| V0809805A | | TELESAT | BRIDGE FTG LFT FWD LONGN Z-AXIS | Z | 0 - 50 | +10G | 1030 | -95 |
| V0809806A | TELESAT | BRIDGE FTG LFT APT LONGN Z-AXIS | Z | 0 - 50 | +10G | 1108 | -95 | |
| V0809807A | TELESAT | BRIDGE FTG KEEL LONGN Y-AXIS | Y | 1.5 - 50 | +8G | 1025 | -? | |
| V08Y9275A | MICROPHONES | DFI | NO. 1 UPR FWD OUTBD CORNER | 0 | 5 - 2K | 155 dB | 1139 | -68 |
| V08Y9276A | | DFI | NO. 2 LMR FWD INBD CORNER | 0 | 5 - 8K | 155 dB | 1139 | +20 |
| V08Y9277A | | DFI | NO. 3 UPR FWD OUTBD CORNER | 0 | 5 - 8K | 155 dB | 1219 | -68 |
| V08Y9278A | | DFI | PALLET CONN PL L.H. | 0 | 5 - 2K | 155 dB | 1194 | -44 |
| V08Y9279A | | DFI | PALLET COOL PUMP BRACKET | 0 | 5 - 2K | 155 dB | 1192 | +5 |
| V08Y9280A | | DFI | NO. 2 UPR FWD OUTBD CORNER | 0 | 5 - 8K | 155 dB | 1139 | +68 |
| V08Y9281A | | DFI | NO. 3 LMR APT CORNER | 0 | 5 - 8K | 155 dB | 1219 | -68 |